Journal of the Royal Society of Western Australia, 106: 1–8, 2023

Changing ideals and realities: a longitudinal view of rural Western Australia

ROY JONES

Curtin University, Perth, Western Australia

✉ *r.jones@curtin.edu.au*

ABSTRACT

This state-wide and long-term overview of rural change in Western Australia employs Craig Colten's hierarchical categorisation of rural change into transitions and adaptations. It identifies two major transitions in the nature of human use of Western Australia's rural land. The first was the shift from a localised subsistence economy and society spanning tens of millennia, as practised by the Indigenous population, to a commercially productive and imperial system between the early nineteenth and the early twentieth centuries as British colonisation and Indigenous dispossession progressed. Then, from roughly the mid-twentieth century onwards, there has been a 'multifunctional rural transition'. Whereas commercial and productive activities have remained an important function of rural Western Australia, these have been increasingly complemented by, and may even be in competition with protection of the state's pre-existing environments and ecosystems, and consumption of non-metropolitan Western Australia's aesthetic and recreational resources by a predominantly urban population from within and without the state. Adaptations have continued throughout and across both transitions, but they have become more frequent and necessary as global rates of technological, political and social change have accelerated. A case study of the social, economic and land use shifts in the Margaret River region illustrates these processes.

KEYWORDS: Rural change, Transition, Adaptation, Subsistence, Productivism, Protection and consumption of rural areas, Multifunctionality, Margaret River wine region

Manuscript received 15 February 2023; accepted 8 April 2023

INTRODUCTION

In assessing agriculture and other rural activities in Western Australia, the contention attributed to Heraclitus that change is the only constant in life can be accepted as a truism. However, it is the nature, rate and direction of the many changes in rural Western Australia, some of which are continuing, that require attention if trends and patterns are to be identified. The historical geographer Craig Colten used a hierarchical categorisation of change into (fundamental) transitions and (contingent) adaptations in a historical study of coastal management in Louisiana (Colten 2019). Although such change can be studied through a range of lenses, from the empiricism of traditional historical geography to theoretical approaches such as Marxism and evolutionary economic geography (Flood Chavez *et al.* 2023), Colten's categorisation is useful in this context because it can accommodate varying scales in both space and time. Coltern's framework provided the basis for a highly localised case study of rural change on the coastal plain in the Shire of Dandaragan (Jones *et al.* 2022), and is used again in the present overview of Western Australia's rural past, present and prospects.

Colten (2019, p. 417), sees adaptations as 'human actions taken in an effort to *perpetuate* (my emphasis) a society, even if modified in some way'. As such, they may change how people undertake agriculture, or any other rural activity, but they do not change the reason(s) for these activities. Therefore, adaptations 'do not fundamentally alter society' and, even though 'they often take place over years or decades, [they] are often local or regional in scale' (Colten 2019, p. 417). By contrast, transitions result from 'multiple adaptations, deliberate or ad hoc, coordinated or uncoordinated' (Colten 2019, p. 417). He cites the transition from hunting and gathering to agricultural lifestyles as an example of a major shift in human history incorporating numerous adaptations that 'thoroughly infused multiple aspects of society and demanded social, political, technological and economic transformations' (Colten 2019, p. 417). He therefore sees transitions as arising at larger temporal and spatial scales than adaptations, and as bringing about significant changes in human lifestyles and attitudes, whereas adaptations seek to preserve at least some aspects of the status quo.

In Western Australia, three periods of rural occupancy, separated by two transitions can be discriminated. The most clearly defined was the ca. 50,000 – 60,000 years of Indigenous occupation, when land use was largely localised and at a subsistence level (Hallam 1981; Clarkson *et al.* 2017; Dortch *et al.* 2019). This ended with the transition brought on by British colonisation and the development of a commercial and, at least initially, imperial system of agriculture, mining, forestry and fishing between the early nineteenth and early twentieth centuries. A less clear-cut but nonetheless significant shift, which Holmes (2006) terms a 'multifunctional rural transition', has taken place since then. Over this period, the commercial and productivist value system, which had characterised rural Western Australia since colonisation, has been increasingly complemented by the values of protection of the environments and ecosystems that pre-dated colonisation and consumption of the state's rural landscapes and resources as a 'lifestyle product'. Such changes have largely been by visiting recreationists and new residents such as retirees, tree changers, electronic cottagers and second homeowners (Curry *et al.* 2001; Burnley & Murphy 2004). These transitions and their contingent adaptations are described in more detail in the sections below, in terms of ideals and realities, followed by a case study of rural transitions in the Margaret River region.

TRANSITIONS AND ADAPTATIONS IN RURAL WESTERN AUSTRALIA

Indigenous occupation and adaptation

Indigenous groups of people have lived in Western Australia for some 60,000 years (Clarkson *et al.* 2017; Dortch *et al.* 2019). During this period, they operated an economy based on local subsistence and a value system based on sustainability, thereby developing a strong cultural and spiritual attachment to each group's specific territories (McDonald 2020). Noongar elder Noel Nannup (2006) has described this local role and relationship as being 'the carers of everything'.

Whereas the arrival of the first humans to settle in Western Australia could be considered a transition in itself, Indigenous occupation across the state spanned tens of millennia and was characterised by the maintenance of a subsistence and sustainability-oriented lifestyle at a local scale. However, this did not mean that there were not numerous and significant adaptions. As the first human inhabitants of Western Australia diffused southwards from their first foothold in the Kimberley, they exchanged a tropical monsoonal environment, initially for an arid one and subsequently for the highly seasonal temperate conditions of much of the southern part of the state (Dortch *et al.* 2019). There is evidence of Aboriginal occupance at Devil's Lair in the far South West as long ago as 48,000 years BP (Turney *et al.* 2001), which provides a broad time frame for the spread of Indigenous people across the state from north to south. The first inhabitants were required to make significant adaptions during their first 10 millennia or so in Western Australia to survive in different, but generally challenging, physical environments across the state. Nevertheless, over many generations, individual Aboriginal groups developed extremely sophisticated knowledges of their local resources and the most sustainable means of using them. This included the use of fire to clear pathways through the bush, facilitate hunting and selectively encourage plant growth (Hallam 1975). The extent to which this Aboriginal use of the Australian environment was agricultural rather than hunting and gathering is a subject of current debate (Pascoe 2014; Sutton & Walshe 2021). However, as early as 1837, George Grey described turned-over yam grounds north of Perth as more than he 'could have believed in the power of uncivilised man to accomplish' (Grey 1841, cited in Broome *et al.* 2020).

The Aboriginal occupants of Western Australia were obliged to adapt because of environmental variations not only over space, but also over time. During the Last Glacial Maximum, the most recent advance and retreat of global ice sheets, which reached their maximum extent around 25,000 years BP, much of Australia experienced significant drying (Broome *et al*. 2020, p. 12). This climatic shift was also associated with a fall, followed by a rise, in sea levels. Bolton (1992, p. 6) pointed out that '[a]bout 15 per cent of the continent's land surface has sunk below sea level since the first Aborigines settled on it' whereas Williams *et al.* (2018) provided a figure of a 22% reduction in Australia's land area relative to its largest extent. Adaptation to major climatic and environmental change is by no means a recent phenomenon in rural Western Australia.

The information provided in this section relies primarily on archaeological evidence, which is still being collected and assessed. While much Indigenous knowledge has been retained through oral traditions, these sources provide only a partial picture of Aboriginal adaptations to changing environments over time given the serious disruptions to Aboriginal knowledge transmission systems, such as songlines, which accompanied the transition brought about by colonial dispossession.

Commercial and imperial agricultural expansion

The British colonisation of Western Australia from 1826 onwards saw the arrival of a population with extremely different views of the land and their responsibilities in relation to it, and their spiritual and economic roles, compared to the earlier occupants. The prevailing Christian, and especially Protestant, view of the British population in the early nineteenth century was that 'man'—meaning particularly white, Christian men—was separate from and possessed divinely granted domination over 'nature' (Tawney 1964). Furthermore, because the British crown had claimed Western Australia, the colonists saw themselves as being at liberty to develop it for their personal gain, albeit subject to such property and other regulations imposed on them by the colonial and imperial authorities. However, for much of the nineteenth century, such regulation over this large and sparsely populated area was inevitably limited (Bolton 1992). Colonisation and Aboriginal dispossession therefore represented a clear transition whereby the localised and sustainability-oriented land use patterns of the Aboriginal population were supplanted by commercial systems of agricultural and pastoral production, together with forestry, fishing and mining, which were characteristically oriented to supplying the needs of a motherland half a world away.

The colonists had to accept that they were not farming in Britain and that there were limits on the extent to which British farming practices could be transferred to Western Australia. As Powell (1974, p. 15) argued, '[t]he physiognomy of rural Australia is predominantly a continuing expression of the efforts of European people adapting their changing aspirations to an increasing but still relatively slender knowledge about the physical environment'. For the first Western Australian colonists, this adaptation commenced soon after they realised that the soil fertility of the Swan

River Colony had been vastly overestimated by the first British explorers and that poisonous plants were common (Cameron 1981). Shepherds noticed that their flocks rapidly ate out the more nutritious grasses and that their animals' hooves rapidly degraded the fragile soils. This caused them to keep moving to new pastures thereby extending the pastoral frontier from the Avon Valley to the most remote parts of the state in less than a century. Another nineteenth-century adaptation was the admission of convicts into what had been intended to remain a 'free' colony from 1850 onwards to boost the agricultural labour force and prevent economic collapse. Nevertheless, the ideal of creating an English landscape of small, family-run farms died hard. Premier John Forrest's promotion of a 'bold yeomanry' of this type (Tonts 2002) was reflected in Western Australia's land settlement and infrastructure policies extending into the early twentieth century. Their imprint can still be seen in the relatively dense pattern of rail lines and designated town sites provided for the development of the wheat belt in the early twentieth century (Glynn 1975), which almost immediately were rendered obsolete by the onset of motorised road transport, and has been in a state of ongoing adaptation ever since.

Alongside these what might be termed political and economic shifts, farmers, fishers, foresters and miners were constantly making adaptations to their methods of production. These were in response to both the understandings they developed of the potentials and pitfalls of the local environments in which they operated and the increasingly rapid technological advances, such as new machines, crop strains, stock breeds, pesticides and fertilisers—in short, entirely new methods of production—available to them. Tonts *et al.* (2010) provided an illustration of this process with reference to cattle breeding.

In spite of the massive technological and socioeconomic changes that took place during the first century of (predominantly) European settlement in Western Australia, in Colten's terms this period can still be considered as one of adaptation. While changes in the sites and methods of production transformed the colony's/state's non-metropolitan areas between the early nineteenth and early twentieth centuries, Western Australia's farming, fishing, forestry and mining industries remained productive, profit-oriented and largely British Empire-focused throughout.

The multifunctional rural transition

Holmes (2006, p. 143) discerned three 'impulses' towards a multifunctional rural transition, which gained momentum across Australia and many other parts of the developed world as the twentieth century progressed. The first impulse, which is related to productivist advances, he termed 'agricultural overcapacity'. He argued that technological and other agricultural adaptations, some of them political, have led to commodity and therefore to (farm)land surpluses. This can render some farmland redundant for productive purposes, thereby making it available for alternative uses. Secondly, he identified 'the emergence of market-driven amenity-oriented uses'. The increasing affluence, mobility and leisure time of urban populations over this period provided them with greater opportunities to reassign at least some of the rural areas for recreational, tourism and even residential purposes. This enabled some rural land, particularly if it was scenic or close to metropolitan areas, to gain what he termed an 'amenity premium' in its land value. It therefore became more profitable to reallocate such land to consumption-related uses, rather than to continue using it for productive purposes. Finally, the twentieth century has seen 'changing societal values' with respect to both the environment and social justice. These concerns, especially those relating to sustainability, the maintenance of biodiversity and Indigenous land rights, have given rise to political movements and subsequently government policies to protect at least some rural areas from the environmental degradation resulting from productive rural activities such as land clearance, forestry and mining.

Taken together, these impulses have changed—that is, they have brought about a transition in—the ways in which Western Australia's rural resources are appraised, allocated, used and managed. Overall, this multifunctional transition has yielded 'increasing diversity, complexity and spatial heterogeneity in [the] modes of rural occupance' (Holmes 2006, p. 144). Holmes identified several generalised modes of human occupancy that he claimed are identifiable in contemporary rural Australia. One of these, the conservation and Indigenous mode, in which protection values are emphasised, correlates closely with the period of sole Indigenous occupation when Country was cared for to support local populations sustainably at a subsistence level. Another, the productivist agricultural mode, in which production values are dominant, characterised most, if not all, of rural Western Australia by the end of the first century of British colonisation. A third, the rural amenity mode, in which consumption values are dominant, can be discerned in highly localised forms in the contemporary countryside. These include hobby farms, tourist resorts and rural residential subdivisions. In his three other modes (pluriactive, peri-metropolitan and marginalised agricultural), production, protection and consumption value systems interact.

What is currently intensifying the 'diversity, complexity and spatial heterogeneity' of rural Western Australia, therefore, is not only the local dominance of production, consumption and protection values in specific rural areas of the state but also the intricate sets of processes whereby these three value systems interact with each other, either negatively through competition or positively through complementarity. These processes are illustrated below in a case study of rural change in the Margaret River wine region, by considering how these value systems have contested and collaborated as the region's rural economy and society have both transitioned and adapted over time.

CHANGING IDEALS AND REALITIES IN THE MARGARET RIVER WINE REGION

Indigenous groups occupied this region for tens of millennia (Turney *et al.* 2001), adapting to the specific conditions of the local environment and to long-term climatic changes. They refined their hunting, fishing, gathering and, arguably, agricultural practices to ensure sufficient resources to maintain themselves at a subsistence level on their local territories in the short and long term. Whereas the purpose of their occupation of this region remained constant over a long period, this did not mean a lack of innovation. Archaeological finds at the Devil's Lair site, for example, provide evidence of some of the oldest symbolic objects (in this case jewellery) found anywhere in the world (Bednarik 1997).

British colonisation resulted in the arrival of a population with vastly different ideals to those of the Indigenous population. The first European settlers in the area arrived in 1830 and were possessed of a frontier ideology that perceived the local resources as inexhaustible (Sanders 2005; Flood Chavez *et al.* 2023). Nevertheless, initial attempts to develop agriculture in the region met with limited success. Fishing and whaling fared a little better, especially at Augusta/Flinders Bay, though the whale stocks were rapidly depleted (Gaynor 2014). However, in the latter part of the nineteenth century, adaptations such as the introduction of convict labour and partial mechanisation in the form of railways and steam-powered mills facilitated the development of a significant timber industry. This activity was clearly productivist, but the scale of its operations proved unsustainable with supplies of accessible timber declining by the end of the century.

During the timber operations, spectacular limestone cave systems were discovered along the ridge between Cape Naturaliste and Cape Leeuwin. It was at this point that the first impulses towards a multifunctional rural transition became apparent locally. Not only did this add consumption values to the area as the caves became one of the state's first rural tourist attractions, but it also brought about protection initiatives. In 1900, the WA government created a reserve of 6,600 hectares around the cave sites, undertook an inventory of the cave systems and set up a caves conservation committee (Rundle 1996; Flood Chavez *et al.* 2023). This early mixing and, in many ways contesting, of production, consumption and protection values presaged much larger and longer-term interactions between them in the twentieth century.

However, the next major rural initiative in this area, the Group Settlement Scheme (Gabbedy 1988), was solely productivist and strongly imperial. The state government was seeking to both diversify the economy and offer more widespread employment opportunities in the aftermath of the gold rush and the First World War. Following the modest success of its initiatives for the expansion of the wheat belt (Glynn 1975; Tonts & Horsley 2019), in the 1920s the state entered into a partnership with the British government to bring out migrants who would, it was hoped, establish dairy farms in the South West, particularly in the region surrounding Margaret River (Fig. 1). This scheme strongly adhered to John Forrest's ideal of a bold yeomanry and was widely promoted in Britain as a process of 'giving away farms' (Brayshay & Selwood 2002). In practice, however, it was a spectacular failure. The British migrants, almost all of whom had no prior experience of farming, were provided with manifestly inadequate support and guidance. They were set unrealistic targets and timelines for clearing their land, and establishing herds before they were expected to commence repayments for their passage, their land and the initial support offered to them. For the minority who struggled on to the end of the decade, the collapse in agricultural prices following the 1929 stock market crash and the 1930s depression was, in most cases, the final straw (Bolton 1994).

Although the vast majority of Group Settlers abandoned their properties within a few years of their arrival (Brunger & Selwood 1997), the basis of a road network had been established in the area and numerous small agricultural plots had been at least partially cleared. In the more favourable economic circumstances following the Second World War, the state government again used these assets in the hope of developing a local dairy industry, this time with Australian soldier settlers (Sanders 2005). Again, this met with limited success. It was not until the 1960s that this rural region embarked upon a far more multifunctional and what until now appears to be a more sustainable trajectory of economic and social development.

Early attempts at productivist development in the South West ignored the environmental reality of a finite timber resource, and the economic and social realities of setting up a dairy industry from scratch while using a labour force lacking in capital, skills and local knowledge. In the 1960s, however, an agricultural scientist (Gladstones 1965) pointed out that the soils of the Leeuwin–Naturaliste limestone ridge were eminently suited to the production of premium wines. Fortuitously, the state was going through a mineral boom at that time, and local investors with sufficient capital to cover the time required to develop vineyards and quality wines were both available and interested. This development also coincided with a considerable increase in demand from a variety of groups for consuming aspects of Margaret River's rural environment, including surfers, alternative lifestylers (hippies), retirees, second homeowners and 'electronic cottagers' (Gold 1991; McDonald-Lee 2016; Curry *et al.* 2001; Sanders 2005). All these groups were attracted by the natural assets of the Margaret River environment, such as the surf breaks, the scenic coastline and the (remaining) karri and jarrah forests, all of which facilitated a rapid growth in the area's tourism industry from the 1960s onwards.

Over the intervening decades this area—in contrast to many of the state's other rural areas—has experienced significant demographic and economic growth during which the combination of production, consumption and protection values has generated numerous synergies. The local production of premium wine has succeeded with many Margaret River wineries winning national awards and establishing a global reputation. They have also become tourist (and consumption) attractions offering cellar-door sales and, in many cases, dining facilities showcasing other local produce including lamb, seafood and organic and heritage vegetables. This has stimulated the local creation of a range of typically niche, agricultural enterprises supplying such products as venison and gourmet cheese.

Perhaps the most advantageous combination of production, consumption and protection is to be found in the aesthetics of the viticultural, agricultural and forested landscapes of the region, which remain an attraction for tourists, retirees, second homeowners and electronic cottagers alike. A section of the 'incomer' population that is perhaps more idiosyncratically West Australian are the

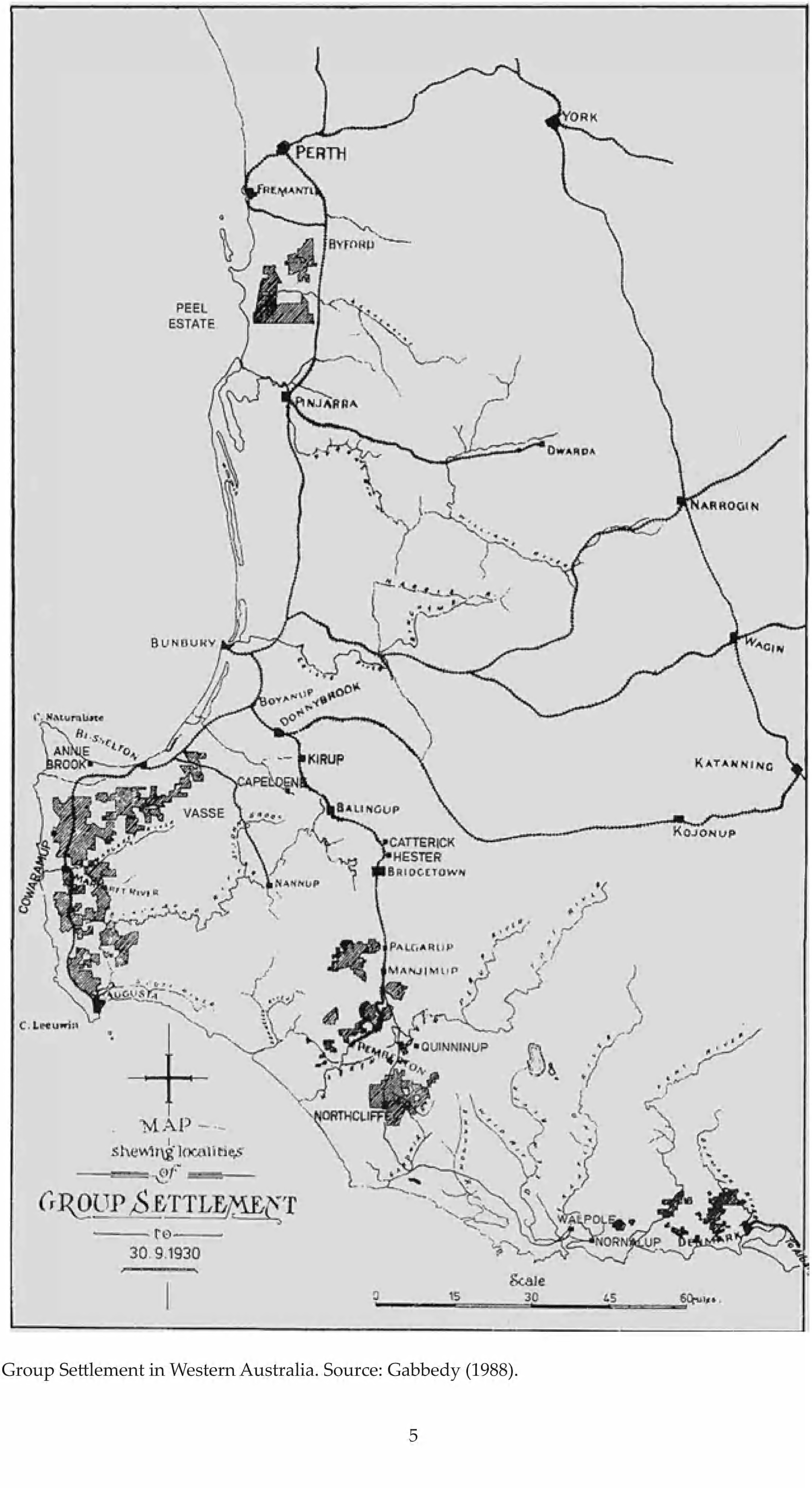

Figure 1. Group Settlement in Western Australia. Source: Gabbedy (1988).

FIFO (fly-in, fly-out) families whose wage earners live in scenic, temperate Margaret River but work in the mines of the state's North West. The protection and preservation of this landscape is therefore vital to those involved in production—the vignerons and other agriculturalists—and in consumption for tourism operations. Recent studies (Jones *et al.*) underline not only the high levels of environmental concern among large sections of the local business and wider communities but also an awareness of how relevant this concern is to the sustainability of the area's agricultural and tourism industries. Findings from surveys and focus groups (Jones *et al.* 2010) indicated that vignerons and tourism operators alike saw pursuing high environmental standards for their operations, and thereby achieving major environmental accreditations, as a valuable tool for attracting and maintaining future custom. For example, in 2012, Margaret River became the first place in Australia to join the global Transition Towns network.

The Margaret River region provides an example of the transition to rural multifunctionality in Western Australia. It is one that has been replicated to a greater or lesser degree in other climatically, scenically and/or locationally favoured areas of the state—that is, those benefiting from an 'amenity premium' (Argent *et al.* 2014). Inevitably, the colocation of proponents of these values in small but growing rural areas like Margaret River will lead to competition and even conflict. As long ago as the 1990s, an article on 'growing pains down south' (Amalfi 1994) referred to the Margaret River region as 'Cape Fear'. At the same time, the shire planning officer in the smaller and more remote settlement of Denmark was expressing concerns over his shire becoming 'like Margaret River' in terms of its population growth and development controversies (Selwood *et al.* 1996, p. 222), while Greive and Tonts (1996) referred to 'creative destruction' in Donnybrook, another South West country town. In all of these cases, both long-term and more recent residents raised concerns about what they saw as the negative impacts of further population and economic growth.

As Selwood *et al.* (1996, p. 223) observed, 'increasing numbers of residents, visitors and investors in coastal Australia are deeming a number of demographic trends, economic flows and physical developments good or bad by virtue of their different ways of seeing and thinking about these trends. The different ways in which these diverse groups react to such trends will pose an increasing number of problems for local planning systems.' Almost three decades on, these differences (of vision) and concerns (over local realities) remain. Hopefully, Margaret River will adapt to its multifunctional transition in a manner that is more sustainable than that which resulted from colonial dispossession almost two centuries ago. However, whether it be from economic necessity—such as the development of farm and station stays—or government regulation in the form of environmental restrictions, most rural areas in the state are now affected by the addition of at least some consumption and/or protection values to those of production as their residents, governments and investors plan for their futures.

CONCLUSION: REALITIES AND IDEALS IN SPACE AND TIME

The environmental realities of changing climatic, pedological and physiographic conditions over space have ensured that varied forms of occupancy have always characterised Western Australia's diverse rural and remote regions. Over time, the human realities of economic, technological, political and social changes have ensured that the rate and intensity of rural adaptation have increased significantly. This accelerating but simple trajectory of adaptation to the realities faced by Western Australia's population can be contrasted with the increasingly complex ideals possessed by these same inhabitants as a multifunctional rural transition progresses.

The first rural transition, from Indigenous to colonial occupancy, supplanted one set of ideals with another. In Holmes's terms, largely protectionist values were replaced by predominantly productivist ones through the often violent process of colonisation. In each period—before and after this transition—a single set of values or ideals was held, if not by the whole population, then at least by those controlling Western Australia's destinies. By contrast, the second transition came about through the replacement of a single set of ideals, or values, by a multiplicity of them. Whereas these ideals/values can be expressed as a simple triad of production, consumption and protection, this does not adequately describe how these values are actualised either on the ground or conceptually. Just as multiple values are manifested in place—for example by a vineyard with a cellar door, gourmet restaurant and waterwise irrigation system, or by a pastoral property offering station stays and ecotours—these values are also balanced and integrated by enterprise operators, land managers and politicians who oversee and regulate these places, and by the population of non-metropolitan Western Australia.

Ultimately, the future of agriculture and other rural land uses in Western Australia can be assured only if some of the ideals from its distant past, notably sustainability, are balanced against the economic, political and environmental realities of its complex present. In the United Kingdom, Cloke & Little (1997) have written of 'Contested Countryside Cultures' and of the marginalisation of certain rural groups. Rural Western Australia, from Noonkanbah (Hawke & Gallagher 1989) to Northcliffe (Crawford & Crawford 2003) via Ningaloo (Jones *et al.* 2007), has also experienced bitter disputes over values in the past and will likely continue to do so. Nevertheless, the contemporary, if not always harmonious, juxtaposition of such ideals and values in Margaret River, the site of one of the state's most spectacular agricultural failures, may offer some pointers to a more sustainable way forward.

ACKNOWLEDGEMENT

I thank Dr Graham Thompson of Curtin University and Dr Joseph Christensen of the University of Western Australia for their advice on earlier versions of this paper.

REFERENCES

Amalfi C 1994. Cape Fear: growing pains down south. *West Australian Big Weekend.* August 6.

Argent N, Tonts M, Jones R & Holmes J 2014. The Amenity Principle, Internal Migration and Rural Development in Australia. *Annals of the Association of American Geographers* **104**, 305–318.

Bednarik R 1997. Pleistocene stone pendant from Western Australia. *Australian Archaeology* **45**, 32–34.

Bolton G 1992. *Spoils and spoilers: a history of Australians shaping their environment* (second edition). Allen & Unwin, North Sydney.

Bolton G 1994. *A fine country to starve in.* (new edition). University of Western Australia Press, Nedlands.

Brayshay M & Selwood J 2002. Dreams, propaganda and harsh realities: landscapes of group settlement in the forest districts of Western Australia in the 1920s. *Landscape Research* **27**, 81–101.

Broome R, Fahey C, Gaynor A & Holmes K 2020. *Mallee country: land, people, history.* Monash University Publishing, Clayton, Vic.

Brunger A & Selwood J 1997. Settlement and land alienation in Western Australia: the Shire of Denmark. *Journal of Historical Geography* **23**, 478–495.

Burnley I & Murphy P 2004. *Sea change: movement from metropolitan to arcadian Australia.* UNSW Press, Sydney.

Cameron J 1981. *Ambition's fire: the agricultural colonization of pre-convict Western Australia.* University of Western Australia Press, Nedlands.

Clarkson C, Jacobs Z, Marwick B, Fullagar R, Wallis L, Smith M, Roberts R, Hayes E, Lowe K, Carah X, Florin A, McNeil J, Cox D, Arnold L, Hua Q, Huntley J, Beard H, Manne T, Faribarn A, Shulmeister J, Lyle L, Salinas M, Page M, Connell K, Park G, Norman K, Murphy T, & Pardoe C 2017. Human occupation of northern Australia by 65,000 years ago. *Nature* **547**, 306–310.

Cloke P & Little J (editors) 1997. *Contested countryside cultures: rurality and socio-cultural marginalisation.* Routledge, London and New York.

Colten C 2019. Adaptive transitions: the long-term perspective on humans in in changing coastal settings. *Geographical Review* **109**, 416–435.

Crawford P & Crawford I 2003. *Contested country: a history of the Northcliffe area of Western Australia.* University of Western Australia Press, Crawley.

Curry G, Koczberski G & Selwood J 2001. Cashing out, cashing in: rural change on the south coast of Western Australia. *Australian Geographer* **32**, 109–124.

Dortch J, Balme J, McDonald J, Morse K, O'Connor S & Veth P 2019. Settling the West: 50,000 years in a changing land. *Journal of the Royal Society of Western Australia* **102**, 30–44.

Flood Chavez D, Niewiadomski P & Jones T 2023. Interpath relations and the triggering of wine-tourism development. *Tourism Geographies* DOI: 10.1080/14616688.2023.2168041

Gabbedy J 1988. *Group settlement. Part 1: its origins, politics and administration.* University of Western Australia Press, Nedlands.

Gaynor A 2014. Shifting baselines or shifting currents? An environmental history of fish and fishing in the South West Capes region of Western Australia. Pages 231–250 *in* J Christensen and M Tull, editors, *Historical perspectives of fisheries exploitation in the Indo-Pacific.* Springer Science+Business Media, Dordrecht.

Gladstones J 1965. The climate and soils of Western Australia in relation to vine growing. *Journal of the Australian Institute of Agricultural Science* **31**, 275–288.

Glynn S 1975. *Government policy and agricultural development: a study of the role of government in the development of the Western Australian Wheat Belt 1900–1930.* University of Western Australia Press, Nedlands.

Gold J 1991. Fishing in muddy waters: communication media and the myth of the electronic cottage. Pages 327–341 *in* S Brunn & T Leinbach, editors, *Collapsing space and time: geographic aspects of communication and information*. Harper Collins, London.

Greive S & Tonts M 1996. Regulation, land development and the contested countryside: reflections on Bridgetown, Western Australia. *New Zealand Geographer* **52**, 18–23.

Hallam S 1975. *Fire and hearth: a study of Aboriginal usage and European usurpation in South-western Australia.* Australian Institute of Aboriginal Studies, Canberra.

Hallam S 1981. The first comers. Pages 35–71 *in* T Stannage, editor, *A New History of Western Australia.* University of Western Australia Press, Nedlands.

Hawke S & Gallagher M 1989. *Nookanbah, whose land, whose law.* Fremantle Arts Centre Press, Fremantle.

Holmes J 2006. Impulses towards a multifunctional rural transition: gaps in the research agenda. *Journal of Rural Studies* **22**, 140–160.

Jones R, Burke G & Stocker L 2023. Chapter 24: Climate change, tourism and rural sustainability in the Margaret River wine region of Western Australia. Pages 347–357 *in* M Koscak and T O'Rourke, editors, *Ethical and responsible tourism: managing sustainability in local tourism destinations* (second edition). Routledge, London and New York.

Jones R, Ingram C & Kingham A 2007. Waltzing the heritage icons: 'Swagmen', 'Squatters' and 'Troopers' at North West Cape and Ningaloo Reef. Pages 79–94 *in* R Jones & B Shaw, editors, *Geographies of Australian heritages: loving a sunburnt country?* Ashgate, Aldershot.

Jones R, Jones T & Ingram C 2022. Re-turning inwards or opening to the world? Land use transitions on Australia's western coast. *Geographical Review* **112**, 422–443.

Jones R, Wardell-Johnson A, Gibberd M, Pilgrim A, Wardell-Johnson G, Galbreath J, Bizjak S, Ward D, Benjamin K & Carlsen J 2010. *The impact of climate change on the Margaret River region: developing adaptation and response strategies for the tourism industry.* Sustainable Tourism Cooperative Research Centre, Gold Coast.

McDonald J 2020. Serpents Glen (*Karnatukul*): new histories for deep time attachment to Country in Australia's Western Desert. *Bulletin of the History of Archaeology*, **30**, 5. DOI: http://doi.org/10.5334/bha-624

McDonald-Lee T 2016. Three generations of surfing nomads. *YOUR RAC Magazine* June/July, 28–32.

Nannup N 2006. *Moondang-ak kaaradjiny: the carers of everything.* Batchelor Press, Batchelor NT.

Pascoe B 2018. *Dark Emu, Aboriginal Australia and the birth of agriculture* (second edition). Magabala Books, Broome.

Powell J 1974. Introduction. Pages 11–24 *in* J Powell, editor, *The making of rural Australia.* Sorrett Publishing, Melbourne.

Rundle G 1996. History of conservation reserves in the South West of Western Australia. *Journal of the Royal Society of Western Australia* **79**, 225–240.

Sanders D 2005. From colonial outpost to popular tourism destination: an historical geography of the Leeuwin – Naturaliste region 1929–2005. PhD thesis, Murdoch University.

Selwood J, Curry G & Jones R 1996. From the turnaround to the backlash: tourism and rural change in the Shire of Denmark, Western Australia. *Urban Policy and Research* **14**, 215–225.

Sutton P & Walshe K 2021. *Farmers or hunter-gatherers? The Dark Emu debate.* Melbourne University Publishing, Melbourne.

Tawney R 1964. *Religion and the rise of capitalism.* Penguin, Harmondsworth.

Tonts M 2002. State policy and the yeoman ideal: agricultural development in Western Australia 1890–1914. *Landscape Research* **27**, 103–115.

Tonts M & Horsley J 2019. Policy mobilities and settlement schemes: the emergence of homesteading in Western Australia. Pages 28–47 *in* R Jones and A Diniz, editors, *Twentieth Century Rural Settlement Schemes*. Routledge, London and New York.

Tonts M, Yarwood R & Jones R 2010. Global geographies of innovation diffusion: the case of the Australian cattle industry. *Geographical Journal* **176**, 90–104.

Turney C, Bird M, Fifield L, Roberts R, Smith M, Dortch C, Grun R, Lawson E, Ayliffe L, Miller G, Dortch J & Cresswell R 2001. Early human occupation at Devil's Lair, Southwestern Australia 50,000 years ago. *Quaternary Research*. **55**, 3–13.

Williams A, Ulm S, Sapienza T, Lewis S & Turney C 2018. Sea level change and demography during the last glacial termination and early Holocene across the Australian continent. *Quaternary Science Reviews* **182**, 144–154.

Journal of the Royal Society of Western Australia, 106: 9–21, 2023

Holocene beaches, bedforms and sediment dynamics of Geographe Bay, southwestern Australia

R DENNIS GEE

Busselton, Western Australia

✉ *dennis.gee@bigpond.com*

Abstract

Geographe Bay is a large near-symmetrical north-facing bay in southwest Australia, characterised by a continuous arcuate sandy beach extending over 50 km, and a wide microtidal shallow inner continental shelf devoid of significant currents. It displays shoreline features in dynamic equilibrium with present metocean conditions, superimposed on relict bed-forms dating from the end of the Last Glacial Maximum. Records of historic shorelines, in places going back to 1941, show that about 90% of the bay's beachline is accreting, whereas only about 10% is subject to natural erosion. Accretion is progressive, but not cyclic—estimates indicate the beach accumulates sand at about 100,000 m^3/yr. Total long-shore littoral sand fluxes on both western and eastern arms of the bay are about 42,000 m^3/yr, implying a remarkable addition of 142,000 m^3/yr to the system. It is unlikely that such a volume was generated by coastal erosion, rivers draining into the bay, or erosion of offshore sandbars and ridges.

Large, linear, stationary, sand ridges oriented at about 60° to the beachline are a distinctive bathymetric feature of Geographe Bay and extend to the 10 m isobath. These ridges are largely stabilized by seagrass meadows and are interpreted as relics from sometime in the last 7,000 years as their size, asymmetry and orientation are incompatible with present metocean conditions. They possibly formed due to intense high-pressure continental systems at the conclusion of the last Pleistocene glacial event after which a strong clockwise gyre may have operated in the bay. Small shore-attached sandbars, about 30° oblique to the beach, overprint the larger ridges to form a complex network bare of seagrass. Although locally reworked, they have been stationary for the past 80 years, and do not contribute to the sediment budget. The large Dunn Bay bars at the western end of the bay commenced building soon after sea-level recession from the Holocene highstand reached its present stillstand at about 3,770 yrs BP.

A field of small, northeastly ripples, between the 6 m and 9 m isobaths, are evident on LIDAR bathymetry as fine lineaments that bulge shoreward into the seaward limits of the larger bedforms. They relate to refracted Southern Ocean swells that pass around Cape Naturaliste but are not actively importing sediment into the bay. The sand influx probably comes from seaward of seagrass meadows at depths of 10–15 m on the inner continental shelf. There is an inexhaustible supply of sandy sediment on the now-inundated post-glacial plain, derived from erosion of the Cretaceous Leederville Formation during the protracted sea-level falls from much higher levels through the Cenozoic. At present, northwesterly winter storm waves feed sediment into the bay where it is dispersed by seasonal wind-generated waves. Southwesterly winter fronts and summer sea breezes drive the major dispersal of ~35,000 m^3/yr along the eastern arm of the bay, whereas a minor pathway of ~7,000 m^3/yr along the western arm is driven by easterly winds. Under this regime, coastal erosion is not a major threat to Geographe Bay.

Keywords: Geographe Bay, Holocene, sediment cells, beach accretion, oblique sand ridges, palaeorivers, sand budget, gyre, relict bedforms, palaeoclimate

Manuscript submitted 23 February 2023; accepted 3 May 2023

INTRODUCTION

Potential threats of erosion and inundation in Geographe Bay have been assessed as products of coastal processes (Shore Coastal 2018; Eliot 2013), mostly by engineering and research consultancies jointly commissioned by the City of Busselton and the Western Australia Department of Transport (DoT). Their focus has been on localized erosion, loss of amenity and infrastructure protection, rather than a quantitative, whole-of-bay, sediment-budget approach that takes the geological evolution of the bay into account. Previous studies demonstrated quantifiable sediment transport by littoral drift relating to seasonal winds, but also invoked migration of the offshore sandbars. These studies underpin many proposals in coastal hazard risk management and adaptation plans (City of Busselton 2022).

Coastal engineering investigations have identified two leading features in Geographe Bay. Firstly, significant beach accretion for which Damara (2011) provided a qualitative estimate with no explanation of the source of the sediment nor a discussion of the implications of this phenomenon. Secondly, the origin of the atypical shore-oblique sandbars is poorly understood, as pointed out by Pattiaratchi *et al.* (2017).

There is a general perception that historic records show cycles of accretion and erosion influenced by sediment fed from migrating offshore sandbars (Damara 2011; Shore Coastal 2018). However, neither the historic records nor the seabed forms in the bay substantiate this claim. Importantly, many of the coastal and seabed features are incompatible with current meteorological and oceanic (metocean) conditions. Moreover, no definite quantitative sediment budget has been developed despite the abundance of historic beachline data dating back 80 years and available on the Shared Location Information Platform (SLIP) website maintained by DoT. (https://maps.slip.wa.gov.au/Marine/app/).

The consultant reports referenced here are in the open domain and provide valuable background information on present-day metocean parameters and some commentary on sediment dynamics. Most studies attempt to link observed shoreline and seabed features with present-day coastal parameters, sometimes with numerical models. This can yield inconclusive interpretations for sediment sources, pathways and sinks. Coastal engineering studies have mostly overlooked geological processes and palaeoclimates that have shaped the beaches and seabed forms we see today. This imposes constraints on previous sediment-dynamic models and the effectiveness of proposed geo-engineered remedial actions.

Recently Bufarale *et al.* (2019) presented a realistic geological framework as a basis for interpreting bathymetric features in Geographe Bay. However, their study did not explain the significance of some seabed features, or the sediment dynamics in terms of sources, sinks and pathways. This paper reinterprets some of the bedforms of the bay, and provides a model for sediment dynamics, in terms of sources, sinks and processes throughout the Holocene.

GEOLOGICAL EVOLUTION OF GEOGRAPHE BAY

Geographe Bay is a broad, shallow, northwest-facing sand-enriched bay formed over the last 40 million years by marine erosion of poorly consolidated sedimentary rocks of the Perth Basin, which is flanked by hard metamorphic rocks of the Naturaliste Ridge to the west and granitic rocks of the Yilgarn Craton to the east. The hinterland is characterised by a series of ancestral coastal plains and scarps carved into the 150 m-thick Lower Cretaceous Leederville Formation, which postdates the break-up unconformity created by the separation of India from Australia (Thomas 2018; Gee 2022).

Cenozoic Evolution

The J-shape of the bay evolved by marine erosion during a protracted but episodic fall in sea level from the highstand at about 90–110 m above sea level (ASL) of the Eocene Climatic Optimum, through the glacio-eustatic sea-level oscillations of the Pleistocene to the present (Gee 2022). Episodic sea-level falls formed a progressive series of concentric strand lines that mimic the present-day outline of the bay (Fig. 1). Onshore erosion extended through the late Eocene and Miocene, when the Leederville Formation was eroded locally to form the Whicher Scarp. This process moved a large volume of sand onto the continental shelf offshore from Geographe Bay.

The Ambergate Plain at the foot of the Whicher Scarp is a marine-cut platform with a veneer of paralic strand-line sand and estuarine mud, formed during the Pliocene marine regression (Gee 2022). The plain slopes gently seaward from 41 m ASL at the toe of the Whicher Scarp to the marine-cut Cemetery Scarp at 9–21 m ASL at the seaward edge of the Ambergate Plain. The scarp corresponds to one or more of the Pleistocene Marine Isotope Stage (MIS) highstands such as MIS 5e, MIS 7 or even MIS 9. Its formation corresponds to the end of lateritisation in the Cenozoic warm periods, and the end of substantial hinterland erosion, as well as the beginning of the geologically benign processes that prevail today.

Seaward of Cemetery Scarp is the near-coastal Ludlow Plain, at 3–5 m ASL, which is underlain by a 6 m-thick sheet of shelly coralline Tamala-type calcarenite. This unit was deposited against the Cemetery Scarp and a marine erosional surface cut into the Leederville Formation at 1 to 3 m below sea level. Correlation with similar deposits in the southwest suggests the coralline calcarenite accumulated during MIS 5e at 124 ka BP (McCulloch & Mortimer 2008). The seaward edge of the Ludlow Plain at 2–3m ASL records the Holocene highstand at about 7 ka BP.

Water bores and geotechnical probes near the present shoreline indicate the base of the Pleistocene and Holocene deposits is erosional on the Leederville Formation or the overlying Osborne Formation. Subsurface data also suggests erosion of the now buried calcarenite segmented this unit to form discrete bars parallel to the present coast. Bufarale *et al.* (2019) demonstrate similar calcarenite segments or 'ridges' in water depths of <10 and ~20 m.

The seabed of Geographe Bay shelves gently northwest for 75 km across the continental shelf to the continental slope, which starts at around 170 m below present sea level. Bufarale *et al.* (2019) investigated the nearshore seabed and substrate of the bay using acoustic seismic profiling, augmented by seabed sampling. Their study identified a thin unconsolidated Holocene mixed carbonate-silicate sediment, and an 'acoustic basement' around 15 m below the seabed, postulated to be Leederville Formation, but which also could include younger strata.

Rivers from the hinterland, principally the Carbunup, Vasse, Sabina, Abba and Capel rivers (Fig. 1), developed soon after formation of the Whicher Scarp in the Eocene-Miocene (Gee 2022). Stranded alluvial fans at the foot of the Whicher Scarp, and micro-deltas where the rivers (especially Sabina River) debouch onto the coastal wetlands behind the present beach dunes, demonstrate a progressive decline in sediment load to a now insignificant volume.

The nature of the substrate near the shore in the bay is unclear as there has been no drilling. In a review of the Southern Perth Basin, Thomas (2017, plate 6), used exploration seismic-reflection data to infer a post break-up sedimentary section at least 200 m thick about 5 km

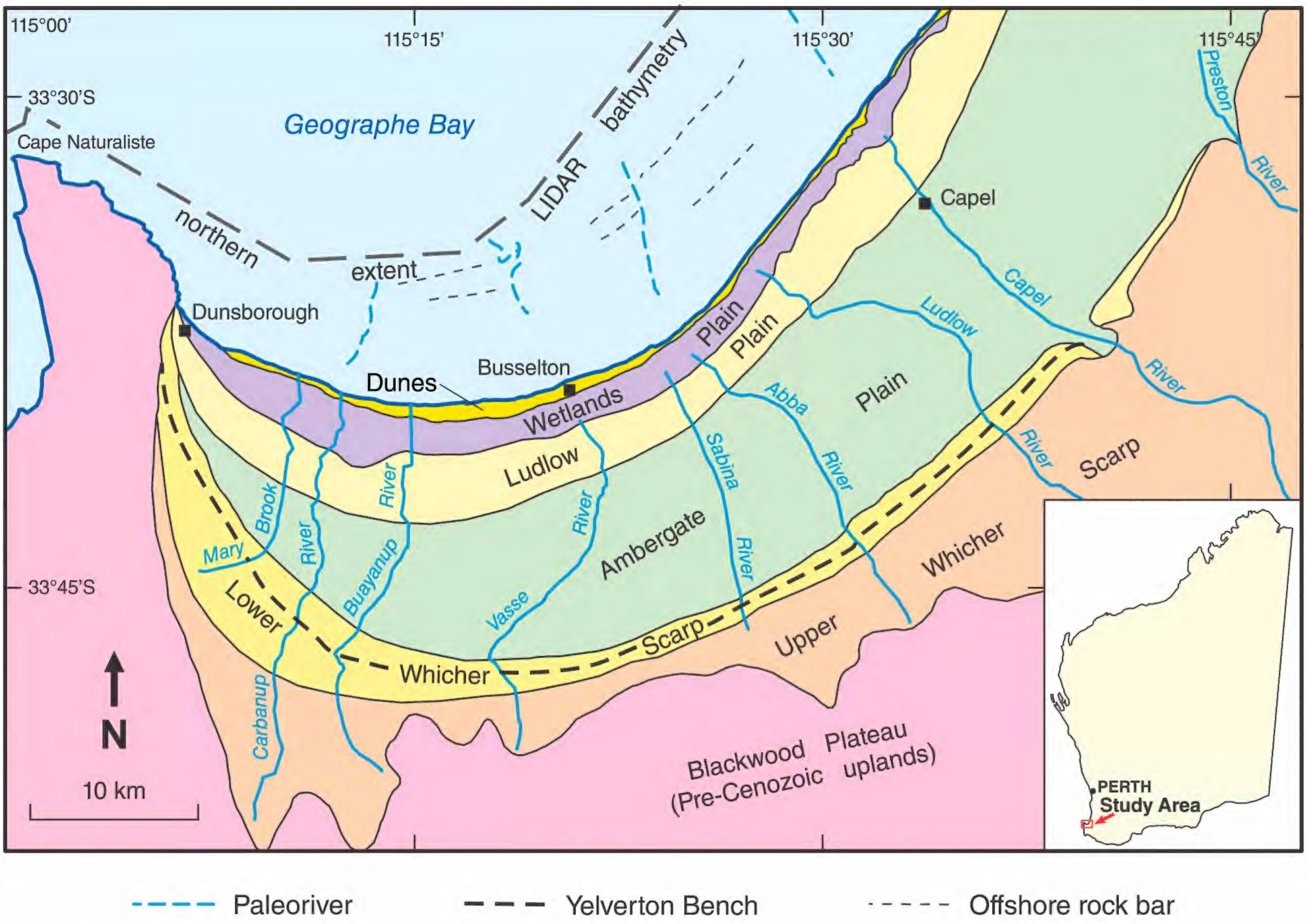

Figure 1. Onshore geomorphic elements (after Gee 2022) of Geographe Bay, showing the extent of LIDAR bathymetric coverage, offshore palaeo-shorelines and palaeorivers.

offshore, thickening considerably to the northwest. This section could include Leederville Formation and offshore facies of the overlying Upper Cretaceous Coolyena Group, such as Osborne Formation, together with a large amount of sand eroded from onshore sections of the Leederville Formation during the Eocene–Miocene evolution of the Whicher Scarp.

Pleistocene–Holocene Evolution

Sea level changes during Pleistocene glacial–interglacial events were important in the development of shoreline and seabed features of the bay. Coastal aeolianite deposits and now-drowned shorelines provide records of these events along much of the western coast of the State (Brooke *et al*. 2014) but not in and around Geographe Bay because of the long-standing protection provided by the Naturaliste Ridge.

At about 17,000 years BP, global sea levels were approximately 130 m below their present level (Miller *et al*. 2020) thereby exposing the present continental shelf for about 75 km northwestward of Busselton. At that time a cool arid plain formed, on which veneers of stranded beach sands, shell and coral debris, wind-blown dunes, alluvial channels and sheetwash material presumably accumulated. Based on the sea-level curve of Twiggs & Collins (2010) for the Abrolhos coast, 700 km to the north of Geographe Bay, the marine transgression prior to the present interglacial passed the present position of the coast at 7,500 yr BP, and reached the Holocene highstand 2–3 m above present sea level at 7,000 yr BP. Since then, the sea level has slowly receded to its present position.

The entire beach around the bay is backed by twin-ridge aeolian dunes (Quindalup Dunes; McArthur & Bettenay 1960), which have a low profile at the head of the bay and progressively increase in size to the east (Gee 2022). The landward dune first developed at about 6,580 yr BP as the sea level fell from the Holocene highstand to the present, and the seaward foredune developed on a layer of seagrass with a carbon age of about 3,770 yr BP (Hamilton & Collins 1997). These dunes are largely built by wind-blown sand from the beaches, a process that continues today.

METOCEAN CONDITIONS OF GEOGRAPHE BAY

The seabed of Geographe Bay gently slopes to the northwest with a gradient of 1:275 between the coast and the 30 m isobath, which is the effective wave base for sediment disturbance on the inner shelf during storms. The bay is subject to diurnal tides with an average range of 0.5 m, and lowest to highest astronomical tides of 1.2 m (Fahrner & Pattiaratchi 1994). This is at the lower end a micro-tide classification (<2 m). As such, tidal currents play no significant part in sediment movement within the bay.

The Leeuwin Current (Smith *et al*. 1991; Pattiaratchi & Woo 2009) flows southwards near the 200 m isobath, on the upper continental slope, well to the west of the coast and does not enter the bay. Neither does the counter Capes Current (Pearce & Pattiarachi 1999), near the 50 m isobath, although it has the potential to augment any current exiting the bay via the Naturaliste headland.

In summer, the bay is subject to prevailing easterly winds, associated with high-pressure systems generated within the Great Australian Bight, and to southwesterly sea breezes. In winter, strong winds of storm intensity blow from the north-west quadrant, during the passage of low-pressure systems (Fahrner & Pattiaratchi 1994); however, these winds are insufficient to establish wind-shear currents within the bay.

Seasonal winds can generate nearshore currents capable of moving sand in shallow waters. Thus Gallop *et al*. (2010) and Gallop *et al.* (2012) note sea breeze induced currents of 0.3 – 0.7 m/sec restricted to the top 5 m of the water column. Such currents are insignificant in terms of sediment movements discussed in this paper. Sand movement in the bay is principally by wind-driven waves that impinge obliquely onto the beach face (Farhner & Pattiaratchi 1994) and thereby generate long-shore drift in the surf and swash zones immediately adjacent to the beaches.

SEABED FEATURES

LIDAR bathymetry reveals several seabed features that do not relate to present metocean conditions. These are described below in order of oldest to youngest, as deduced from interactive and superpositional relationships.

Palaeo-shorelines

Low-relief ridges around the 20–28 m isobaths, with arcuate geometries that mimic the current shoreline (Fig. 1), are interpreted as cemented Tamala-type calcarenite. They probably represent palaeo-shorelines formed during still stands related to various sub-stages of MIS 5, coinciding with the marine regression that led into the Last Glacial Maximum (Bufarale *et al.* 2019).

Submarine Palaeochannels

Low-relief palaeochannels on the seafloor extend west to at least the 28 m isobath (Eliot 2015). These align with the seaward extensions of the present-day Carbunup, Vasse and Capel rivers prior to their deflection by Holocene beach dunes (Fig. 1). They represent river channels that flowed across a wind plain during the Last Glacial Maximum. Modern sediment infill in the nearshore zone obscures parts of the palaeochannels (Bufarale *et al.* 2019).

Large oblique offshore sand ridges

Large linear sand ridges oblique to the shoreline are a characteristic feature of Geographe Bay (Fig. 2). On LIDAR bathymetric imagery, they extend as much as 6 km to water depths of 12 m, where they gradually diminish. The ridges have wavelengths of 1 to 1.5 km, and amplitudes of up to 5 m. Their axes trend WNW–ESE along the eastern arm of the bay, swinging to NNW–SSE in the western arm, thereby maintaining a constant 50° obliquity to the shore. LIDAR bathymetry indicates steeper side to the south, which implies growth by southward migration. Seemingly, the sand ridges formed from clockwise currents along the coast. However, the large sand ridges are now stationary. Geo-referenced ortho-rectified aerial photo mosaics (provided by DoT), dating back to 1959, show no lateral movement in the ridge axes and that current nearshore processes only disturb their nearshore tips.

Large sand ridges are out of place in the present microtidal, minimal-current coastal environment of Geographe Bay. Elsewhere in the world, strong tidal currents form similar large linear or curvilinear sand ridges, typically on inner-shelf platforms at depths of 20–40 m (Dronkers 2016). Their origin in Geographe Bay is enigmatic. Possibly, they formed by active bottom currents, seemingly initiated under surface currents associated with marine transgression after the Last Glacial Maximum and then re-shaped by bottom currents, in a similar manner to ridges on the Spitzbergen Shelf of the Barents Sea (Bellec *et al*. 2019). Off the Atlantic coast of the USA large oblique sand ridges formed as parallel offshore ridges during lower sea levels and grew shoreward at their down-current tips in response to southwest-directed storm currents during rising sea levels (Swift & Field 1981; Trowbridge 1995; Garnier 2006; Nnaffie 2014). The ridges exhibit landward-flank erosion where the current deviates seaward, allowing seaward-flank deposition when the current turns landward. The resulting toroidal current causes landward migration of the down-current tip, leaving an up-current trailing moribund ridge. Numerical modelling requires constant nearshore wave stirring and strong longshore currents of about 0.8 m/sec (Nnafie 2014). This process may have acted in Geographe Bay on the smaller, shore-attached oblique sandbars, in the nearshore zone, but is unlikely to apply to the large oblique ridges.

In terms of seabed morphology, the most likely analogue is the oblique linear sand ridges off the KwaZulu coast of South Africa, which are related to the southwest-directed Agulhas geostrophic current (Green *et al*. 2022). These ridges splay seaward off the coast, are asymmetric, possess internal cross-stratification, have rounded crests, and display evidence of down-current-over-riding of smaller bars by larger ones. Ridges migrate down current and grow in height due to amalgamation of smaller ridges. In Geographe Bay a constant supply of locally available sediment is needed to build such large ridges, so they possibly developed soon after the retreat from the Holocene highstand during a climatic phase dominated by strong northerly or north-northeasterly winds.

Small nearshore oblique sandbars

Pattiaratchi *et al*. (2017) have drawn attention to enigmatic nearshore, apparently shore-attached oblique sandbars between Busselton Jetty and Port Geographe. In contrast to the large ridges described above, these bars are restricted to the eastern arm of the bay, where they extend no more than 1.5 km seaward, are 200–400 m apart, have irregular wavelengths, amplitudes of 3–4 m and no seagrass. They lie at 30° to the beachline and swing gently

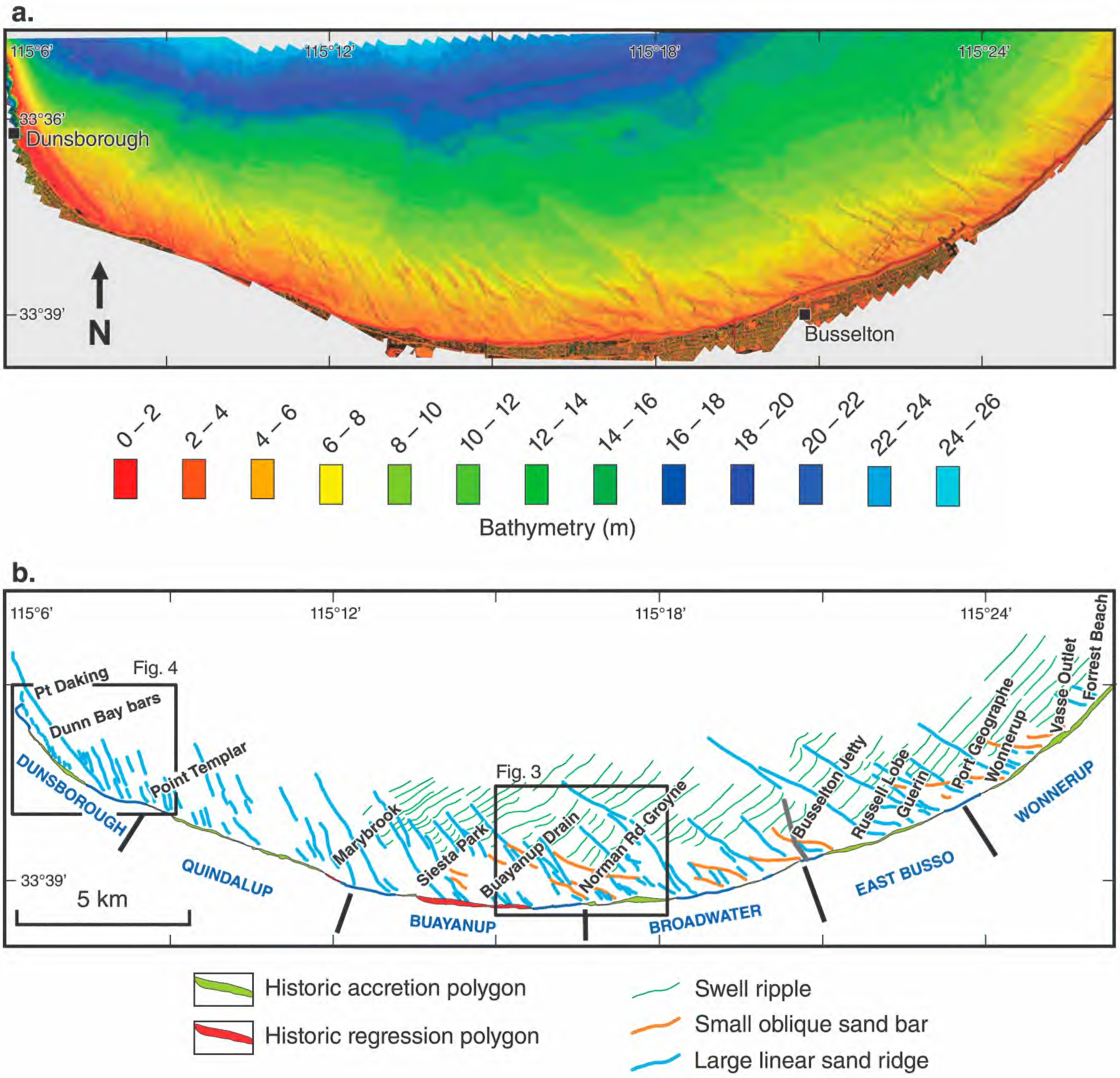

Figure 2. **a)** LIDAR image of area of study; **b)** Main morpho-dynamic seabed features of Geographe Bay; large linear sand ridges, (pink), small shore-attached oblique sandbars (orange), seafloor swell ripples (green), accretion polygons (green) and regression (red), showing beach sectors and localities mentioned in text, and the location of Figures 3 and 4.

with the curvature of the eastern arm of the bay. Thus, they point northeasterly in the direction of the littoral drift. Sense of asymmetry is equivocal, and difficult to determine from the bathymetry. Seismic profiles (Bufarale *et al*. 2019) suggest some may have northward asymmetry. Although they closely approach the shore, there is invariably a runnel between their nearshore tip and the shore. They overprint and modify the shoreward tips of the large linear ridges to form a complex interlaced network of bedforms (Figs 2b, 3). LIDAR bathymetry shows no evidence of lunate scours, or shore-parallel sandbars, reported by Searle & Logan (1978) and Riedel & Byrne Ltd (1989). Such supposed scours are better interpreted as part of a complex network of ridges and bars of different generations.

Historical aerial photographs and satellite imagery (dating back to 1941 and 1984, respectively) indicate no measurable change in the overall position of the sandbars although there is evidence that their shoreward tips have grown slightly. Thus, Rogers (2015, fig. 3.6) shows the immediate shoreward tip of a bar at Broadwater has grown down-current and turned shoreward in response to the development of a 1 km-long regression pocket following the construction of the Holgate groyne in 1999. Importantly, in Rogers (2015), the same figure shows no measurable movement on this specific sandbar. Thus, his often-quoted metric of down-current migration at 8.5 m/yr cannot be used to assert that these small oblique sandbars are still active.

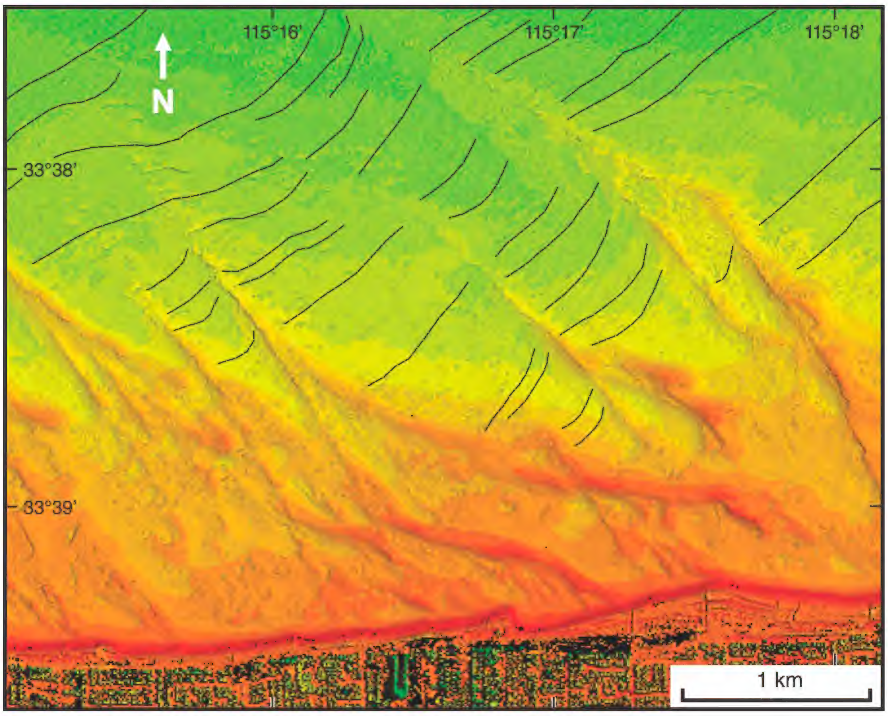

Figure 3. Bathymetric detail of small oblique sandbars superimposed on older sand ridges at boundary of eroding Buayanup (left) and accreting Broadwater (right) sectors at head of the bay. Note the asymmetry of linear ridges, and swell ripples (black) pushing shoreward between ridges. Location shown on Figure 2.

The toroidal dynamic model proposed by Trowbridge (1995) and numerically modelled by Garnier *et al*. (2006), may well apply to the modifications on the shoreward tips of the sandbars, but not to their original construction. Such small apparent shore-attached oblique sandbars in the bay appear to be inactive and not substantially eroding.

Seafloor swell ripples

An area of seabed ripples forms an arcuate field extending from the Carbunup palaeochannel, eastward to the Wonnerup palaeochannel (Fig. 2b and 3). The field is constrained between the 9 m and 6 m isobaths where it interacts with the nearshore sandbars. These features are evident as fine striations with spacing of 30–50 m, and amplitude of about 1 m on LIDAR bathymetry images. Shoreward, they refract at the leading tips of the large linear sand ridges (described above), and bulge into the swales between the ridges (Fig. 3). The general orientation of the axes and the restriction to a specific depth zone indicate these are oscillatory ripples related to refracted Southern Ocean swells as they pass around Cape Naturaliste and turn into Geographe Bay. Whereas Searle & Logan (1978), and several subsequent authors, propose this mechanism for the formation of sandbars in Geographe Bay, it is more likely that the sandbars and ridges are pre-existing features bearing no relationship to the theoretical or observational orientation of the swell-generated seafloor ripples.

Dunn Bay Sandbars

The most striking feature of the far-western part of Geographe Bay is the large composite sandbar in Dunn Bay (Fig. 2b and 4). Damara (2011) noted this is different to the other sandbars within the bay but provided no explanation of its origin. The bar contains two adjacent bare sandbars, separated by a 6 m deep swale covered by seagrass. Together they extend for over 4.6 km and are 0.7 km across. They shoal at low tide where they lie in waters of 6 m or shallower.

The outer bar is narrow and asymmetrical with a shallow seaward face and a steep landward face, implying the bar was built from the northeast. The seaward face possesses small lunate ripples, probably due to present-day storm currents. The inner bar is 'locked' within the curvature of Dunn Bay. It is broader and more irregular in shape, and its surface takes the form of a series of small, en echelon, curvilinear, nearshore oblique sandbars similar to those farther east. Offshore sandstone bars at Quindalup, just to the east of Dunn Bay, are probably composed of the Leederville Formation (Justin Parker, pers comm. 2020). Thus, the NW–SE banding, marked in Figure 4, is probably a sandstone pavement of that formation.

The Dunn Bay bars cover 2.5 km^2. Considering the bar and swale profiles, the average thickness is conservatively estimated at 5 m, giving a volume of over 12 million m^3 of sand in 'storage'. Although the oldest aerial photos for this area only go back to 1975 and cover only the southeastern half of the Dunn Bay bars, they are sufficient to show that the outer bar did not have measurable movement in the past four to five decades, either longitudinally or transversely. In contrast, the inner bar has moved seaward by over 100 m, along with an equivalent amount of beach accretion behind it, partially closing the swale.

Beach morphology

Geographe Bay possesses a typical wave-dominated, low-angle sandy beach with an average width of 40 m, as measured between mean sea level and the vegetation line at the base of the foredune system. It is dominantly

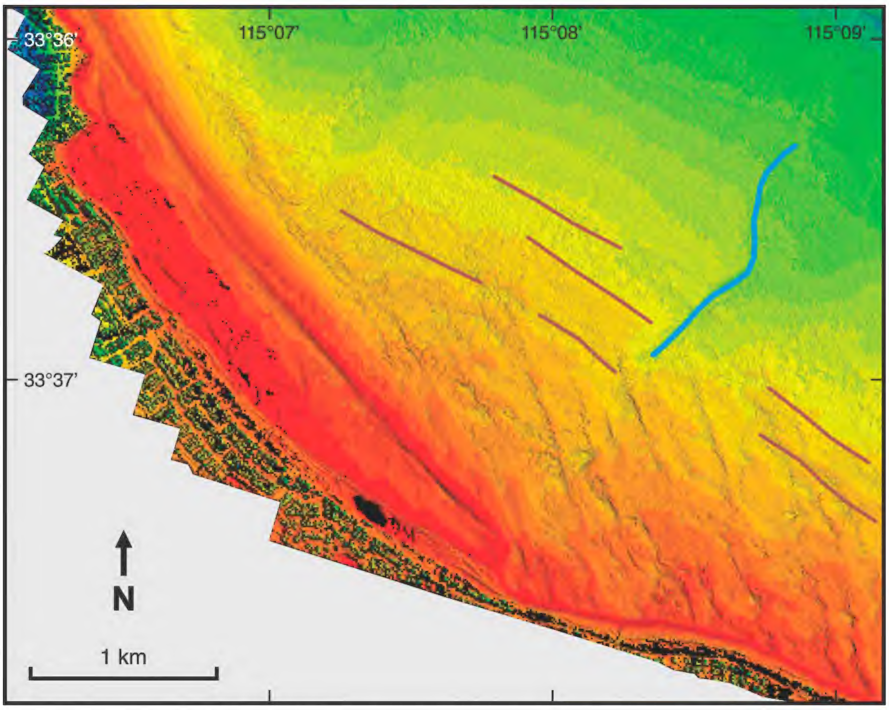

Figure 4. Detail of relict Dunn Bay sandbars at western end of Geographe Bay, showing stacking of relict sand ridges against bar; northwesterly features, interpreted to be Leederville Formation rock bars (brown), are cut by palaeochannel. Location shown on Figure 2.

composed of fine-grained spherical quartz grains, with lesser contribution from biogenic carbonate grains.

The beachline is characterised by lobes that bulge seaward for about 100 m from the adjacent smoothly scalloped embayments, with wavelengths of about 5 km (Fig. 6d). In this respect, they are not the common rhythmic cusps of wave-dominated beaches, nor do they relate to any natural or artificial hard feature. The spatial relationship between the lobes and the shoreward projection of the larger oblique offshore sand ridges points to the lobes accreting where they are protected from wave action by offshore sandbars, whereas the embayments are less protected. Wider tracts of beach, particularly the areas behind the lobes, have a wide berm (the flat surface above the beach face), which displays incipient lines of foredunes, indicative of an overall beach accretion. Thus, the position of the offshore bars and ridges determines that of the lobes, not the reverse.

HISTORIC BEACH CHANGES OF GEOGRAPHE BAY

The Coastal Infrastructure Section of DoT provides data that enables the tracking of coastal movement by way of a series of ortho-rectified aerial photos for the years: 1941, 1964, 1965, 1974, 1975, 1980, 1982, 1985, 1986, 1993, 1996, 2009, 2014, 2016. Some of this imagery is available via the Shared Location Information Platform. From these data the following lines of various ages have been extracted into MapInfo GIS:

- Vegetation line - essentially marking the back of the beach berm.
- Australian Height Datum (AHD) 0 m line – mean sea level for all years, except 1941.
- Natural water line – water line at time of photograph.

Historic changes in beach aspect were analysed using the concept of sediment cells, i.e. spatially discrete areas of the coast within which marine and terrestrial landforms are likely to be connected through processes of sediment exchange (Stul *et al.* 2012). These processes require sediment supply (source), sediment loss (sink), and linking transport pathways, which can include both along-shore and cross-shore processes. Cells provide the framework for a sediment budget.

The usefulness of sediments cells is somewhat limited as they do not account for long-term changes in sediment behaviour related to palaeoclimate, effects of which are evident in Geographe Bay. Nevertheless, they provide a convenient framework for analysis and description. Accordingly, the bay was analyzed along six shoreline sectors (Fig. 2b), which correspond closely to the tertiary sediment cells of Gozzard (2011). To provide relevance to local issues relating to Port Geographe, his Busselton to Wonnerup Cell is divided into two sectors. From west to east the cells are:

1. **Dunsborough** – Point Darkling (rocky headland) to Point Templar.
2. **Quindalup** – Templar lobe to Marybrook (Carbunup River Drain).
3. **Buayanup** – Marybrook to Norman Road groyne.
4. **Broadwater** – Norman Road groyne to Busselton Jetty.
5. **East Busso** Busselton Jetty to Port Geographe.
6. **Wonnerup** – Port Geographe to Forrest Beach.

Historical beach areas

Historical changes in beach areas, defined as lying between the edge of vegetation and the 0 m AHD datum, were examined from images spanning 51 years. The oldest dataset is for 1965, which can be compared directly with equivalent imagery for 2016. Whereas there is a 1941 vegetation line, there is no AHD for 1941. Although a 1941 waterline is mappable from the aerial photos, the tide elevation at the time of their acquisition is unknown. The respective beach boundaries for 1965 and 2016 were digitized across the six sectors, from Point Darkling in the west, to the northern extent of the Wonnerup lagoons, 10 km north of the Vasse River outlet.

No significant change in beach area is evident for the last 51 years. The small reduction in the Dunsborough sector (0.07 km^2; Table 1) is due to installed revetments, seawalls and boat ramps, plus accelerated dune rehabilitation. This preservation indicates the beaches are in dynamic equilibrium with the current geomorphic and metocean elements. Such equilibrium does not imply that beaches are stationary—they have moved significantly in most areas.

Beach accretion

Beach movement is analysed by comparing 1941 vegetation lines (from the earliest available rectified aerial photographs) and 2018 vegetation lines (from Google Earth) in the complete arc from Point Daking to Wonnerup Lagoons (Fig. 2b). Where the 2018 vegetation line is seaward of the 1941 line there has been accretion, and where landward of the 1941 line, there has been regression/erosion.

The two timelines mostly track together and sinuously interweave. Their interconnection defines the deviation polygons shown in Figure 2b. The green polygons indicate accretion and the red polygons regression. Polygons smaller than 20 × 400 m are considered insignificant and therefore not displayed in Fig. 2b).

The greatest accretion is in the east, notably along the Broadwater, East Busso and Wonnerup sectors, which total 863,360 m^2. There is also substantial accretion in the Dunsborough and Quindalup sectors in the west, totaling 388,070 m^2. The only significant regression is within Buayanup sector east of Siesta Park groyne where the main polygon indicates the loss of 350,600 m^2. The estimate for net accretion across Geographe Bay over 77 years is 866,210 m^2 (Table 2). In detail, the largest accretion is in lobes of new sand, but significant accretion is also evident on the intervening scalloped embayments. Lobes show growth lines marked by incipient vegetation, which become the next generation of foredunes along the coast.

Table 2. Mass accretions and losses Geographe Bay Beaches in 77 years. Note: GIS derived values are not rounded, stated precision not implied.

	m^3	Thickness	m^3	m^3/year
Western sectors	388,070	6.5	2,522,455	32,759
Buayanup central	-350,600	3.5	-1,227,100	-15,936
Eastern sectors	863,360	7.5	6,475,200	84,094
Net Totals	866,210		7,544,517	100,096

The accretionary lobes and beach berms in the eastern sectors reach 3.5 m ASL, and are assumed (Damara 2011) to lie on a 4-m thick mobile substrate, giving an accretionary prism 7.5 m thick (volumes estimates in Table 2). For the western sectors, a marginally thinner prism seemingly reflects lower energy accretion. The eroded prism at Buayanup is assumed to be similarly thin, or thinner. Net sand accumulation for Geographe Bay is about 7,545,000 m^3 over 77 years, implying a net annual addition of around 100,000 m^3 (Table 2). This accords with the estimate by Damara (2011) using a non-polygonal method.

Rates of Accretion

Linear measures of seaward accretion for representative sections (Table 3) include the Buayanup regression polygon for reference. Growth curves (Fig. 5) show accretion is progressive, quasi-linear, with no evidence of cyclic accretion and regression. Cyclone Alby in 1978 left ephemeral dips in the Guerin and Russell sections. Small sections of artificial recession related to engineered structures are not included in this analysis. An example is a small pocket of starvation immediately east of Port Geographe revetment in an otherwise accreting coast. The shoreline in this pocket is still seaward of the 1941 position.

Table 3. Seaward movement of accretionary lobes

Sector	Feature	Distance m
Dunnsborough	Dunnn Bay Beach	120
Quindalup	Templar Point lobe	72
Buayanup	**Siesta Park regression**	**-150**
Broadwater	Maryilla lobe	120
East Busso	Russell St lobe	82
Wonnerup	Baudin lobe	107
	Vasse River lobe	170

Table 1. Comparison of beach areas (in m^2) between 1965 and 2016.

Sector	From	To	1965 Beach Area M^2	2016 Beach area M^2
Dunsborough	Point Daking	Pt Templar	116,100	185,600
Quindalup	Pt Templar	Marybrook	224,100	221,000
Buayanup	Marybrook	Norman Rd groyne	215,840	171,330
Broadwater	Norman Rd groyne	Busselton Jetty	357,760	270,350
East Busso	Busselton Jetty	Port Geographe	157,800	235,100
Wonnerup	Port Geographe	Wonnerup Lagoons	245,890	163,850
Totals (m^2)			**1,317,490**	**1,247,230**

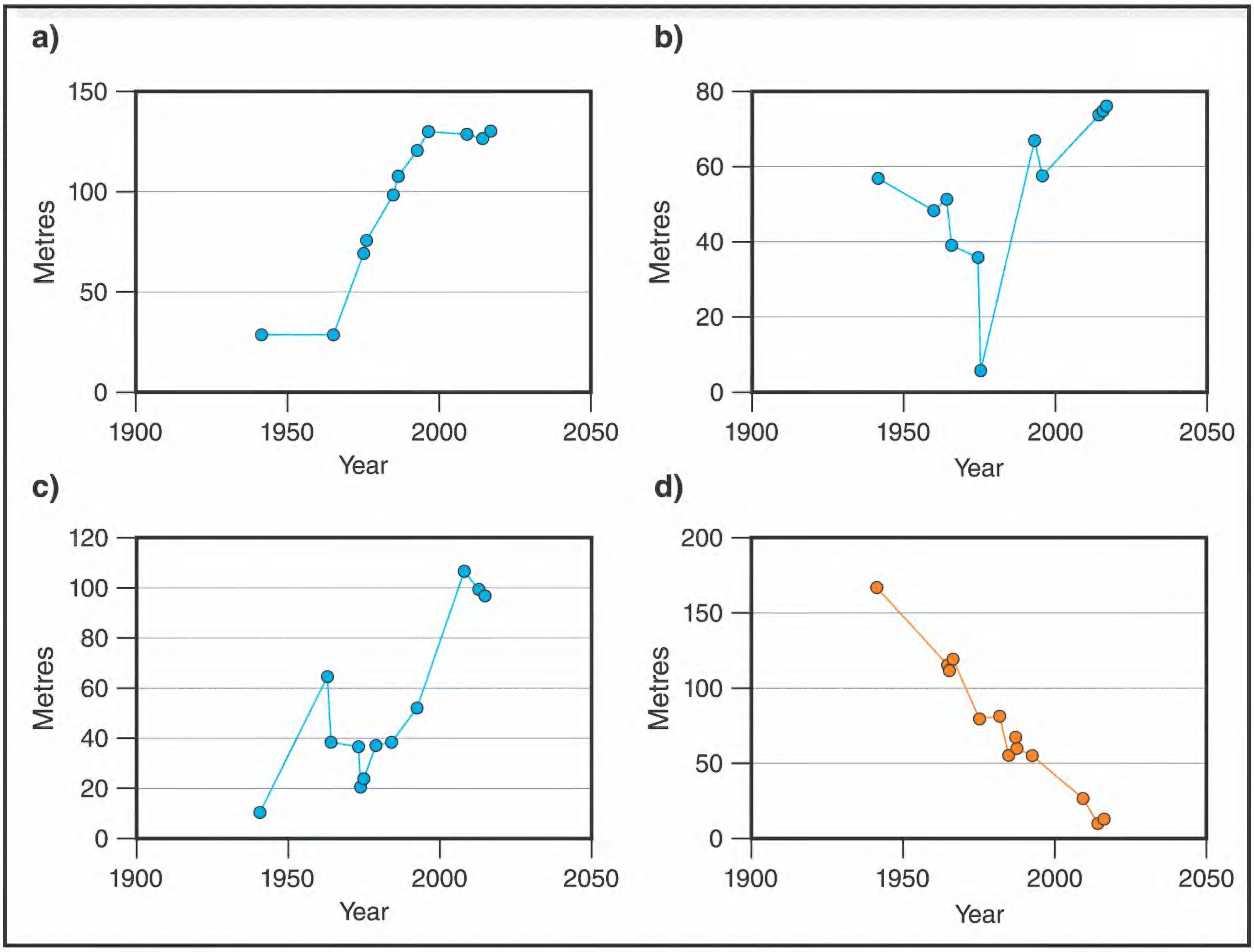

Figure 5. Time series graphs of historic vegetated beachlines extracted from the SLIP Website, showing rates of progressive accretion at representative sites: **a)** Wonnerup at Vasse River outlet; **b)** Guerin Street; **c)** Russell Street lobe; and **d)** Buayanup.

Buayanup regression

The Buayanup sector contains the only natural regression polygon along the entire bay. It covers 350,600 m^2 along 3.3 km, and records a landward retreat of 150 m since 1941. Although this erosion is locally significant, it has only made a minor contribution to the sediment budget (Table 2). The regression polygon starts at the 130 m-long Siesta Park groyne, which was installed in 1960, ostensibly to prevent erosion. West of the groyne an accretion wedge contributes to localized sediment starvation immediately down-drift of the groyne. The Buayanup recession curve (Fig. 5d), 1 km east of the groyne, shows a remarkable linear regression of 1.8 m/yr, and presumably is ongoing.

A popular belief is that the Siesta groyne is responsible for erosion. This can only apply to the small pocket against the groyne, but not the regression polygon. Erosion at this location is likely related to present metocean conditions. Offshore bathymetric features (Fig. 3) are no different in this sector to any other part of the bay. Damara (2011) observed that this sector, being at the head of the bay, receives full frontal amplification of northwesterly storms. Regression in this part of the bay is a natural part of its progressive evolution.

LITTORAL DRIFT IN GEOGRAPHE BAY

Wind-driven waves provide the principal mechanism of sand movement around the bay. Individual grains move obliquely up the beach face by obliquely impinging waves, and rill orthogonally down the beach face. Thus, sand migrates down-wind. Littoral drift adds no sediment to the total system and may lose material if blown into the foredunes. Asymmetry of accretionary lobes and intertidal micro-deltas at drain outlets provide vectors and quantitative measurement of flux where they build against artificial groynes.

Drift indicators along the western arm of the bay are subtle. Micro-deltas at the outlets of river drains, together with sand built up against the old wooden groynes in the Buayanup and Quindalup sectors indicate east-to-west movement. Asymmetry of the Templar accretionary lobe in the Quindalup sector indicates a similar sustained movement. Westerly littoral drift in the western arm relates to the easterly component of the present-day bimodal wind pattern.

East of the Buayanup sector, vectors are consistently to the east. The elbow against the western groyne of Port Geographe has accreted 110 m since its reconfiguration in 2015. Asymmetry of the Russell Street accretionary lobe, which shows seaward growth of 82 m, indicates sustained easterly movement. Easterly littoral drift relates to the southwest component of the present-day bimodal wind pattern.

SEDIMENT BUDGET

Using sand built up against artificial structures, Damara (2011) estimated a sediment flux of 25,000 – 35,000 km^3/yr at west Busselton. Reidel & Byrne (1989) estimated 40,000 m^3/yr at Busselton Jetty and 50,000 m^3/yr at Port Geographe, which suggests that the sand-flux increases down drift. In constructing a sediment budget, the annual eastern-arm flux is taken as 35,000 m^3/yr.

The western-arm flux is not easily quantified, but a reasonable assumption can be made by comparing the dimensions of the two arms, and the strengths of the respective driving winds. Thus, a western flux of 20% of the eastern flux, i.e. about 7,000 m^3/yr is assumed. The combined flux is therefore 42,000 m^3/yr, which together with the net amount of annual accretion (100,000 m^3/yr) infers that 142,000 m^3 is being added to the entire system each year. This large volume raises the question of where this sediment is coming from.

Input from rivers that drain into the bay is miniscule. Constructed polygons (summarized in Table 2) show that natural erosion at the head of the bay can only provide about 15% of the required amount. Searle & Logan (1978) suggested that wave fronts from Southern Ocean swells refracting around Cape Naturaliste to reach the beaches align with nearshore scour-and-fill structures within the bay and are responsible for sediment input. However, that study pre-dated modern bathymetric data and lacked estimates of the magnitude of the required sediment. It is now evident that the sediment movement by refracted ocean waves is limited to seabed micro-ripples.

Sand distribution patterns and stability of nearshore bars are evidence against the contribution of sand around Cape Naturaliste to accumulate in Dunn Bay. Moreover, waters off Cape Naturaliste are too deep (>40 m) to

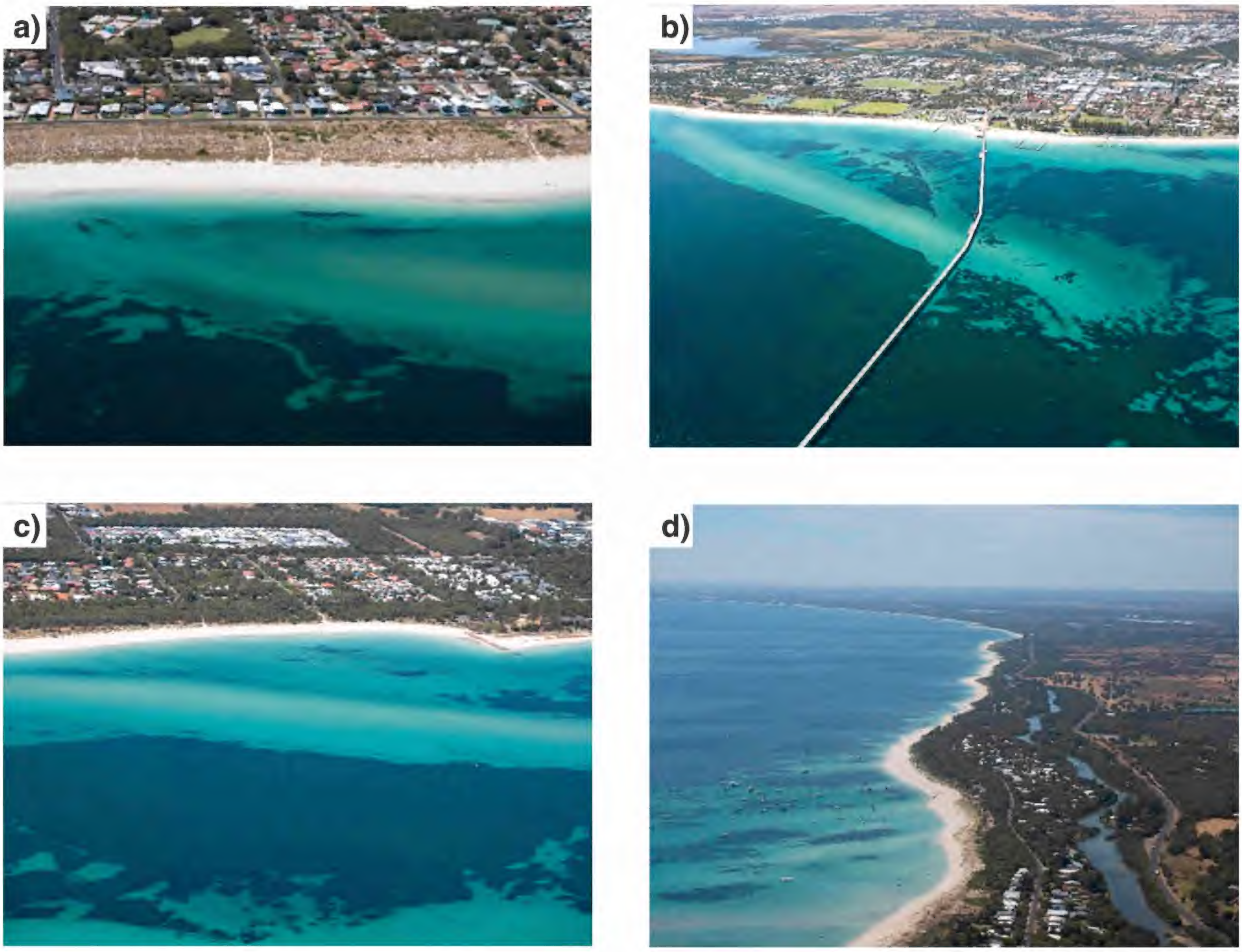

Figure 6. Aerial images along Geographe Bay: **a)** accreting beach encroaching onto relict sand ridges, Russel Street lobe. Thinly vegetated strip behind beach marks accretionary growth; **b)** relict linear sand ridge at Busselton Jetty; historic records show no migration. Dark area is seagrass meadow; **c)** sand starvation at Broadwater groyne has returned the beachline back to its 1960s position; oblique sandbar has not migrated in historic time; and **d)** lobes and sand-ridges on western arm of Geographe Bay looking east; back-beach lagoon is in the swale between dual ridges of Quindalup Dunes (Photographs by Ron Jensen, Dec 2021).

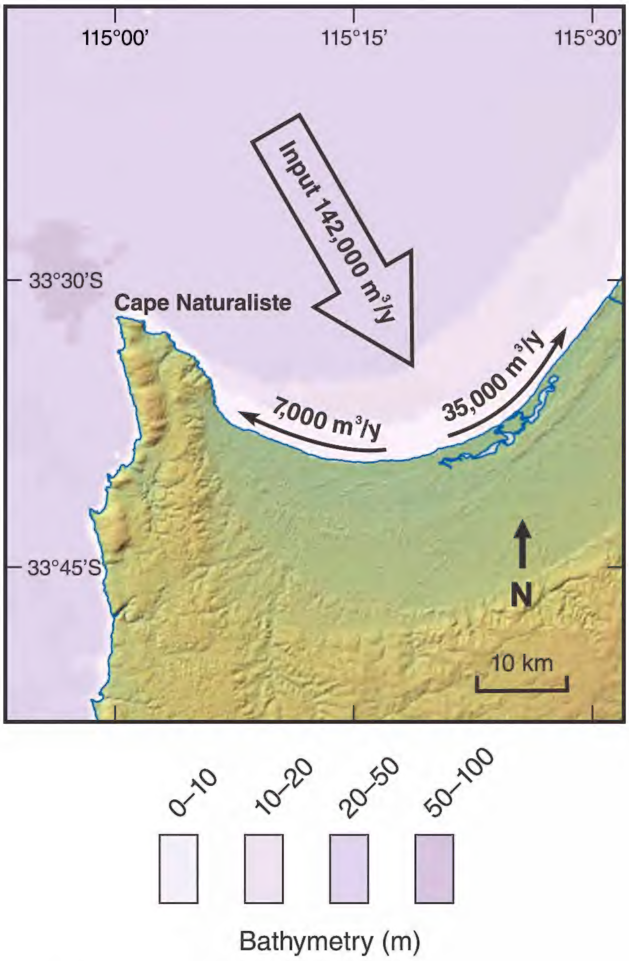

Figure 7. Model of sediment sources, pathways and sinks. The difference between input and dispersal is the amount sequestered by accretion (100,000 m^3/y).

allow seabed sand transport. Dunn Bay bars presumably were built up by sediment overwash within the bay, but present-day metocean conditions are insufficient to do this. Dunn Bay is a sediment sink, and not a source for contemporary accretion, as proposed by Barr & Eliot (2011). Thus, the Dunn Bay bars represent relicts of a past climate. The volume in storage (12 × 10^6 m^3) and the assumed flux (7,000 m^3/y) suggest Dun Bay bars took about 2,000 years to accumulate, commencing soon after 3770 yrs BP, when sea-level recession from the Holocene highstand reached its present position.

Damara (2011) recognised an onshore sand flux, albeit understated, and assumed offshore sandbars were the source. In the absence of detailed bathymetric data over many decades, his assumption is difficult to susteain, but the stationary nature of the ridges and bars indicates this is unlikely. The large oblique sand ridges are stationary as they are now stabilized by sea grass, and so are interpreted as relics of a past climate. They are active only at their innermost tips, where consumed by the accreting shoreline. Similarly, small oblique sandbars show no sense of movement, and they have maintained their positions and gross morphology over many decades. In the surf zone, they are remolded rather than migrated. Their remarkable persistence for over 60 years indicates they cannot be a source of accretionary sand.

Seabed data within Geographe Bay, collected as part of the post-glacial sampling program of the southern Rottnest platform, does not include detailed mineralogy, which could help determine the provenance of this sediment. Data from samples collected by Collins (1983) and Carrigny (1956) has been collated in the Geoscience Australia Marine Sediments (MARS) Database (http://dbforms.ga.gov.au/pls/www/npm.mars.search). Samples from depths down to 30 m are predominantly well-sorted quartz sand (with <30% $CaCO_3$) of 0.45 mm to 0.8 mm diameter, with an average of 0.64 mm. Similarly, the 'loose Holocene layer' Bufarale (2019) encountered at depths around 10 m contains 60–90% medium-grained quartz of medium sphericity. Significantly, some sampling sites failed as they encountered hard surfaces indicating local stripping of the loose sand from the seabed.

DISCUSSION

In terms of geomorphological evolution, the formation of large oblique linear ridges marked the beginning of a substantial ingress of sand into the bay, after it had achieved its present shape and position, some 7,000 years ago. It is notable that the larger ridges form clusters around the positions of the palaeo-outlets of the ancestral Capel and Vasse rivers. Alluvial fans and marine deltas related to these rivers could be the source of the sediment in these ridges.

Considering their size, shape and position, the large ridges would have required strong prevailing northeast winds to form. For southwestern Australia, such wind direction is associated to anti-cyclonic high-pressure cells on the continental interior but, in the present-day climate, these winds are not strong enough to generate such significant features. However, at the termination of the Last Glacial Maximum, intense anti-cyclonic cells operated over western continental Australia, as shown by the quasi-circular pattern of longitudinal desert dunes, dated by optically stimulated luminescence methods at 45,000–17,000 yr BP (Rhodes *et al.* 2004). Such intense anticyclonic winds may have persisted through the Holocene when the marine transgression reached the position of the present coast at about 7,500 yr BP. At that time, the Leeuwin Current was operating (Collins *et al.* 1991) as probably also was the counter north-flowing Capes Current, closer to Cape Naturaliste. The Capes Current, combined with strong anti-cyclonic winds, could have generated a clockwise gyre of sufficient strength to form the large sand ridges around the bay, and to build the Dunn Bay bars.

The formation of the smaller nearshore oblique sandbars with east–west axes that overprint the large sand ridges probably signals a moderating shift to more northerly prevailing winds, and possibly the advent of direct storm influence. Thereafter, the bay became a sink for introduced sand. It is likely that seasonal storms brought in the bulk of present-day sand. The highest intensity modern storms are from the north-northwest, down the axis of the bay. Geographe Bay experiences 5 to 15 such events per year, with storm-wave amplitudes averaging 3.3 m and peaking at 5 m (Damara 2011). Waves of this magnitude have a wave base of 15–20m, sufficient to move sand landwards from beyond the seagrass meadows.

The large volumes of sand stripped from the Leederville Formation through the Cenozoic have provided an almost inexhaustible source of sand on the inner continental shelf off Geographe Bay. This process may have operated for at least the last 2,000 years. Seasonal winds then generated along-shore dispersal pathways. The major pathway is northeasterly along the eastern arm of the bay, driven by the southwesterly tails of winter storms and summer sea breezes. A minor pathway is northwesterly along the western arm, driven by easterly winds. The large volume of sediment entering the system is much more than long-shore littoral drift can disperse, thereby accounting for the extensive accretion around the bay.

CONCLUSIONS

The beachline along Geographe Bay is rapidly accreting due to the influx of large amounts of sand, estimated at 142,000 m^3/yr. Accretion is progressive and not cyclic. Some sectors of the coast have advanced as much as 170 m seawards since the 1940s. Only a small sector 3 km in length at the head of the bay is subject to natural erosion. Pockets of sand depletion adjacent to engineered groynes and revetments are of local concern, but do not signify a fragile coast, which overall is robust.

Accreting sediment comes from the mobile sand layer on the inner continental shelf that accumulated during lower sea levels associated with global Pleistocene glacial cycles, rather than from eroding offshore sandbars, as is commonly thought. The offshore ridges and bars show no evidence of migration over the last six to eight decades. The large offshore linear, oblique ridges pre-date present metocean conditions, and are interpreted as submarine migrating sand ridges formed by a clockwise gyre in the bay related to strong anti-cyclonic winds at the beginning of the present interglacial, about 7,000 years ago. Landward tips of the large ridges are being disturbed by the advancing beaches. This disturbance may provide minor sediment feed for the development of nearshore oblique sandbars that are effectively stationary.

Geographe Bay is a large sediment sink, and possibly has been so for the last 5,000 years. Sediment dynamics is best interpreted in terms of evolutionary sequences related to palaeoclimatic conditions, rather than attempting to fit bed forms into present-day metocean conditions. It is not an intention of this study to make recommendations on coastal management by geo-engineering actions; however, such actions need to take into account the geological interpretations of this study, which imply doubtful benefits in the installation of groynes and sunken seawalls in stable sectors of the beachline.

ACKNOWLEDGEMENTS

I am grateful to the geographic information officers Ralph Talbot-Smith, Rick Mahoney and Steven James of the Coastal Infrastructure section of the Western Australian Department of Transport for generously providing georeferenced historical imagery and historic beach-line spatial data for Geographe Bay. I have benefited from discussions on beach processes with Matt Eliot of Damara and Seashore Engineering. Prof Chari Pattiarachi of the Oceans Institute at the University of Western Australia kindly provided published and unpublished material on oblique shore-attached sandbars. Arthur Mory assisted with technical aspects of the sedimentological model developed in this paper. Rob Seggie, Colin Murray-Wallace and Peter Baillie are thanked for their helpful review of the paper. Thanks are due to Giada Bufarale for enhancing the initial manuscript, Ron Jensen for the helicopter-borne aerial photographs, and Art Hoffmann for professionally re-creating my figures.

REFERENCES

Barr S & Eliot M 2011. Busselton Coastal Protection. Coasts and Ports conference (20th Australasian Coastal and Ocean Engineering Conference 2011 and the 13th Australasian Port and Harbour Conference 2011), Perth 28–30 September 2011, 739–744. Published by Engineers Australia, Barton ACT

Bellec V K, Boe R, Bjarnadottir L R, Albretsen J, Dolan M, Chand C, Thorsnes T, Jakobsen F W, Nixon C, Plassen L, Jensen H, Baeten N, Olsen H & Elvenes S 2019. Sandbanks sandwaves and megaripples on Spitsbergenbanken, Barents Sea. *Marine Geology* **416**, 105998. doi: 10.1016/j.margeo.2019.105998

Brooke B P, Olley J M, Pietsch T, Playford P E, Haines P W, Murray-Wallace C V & Woodroffe C D 2014. Chronology of Quaternary coastal aeolianite deposition and the drowned shorelines of southwestern Western Australia — a reappraisal. *Quaternary Science Reviews* **93**, 106–124.

Bufarale G, O'Leary M & Bourget J 2019. Sea level controls on the geomorphic evolution of Geographe Bay, southwest Australia. *Journal Royal Society Western Australia* **102**, 83–97.

Carrigny M A 1956. Continental shelf sediments of south-western Australia. Hons Thesis, University of Western Australia (unpublished).

City of Busselton 2022. Coastal Hazard Risk Management Adoption Plan. https://www.busselton.wa.gov.au/documents/2443/chrmap-final-october-2022

Collins L B 1983. Postglacial sediments and history, Southern Rottnest Shelf, WA. PhD Thesis, University of Western Australia (unpublished).

Collins L B, Wyroll K-H & France R E 1991. The Abrolhos carbonate platforms: geological evolution and Leeuwin Current activity. *Journal of the Royal Society of Western Australia* **74**, 47–57.

Damara WA Pty Ltd 2011. Coastal Erosion Study: Assessment of Climate Change Impacts. Prepared for the Shire of Busselton, Report 96-00-01. https://www.busselton.wa.gov.au/documents/526/coastal-erosion-study-assessment-of-climate-change

Dronkers J 2016. *Dynamics of Coastal Systems* (2nd edition). Advanced Series on Ocean Engineering: Volume 41, World Scientific Publ. Co., Singapore, 780 pp.

Eliot M2013. Application of Geomorphic Frameworks to Sea-level Rise Impact Assessment. Report 193-01. Prepared for Geoscience Australia. Damara WA Pty Ltd, Western Australia. https://www.dcceew.gov.au/sites/default/files/documents/geomorphic-frameworks.pdf

Fahrner C K & Pattiaratchi C B 1994. The physical oceanography of Geographe Bay, Western Australia. Report for the Water Authority of Western Australia. https://research-repository.uwa.edu.au/en/publications/the-physical-oceanography-of-geographe-bay-western-australia

Gallop S L, Verspecht F & Pattiaratchi C H 2012. Sea breezes drive currents on the inner continental shelf off southwest Western Australia. *Ocean Dynamics* **62**, 569–583.

Gallop S L, Bossarelle C & Pattiaritchi C H 2010. Current response to sea breezes in southwestern Australia. Proceedings 15th Physics of Estuaries and Coastal Seas (PECS) conference, Colombo, Sri Lanka, 14–17 September 2010. doi: 10.13140/2.1.3937.1202

Garnier R, Calvete D, Falques A & Cabelleria M 2006. Generation and non-linear evolution of shore-oblique / transverse sandbars. *Journal of Fluid Mechanics* **567**, 327–360.

Gee R D 2022. Landscape evolution and Cenozoic sea-levels of the Geographe Bay hinterland, southwestern Australia. *Journal of the Royal Society of Western Australia* **105**, 1–19.

Green A N, Flemming B W, Cooper J A G & Wanda T F, 2022. Bedform evolution and dynamics of a geostrophic current-swept shelf, northern KwaZulu-Natal, South Africa. *Geo-Marine Letters* **42**, 5. doi: 10.1007/s00367-021-00722-7

Gozzard J R 2011. WA Coast – Cape Naturaliste to Lancelin. Geological Survey of Western Australia, Digital Data Product, https://dmpbookshop.eruditetechnologies.com.au/product/wa-coast-cape-naturaliste-to-lancelin.do

Hamilton N T M & Collins L B 1997. Morphostratigraphy and evolution of a Holocene composite barrier at Minninup, southwestern Australia. *Australian Journal of Earth Sciences* **44**, 113–124.

McArthur W M & Bettenay E 1960. The development and distribution of soils on the Swan coastal plain. *CSIRO Australia Soil Publication* **16**, 1–55.

McCulloch M T & Mortimer G E 2008. Applications of the ^{238}U–^{230}Th decay series to dating fossil and modern corals using MC-ICPMS. *Australian Journal of Earth Sciences* **55**, 955–965.

Miller K G, Browning J V, Schmelz J, Kopp R E, Mountain G S & Wright J D 2020. Cenozoic sea-level and cryospheric evolution from deep-sea geochemical and continental margin records. *Science Advances* **6**, doi: 10.1126/sciadv.aaz1346

Nnafie A, de Swart H E, Garnier R & Calvete D 2014. Effects of sea level rise on the formation and drowning of shoreface-connected sand ridges, a model study. *Continental Shelf Research* **80**, 32–48. doi:10.1016/j.csr. 2014.02.017

Pattiaratchi C B & Woo M 2009. The mean state of the Leeuwin Current system between North West Cape and Cape Leeuwin. *Journal of the Royal Society of Western Australia* **92**, 221–241.

Pattiaratchi C B, Wijeratne S, Roncevich L & Holder J 2017. The influence of near-shore sandbars on coastal stability in Port Geographe, south-west Australia. Pages 865–871 *in* T Baldock, editor, *Australasian Coasts & Ports 2017: Working with Nature*, Coast and Ports Conference Cairns 21–23 June 2017, Engineers Australia, Barton ACT.

Pearce A & Pattiaratchi C 1999. The Capes current: a summer countercurrent flowing past Cape Leeuwin and Cape Naturaliste, Western Australia. *Continental Shelf Research* **19**, 401–20.

Rhodes E, Fitzsimmons K, MacGee J, Chappell J, Miller G & Spooner N 2004. The history of aridity in Australia: Preliminary chronological data. Pages 299–302 *in* I C Roach, editor, *Regolith 2004*, Cooperative Research Centre for Landscape Environments and Mineral Exploration.

Riedel & Byrne Consulting engineers Pty Ltd 1989. Port Geographe coastal processes study. Report to Department of Marine and Harbours (unpublished, available from their library, item M/1988, 06853).

Rogers M P & Associates Pty Ltd 2015. Broadwater Beach Coastal Erosion Investigation. R614, Report to City of Busselton, DOC ID 5134631.

Searle D J & Logan B W 1978. A Report on Sedimentation in Geographe Bay. Sedimentology and Marine Geology Group, Department of Geology, University of Western Australia (unpublished; available from the Reid Library Special Collections University collection, Q 551.46083 1978-50).

Shore Coastal 2018. City of Busselton Coastal Management Program 2020-2030. Prepared for City of Busselton. www.busselton.wa.gov.au/documents/307/busselton-coastal-management-2020-2030

Smith R L, Huyer A, Godfrey J S & Church J A 1991. The Leeuwin current off Western Australia, 1986–1987, *Journal of Physical Oceanography* **21**, 323–45.

Stul T, Gozzard J R, Eliot I G & Eliot M J 2012. Coastal Sediment Cells between Cape Naturaliste and Moore River, Western Australia. Report prepared by Damara WA Pty Ltd and Geological Survey of Western Australia for the Western Australian Department of Transport, Fremantle. www.researchgate.net/publication/282617218_Coastal_Sediment_Cells_for_the_Vlamingh_Coast_Between_Cape_Naturaliste_and_Moore_River_Western_Australia

Swift D J P & Field M E 1981. Evolution of a classic sand ridge: Maryland sector, North American inner shelf. *Sedimentology* **28**, 461-482.

Thomas C M 2018. Regional seismic interpretation and structure of the Southern Perth Basin. *Geological Survey of Western Australia Report* 184.

Trowbridge J H 1995. A mechanism for the formation and maintenance of shore-oblique sand ridges on storm-dominated shelves. *Journal Geophysical Research* **100**(C8), 16071–16086.

Twiggs E J & Collins L B 2010. Development and demise of a fringing coral reef during Holocene environmental change, eastern Ningaloo Reef, Western Australia. *Marine Geology* **275**, 20–36.

Journal of the Royal Society of Western Australia, 106: 23–24, 2023

Basil Eric Balme

13th June 1923 – 10th July 2023

Doyen of Australian palynology

One of the leading figures of post-war palynology, Basil Eric Balme, passed away on 10 July 2023 in his 100th year. He was born on 13 June 1923 in Perth, Western Australia. His grandfather hailed from Yorkshire and his father had been involved in the Battle of Passchendaele in WW1 as a member of the Australian forces. After the war, his father worked in Collie and farmed at Meckering before becoming a shopkeeper in Victoria Park and then South Perth. Consequently, Basil attended a variety of primary schools before gaining entry to Scotch College as a Coombe Scholar with a Council Scholarship. There he made his mark playing Australian Rules football and cricket, and was Head Boy in his final year. Basil commenced studies at the University of Western Australia (UWA) in 1941, initially in engineering before switching to science, majoring in geology, where the lecturer in palaeontology was the internationally renowned Curt Teichert (1905-96). However, in 1942 he suspended his studies to enlist in the Royal Australian Navy. Initially, he received intensive training in the then-new radar technology and went on to serve as a radar operator and eventually Petty Officer on ships in the Mediterranean and Pacific. He recalled serving for several months on a ship and had several discussions with Philip Mountbatten (subsequently Prince Philip, Duke of Edinburgh).

Basil returned, post-war, to UWA in 1946 to complete his undergraduate studies, achieving first class honours in 1948. For his honours project, he was invited by Joe Lord, then a geologist with the Geological Survey of Western Australia, to investigate spore-pollen assemblages from the Collie Coalfield, 160 km south of Perth, with a view to correlating the coal seams in Joe's pet project. He was under no illusion about the difficulty ahead, noting "it is with some trepidation that one approaches the task of employing miospores as fossils for stratigraphical purposes". Despite his reservations, Basil was able to describe and illustrate 36 types of spores and pollen from 35 mine face and borehole samples. This enabled him to distinguish two assemblage types and compare his material with published descriptions from New South Wales, Queensland and India: a remarkable achievement for the time. This work was published in 1952 as part of a Bulletin on the Collie Mineral Field. It was the first study of palynomorphs of any age from Western Australia, and one of the few from anywhere in Australia. As an undergraduate, Basil was awarded the Lady James Prize in Natural Science and the E.S. Simpson Prize in Mineralogy (both jointly with John Glover) and a CSIR Junior Scholarship. He continued his sporting interests, playing cricket and Australian Rules football for the university and was treasurer of the Guild of Undergraduates.

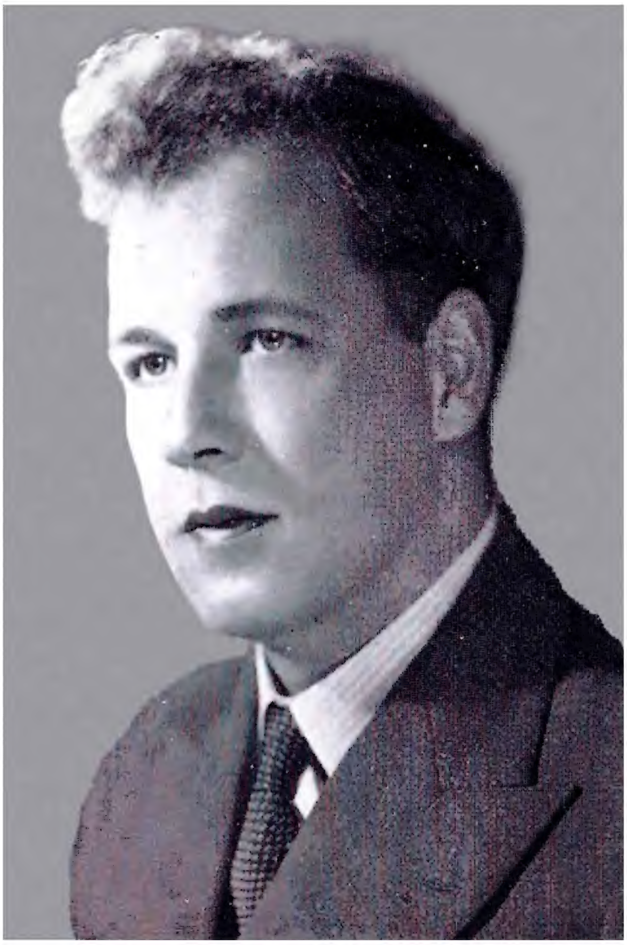

Travelling to England in 1949, he married Helen Cook from Dumbleyung, Western Australia, who at the time was an entomologist at the Natural History Museum, London. Basil joined the National Coal Board's Coal Survey Laboratories in Sheffield, collaborating with Mavis Butterworth and Harold Smith in the study of miospores from British Carboniferous coalfields. He returned to Australia in 1952 to work in the CSIRO Coal Research Section in Sydney. While in this position, he published three papers in 1955-56, co-authored with John Hennelly, on Permian spore-pollen taxonomy. These included many taxa from the Collie Basin that he had first encountered as a UWA honours student.

In mid-1957, Basil accepted a position as Lecturer in Geology at UWA. There he spent the rest of his academic career, progressing to Reader in Geology in 1969 and serving as Dean of Science (1979-81) and Head of the Geology Department (1983-85). His return to Perth in 1957 coincided providentially with the expansion of oil exploration in the state by West Australian Petroleum Pty Ltd (WAPET), a company with leases covering vast tracts in the Phanerozoic sedimentary basins of Western

---

Australia. Basil had previously examined numerous samples from WAPET exploration wells, and with his return to the state this collaboration expanded. The general paucity of surface outcrop of Palaeozoic and Mesozoic strata – nevertheless, extensive at depth in all the state's Phanerozoic sedimentary basins – was the impetus for using palynology from boreholes and petroleum wells. His taxonomic publications describing spores-pollen from subsurface Devonian, Permian and Triassic strata provided the essential basis for much of the ensuing biostratigraphic correlations. Many of his papers detailed geological boundary correlations, particularly the Permo–Triassic boundary, and he contributed to numerous international volumes. He also supervised at least seven higher-degree theses on palynological topics and most of the students proceeded to careers in palynology or joined the petroleum industry in other capacities. Furthermore, Basil was instrumental in supplying rock material to his colleague, Isabel Cookson (1893-1973) at the University of Melbourne, accompanied by precise geological formation and age data. From this material, she with her principal co-author, Alfred Eisenack, described a large number of dinoflagellate cyst taxa that became the foundation of many subsequent taxonomic and biostratigraphic studies of Jurassic, Cretaceous and Cenozoic dinoflagellate cysts.

Basil was awarded a D.Sc. from UWA in 1968 and the W.R. Browne Medal of the Geological Society of Australia in 1988. He became President of the Western Australian Division of the Geological Society of Australia in 1961 and President of the Royal Society of Western Australia in 1976. During overseas study leave, he has been Visiting Professor of Micropaleontology at New York University/American Museum of Natural History in 1962-63, Visiting Research Scientist at Chevron Oilfield Research Laboratory, Los Angeles (1971-72), and Occasional Lecturer at Aarhus University, Denmark (1978-79). A festschrift volume – published in his honour (*AAP Memoir* 5, 1988) and edited by Peter Jell and Geoffrey Playford – contains many papers by his colleagues and former students.

Following retirement in 1988, Basil continued in an adjunct position at UWA, eventually sharing, with his long-standing colleague John Glover, a very small office that had for many years been his microscope room. In 1995, he published a very comprehensive (242 pp.) catalogue of in-situ spores and pollen grains. This substantial reference work – the result of sustained effort over several years – is unlikely to be superseded. During 1999-2001, he collaborated on an extensive work on the Late Triassic palynology of the Rankin and Goodwyn gas fields in the Carnarvon Basin. This constituted his last palynological contribution.

In concluding this eulogy, it is appropriate to reproduce here paragraphs from the preface to the 1988 volume honouring Basil (*Australasian Association of Palaeontologists, Memoir* 5): "For many of us, it is his love of words that we associate with Basil. In conversation, in letters, and his scholarly writing there is so often evident his apt, original, and vivid use of language. Who else could describe his hometown of Perth as 'something between Dallas and Cheltenham?' He was a masterly lecturer and an entertaining speaker; his after-dinner address to the Gondwana Symposium in Canberra in 1973 is recalled with affection as something of a landmark of light-hearted oratory in Australian geological circles. The same wry humour enlivened his lectures to undergraduates. It was a love of words which no doubt led him into his association with university theatre in Western Australia, and to roles in such plays as Capek's 'The Insect Play', Shaw's 'St. Joan', T.S. Eliot's 'The Cocktail Party'. There was too his role as the soothsayer in Sophocle's 'Oedipus Rex' played in the lovely setting of the Sunken Garden, and on one occasion before a daunting audience which included Sir Laurence Olivier. Basil has a rare skill as a written communicator. Those of us fortunate enough to have undertaken research under his supervision will recall his always apposite and tactful recommendations for remedying disorganized observations and faulty syntax. We recall with gratitude, too, his wise counsel, his unfailing accessibility to us and our ideas, his good humour, and his tolerance."

Basil's wife, Helen, predeceased him in 2008. He is survived by their three children, five grandchildren and two great-grandchildren.

John Backhouse

Honorary Research Fellow, The University of Western Australia, Perth

Geoffrey Playford

Professor Emeritus, The University of Queensland, Brisbane

Journal of the Royal Society of Western Australia, 106: 25–44, 2023

Lunulite bryozoan biogeography—a convergent global success with a distinct Western Australian twist

ECKART HÅKANSSON[1]*, AARON O'DEA[2,3] AND ANTONIETTA ROSSO[4]

[1] *School of Earth Sciences, The University of Western Australia*

[2] *Smithsonian Tropical Research Institute, Balboa, Panamá*

[3] *Sistema Nacional de Investigación, SENACYT, Panamá*

[4] *Department of Biological, Geological and Environmental Sciences, University of Catania, Italy*

* *Corresponding author:* ✉ *eckart.hakansson@uwa.edu.au*

Abstract

Lunulites are a polyphyletic group of marine bryozoans that have been a conspicuous element of marine shelf faunas from the Late Cretaceous to the present. They are easily recognisable by their domed colony form and free-living mode of life on sea floor sediments. Here we explore the waxing and waning of the major lunulitiform groups and their unique morphology and mode of life from the Cretaceous to the present day. Because relatively few and simple modifications are needed to transition from an encrusting form into this highly specialised lifestyle, shared colonial features are rampant and we find examples of both convergent and iterative evolution across several unrelated clades, although detailed phylogenetic relationships remain largely unresolved. The early chapter of the 'lunulite story' is focused on the Late Cretaceous European Chalk Sea, which appears to have been a crucible for the evolution of 'lunulites'. At least six, and likely more, cheilostome groups independently evolved a free-living mode of life in this tropical shelf region. To what extent any of these free-living clades gave rise to post-Cretaceous groups remains unclear. The Cenozoic chapter is more complex, comprising at least three independently evolved major clades, two of which are extant: (1) the Lunulitidae *s. str.*, a North American/European cluster, encompassing the classic *Lunulites*, which became extinct in the late Neogene; (2) the Cupuladriidae, which reached circum-global tropical and sub-tropical distribution in the Miocene; and (3) the 'Austral lunulite' cluster, which is almost certainly polyphyletic and through most of its history confined to Australia and New Zealand, bar a comparatively brief colonisation of the southern part of South America, with the earliest representatives from northwestern Western Australia.

Key words: free-living bryozoans, biogeography, phylogeography, Cupuladriidae, Lunulariidae, Lunulitidae, Otionellidae, Selenariidae

Manuscript submitted 16 April 2023; accepted 11 May 2023

INTRODUCTION

The Bryozoa is a diverse, highly successful phylum of suspension-feeding, predominantly benthic marine invertebrates with an excellent fossil record dating back to the Early Ordovician, and with a sporadic, albeit disputed, record commencing at the beginning of the Cambrian (Zhang *et al.* 2021; Yang *et al.* 2023). All members of the phylum (with one possibly derived exception) form colonies by repetitive asexual budding of individual zooids, allowing polymorphic diversification in both the shape and function of zooids. Sexual reproduction involves a freely moving larval stage lasting from a few hours to several months (e.g., Driscoll *et al.* 1971; Cook & Chimonides 1983; Taylor 1988; Winston 1988). The overwhelming majority of bryozoans require a substrate for their larva to successfully settle and metamorphose into an ancestrula or ancestrular complex, thus initiating the new colony. Most bryozoans select stable positions that provide sufficient space to enable the proper development of the colony (Winston 1988; Håkansson & Thomsen 2001). In the case of the free-living bryozoans, however, the lecithotrophic larvae mostly settle on sand grains, typically less than 2 mm; far too small to provide stability or space for the adult colony. By outgrowing or integrating the small substrate and adopting heteromorphic zooids called vibracula that possess long, bristle-like setae (Fig. 1), the bryozoan colony becomes free-living. The adoption of this mode of life allowed several groups of cheilostome bryozoans to colonise the vast expanses of fine-grained shelf sediments across the globe with tremendous success. In some instances, lunulite bryozoans are the most abundant epifaunal element of benthic soft-sediment communities (Fig. 2) with 2,000 to 3,000 colonies/m^2 reported by Marcus & Marcus (1962) and an exceptional number of more than 15,000 live colonies/m^2 reported by Cadée (1975).

The free-living—or lunulitiform—bryozoans are characterised by small (usually less than 2 cm in

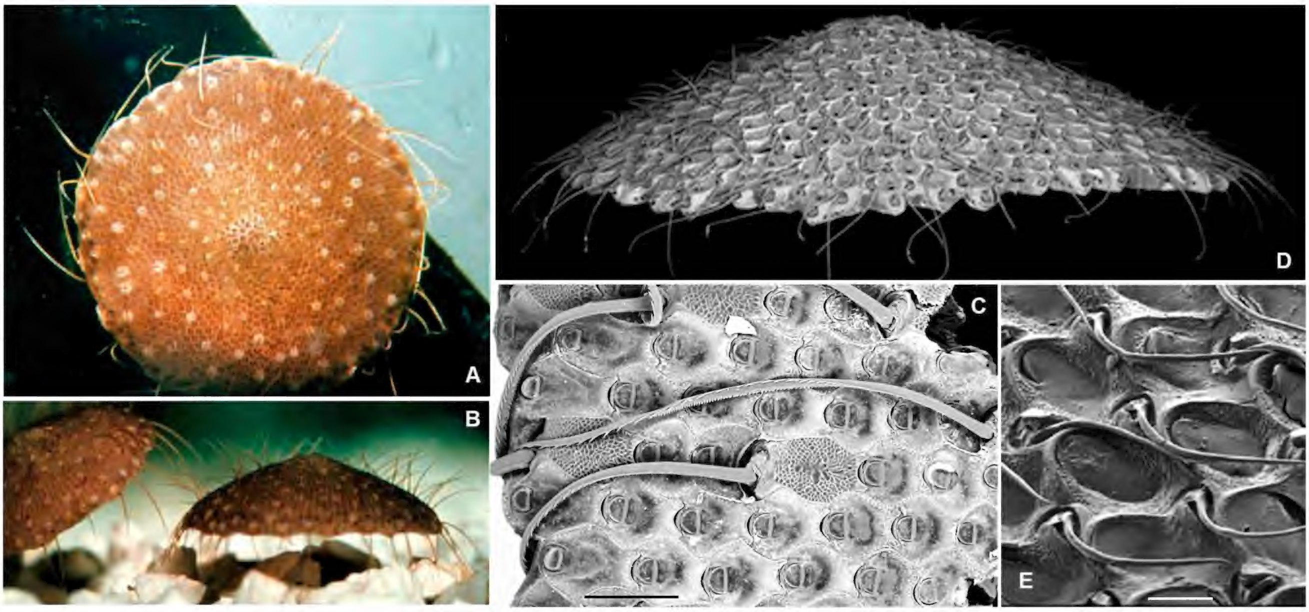

Figure 1. Live free-living lunulite bryozoans 'walking'; note the long, flexible bristle-like setae characterising these species. **A–C,** *Selenaria maculata* (Busk 1852a), Great Barrier Reef (**A–B** colonies are just over 1 cm in diameter; courtesy P. L. Cook); **C**, note the low proportion of vibracula, with extremely long, serrated setae (scale bar 500 µm). **D**, *Cupuladria biporosa* (Canu & Bassler 1923), Panama, with comparatively long setae (the colony is about 12 mm in diameter). **E**, *Cupuladria guineensis* (Busk 1854), with short setae (courtesy P. Bock, Melbourne); note the 1:1 proportion between autozooids and vibracula with smooth setae (scale bar 200 µm).

diameter) discoid, flat to domed colonies, typically with all zooids confined to the frontal side. Their most conspicuous element is the presence of regularly distributed vibracula with individually movable long setae (Fig. 1) some of which extend beyond the colony margin, raising it slightly above the seafloor. Representatives of two families, Cupuladriidae and Selenariidae, both illustrated in Figure 1, have been observed to move across the seafloor, as well as digging into or out of the seafloor sediment through coordinated movement of their setae (Cook & Chimonides 1978; Håkansson & Winston 1985; O'Dea 2009)—a most unusual capability amongst bryozoans and colonial organisms.

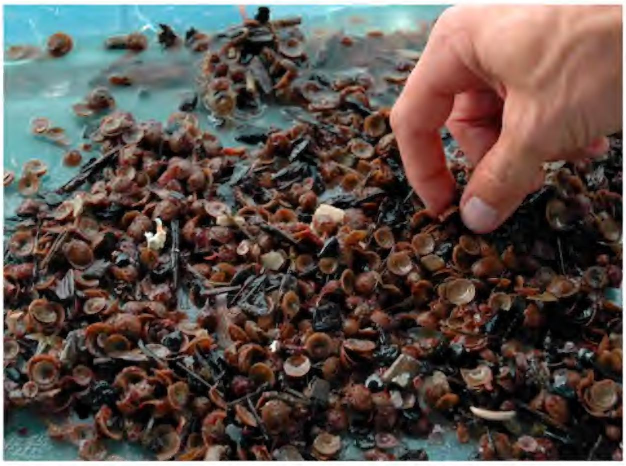

Figure 2. Hundreds of living colonies of *Cupuladria biporosa* collected in a van Veen grab sample in Golfo de los Mosquitos, Caribbean Panama (35 m; 8.8750, -80.9992).

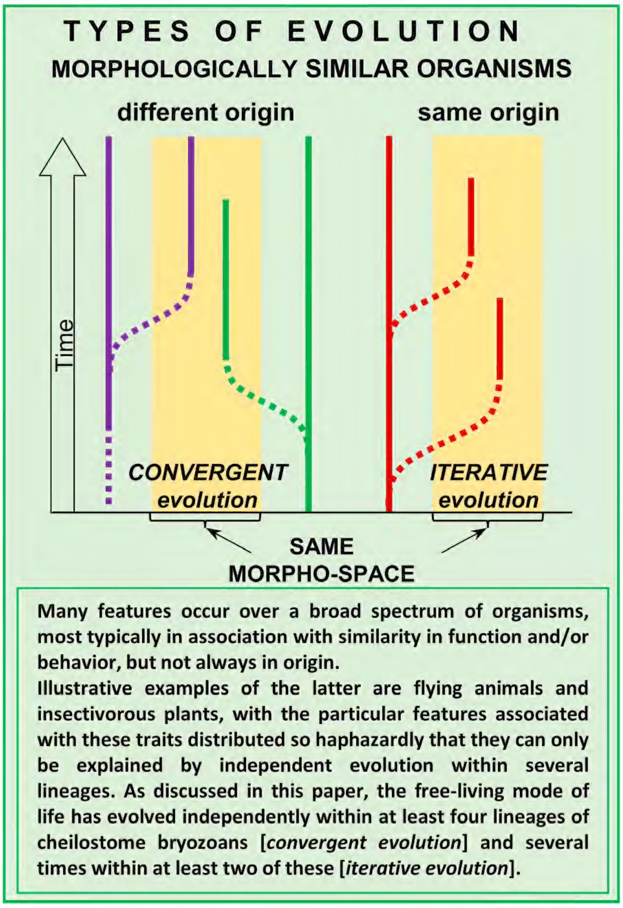

Many features occur over a broad spectrum of organisms, most typically in association with similarity in function and/or behavior, but not always in origin.
Illustrative examples of the latter are flying animals and insectivorous plants, with the particular features associated with these traits distributed so haphazardly that they can only be explained by independent evolution within several lineages. As discussed in this paper, the free-living mode of life has evolved independently within at least four lineages of cheilostome bryozoans [*convergent evolution*] and several times within at least two of these [*iterative evolution*].

Figure 3. Convergent and iterative evolution. The yellow zone represents the free-living morpho-space, and the line colors represent separate clades.

Because of the morphological constraints imposed by their mode of life, free-living, lunulitiform bryozoans are generally easily distinguishable and, as such, a few genera were formally recognised early in the study of the bryozoans. Thus, pairs of generic names *Lunulites* Lamarck 1816 vs. *Lunularia* Busk 1884 and *Cupuladria* Canu & Bassler 1919 vs. *Cupularia* de Blainville 1830 [now abandoned], have been confused and sometimes interchanged ever since. Because of their superficial morphological similarities, higher level classification of the groups has been persistently 'dynamic' with several family-level taxa proposed, combining the lunulitiform genera in virtually all combinations possible. Although the genus *Lunularia* has been formally restricted to a small group of exclusively Austral (i.e., from Australia and New Zealand) species referred to the monotypic family Lunulariidae (Levinsen 1909), the name *Lunulites* remains in broad use.

Researchers have attempted to clarify the resulting systematic quagmire. A series of papers by P. L. Cook in collaboration with P. Chimonides (1978–1994) and P. Bock (1998–1999), among others, led to a growing realisation that convergent and iterative evolution (Fig. 3) were likely widespread among the free-living bryozoans, a notion we support and are exploring further in a parallel investigation.

Currently, all formally described lunulitiform taxa considered here are referred to either the family Cupuladriidae or the superfamily Lunulitoidea (most recently by Bock 2022), albeit commonly with some reservation. Although the Cupuladriidae as a monophyletic family is well-supported, we do not support the unification of all other major lunulite groups into one superfamily.

BIOGEOGRAPHY OF THE FREE-LIVING BRYOZOANS

The general pattern of free-living bryozoan biogeography is rapid occupation (and domination) of soft shelf sediments in warm waters following their emergence

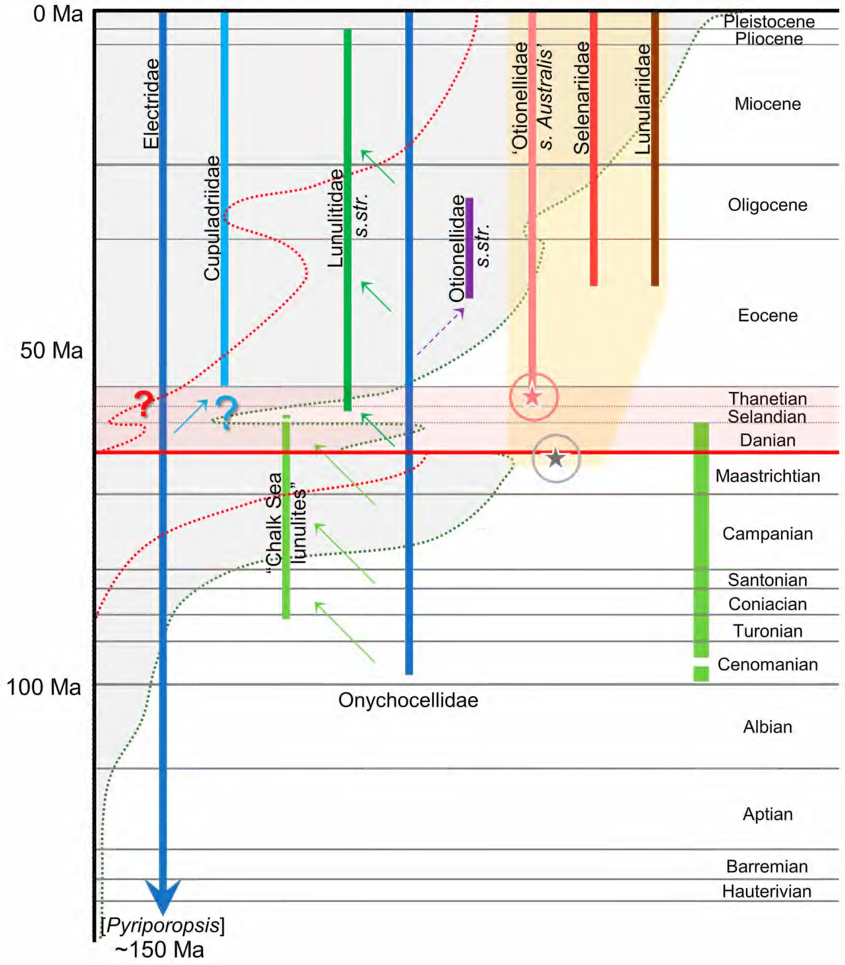

Figure 4. Stratigraphic distribution of the main lunulite clades referred to in the text. Two non-free-living families (dark blue lines) are included as the likely ancestors to most or all free-living clades (indicated by thin arrows). Electridae, the longest ranging cheilostome family, includes the probable ancestor to the Cupuladriidae (as well as the oldest known cheilostome genus, *Pyriporopsis* Pohowsky 1973), whereas the Family Onychocellidae is considered the likely ancestor of several 'lunulite' clades. Relative temporal diversity estimates in green stippled curves are for the Order Cheilostomata; the red stippled line is for free-living cheilostomes (not to scale). The Paleocene 'dead zone' is shaded red; the 'Austral Realm', yellow; the temporal extent of the Northern European Chalk Sea is the broad green line; the two asterisks show the stratigraphic position of the two oldest known Austral lunulite records (discussed in the text).

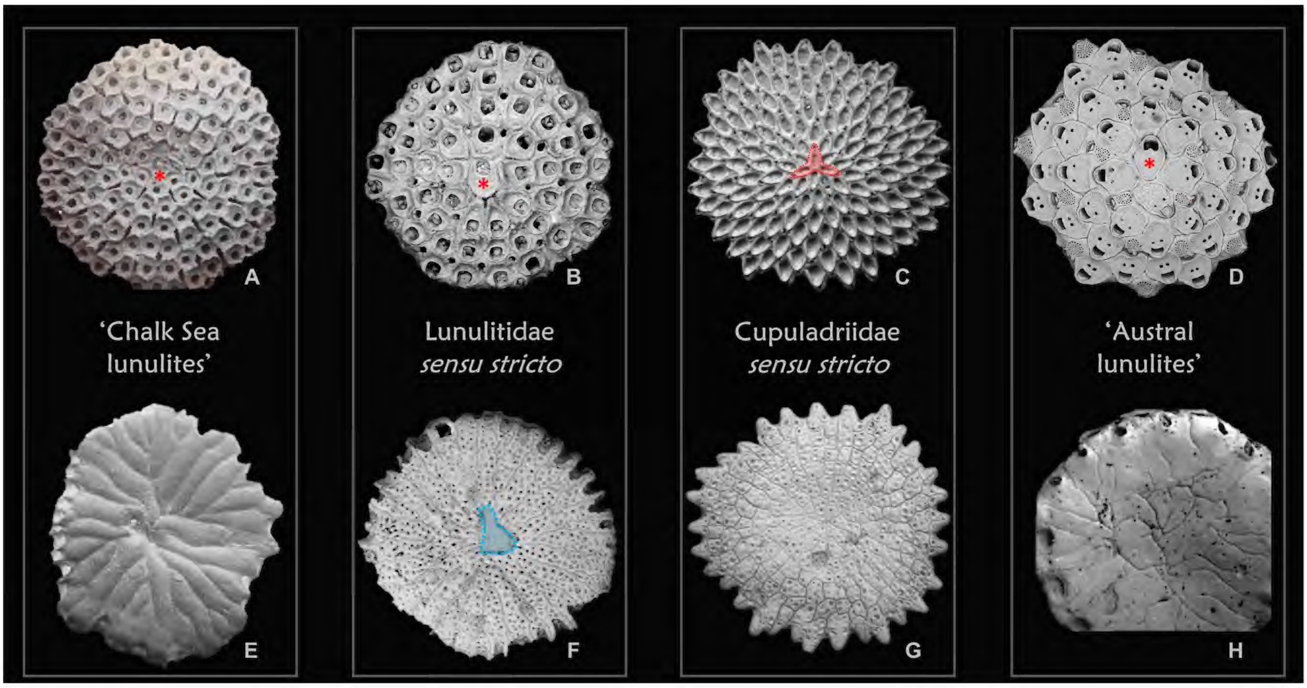

Figure 5. The four main clusters of lunulite bryozoans, showing both frontal (top) and basal aspects. Ancestrula and ancestrular complex indicated in red (asterisk and shaded, respectively); substrate visible only in **G** (shaded blue). **A**, *Lunulites goldfussi* von Hagenow 1839 (Maastrichtian, Denmark). **B**, **F**, *Lunulites androsaces* Michelotti 1838 (Late Pliocene, Altavilla, Italy). **C**, **G**, *Cupuladria biporosa* (Canu & Bassler 1923); (recent, Florida; ancestrular triplet shaded red). **D**, *Selenaria punctata* Tennison Woods 1880 (recent, New South Wales). **E**, *Lunulites beisseli* Marsson 1887 (Maastrichtian, Denmark). **H**, *Otionellina ampla* Bock & Cook 1999 (Miocene, Victoria).

(Fig. 4). The main trends in their biogeography are explained herein using the dominant four clusters of lunulitiform free-living bryozoans, which we believe are all phylogenetically distinct, although no formal phylogenetic analyses have been made. The following summaries are based on published records and personal observations.

'Chalk Sea lunulites'

This cluster of lunulites (Fig. 5 A, E) originated in the Late Cretaceous northeast Atlantic shelf seas, particularly the Northern European Chalk Sea, where the diversity of free-living bryozoans, from a fledgling beginning in the Late Turonian (Koromyslova & Pervushov, 2022), formed an evolutionary hotspot reaching approximately 100 species in the Maastrichtian. The group appears to have been geographically and ecologically constrained by the unique depositional environments of the Chalk Sea province with an assumed total range of Late Cenomanian to Danian (Håkansson *et al*. 1974; Surlyk 1997). The group is unequivocally polyphyletic (e.g., Håkansson & Voigt 1995), with calcitic skeletons and non-porous basal walls dominating. The group is very rare in the ultimate phase (Danian) of the Chalk Sea as well as within later Paleocene deposits in the region and has uncertain relations to isolated Late Cretaceous species in central Gondwanan fragments (cf. Taylor 2019) and North America (undescribed). There is no indication that any member of this cluster has migrated into the Austral Realm.

Lunulitidae

A separate group of lunulites, the family Lunulitidae *s. str.* (Fig. 5 B, F) originated in and dominated, both in abundance and diversity, the North Atlantic shelf seas, with an assumed range of Selandian to Pliocene (e.g., Cipolla 1921; Lagaaij 1952; pers. obs.). Within the family, two hotspots developed: one in the northwest Atlantic during the mid-Paleogene, and a minor one in European seas during the Neogene. The group is probably polyphyletic, typically with a bimineralic or, less frequently, an entirely aragonitic skeleton (Taylor *et al*. 2009) with basal-wall pores. There appears to have been little migration outside the North Atlantic Realm, and there is no indication that any member related to this cluster migrated into the Austral Realm.

Cupuladriidae

The family Cupuladriidae (Fig. 5 C, G) probably originated in the tropical eastern Atlantic (Gorodiski & Balavoine 1961). It has a known range of Thanetian or Ypresian to Recent, is apparently monophyletic (Dick *et al*. 2003) with a dominantly aragonitic skeleton (e.g., Taylor *et al*. 2009), and commonly exhibits basal-wall pores. Although highly localised and rare through the Paleogene, the family underwent a large-scale expansion into near-circumtropical seas at the onset of the Miocene (e.g., Laagaij 1963), forming a hotspot around the central Atlantic region. The Cupuladriidae have been present, and often prolifically so, in the mid-Atlantic and Caribbean, tropical west Pacific and Indo-Pacific archipelago since the Miocene, although their diversity and abundance in the latter two realms remains poorly documented. A few taxa are recorded from the Miocene in southern South America (Philippi 1887; Canu 1904, 1908), and a single cupuladriid species migrated into the Austral Realm in the Miocene (Cook *et al*. 2018b).

'Austral lunulites'

A distinct group of free-living lunulite bryozoans (including Lunulariidae, Selenariidae, 'Otionellidae *sensu australis*'; Fig. 5 D, H) developed in the Austral Realm. Limited evidence indicates this cluster most likely originated along the northwestern margin of Australia, with a total range of Maastrichtian or Thanetian to Recent (Bock & Cook 1998, 1999; pers. obs.). The group is polyphyletic, comprising at least four families, with dominantly aragonitic skeletons (Taylor *et al*. 2009). Although geographically isolated through most of their history (see 'The Austral lunulites' below), they had spread around all of Australia and New Zealand by the Oligocene (Bock & Cook 1999) to form a prominent, ongoing hotspot with temporary migration into southern South America in the Late Oligocene, possibly via Antarctica. No austral 'lunulites' are known to have crossed the Wallace Line into Eurasia.

Among the four groups outlined above, the Lunulitidae *s. str.*, together with its nominal genus *Lunulites*, remains particularly loosely constrained. Both names have been assigned extensively to taxa in both clusters of lunulites distinguished above, separated by not only the end-Cretaceous mass extinction, but also the subsequent Paleocene 'dead zone' (Fig. 4), which obscures any possible relationship between these two cohorts of '*Lunulites*'. It is noteworthy that the scarcity of free-living bryozoans otherwise characterising the Paleocene does not apply to the Austral Realm, which was the scene of a separate, spectacular evolutionary radiation, seemingly without contribution from any lunulite clade from outside the realm (see below). As demonstrated from the groupings above, we suggest that the two '*Lunulites*' clusters are phylogenetically distinct, with 'Chalk Sea lunulites' effectively becoming extinct at the Mesozoic–Cenozoic boundary, bar a few survivors into the Paleocene 'dead zone' (Håkansson *et al*. 2019, and ongoing research). Together with a mixed group of unique free-living bryozoans without setae, the 'Chalk Sea lunulites' forming an as yet unrivaled diversity hotspot of free-living bryozoans during the later phases of the Late Cretaceous Chalk Sea in northern Europe (e.g., Håkansson & Voigt 1995).

THE 'AUSTRAL LUNULITES'

The Austral Realm occupies a prominent position in the study of Cenozoic and modern bryozoans—including the lunulites—with studies of their highly diverse faunas dating back to the early 19th century. Initially these studies were based, albeit rather chaotically, on the collections from the French Baudin expedition (1801–1803), but following the British *Rattlesnake* expedition (1846–1850) and subsequent local collecting, more systematic descriptions of the bryozoan faunas commenced (e.g., Busk 1852a, b, 1854; Hincks 1881a,b, 1882; MacGillivray 1881, 1886; and the overview by Cook *et al*. 2018a). The earliest work on fossil bryozoans includes that by Tenison Woods (1865) as well as a monograph by MacGillivray (1895), with early works on fossil lunulite bryozoans by Tenison Woods (1880) and Maplestone (1904). All referred

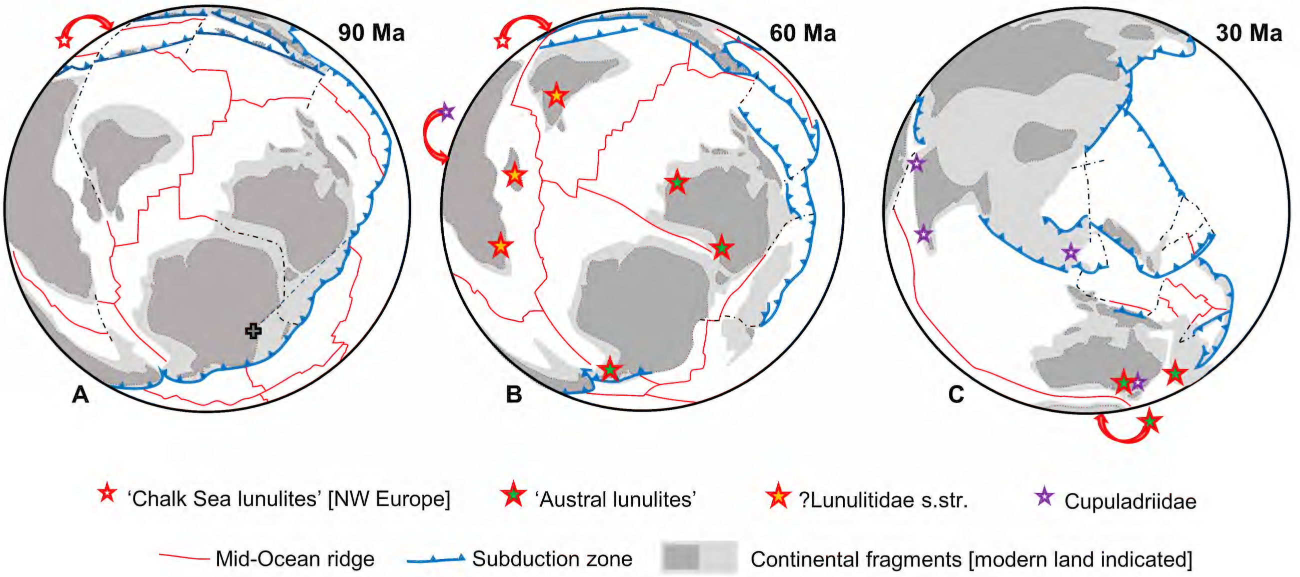

Figure 6. Consecutive plate configurations (simplified from Müller *et al*. 2021) as background for the distribution of lunulite bryozoans from their first appearance in the Late Turonian, in the European Chalk Sea, through to the early Neogene. **A**, The early part of the Chalk Sea; few lunulites and only in northern Europe and Asia. The rough position of the 90 Ma South Pole is indicated (with a cross), with only limited subsequent change in position. **B**, Encompassing the rapid change across the Mesozoic–Cenozoic transition (including data for the period Maastrichtian – Early Eocene). **C**, Encompassing the comparatively short period with invasion of Austral lunulites into southern South America (Late Oligocene – Middle Miocene). Note the continuous isolation of the Australia – Antarctica – New Zealand – southern South America remnants of Gondwana locked in high latitudes traditionally considered unsuited for lunulite bryozoans.

these Austral lunulitids to the family Selenariidae (see below).

The Austral free-living bryozoans appear to have remained largely isolated from external influences throughout most of their history, a proposition hinted at previously by Cook & Chimonides (1985b) and Bock & Cook (1998), for example. Whereas such propositions were based primarily on ancient and modern distributions of the different groups, they are consistent with Australia's post-Gondwanan history of isolation (Fig. 6). By the time the first free-living cheilostome bryozoans evolved in Eurasia (in the latest Turonian), only Australia and Antarctica, with New Zealand still attached, formed an isolated, southern continent within a major ocean including a cold-water barrier across Antarctica and into South America (see e.g., Müller *et al*. 2019). Late Paleogene separation between these three terranes sent Australia and New Zealand on somewhat different northward trajectories preceding the post-Miocene closure of the Tethyan Ocean north of Australia, with only a few, narrow deep-water straits across the Indonesian archipelago remaining (e.g., Barber *et al*. 2000). In short, these terranes did not reach a position facilitating at least some warm, shallow water connections to the rest of the world until the Middle Eocene (specifically southeast Asia, as shown by the first occurrence of warm-water benthic foraminifera in Australia; Haig *et al*. 1997). Prolonged isolation of the shallow marine margins of the Australian continent, commencing well before the appearance of the first lunulite bryozoan in Europe, supports the notion that the 'Austral lunulites' evolved into free-living organisms independently, with none of the traits particular to this mode of life inherited from other free-living clades. Importantly, this therefore provides an independent parallel to the simultaneous evolution of such traits in the Lunulitidae *s. str.* and the Cupuladriidae (Håkansson *et al*. 2019).

The origin of the distinct Austral group of free-living bryozoans remains somewhat ambiguous due to a patchy early fossil record. The Late Aptian record of *Lunulites abnormalis* Etheridge 1901 from Queensland was refuted by Håkansson *et al*. (in press) in the absence of the original and only known, but poorly described and illustrated, specimen. The potentially earliest known appearance is a record referred to the uppermost Maastrichtian Miria Formation (following terminology of Hocking *et al*., 1987) in the Southern Carnarvon Basin of Western Australia, as reported by Cook & Chimonides (1986). Unfortunately, according to their labels, these two specimens were collected loose, leaving the possibility that they may belong to the earliest substantiated free-living fauna, comprising at least 10 species-level taxa from the Thanetian Boongerooda Greensand Member of the Cardabia Calcarenite (following terminology of Hocking *et al*., 1987; EH collections; see 'Origin of the Austral lunulite hotspot' below).

Nevertheless, by the Late Eocene all modern families of lunulite bryozoans in the Austral Realm were already established in the significant expansion of Austral free-living genera, with dominance and diversity peaks shifting to southeastern Australia and, in the Oligocene, to New Zealand, thereby forming an independent Austral lunulite hotspot that reached its diversity maximum in the Miocene (Bock & Cook 1999). Around the same period, the Austral free-living fauna experienced a brief interval of extra-continental expansion into southern South America, possibly facilitated by a more favourable Late Oligocene – Middle Miocene temperature regime (see 'The South American connection' below).

Even though it appears unlikely that any Austral free-living taxon has a free-living ancestral connection outside the region (the apparently Miocene immigrant *Cupuladria guineensis* Busk 1854 being the exception), the group is probably polyphyletic, reinforcing the conclusion that becoming a free-living bryozoan may be relatively easily achieved. We currently consider the following family level clades to have originated in the Austral Realm: Lunulariidae, Selenariidae and 'Otionellidae *sensu australis*' (amended, see below), all of which are

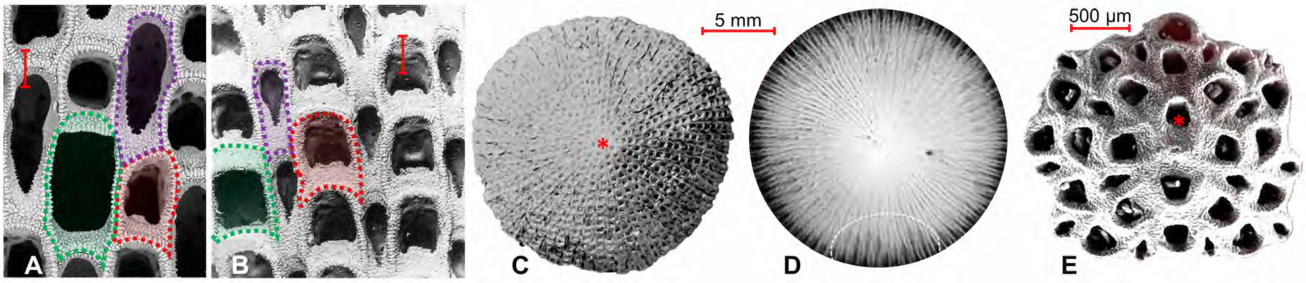

Figure 7. Selected species of Lunulariidae. **A**, *Lunularia repanda* Maplestone 1904; Investigator Strait, South Australia, recent. Detail showing zooidal morphology, note the significant size increase in female zooids. **B**, *L. capulus* (Busk 1852a); recent; detail showing zooidal morphology; note that female zooids are externally recognisable only by their slightly enlarged, square opesia. **C**, *L. capulus* (Busk 1852a); recent; frontal side of small, mature colony with perfect radiating symmetry (ancestrula marked with red asterisk), and **D**, X-ray image of the same colony revealing the distribution of the internally enlarged female zooids (diffuse, light grey shades) in incomplete circles near the margin of the colony; one cluster indicated by thin white stipples. Note the complete lack of a substrate. **E**, *L. capulus* (Busk 1852a); (from NHMUK 1984.12.24.71, recent; Juvenile colony). Zooidal colour codes (Figs 7–10): autozooids red, vibracula purple, female zooids (ovicells) green, male zooids blue. Scale bars: **A**, **B** 200 µm. (**A**, **B** courtesy Phil Bock, Melbourne, **E** courtesy P. J. Chimonides, NHM London).

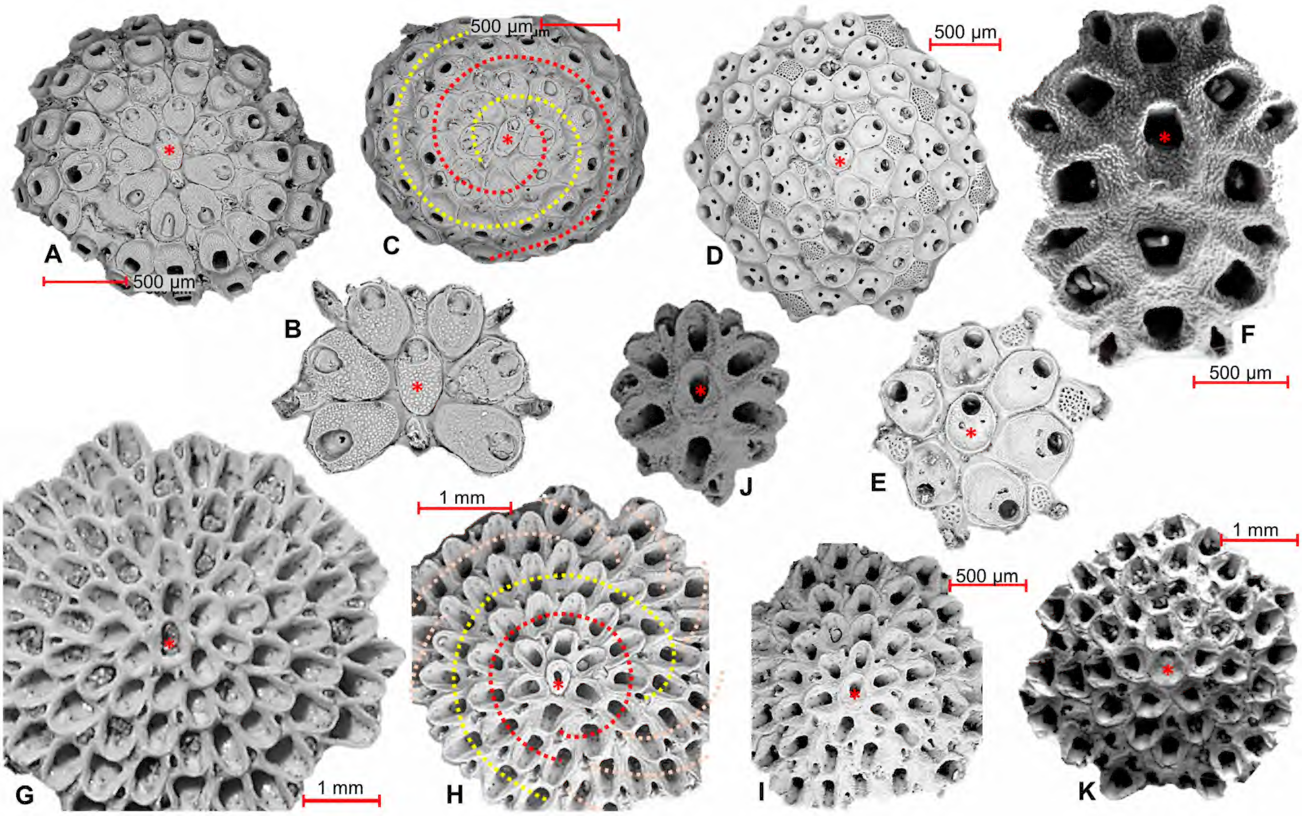

Figure 8. Colony architecture and growth pattern in selected free-living Austral species (ancestrula indicated with red asterisk). **A**, **B**, *Otionellina cupula* (Tennison Woods 1880); Victoria, Miocene. Frontal side of complete colony, with the ancestrular complex magnified (**B**); note closure of the central zooids. **C**, *Helixotionella spiralis* (Chapman 1913); Victoria, Miocene). Frontal side of complete colony, with the two spiral budding rows indicated (red and yellow stipple). **D**, **E**, *Selenaria punctata* Tennison Woods 1880; New South Wales, recent. Frontal side of complete colony, with the ancestrular complex magnified (**E**). **F**, Ancestrular complex of *Lunularia capulus* (Busk 1852a); from NHMUK 1984.12.24.71, recent; cutout from Figure 6 E. **G**, *Discoradius*(?) *rutella* (Tenison Woods 1880); Victoria, Miocene. Complete colony with radiating budding; note the four vibracula in association with the ancestrula. **H**, *Kausiaria magna* Bock & Cook 1998; Victoria, Late Eocene. Frontal side of complete colony with the complex spiral growth pattern indicated, with the ancestrular complex magnified (**E**). **I**, **J**, *K. jamesi* Bock & Cook 1998; Victoria, Late Eocene. Complete colony showing the more traditional radial budding pattern. **K**, Complete colony of *Petasosella lata* (Tennison Woods 1880); Victoria, Miocene. (Images courtesy Phil Bock, Melbourne, except **J**, courtesy P. J. Chimonides, NHM, London, and **G**).

well known from Upper Eocene to recent strata (see Bock & Cook 1998, 1999 & references therein). Ongoing work on the undescribed faunas from the Thanetian and Maastrichtian(?) in Western Australia should add at least two new families from the Thanetian (presented informally below) and possibly an additional new family from the Maastrichtian.

Lunulariidae Levinsen 1909

The monogenetic Family Lunulariidae Levinsen 1909 (Figs 7, 8 F) is known from the Late Eocene to modern faunas in Australia and from the Miocene onwards in New Zealand (Bock & Cook 1998). Female zooids (barely distinguishable from the exterior in some species) are interiorly expanded to accommodate the ovisac for brooding large, presumably nutrient-packed, larva (Cook & Chimonides 1986). This, in turn, allows for a prolonged metamorphosis leading to a large ancestrular complex with up to 12 autozooids (ordinary feeding zooids) before the onset of feeding (EH unpublished data on *Lunularia capulus*, *in* Cook & Chimonides 1986). Despite several clear statements to the contrary (e.g., Bone & James 1993), the ancestrular complex is consistently found without a substrate (Håkansson 1981; Cook & Chimonides 1986; Cook *et al*. 2018b).

Lunularia Busk 1884 is close to the genus *Lunulites*, in many ways, with several morphological features resembling members of both the 'Chalk Sea lunulites' and the Lunulitidae. Conversely, the presence of an interior ovisac seemingly parallels the reproductive life history strategy of the Cupuladriidae (cf. Ostrovsky *et al*. 2009; Ostrovsky 2013, and references therein). Members of this genus form some of the largest known free-living colonies, reaching diameters over 7 cm, as estimated from the size of fragmented colonies (EH data, from the Geology collections at University of South Australia, Adelaide). The ancestrula is comparable in size to the periancestrular autozooids, and there are no vibracula in direct contact with the ancestrula.

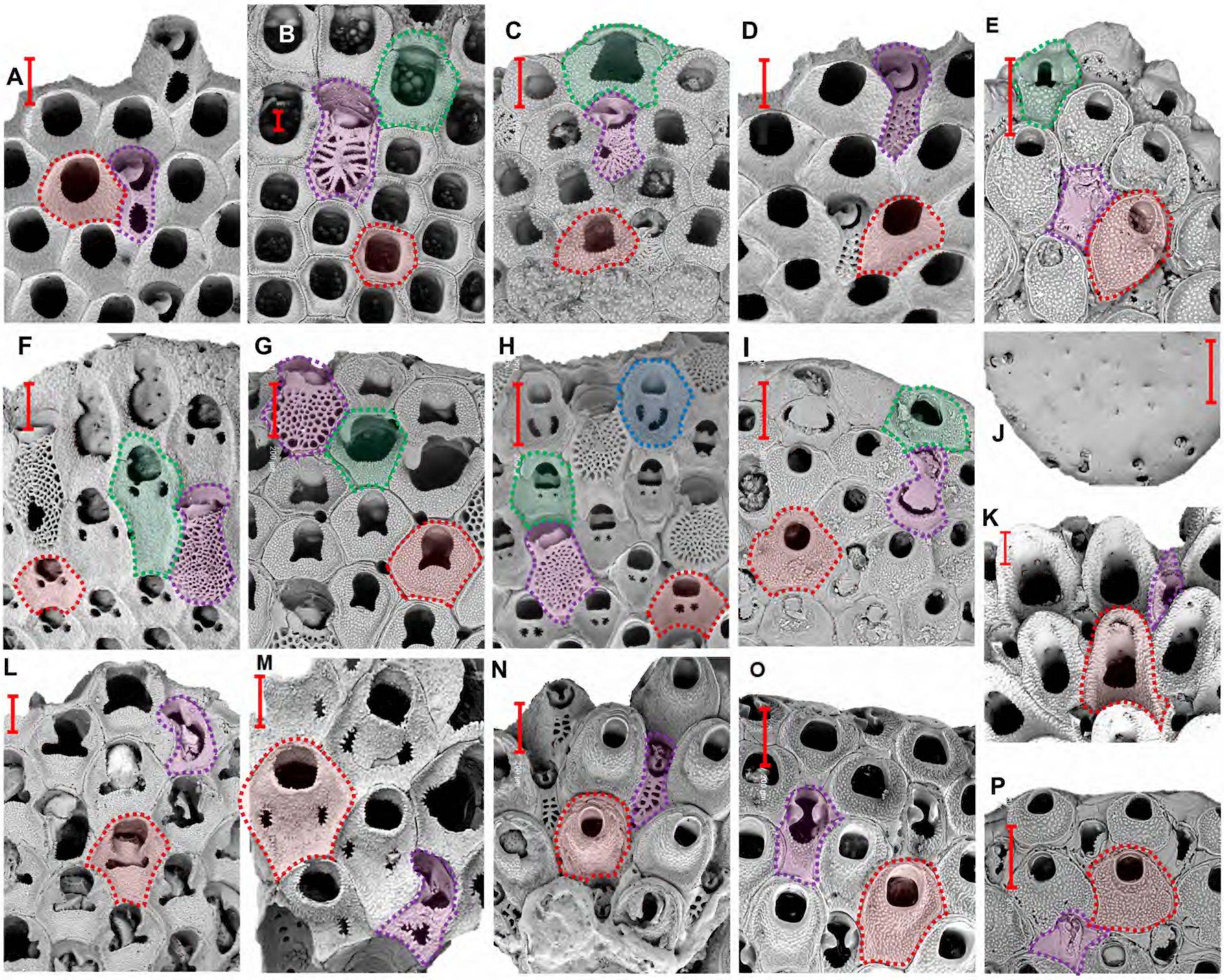

Figure 9. Selected Recent and fossil species of Selenariidae (**A**–**H**) and 'Otionellidae *sensu australis*' (**I**–**P**) illustrating the range of zooidal polymorphism characterising these families: two to four types of zooids in the Selenariidae, and two to three types in the 'Otionellidae *sensu australis*'. **A**, *Selenaria concinna* Tennison Woods 1880; Victoria, recent. **B**, *S. hexagonalis* Maplestone 1904, Investigator Strait, South Australia, recent. **C**, *S. verconis* Parker & Cook 1994; Victoria, Miocene. **D**, *S. kompseia* Cook & Chimonides 1987; New South Wales, recent. **E**, *S. initia* (Waters 1883); Victoria, Miocene. **F**, *S. bimorphocella*, Mapelstone 1904; South Australia, recent. **G**, *S. minor* Maplestone 1911; Victoria, recent. **H**, *S. punctata* Tennison Woods 1880; recent. **I**, **J**, *Helixotionella scutata* Cook & Chimonides 1984b; Western Australia, recent. **K**, *Kausaria magna* Bock & Cook 1998; Victoria, Late Eocene. **L**, *Petasosella alata* Tennison Woods 1880; Victoria, Miocene. **M**, *P. magnipunctata* (Maplestone 1904); Victoria, Miocene. **N**, *Otionellina squamosa* (Tennison Woods 1880); New Zealand, Pleistocene. **O**, *O. australis* Cook & Chimonides 1985; Victoria, recent. **P**, *H. spiralis* (Chapman 1913); Victoria, Miocene. (Scale bars 200 µm; zooidal colour codes as in Fig. 6. Images courtesy Phil Bock, Melbourne).

Selenariidae Busk 1854

The monogenetic Family Selenariidae Busk 1854 (Figs 8 D, E, 9 A–H) spans the Late Eocene to present, with many Australian species. In addition, a single, recent species was reported from New Zealand (Bock & Cook 1999), and there are at least two taxa from southern Argentina and Chile of Early and Middle Miocene age, respectively (López-Gappa *et al*. 2017; EH collections). The family is characterised by advanced sexual polymorphism with distinct male and female zooids in many taxa (Cook & Chimonides 1985a, 1985b, 1987; Bock & Cook 1999, and references therein).

Selenaria Busk 1854 is characterised by the zonal distribution of sexual polymorphs and large, scattered, commonly highly complex vibracula (significantly fewer than autozooids), with long setae observed to facilitate locomotion in several species (Cook & Chimonides 1978). The frontal walls of both autozooids and vibracula are highly variable. The ancestrula is comparable in size to the periancestrular autozooids and there are typically no vibracula in direct contact with the ancestrula (Fig. 8 E).

'Otionellidae *sensu australis*'

At present the family Otionellidae Bock & Cook 1998 (Figs 8 A–C, H–K, 9 I–P) contains five genera: the nominate genus *Otionella* Canu & Bassler 1917; *Otionellina* Bock & Cook 1998; *Helixotionella* Cook & Chimonides 1984b; *Petasosella* Bock & Cook 1998; and *Kausiaria* Bock

& Cook 1998. However, the nominal genus of the family Otionellidae only accommodates a few closely related species from the Middle Eocene to Lower Oligocene in North America, whereas all other genera have a distinct Austral distribution. In our opinion, biogeography as well as pronounced morphological differences suggest a separation between a restricted, North American family Otionellidae *s. str.*, and a strictly Austral, – as of yet – unnamed, family, here provisionally referred to as 'Otionellidae *sensu australis*'. It includes at least four genera, three of which were also briefly present around southern South America (Canu 1904; Bock & Cook 1998; Pérez *et al.* 2015; EH collections). Based on the distribution of the periancestrular autozooids and vibracula, these genera may be further subdivided into two groups: one without vibracula in direct association with the ancestrula (*Petasosella* and *Kausaria*), and the other with a distolateral and proximal vibraculum in direct contact with the ancestrula (*Otionellina* and *Helixotionella*). Based on morphological similarities in the skeletal structure of the vibracula, as well as sexual polymorphism (Fig. 9), it is possible that the latter group of this geographically restricted and currently unnamed family shares a common ancestry with the Selenariidae.

Petasosella Bock & Cook 1998 (Figs 8 K, 9 L–M) is characterised by a radiating budding pattern with an ancestrula surrounded only by autozooids. The scattered vibracula are large and significantly less abundant than the autozooids. As no skeletal sexual polymorphism has been noted, brooding was possibly in interior ovisacs. The genus is known from the Upper Eocene to Recent of southeastern Australia and, plausibly, Upper Oligocene to Lower Miocene deposits in southernmost South America (Canu 1904; Bock & Cook 1998; EH collections).

Kausiaria Bock & Cook 1998 (Figs 8 H–J, 8 K) is characterised by comparatively large colonies, an ancestrula surrounded exclusively by autozooids, and a variable budding pattern, as radial or composite sinistral spirals (Figs 8 D & I, respectively). The vibracula are small and equivalent in number to autozooids. Colonies consistently lack a substrate. The genus is known from the Upper Eocene to Miocene of southeastern Australia, and from the Upper Oligocene to Lower Miocene of southernmost South America (EH collections).

Otionellina Bock & Cook 1998 (Figs 8 A, B, 9 N–O) is characterised by its compact, almost lenticular colonies, with abundant, small vibracula (equal in numbers to autozooids), which are commonly developed also along the colony margin and the basal side of the colony. The ancestrula characteristically has one distal and one proximal vibraculum (Fig. 8 B). The genus—or close relatives—is known from the Thanetian of northwestern Australia (see new informally designated "Family X below), from the Middle Eocene – Recent in southeastern Australia (Bock & Cook 1998, 1999; Schmidt 2007), from the Oligocene – Recent in New Zealand (Bock & Cook, 1999), and from the Upper Oligocene to Middle Miocene in southern South America (Canu 1904; Pérez *et al*. 2015; EH collections), as well as, possibly, from Lower Eocene deposits in Antarctica (Hara *et al*. 2018, their fig. 7, only).

Helixotionella Cook & Chimonides 1984b (Figs 8 C, 9 I–J, P) is characterised by its unusually small, typically lentil-shaped colonies, abundant small vibracula (equal in number to autozooids) and a spiral budding pattern, with two distinct, dextral budding series. The budding series are initiated from the two vibracula associated with the ancestrula. In late astogeny the budding series may bifurcate, and all or most budding series are associated with a (terminal) vibraculum on the basal side of the colony, strongly suggesting terminate growth of the colonies. The genus is known from the Upper Eocene to recent of southeastern Australia, with a potential relative in the Thanetian of northwestern Australia (see "Family X" below).

Incertae sedis

As outlined above, the genus name *Lunulites* has been variously applied also to Austral free-living taxa. Most have subsequently been referred to the endemic Austral genera listed above, but one fossil taxon—quite widespread in the Australian Paleogene and Neogene successions—remains largely unaccounted for in terms of its taxonomic phylogenetic affiliation. Originally described as *Lunulites rutella* Tenison Woods, 1880 (Fig. 8 G), this species has usually been referred to as *Lunulites*, albeit commonly with some reservation (see Bock & Cook 1999, & references therein), but recently it has been transferred to the new genus *Discoradius* Di Martino, Greene & Taylor 2017a, again with some reservation (Di Martino *et al*. 2017b). In our opinion, the zooidal morphology suggests a closer relationship to the austral genus *Kausiaria*. However, the unique early astogeny, with three, or occasionally four, small periancestrular vibracula (a disto-lateral pair of vibracula directed proximally, plus one or two proximal vibracula), suggest yet another independent free-living Austral clade.

New "Family X"

This family (in prep.; Fig. 10 A–G) is thus far known only from the Thanetian and possibly Ypresian of the Southern Carnarvon Basin. Taxa referred to the family are interpreted to have been free-living without setal support (free-lying) and without a substrate, a condition otherwise common only in the Late Cretaceous, Northern European Chalk Sea (Håkansson 1975). This new Austral clade has perhaps four different species all sharing essentially identical zooid morphology, but with significant differences in colony architecture—they resemble most free-lying bryozoans from the Chalk Sea in that they lack setal support, and presumably went through metamorphosis without the physical support of a substrate. To what extent the considerable architectural variation within this new family warrants recognition of more than a single genus is still under consideration.

Two members of this new clade are illustrated here. New species *a* (Fig. 10 A–C) is characterised by small (up to ~4 mm diameter) domed to hemispherical colonies with a consistent budding pattern. The early stage is characterized by a gradually expanding fan-shaped growth pattern with the ancestrula in a marginal position which then, after three budding generations, changes into a radial budding pattern gradually bringing the ancestrula into a more central position (cf. Fig. 10 A). When mature, a single ovicell (brood chamber) may develop from the ancestrula through partial skeletal resorption also involving the distal zooid (Fig. 10 C) in a process and position otherwise unknown in the phylum. In contrast, new species *b* (Fig. 10 D–G) has a budding

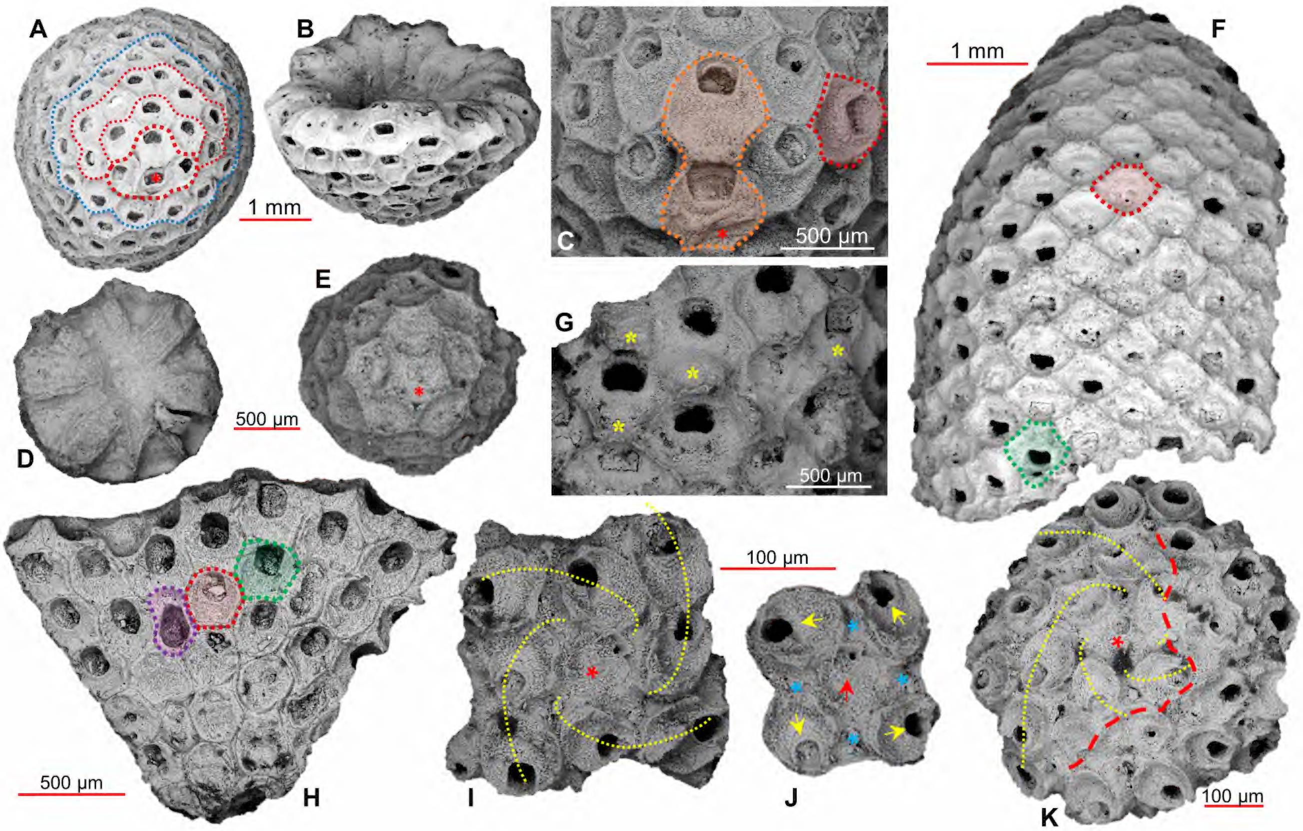

Figure 10. Selected free-living taxa from the Thanetian (Paleocene) of the Southern Carnarvon Basin, Western Australia. **A**–**G**, New "Family **X"**; two unnamed taxa illustrating the morphological range of the family. **A**–**C**, New "species ***a***". **A,** Mature colony; the early fan-shaped growth stages outlined in red stipples (ancestrulas with red asterisk; ancestrular complex with thick stipple), and the first, subsequent stage with radial budding outlined in blue stipple. **B**, Oblique lateral view of the same colony showing the hollow, hemispherical shape. **C**, Detail of the ancestrular region of the same colony showing the single, ovicell complex (orange shading) developed from the ancestrula (red asterisk) late in astogeny, through partial skeletal resorption in the distal autozooid. **D**–**G**, New "species ***b***". **D**, Basal view of juvenile, star-shaped colony demonstrating the symmetric budding pattern radiating from the ancestrula. **E**, frontal view of juvenile colony, maintaining the strict radial budding pattern from the central ancestrula (red asterisk). **F**, Lateral view of a large fragment of a mature colony demonstrating the highly unusual, tall to near cylindrical colony. **G**, Detail of the mature part of the same colony with several ovicells/female zooids (yellow asterisks). **H**–**K**, Two unnamed taxa referred to the provisionally named 'Otionellidae *sensu australis*'. **H**, cf. *Otionellina* n. sp., fragment of discoidal colony with radial budding showing zooidal details. **I**–**K**, aff. *Helixotionella* n.sp. **I**, Complete juvenile colony comprising the first two zooids in each of the four sinistral spiral budding rows (ancestrula indicated with red asterisk, budding rows in yellow stipples). **J**, Cutaway detail of **I** showing the distribution and relative orientation of the ancestrula (red arrow), the initial four autozooids (yellow arrows, indicating orientation) and the four primary vibracula (blue asterisks). **K**, Complete, regenerated colony, with spiral budding (yellow stipples) in the original part of the colony (including the ancestrula, red asterisk) and chaotic budding in the regenerated part (fracture line in red stipples). Additional zooidal colour code as in Figure 6**.**

pattern with a central ancestrula from the onset (Fig. 10 E) and a subsequent, perfectly radial budding symmetry (Fig. 10 D) that rapidly turns the colony into a tall (>1 cm), hollow column with near parallel sides (Fig. 10 F), maintained through a slow increase in the number of budding series. The ancestrula consistently occupies its original, central position at the apex of the column and, unlike species *a*, this taxon develops multiple ovicells in female zooids in a more 'normal' position, several budding generations from the ancestrula (Fig. 10 G).

The remaining, less abundant, free-living taxa from the Boongerooda Greensand consist of several, apparently not closely related taxa, all (potentially) possessing vibracula. The early history of free-living bryozoans in Western Australia is based entirely on taxa yet to be formally described, although there are morphological features indicating that some of these pioneers may be directly related to well-established entities in the later, more fully known Austral faunas—two such examples are illustrated (Fig. 10 H–K).

The taxon "new genus and species aff. *Otionellina*" (in prep.; Fig. 10 H) has flat, discoid colonies with zooids confined to one side, radial budding, and resembling *Otionellina* in its zooid morphology and in the absence of a substrate; however, these specimens lack the thick, lenticular shape and basal side vibracula characteristic of that genus. The autozooids have a depressed, granulated cryptocyst with a large, terminal opesium; ovicells are recognised by their low, hood-like structure distal to the opesium, combined with a more angular, almost quadratic outline of the opesium. The vibracula are large, typically initiating budding rows, and they are mostly slightly asymmetrical with variously developed condyles. Pending information on the early astogeny, this taxon may represent either an early member of the genus *Otionellina* or a new, related genus.

The taxon "new genus and species aff. *Helixotionella"* (in prep.; Fig. 10 I–K) is characterised by its minuscule colonies (mostly <1 mm) with abundant vibracula (equaling autozooids in number) and a spiral budding pattern with four sinistral budding series, each initiated from one of the four vibracula associated with the ancestrula. The taxon is known only from the Thanetian of northwestern Western Australia, and provisionally we consider it to be a relative of, and potential ancestor to, *Helixotionella*.

ORIGIN OF THE AUSTRAL LUNULITE HOTSPOT

Considering the known distribution of fossil free-living bryozoans within the Austral Realm (see comprehensive summaries in Bock & Cook 1998, 1999, supplemented by EH collections from South America, Australia, and New Zealand), the origin of this evolutionarily isolated lunulite cluster was likely the northwestern margin of the Australian continent, in the proximal part of the broad, gently sloping shelf bordering the Indian Ocean in a configuration resembling that of the present. Reflecting its proximal position on this platform, the stratigraphic succession containing these faunas is significantly condensed with sediment accumulation restricted to transgression maxima (Fig. 11). Thus, the two main intervals from which free-living bryozoans have been reported—the Upper Maastrichtian Miria Formation (Cook & Chimonides 1986; two loose specimens) and the immediately overlying Thanetian Boongerooda Greensand Member (EH collections), initiating the Thanetian–Ypresian Cardabia Calcarenite—are both thin (up to a couple of meters), but separated by a significant lacuna across the Mesozoic–Cenozoic boundary interval (Fig. 11).

The two specimens with a lunulite morphology allegedly originating from the Maastrichtian Miria Formation share a dubious provenance. Notwithstanding that their labels indicate they were collected from loose material, it refers them to the Miria Formation (WAM, 80.648 & 80.649, "Miria Marl, Cardabia Station": Cook & Chimonides 1986; Fig. 12). However, there is no adhering sediment to support this assignment and, as seen from Figure 11 it is equally plausible that they originated from the younger Boongerooda Greensand Member and were simply mislabeled. Both specimens are unequivocally free-living, but are poorly preserved, allowing only a limited certainty as to their taxonomic position. Specimen WAM 80.649 (Fig. 12 A–C) may be an early relative of *Otionellina* (cf. Figs 8, 9), but WAM

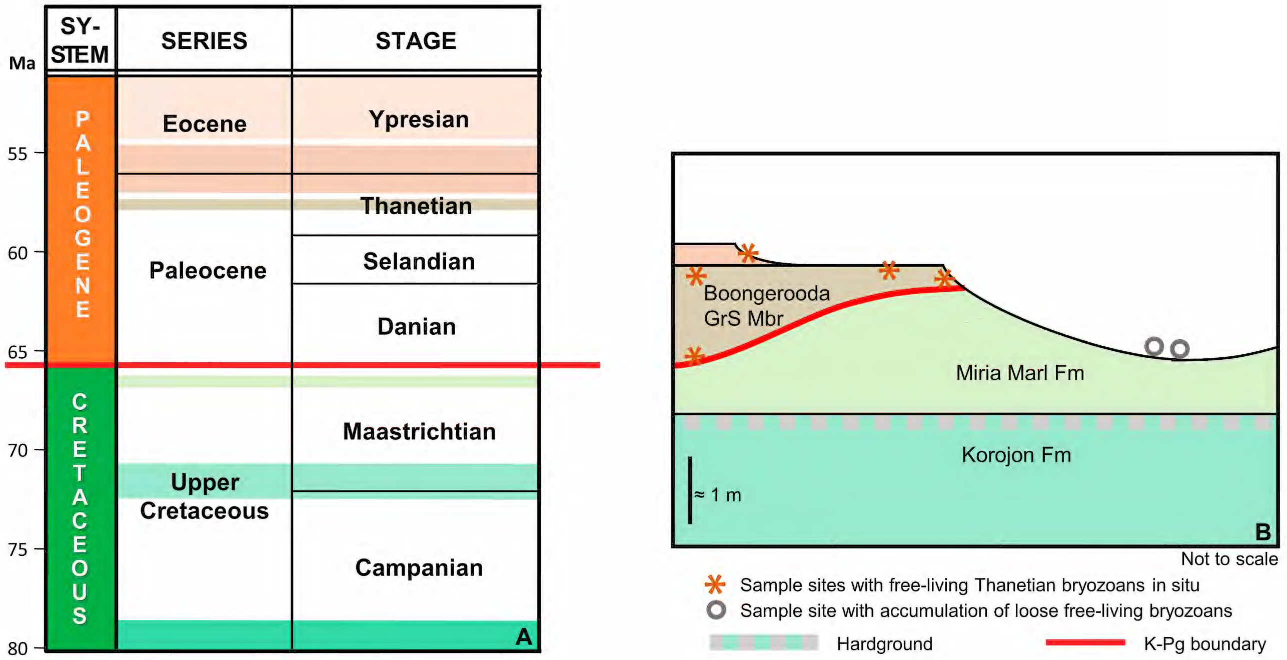

Figure 11. Stratigraphy of the Upper Cretaceous – Lower Paleogene succession in the onshore part of the Southern Carnarvon Basin on the northwestern margin of the Australian continent. **A**, Chronostratigraphic chart covering the Upper Cretaceous and Paleogene strata in the Giralia Anticline. Note the frequent and extensive breaks in accumulation reflecting the position of this succession in the proximal part of a passive continental margin. **B**, Highly stylised cross section illustrating the field relations of the strata investigated. Asterisks indicate levels yielding free-living in situ bryozoans; grey circles indicate the location of loose specimens, including the two allegedly Late Maastrichtian specimens illustrated in Fig. 12; red line shows the end-Cretaceous mass-extinction event; GrS Mbr = Greensand Member; Fm = Formation.

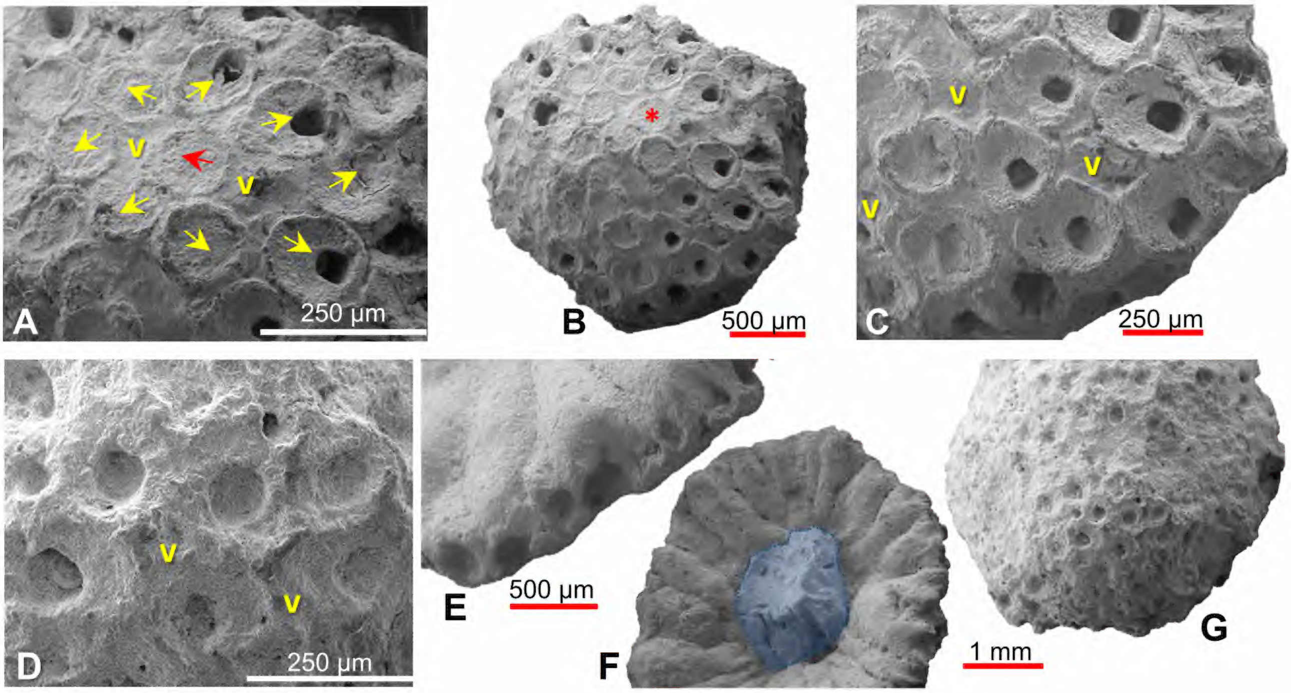

Figure 12. Possibly the oldest lunulite bryozoans from Australia, collected loose and for untold reasons referred to the Upper Maastrichtian Miria Formation (see text). **A**–**C**, Early, potential representative of 'Otionellidae *sensu australis*'; WAM 80.649. **A**. The periancestrular region with arrows indicating the interpreted orientation of the ancestrula (red arrow) and the early autozooids; two potential vibracula marked (v). **B**. Overview, centred around the best-preserved part of the frontal surface; ancestrula indicated. **C**. Colony margin with several well-preserved autozooids and scattered, variously preserved vibracula (v). **D**–**G**, Indeterminate lunulite colony; WAM 80.648. **D**. The 'best' preserved part of the frontal side providing enough detail of the autozooidal morphology to exclude the likeliness of conspecificity with WAM 80.649; potential vibracula indicated (v). **E**. Oblique basal view of the well-preserved colony margin. **F**. Basal surface of the colony displaying distinct budding rows with secondarily thickened calcitic walls and widely scattered minute pits, which may represent basal pores; note the sand-sized substrate (shaded blue). **G**. Overview, showing the seriously corroded frontal side of the colony.

80.648 (Fig. 12 D–G) does not resemble any of the free-living taxa in the overlying Boongerooda Greensand, suggesting it could be Maastrichtian in age. Moreover, the moderately rich free-living fauna from the Thanetian Boongerooda Greensand is reasonably well preserved, and has clear ties with the later, better-known Austral free-living faunas—most obviously, but not exclusively, with the family 'Otionellidae *sensu australis*'. Here, the taxonomic and stratigraphic status of the two specimens referred to the Miria Formation is left open, pending further investigation.

THE SOUTH AMERICAN CONNECTION

Prior to the Late Oligocene, the record of free-living lunulite bryozoans is poor in South America with just a single Paleocene species of *Discoradius* from northeastern Brazil (Buge & Muniz 1974; Di Martino *et al*. 2017b). However, during part of the Early to Middle Miocene, a moderately diverse cupuladriid fauna coexisted with the Austral emigrants around the southern part of the continent (Fig. 13 A), commencing at a time where the Cupuladriidae were rare in the rest of the world. However, both groups are today absent from this part of the continent, probably because of considerable late Miocene to Pleistocene cooling.

The Austral lunulite fauna in Upper Oligocene to Middle Miocene strata in southern Argentina and Chile is summarised as follows (Fig. 13 A). Approximately ten taxa with Austral connections have been distinguished: three species referable to *Selenaria*, one referable to *Otionellina*, two taxa closely associated with *Petasosella*, one referable to *Kausiaria*, as well as two taxa that may warrant the creation of new genera, one related to *Selenaria* and one possibly related to *Otionellina* (Canu 1904, 1908; Pérez *et al*. 2015; López-Gappa *et al*. 2017; supplemented by EH data). For all genera listed, these species represent the only record outside their Austral heartland, thus overwhelmingly pointing to a close faunal relation between the Austral and Magallanes biogeographic provinces during this period.

The existence of a significant Late Oligocene to Miocene marine connection between the Austral Realm and the South American Magallanes province has been pointed out previously, particularly based on various Mollusca that were thought to have dispersed in the circum-Antarctic Currents (e.g., Beu *et al*. 1997). Although the time of deep-water opening between Tasmania and Antarctica is reasonably well established at about the Eocene–Oligocene boundary, the Drake Passage between Antarctica and South America is less so, with estimates ranging from Late Eocene to Early Miocene (Scher

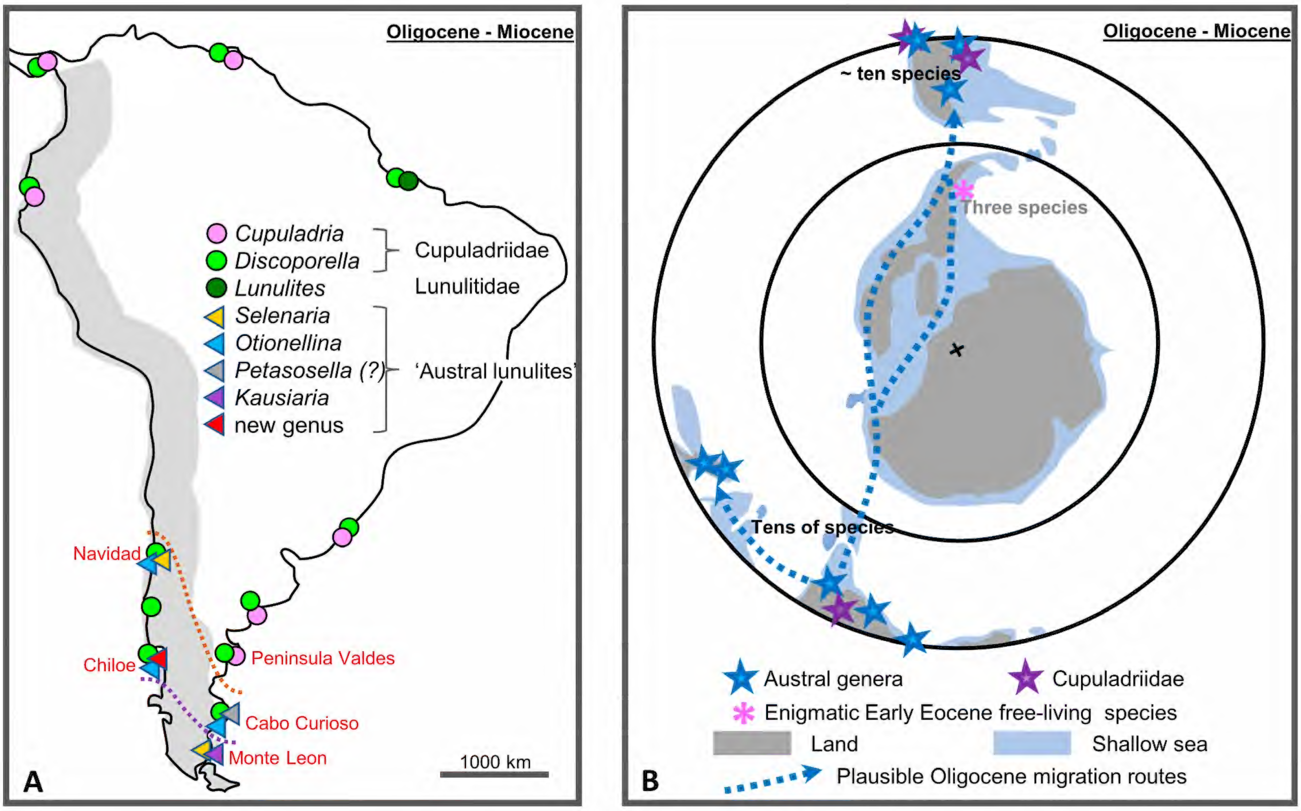

Figure 13. **A**, Distribution of free-living bryozoan taxa in South America during the Late Oligocene – Middle Miocene as presently known. Note the distribution of cupuladriids across the continent (except the most extreme south) overlapping significantly with the Austral genera in the southern part (Canu 1904, 1908; Pérez *et al.* 2015; López-Gappa *et al.* 2017; own observations). The apparent absence of cupuladriids between the known presence of Miocene cupuladriids in Ecuador and Navidad, Chile is likely to reflect insufficient sampling. However, the influence of cold upwelling along the west coast of South America somewhat comparable to the modern situation cannot be dismissed. **B**, Paleogeographic map showing a plausible migration route connecting the Austral Realm to South America via Antarctica; note that all cupuladriid taxa on either side of Antarctica arrived from the north, with no connections across the polar Antarctic seas. Note also that while there is a significant overlap at the genus level between the Austral Realm and southern South America, the three Early Eocene lunulite taxa from Antarctica (Hara *et al.* 2018) do not appear closely related to either of these regions (see text). The paleogeographic outline in **B** is based on Lawver & Gahagan (2003).

& Martin 2006; Dalziel *et al.* 2013; Hodel *et al.* 2021). Nevertheless, as pointed out by Casadio *et al.* (2010), faunal similarities between the Austral and Magallanes provinces declined after the establishment of the circum-Antarctic Current and, therefore, an alternative, shorter route of dispersal via the archipelago formed in the West Antarctic Rift System seems more likely (Fig. 13 B). Considering the assumed short-lived larval stages of modern lunulite taxa, this alternative seems more likely. Whereas rafting of bryozoans on kelp, debris and ships is widespread, one of the key elements in becoming free-living is precisely the opposite—a preference for minute, typically sand-seized substrates.

Three lunulite bryozoan species recently described from the mid-Ypresian of the Antarctic Peninsula (Hara *et al.* 2018) offer some support to the existence of an Austral connection across the West Antarctic Rift System, although just a single species—*Otionellina antarctica* Hara, Mörs, Hagström & Reguero 2018—potentially shows any relation to the core Austral province. Nevertheless, the mere presence of a free-living Antarctic bryozoan fauna clearly demonstrates that suitable habitats were present, providing supporting evidence for a trans-Antarctic route of migration between the Austral Realm and South America along the West Antarctica archipelago (Fig. 13 B; Casadio *et al.* 2010). To further complicate comparisons, it is emphasised that the Antarctic fauna of Early Eocene age is older than both neighbouring faunas and that it shows even less resemblance to the new Late Paleocene – earliest Eocene faunas from northwestern Western Australia.

AN OVERVIEW OF THE GLOBAL BIOGEOGRAPHY OF FREE-LIVING LUNULITE BRYOZOANS

The biogeography of the lunulite bryozoans has been a matter of interest over the years, with a series of distributional maps presented by Cook & Chimonides (1983, figs 3, 4) as the most comprehensive early attempt. Since then, information on the evolution and distribution of these bryozoans has increased considerably. The incorporation of the Austral cluster into the global biogeography of free-living bryozoans

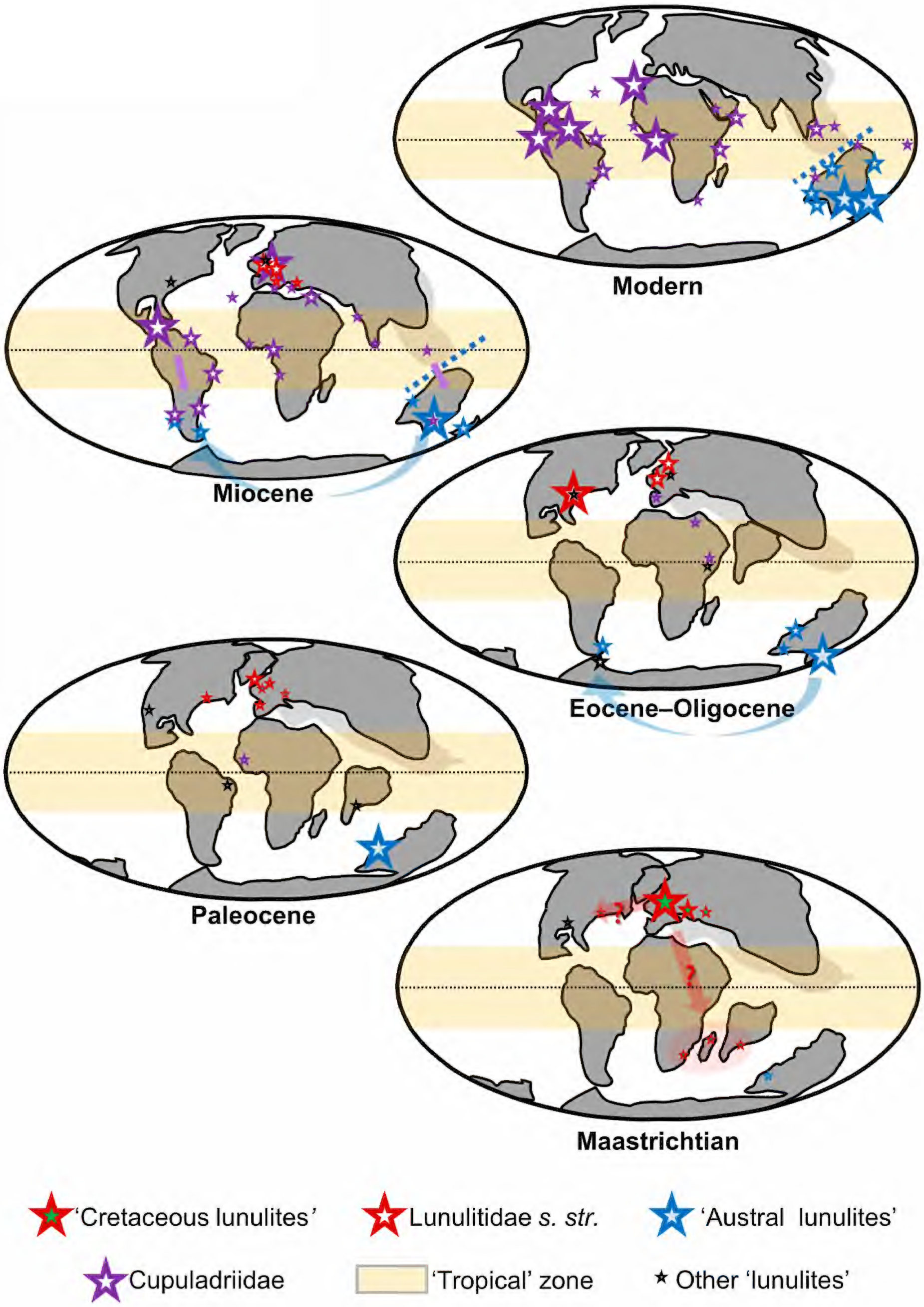

Figure 14. The biogeography of the free-living bryozoans in five steps. Maastrichtian: Global dominance of the Chalk Sea fauna in northern Europe, thinning rapidly towards the Chalk Sea extension into Central Asia; questionable connections to taxa in three Gondwana fragments and North America. Note the possible first trace of the Austral free-living group. Paleocene: The Paleocene 'dead zone' marks an all-time low in both density and diversity in the history of the free-living bryozoans, with the Thanetian fauna from northwestern Western Australia as the exception. Note the possible first trace of the Cupuladriidae in western Africa. Eocene–Oligocene: Re-emergence of lunulites in North America and Europe, developing two Lunulitidae hotspot, separate in both time and space (Fig. 15). The Austral hotspot expands to include New Zealand, with early colonisers in southern South America, coexisting with a few cupuladriids, still only sparingly present in the tropics of Africa and the Mediterranean region. Miocene: The diversity patterns shift dramatically, with a hotspot peak in the Austral Realm (now including the southern part of South America), while the Cupuladriidae is rapidly replacing the lunulites in hot- to warm-water areas across most of the globe. Modern: The Austral free-living hotspot maintains its high diversity level, but the clade is no longer present in South America. The Cupuladriidae have completely replaced the lunulites across the globe, with only a single species in Australia. Continent positions from Scotese (2014, PALEOMAP Project).

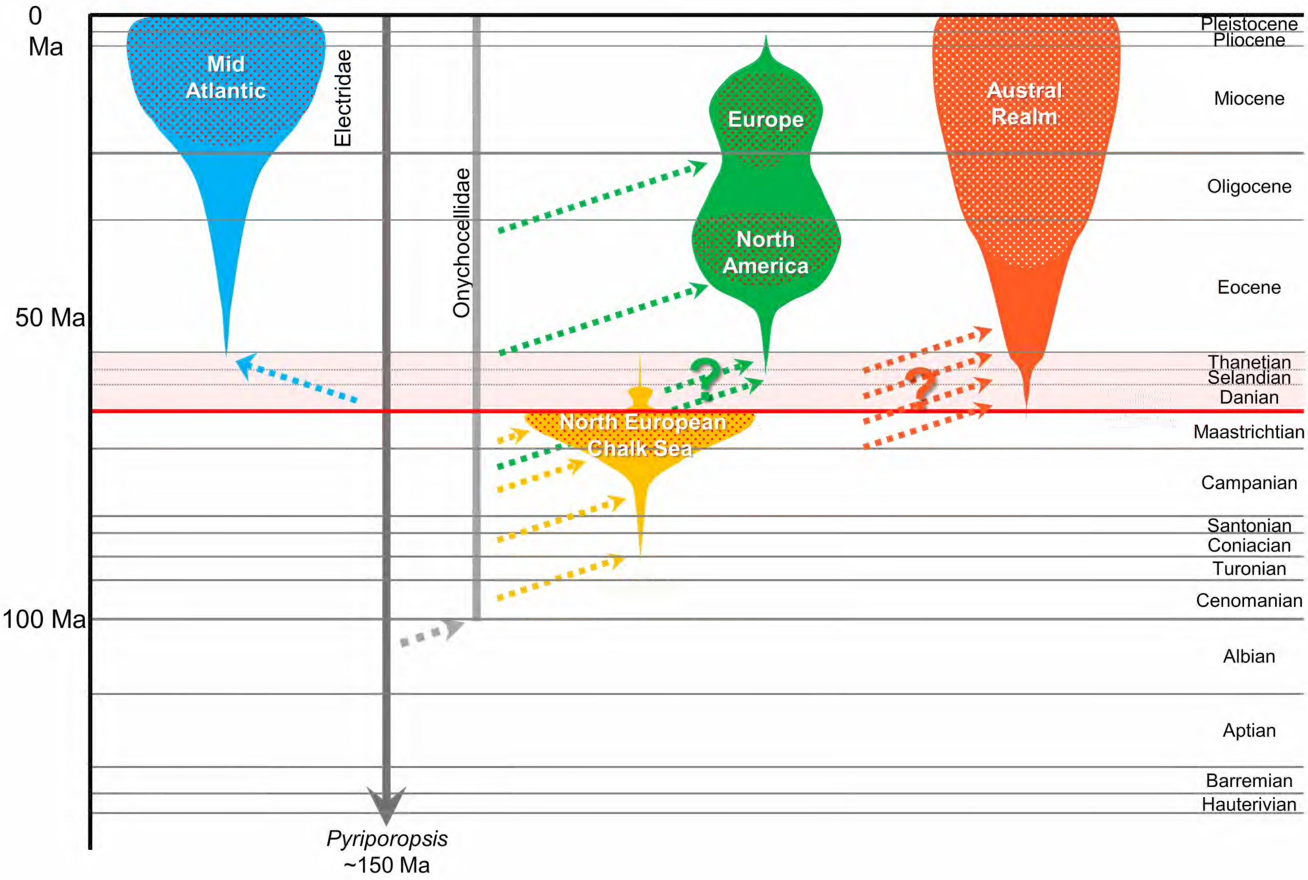

Figure 15. Lunulite hotspots in time and space, main lunulite clusters colour coded, with hotspots dotted. The first, and prominent lunulite hotspot developed in the North European Chalk Sea (yellow): Highly concentrated, 'within-basin', high-frequency iterative evolution, mainly—but not exclusively—from onychocellid roots. Peaks in the Maastrichtian, and terminated in the Maastrichtian–Danian faunal revolution, possibly without descendants. The Lunulitidae s.str. (green) has a longer and more complex story, apparently developing two distinct hotspots. Firstly, with a North American Gulf & Coastal Plains emphasis, with high densities combined with moderate diversity; peaks in the Middle to Late Eocene and fade away in the Oligocene. Secondly, a less prominent hotspot develops in Europe in the Miocene, seemingly independent from the North American hotspot. The strictly monophyletic Cupuladriidae (blue) develop a high-diversity, still-thriving, hotspot centred around the Mid Atlantic early in the Miocene. The origin of the polyphyletic Austral Realm lunulites (red) remains enigmatic due to a long history in plate tectonic isolation (Fig. 6); a prominent, still thriving hotspot was established by the Late Eocene with only a single non-Austral lunulite species present from the Miocene. The earliest cheilostome family (dark grey) and the likely family root of many lunulites (light grey) are included. Arrows indicate origin; stipples indicate probable iterative evolution.

is briefly summarised here in five time slots (Fig. 14), highlighting the unique status of this intriguing group as presented briefly herein. The pattern of shifting hotspots for the free-living bryozoan clades outlined below may, of course, be subject to revision following further investigations. Notwithstanding, with prominent hotspots in comparatively high latitudes, it is clearly at odds with the Tethys-centered temporal global hotspot pattern presented by Yasuhara et al. (2022).

Maastrichtian

On a global scale, the Chalk Sea fauna in northern Europe is unmatched in terms of the diversity of free-living bryozoans (Håkansson & Voigt 1995; & EH data). At least 100 free-living taxa may be recognised, including many specialised forms without setal support (Håkansson 1975). From its northern European hotspot (Fig. 15), this faunal element gradually diminishes to the southeast, towards the Central Asian branch of the Chalk Sea, where only a few lunulite species are found (Voigt 1962, 1967; Favorskaya 1987; Kvachko 1995; Koromyslova & Pervushov 2022). More isolated occurrences of lunulite taxa are known from North America (Ulrich 1901; P. Taylor pers. comm.) and the three separate Gondwana fragments India (*Lunulites annulata* Stoliczka, 1872; Guha & Nathan 1996), Madagascar (*Lunulites pyripora* Canu, 1922; Buge 1951) and South Africa (*Lunulites* sp., Taylor 2019). All three entities had separated from Australia well before the first appearance of any lunulite, with Africa and Madagascar remaining fairly close (Fig. 6). Nevertheless, the three Gondwanan species are quite distinct, and none appears obviously related to taxa from the European Chalk Sea. Note also the possible first appearance of the Austral free-living bryozoans in northwestern Western Australia referred to briefly herein.

As the Chalk Sea clades with some probability suffered near total extinction as a result of the two-step collapse of the long-lived northern European carbonate province and its unique chalk environment (Fig. 4), further exacerbated by the global effects of the K–Pg extinction event (Surlyk 1997; Håkansson & Thomsen 1999; O'Dea *et al*. 2011), the founding role of the few non-European Cretaceous clades is far from obvious due to the Paleocene 'dead zone'.

Why then was this fauna limited to the European Chalk Sea when there were many coeval flooded continents elsewhere? That most of these other regions received greater siliciclastic input than in the European seas obviously plays a role, but the long-lasting stability of the European Chalk Sea environment (30–35 Ma: Surlyk 1997) strongly suggests that the Chalk Sea fauna was uniquely adapted to this particular habitat (e.g., Surlyk 1972; Håkansson 1975; Håkansson & Thomsen 1999; Heinberg 2007). This is nevertheless surprising given subsequent radiations and dominations of similar siliciclastic shelf habitats by free-living bryozoans in subsequent epochs, and thus requires further exploration.

Paleocene

The Paleocene 'dead zone' marks an overall global low in the history of the free-living bryozoans (cf. Fig. 4) mirroring well-established declines in diversity in all bryozoan groups (e.g., Håkansson & Thomsen 1979, 1999; McKinney & Taylor 2001; Stilwell & Håkansson 2012; Moharrek *et al*. 2022) and other marine groups. In Europe, the last Danian remnants of the Chalk Sea province were home to only a few, rare species (Berthelsen 1962; Kvachko 1995), whereas Selandian and Thanetian free-living bryozoans are even more scarce, with four Thanetian taxa reported from Deep Sea Drilling Project site 117 at Rockall Bank (Cheetham & Håkansson 1972) constituting a post-Danian, Paleocene 'hotspot'. However, in marked contrast, the Thanetian fauna from northwestern Western Australia, briefly presented above, stands out as the single, remarkable exception in terms of both density and diversity.

Outside the Austral hotspot, there are therefore good reasons to explore the observation that no post-Paleocene free-living species seem to have pre-Paleocene ancestors and, further, to explore whether the groups 'Chalk Sea lunulites' and Lunulitidae *s. str*. might have coexisted during this comparatively brief interval of time. However, phylogenetic relationships between faunas have not been formally tested.

Somewhat later, in the late Paleocene–Eocene, the first rare representatives of the family Cupuladriidae appear in West Africa (Gorodiski & Balavoine 1961), heralding the global Neogene takeover by this group.

Eocene–Oligocene

The Eocene to Oligocene marked the re-emergence of typical lunulite bryozoans in and around the central north Atlantic, which rapidly developed into a hotspot (Fig. 15), at this time mostly formed by the more advanced and more homogenous group Lunulitidae *s. str*. characterised by their porous, aragonitic basal wall. The hotspot was with a distinct North American Gulf & Coastal Plains emphasis, with high densities combined with moderate diversity, possibly based on iterative evolution from onychocellid roots, peaking in the Middle to Late Eocene and fading away in the Oligocene.

The position of the coeval Austral hotspot changed to the southeastern part of the continent towards the end of the Eocene and expanded to include New Zealand; subsequently, in the latest Oligocene, the first, early Austral colonisers in southern South America appeared. Around Africa and in the Mediterranean, early members of the Cupuladriidae spread sporadically.

Miocene

During the Miocene diversity and distribution patterns shifted dramatically, with the Cupuladriidae rapidly replacing Lunulitidae *s. str.* (Fig. 15) within shallow tropical and subtropical waters across most of the globe bar the Austral Realm. Notwithstanding, a less prominent, seemingly independent hotspot of Lunulitidae *s. str.* developed across Europe overlapping with the rise of the cupuladriids. Further afield, only a single cupuladriid species, *Cupuladria guineensis* (Busk, 1854; Fig. 1 E) appears to have successfully crossed the Wallace Line into Australia while, somewhat later in the Miocene, several unrelated cupuladriid species reached southern South America. In Australia the Austral free-living bryozoan hotspot peaked in diversity during the Miocene, with a limited number of taxa also reaching the southern part of South America. It should be stressed that the cupuladriid taxa reaching their farthest south in Australia and southern South America, respectively, are not closely related, thus allowing the inference that the temperature tolerance levels were different for the Cupuladriidae and the free-living Austral clades.

Modern

The Lunulitidae *s. str.* went extinct in the Pliocene, thus terminating the minor Lunulitidae hotspot in Europe, while the two major Miocene hotspots persevered into the modern faunas. In southern South America, however, free-living bryozoans are no longer present. Rapid Late Neogene cooling may have caused their local extinction, but that does not explain why the Austral part of the fauna was not successful in progressing farther north in South America in accordance with their climatic preferences.

CONCLUDING REMARKS

As we have attempted to illustrate, the free-living lunulite bryozoans had a complex history of rise and demise, with several unrelated groups dispersing and evolving across many continents since the Late Turonian. Their fossils are generally well preserved, their colonial and zooidal characters allow high-level taxonomic differentiation, they are diverse but not excessively so, have modern representatives and are frequently abundant in marine assemblages.

This paper presents new data and a comprehensive review of published information to elucidate the tempo–spatial patterns and morphological evolution of the major free-living groups of bryozoans. Our key findings can be summarised as follows:

1. The fossil record reveals the rise, demise and evolutionary success of several free-living groups over many continents, from the Late Cretaceous (Turonian) to the present, with many of these groups dominating epifaunal loose sediment shelf habitats.
2. The transition to a free-living mode of life in cheilostome bryozoans appears to require only minimal morphological modifications, suggesting a relatively easy shift from a sessile lifestyle to a mobile one.
3. Remarkable morphological convergence among unrelated groups indicates that strong adaptive pressures on habitat, mode of life and growth have shaped the distinctive free-living form.
4. Despite the progress made in understanding the evolutionary history of free-living bryozoans, the relationships between early and subsequent groups remain unclear. Further research using phylogenetic approaches is needed to unravel these evolutionary connections.
5. The absence of free-living groups in high latitudes raises the possibility that the free-living mode of life is metabolically demanding. This observation may provide insights into significant local extinctions within the otherwise highly successful free-living cupuladriid bryozoans during the Cenozoic.
6. The study of free-living bryozoans presents a unique opportunity to explore many evolutionary and ecological questions. However, significant temporal and geographic gaps exist in our knowledge, limiting our ability to confidently understand patterns and processes. We therefore emphasise the importance of focusing on new collections and taxonomic treatments of free-living bryozoans throughout their extensive and intriguing history.

ACKNOWLEDGEMENTS

David Haig (The University of Western Australia) kindly read an early version of the manuscript and provided useful comments and suggestions, and we are grateful to the reviewers, Andrej Ernst (Universität Hamburg) and Abby Smith (University of Otago), for the helpful comments and suggestions provided. Phil Bock (Melbourne) generously provided most of the images of southeastern Australian free-living bryozoans, with additional images provided by the late P. J. Chimonides and Mary Spencer-Jones (Natural History Museum, London). Several SEM images of northwestern Western Australian free-living bryozoans were kindly facilitated by Helen Ryan (Western Australian Museum). We thank Felix Rodriguez and Brigida de Gracia for their help collecting the cupuladriid bryozoans and general assistance. AR is funded by the Università degli Studi di Catania through 'PiaCeRi-Piano Incentivi per la Ricerca di Ateneo 2020–22 linea di intervento 2'. This is the Catania Paleontological Research Group: contribution No. 505.

REFERENCES

Barber P H, Palumbi S R, Erdmann M V & Moosa M K 2000. Biogeography: a marine Wallace's line? *Nature* **406**, 692–693.

Berthelsen O 1962. Cheilostome Bryozoa in the Danian Deposits of East Denmark. *Geological Survey of Denmark, II Series*, **83**, 290 pp.

Beu A G, Griffin M & Maxwell P A 1997. Opening of Drake Passage gateway and Late Miocene to Pleistocene cooling reflected in Southern Ocean molluscan dispersal: evidence from New Zealand and Argentina. *Tectonophysics* **281,** 83–97.

De Blainville H M D 1830. Zoophytes. Pages 535–546 in G F Cuvier (ed.) Dictionnaire des Sciences naturelles, dans lequel on trate méthodiquement des differents êtres de la nature ... par plusieur professeurs du Muséum Nationale d'Histoire Naturelle et des autres principales écoles de Paris **60**. F. G. Levrault, Paris.

Bock P E 2022. The Bryozoa home page. *http://www.bryozoa.net*

Bock P E & Cook P L 1998. Otionellidae, a new family including five genera of free-living lunulitiform Bryozoa (Cheilostomatida). *Memorie di Scienze Geologiche* **50**, 195–211.

Bock P E & Cook P L 1999. Notes on Tertiary and Recent 'Lunulite' Bryozoa from Australia. *Memorie di Scienze Geologiche*, **51**, 415–430.

Bone Y & James N P 1993. Bryozoans as carbonate sediment producers on the cool-water Lacepede Shelf, southern Australia. *Sedimentary Geology* **86**, 247–271.

Buge E 1951. Bryozoaires. In: Collignon, M (ed.): Faune maestrichtienne de la Côte d'Ambatry (Province de Betioky), Madagascar. *Annales Geologiques du Service des Mines (Gouvernement Général de Madagascar et Dépendantes)* **19**, 87–88.

Buge E & Muniz G Da C B 1974. *Lunulites (Heteractis) barbosae* – nouvelle espèce de bryozoaire lunulitiforme (Bryozoa, Cheilostomata) du Paléocène du nord-est du Brésil. *Annales de Paléontologie, Invertébrès, Paris* **60**, 191–201.

Busk G 1852a. An account of the Polyzoa and sertularian zoophytes collected in the voyage of the "Rattlesnake" on the coast of Australia and the Louisiade Archipelago. Pages 343-402 *in* J MacGillivray, editor, *Narrative of the voyage of H.M.S. Rattlesnake commanded by the late Captain O. Stanley during the years 1846–1850* **1**. T. & W. Boone, London.

Busk G 1852b. Catalogue of marine Polyzoa in the collection of the British Museum. I. Cheilostomata. *Trustees of the British Museum (Natural History), London*. 1–54.

Busk G 1854. Catalogue of marine Polyzoa in the collection of the British Museum. II. Cheilostomata. *Trustees of the British Museum (Natural History), London*. 55–120.

Busk G 1884. Report on the Polyzoa collected by H.M.S. Challenger during the years 1873–1876. Part 1. The Cheilostomata. *Report on the Scientific Results of the Voyage of the H.M.S. "Challenger", Zoology* **10**, 1–216.

Cadée G C 1975. Lunulitiform Bryozoa from the Guyana Shelf. *Netherlands Journal of Sea Research* **9**, 320–343.

Canu F 1904. Les bryozoaires du Patagonien. Échelle des bryozoaires pour les terrains tertiaires. *Mémoires de la Société Géologique de France: Paléontologie* **12**, 1–30.

Canu F 1908. Iconographie des bryozoaires fossiles de l'Argentine. Première partie. *Anales del Museo Nacional de Buenos Aires, serie 3*, **10**, 245–341.

Canu F 1922. Bryozoaires. Pages 16–30 *in* Cottreau J, Paleontologie de Madagascar X. Fossiles Crétacés de la côte orientale. *Annales de Paleontologie* **11**. Paris.

Canu F & Bassler R S 1917**.** A synopsis of American Early Tertiary Cheilostome Bryozoa. *United States National Museum Bulletin* **96**, 1–87.

Canu F & Bassler R S 1919. Fossil Bryozoa from the West Indies. *Publications of the Carnegie Institution* **291**, 75–102.

Canu F & Bassler R S 1923. North American later Tertiary and Quaternary Bryozoa. *United States National Museum Bulletin* **125**, 1–302.

Casadio S, Nelson C, Taylor P, Griffin M & Gordon D 2010. West Antarctic Rift system: a possible New Zealand-Patagonia paleobiogeographic link. *Ameghiniana* **47**, 129–132.

Chapman F 1913. Descriptions of new and rare fossils obtained by deep boring in the Mallee. *Proceedings of the Royal Society of Victoria* **26**, 165–191.

Cheetham A H & Håkansson E 1972. Preliminary report on Bryozoa (Site 117). Pages 432–441 & 476–507 *in* Laughton A S, Berggren W A *et al*. *Initial Reports of the Deep Sea Drilling Project* **XII**.

Cipolla F 1921. I briozoi pliocenici di Altavilla presso Palermo. *Giornale di Scienze Naturali ed Economiche Palermo* **XXXII**, 163–330.

Cook P L & Chimonides P J 1978. Observations on living colonies of *Selenaria* (Bryozoa, Cheilostomata) I. *Cahiers de Biologie Marine* **19**, 147–158.

Cook P L & Chimonides P J 1983. A short history of the lunulite bryozoa. *Bulletin of Marine Science* **33**, 566–581.

Cook P L & Chimonides P J 1984a. Recent and fossil Lunulitidae (Bryozoa, Cheilostomata), 1. The genus *Otionella* from New Zealand. *Journal of Natural History* **18**, 227–254.

Cook P L & Chimonides P J 1984b. Recent and fossil Lunulitidae (Bryozoa, Cheilostomata), 2. Species of *Helixotionella* gen. nov. from Australia. *Journal of Natural History* **18**, 255–270.

Cook P L & Chimonides P J 1985a. Recent and fossil Lunulitidae (Bryozoa, Cheilostomata), 3. 'Opesiulate' and other species of *Selenaria*, sensu lato. *Journal of Natural History* **19**, 285–322.

Cook P L & Chimonides P J 1985b. Recent and fossil Lunulitidae (Bryozoa, Cheilostomata), 5. *Selenaria alata* Tenison Woods and related species. *Journal of Natural History* **19**, 337–358.

Cook P L & Chimonides P J 1985c. Recent and fossil Lunulitidae (Bryozoa, Cheilostomata), 4. American and Australian species of *Otionella*. *Journal of Natural History* **19**, 575–603.

Cook P L & Chimonides P J 1986. Recent and fossil Lunulitidae (Bryozoa, Cheilostomata), 6. *Lunulites* sensu lato and the genus *Lunularia* from Australasia. *Journal of Natural History* **20**, 681–705.

Cook P L & Chimonides P J 1987. Recent and fossil Lunulitidae (Bryozoa, Cheilostomata), 7. *Selenaria maculata* (Busk) and allied species from Australasia. *Journal of Natural History* **21**, 933–966.

Cook P L & Chimonides P J 1994. Notes on the family Cupuladriidae (Bryozoa), and on *Cupuladria remota* sp.n. from the Marquesas Islands. *Zoologica Scripta* **23**, 251–268.

Cook P L, Bock P E, Gordon D P & Weaver H J (editors) 2018a: *Australian Bryozoa Volume 1. Biology, Ecology and Natural History.* SIRO Publishing, Melbourne, 200 pp.

Cook P L, Bock P E, Gordon D P & Weaver H J (editors) 2018b: *Australian Bryozoa Volume 2, Taxonomy of Australian Families.* CSIRO Publishing, Melbourne, 320 pp.

Dalziel I W D, Lawver L A, Pearce J A, Barker P F, Hastie A R, Barfod D N, Schenke H-W & Davis M B 2013. A potential barrier to deep Antarctic circumpolar flow until the late Miocene? *Geology* **41**, 947–950.

Dick M H, Herrera Cubilla A & Jackson J B C 2003. Molecular phylogeny and phylogeography of free-living Bryozoa (Cupuladriidae) from both sides of the Isthmus of Panama *Molecular Phylogenetics and Evolution* **27**, 355–371.

Di Martino E, Greene S & Taylor P D 2017a. *Discoradius*, a new name for the genus *Heteractis* Gabb & Horn, 1862 (Cheilostomata, Bryozoa), junior homonym of *Heteractis* Milne-Edwards & Haime, 1851 (Cnidaria, Actiniaria). *Journal of Systematic Palaeontology* **16**, p 445.

Di Martino E, Taylor P D, Cotton L J & Pearson P N 2017b. First bryozoan fauna from the Eocene–Oligocene transition in Tanzania. *Journal of Systematic Palaeontology* **16**, 225–243, doi: 10.1080/14772019.2017.1284163

Driscoll E G, Gibson J W & Mitchell S W 1971. Larval selection of substrate by the Bryozoa *Discoporella* and *Cupuladria*. *Hydrobiologia* **37**, 347–359.

Etheridge R Jr 1901. Additional notes on the palaeontology of Queensland (Part 2). *Bulletin of the Geological Survey of Queensland* **13**, 1–37.

Favorskaya T A 1987. Bryozoans of the Maastrichtian of Eastern Turkmenistan. *Yearbook All-Union Paleontological Society* **XXX**, 82–107.

Gorodiski A & Balavoine P 1961. Bryozoaires crétacés et éocènes du Sénégal. *Bulletin du Bureau de Recherches Géologiques et Minières* **4**, 1–15.

Guha A K & Nathan D S 1996. Bryozoan fauna of the Ariyalur Group (Late Cretaceous), Tamilnadu and Pondicherry, India. *Palaeontologia Indica, new series* **49**, 215 pp.

Hagenow F von 1839. Monographie der Rügen'schen Kreide-Versteinerungen. Abt. 1. Phytolithen und Polyparien. *Neues Jahrbuch für Mineralogie 1839*, 252–296.

Haig D W, Smith M & Apthorpe M C 1997. Middle Eocene Foraminifera from the type Giralia Calcarenite, Gascoyne Platform, Southern Carnarvon Basin, Western Australia. *Alcheringa* **21**, 229–245.

Håkansson E 1975. Population structure of colonial organisms. A palaeoecological study of some free-living Cretaceous bryozoans. *Documents des Laboratoires de Géologie de la Faculté Sciences de Lyon H.S.* **3**, 385–399.

Håkansson E 1981 (abstract). Breeding, brooding and 'parental care' in Recent Lunulites. Page 312 *in* G P Larwood & C Nielsen, editors, *Recent and Fossil Bryozoa*, Fredensborg.

Håkansson E & Thomsen E 1979. Distribution and types of bryozoan communities at the boundary in Denmark. Pages 78–91 *in* T Birkelund & R G Bromley, editors, *Cretaceous–Tertiary boundary events. Symposium, Copenhagen, September 1979,* **1***. The Maastrichtian and Danian of Denmark*. University of Copenhagen, Copenhagen.

Håkansson E & Thomsen E 1999. Benthic extinction and recovery patterns at the K/T boundary in shallow water carbonates. *Palaeogeography Palaeoclimatology Palaeoecology* **154**, 67–85.

Håkansson E & Thomsen E 2001. Asexual propagation in cheilostome Bryozoa: evolutionary trends in a major group of colonial animals. Pages 326–347 *in* J B C Jackson, S Lidgard & F K Mckinney, editors, Evolutionary patterns: growth, form and tempo in the fossil record. University of Chicago Press, Chicago, IL.

Håkansson E & Voigt E 1995. New free-living bryozoans from the northwest European Chalk. *Bulletin of the Geological Society of Denmark* **4**, 187–207.

Håkansson E & Winston J E 1985. Interstitial bryozoans: unexpected life forms in a high energy environment. Pages 125–134 *in* C Nielsen C & G P Larwood, editors, *Bryozoa: Ordovician to Recent*. Olsen & Olsen, Fredensborg.

Håkansson E, Bromley R & Perch-Nielsen K 1974. Maastrichtian chalk of north-west Europe a pelagic shelf sediment. *International Association of Sedimentologists, Special Publications* **1**, 211–233

Håkansson E, Gordon D P & Taylor P D *in press*. Bryozoa from the Maastrichtian Korojon Formation, Western Australia. *Fossils and Strata*.

Håkansson E, O'Dea A & Rosso A 2019. The Free-Living Cheilostome Bryozoans – pursuing the unobtainable. *18 International Bryozoology Association Conference, Liberec, 16–22 June 2019*.

Hara U, Mörs T, Hagström J & Reguero M A 2018. Eocene bryozoan assemblages from the La Meseta Formation of Seymour Island, Antarctica. *Geological Quarterly* **62**, 705–728.

Heinberg C 2007. Evolutionary ecology of nine sympatric species of the pelecypod *Limopsis* in Cretaceous chalk. *Lethaia* **12**, 325–340.

Hincks T 1881a. Contributions towards a general history of the marine Polyzoa. Part VI. Polyzoa from Bass's Straits. *Annals & Magazine of Natural History (Series 5)* **8**, 1–14 & 122–129.

Hincks T 1881b. On a collection of Polyzoa, from Bass's Straits, presented by Capt. Cawne Warren to the Liverpool Free Museum. *Proceedings of the Literary and Philosophical Society of Liverpool* **35**, 249–270.

Hincks T 1882. Contributions towards a general history of the marine Polyzoa. Part X. Foreign Cheilostomata (miscellaneous). *Annals & Magazine of Natural* History (Series 5) **10**, 160–170.

Hocking R M, Moors H T, & Van De Graaff J E 1987. Geology of the Carnarvon Basin Western Australia. *Bulletin of the Geological Survey of Western Australia* **133**, 1–289.

Hodel F., Grespan R, De Rafélis M, Dera G, Lezin C, Nardin E, Rouby D, Aretz M, Steinnman M, Buatier M, Lacan F, Jeandel C & Chavagnac V 2021. Drake Passage gateway opening and Antarctic Circumpolar Current onset 31 Ma ago: The message of foraminifera and reconsideration of the Neodymium isotope record. *Chemical Geology* **570**, 120171, 1–14.

Koromyslova A V & Pervushov E 2022. Uppermost Turonian bryozoans from the Lower Volga River region: scanning electron microscopy and micro-computed tomography studies. *Neues Jahrbuch für Geologie und Paläontologie – Abhandlungen* **305**, 263–295.

Kvachko V I 1995. Late Cretaceous and Paleocene bryozoans of the genus *Lunulites* from the Middle Volga, Crimea and Mangyshlak. *Paleontological Journal* **29**, 36–45

Lagaaij R 1952. The Pliocene Bryozoa of the Low Countries and their bearing on the marine stratigraphy of the North Sea region. *Mededelingen van de Geologische Stichting* **5**, 233pp.

Lagaaij R 1963. *Cupuladria canariensis* – portrait of a bryozoan. *Palaeontology* **6**, 172–217.

Lamarck J B P A de M de 1816. Histoire naturelle des Animaux sans Vertèbres ... précédée *d'une introduction offrant la détermination des caractéres essentiels de l'animal, sa distinction du végétal et des autres corps naturels, enfin, exposition des principes fondamentaux de la zoologie*. Verdiere, Pari. 568 pp.

Lawver L A & Gahagan L M 2003. Evolution of Cenozoic seaways in the circum-Antarctic region. *Palaeogeography, Palaeoclimatology, Palaeoecology* **198**, 11–37.

Levinsen G M R 1909. *Morphological and systematic studies on the cheilostomatous Bryozoa*, Nationale Forfatterers Forlag, Copenhagen. 431pp.

López-Gappa J, Pérez L M & Griffin M 2017. First record of a fossil selenariid bryozoan in South America. *Alcheringa*, **41**, 365–368.

MacGillivray P H 1881. Polyzoa. Pages 27-46, *in* McCoy F, editor, *Prodromus of the Zoology of Victoria* **1**.

MacGillivray P H 1886. Polyzoa. Pages 63-73, *in* McCoy F, editor, *Prodromus of the Zoology of Victoria* **2** (12).

MacGillivray P H 1895. A monograph of the Tertiary Polyzoa of Victoria. *Transactions of the Royal Society of Victoria* **4**, 1–166.

Maplestone C M 1904**.** Notes on the Victorian fossil Selenariidae, and descriptions of some new species (Recent and fossil). *Proceedings of the Royal Society of Victoria (new series)* **16**, 207–217.

Maplestone C M 1911**.** The results of deep-sea investigations in the Tasman Sea. 1 - The expedition of the H.M.C.S. "Miner". 5 - Polyzoa supplement. *Records of the Australian Museum* **8**, 118–119.

Marcus E & Marcus E 1962. On some lunulitiform Bryozoa. *Boletim da Faculdade de Filosofia, Ciências e Letras, Universidade de São Paulo, Zoologia* **24**, 281–342.

Marsson T 1887. Die Bryozoen der weissen Schreibkreide der Insel Rügen. Palæontologische Abhandlungen herausgegeben von W. Dames und E. Kayser **4**, 112 pp.

McKinney F K & Taylor P D 2001. Bryozoan generic extinctions and originations during the last one hundred million years. *Palaeontologia Electronica* **4** (1), 26pp. http://palaeo-electronica.org/2001_1/bryozoan/issue1_01.htm

Michelotti G 1838. Specimen zoophytologiæ diluvianæ. Turin 227 pp.

Moharrek F, Taylor P D, Silvestro D, Jenkins H L, Gordon D-P & Waeschenbach A 2022. Diversification dynamics of cheilostome bryozoa based on a bayesian analysis of the fossil record. *Palaeontology* **65**. doi: 10.1111/pala.12586

Müller R D, Zhirovic S, Williams S E, Cannon J, Seton M, Bower D J, Tetley M G, Heine C, Le Breton E, Liu S, Russel S H J, Yang T, Leonard J & Gurnis M 2019. A Global Plate Model Including Lithospheric Deformation Along Major Rifts and Orogens Since the Triassic. *Tectonics* **38**, 1884–1907

O'Dea A 2009. Relation of form to life habit in free-living cupuladriid bryozoans. *Aquatic Biology* **7**, 1–18.

O'Dea A, Håkansson E, Taylor P & Okamura B 2011: Environmental change prior to the K-T boundary inferred from temporal variation in the morphology of cheilostome bryozoans. *Palaeogeography, Palaeoclimatology, Palaeoecology,* **308**, 502–512.

Ostrovsky A N 2013. *Evolution of Sexual Reproduction in Marine Invertebrates. Example of Gymnolaemate Bryozoans.* Chapter 2 Cheilostome Brood Chambers: Structure, Formation, Evolution. Springer, Dordrecht. 115–228. doi: 10.1007%2F978-94-007-7146-8

Ostrovsky A N, O'Dea A & Rodríguez F 2009. Comparative Anatomy of Internal Incubational Sacs in Cupuladriid Bryozoans and the Evolution of Brooding in Free-Living Cheilostomes. *Journal of Morphology* **270**, 1413–1430.

Parker S A & Cook P L 1994. Records of the Bryozoan family Selenariidae from Western Australia and South Australia, with the descriptions of new species of *Selenaria*. *Records of the South Australian Museum* **27**, 1–11.

Pérez L M, López-Gappa J & Griffin M 2015. New and little-known bryozoans from Monte León Formation (early Miocene, Argentina) and their paleobiogeographic relationships. *Journal of Paleontology* **89**, 956–965.

Philippi R A 1887. *Die Terrtiären und Quartären Versteinerungen Chiles*. Leipzig, F A Brockhaus. 266 pp.

Pohowsky R A 1973. A Jurassic Cheilostome from England. In: Larwood G P (ed.) *Living and Fossil Bryozoa*. Academic Press, London and New York. 447–461.

Scher H D & Martin E E 2006. Timing and Climatic Consequences of the Opening of Drake Passage. *Science* **312**, 428.

Schmidt R 2007. Australian Cainozoic Bryozoa, 2: Free-living Cheilostomata of the Eocene St Vincent Basin, S.A., including *Bonellina* gen nov. *Alcheringa* **31**, 67–84.

Scotese C R 2014. Atlas of Neogene Paleogeographic Maps (Mollweide Projection), Maps 1–7, Volumes 1, The Cenozoic, *PALEOMAP Atlas for ArcGIS,PALEOMAP Project,* Evanston, IL.

Stilwell J D & Håkansson E 2012. Survival, but......! New tales of 'Dead clades walking' from Austral and Boreal Post-K–T Assemblages. Pages 795–810 *in* Talent J D (ed.): *Earth and Life, International Year of Planet Earth.* Springer Science. doi: 10.1007/978-90-481-3428-1_26

Stoliczka F 1872. The Cretaceous fauna of southern India. The Ciliopoda. *Memoir of the Geological Survey of India. Palaeontologica Indica* **4**, 33–68

Surlyk F 1972. Morphological adaptations and population structures of the Danish chalk brachiopods (Maastrichtian). *Det Kongelige Danske Videnskabernes Selskab. Biologiske Skrifter* 19, 57pp.

Surlyk F 1997. A cool-water carbonate ramp with bryozoan mounds: Late Cretaceous-Danian of the Danish Basin. Pages 293–307 *in* N P James & J D A Clarke, editors, Cool-water carbonates. *SEPM Special Publication* **56**.

Taylor P D 1988. Major radiation of cheilostome bryozoans: Triggered by the evolution of a new larval type? *Historical Biology* **1**, 45–64.

Taylor P D 2019. A brief review of the scanty record of Cretaceous bryozoans from Gondwana. *Australian Palaeontological Memoir* **52**, 147–154.

Taylor P D, James N P, Bone Y, Kuklinski P & Kyser T K 2009. Evolving mineralogy of cheilostome bryozoans. *Palaios* **24**, 440-452.

Tenison Woods J E 1865. On some Tertiary fossils in South Australia. *Transactions and–Proceedings of the Royal Society of Victoria* **6**, 3–6.

TENISON WOODS J E 1880. On some Recent and fossil species of Australian Selenariidae (Polyzoa). *Transactions of the Royal Society of South Australia, Adelaide* **3**, 1–12.

ULRICH E O 1901. Bryozoa. Pages 205-222 *in* W B Clark & G C Martin G C. *The Eocene deposits of Maryland*. Johns Hopkins Press, Baltimore.

VOIGT E 1962. Oberkreide-Bryozoen des europäischen Teils de UdSSSR und einiger anliegender Gebiete [in Russian]. *Moskwa University*, 125 pp. Moskwa

VOIGT E 1967. Oberkreide-Bryozoen aus den asiatischen Gebieten der UsSSR. *Mitteilungen aus dem Geologischen Staatsinstitut in Hamburg* **36**, 5–95.

WATERS A W 1883. Fossil Cheilostomatous Bryozoa from Muddy Creek, Victoria. *Quarterly Journal of the Geological Society* **39**, 423–443

WINSTON J E 1988. Life histories of free-living bryozoans. *National Geographic Research* **4**, 528–539.

YASUHARA M, HUANG H H M, REUTER M, TIAN S Y, CYBULSKI J D, O'DEA A, MAMO B L, COTTON L J, DI MARTINO E, FENG R & TABOR C R 2022. Hotspots of Cenozoic tropical marine biodiversity. Pages 243–300 *in* S J Hawkins, editor, *Oceanography and Marine Biology: An Annual Review* **60**. CRC Press.

YANG J, LAN T, ZHANG X & SMITH M R 2023. *Protomelission* is an early dasyclad alga and not a Cambrian bryozoan. *Nature* **615**, 468–471. doi: 10.1038/s41586-023-05775-5

ZHANG Z, ZANGH Z, MA J, TAYLOR P D, STROTZ L C, JACQUET S M, SKOVSTED C B, CHEN F, HAN J & BROCK G A 2021. Fossil evidence unveils an early Cambrian origin for Bryozoa. *Nature* **599**, 251–255. doi: 10.1038/s41586-021-04033-w

Journal of the Royal Society of Western Australia, 106: 45–59, 2023

Effect of stand density on growth and allometry of marri (*Corymbia calophylla*) in the high rainfall zone of southwest Western Australia

SHES K. BHANDARI [1,2,3*], **ERIK J. VENEKLAAS** [2,4], **LACHLAN MCCAW** [5], **RICHARD MAZANEC** [6], **MICHAEL RENTON** [2,4]

[1] *Deparment of Renewable Resources, University of Alberta, Edmonton, Canada*

[2] *School of Biological Sciences, the University of Western Australia, Perth, Australia*

[3] *Institute of Forestry, Tribhuvan University, Nepal*

[4] *School of Agriculture and Environment, the University of Western Australia*

[5] *Department of Biodiversity, Conservation and Attractions, Manjimup, Australia (retired)*

[6] *Department of Biodiversity, Conservation and Attractions, Perth, Australia*

[*] *Corresponding author:* ✉ sheskant@ualberta.ca

ABSTRACT

Marri (*Corymbia calophylla*), an endemic and keystone tree species of southwest Western Australia (SWWA), provides significant environmental, conservation, economic and cultural values. This study aims to analyse the effect of stand density, manipulated through thinning, on growth and allometry of marri-dominated forest. Although individual tree diameter (DHBUB, diameter at breast height under bark), basal area, height and crown-width (CW) growth was stimulated by thinning, stand basal-area growth was highest in denser (less thinned) stands. Stand density had a significant effect on the allometry between DBHUB and each of height and height-diameter ratio (HDR). Height and CW increased with an increase in DBHUB although the relationship with CW was not statistically significant; HDR was inversely related to DBHUB. Thinning has the potential to increase yields of merchantable timber, firewood, and enhance ecological values including tree hollows for arboreal fauna and marri-fruit production (important for cockatoos) that depend on retention of sufficient large old trees. Reduction of stand density through thinning reduces inter-tree competition and may help in reducing the risk of marri canker disease.

Keywords: Allometry; increment; marri; Mediterranean forest; stand density; thinning

INTRODUCTION

Marri (*Corymbia calophylla* (R. Br. ex Lindl.) K.D. Hill & L.A.S. Johnson), previously known as *Eucalyptus calophylla* (Hill & Johnson 1995), is one of the keystone and endemic tree species found in association with jarrah (*Eucalyptus marginata*) and karri (*Eucalyptus diversicolor*) in the forests of southwest Western Australia (SWWA). Marri is an evergreen broadleaved tree of a medium to large size (up to 40 m height and 1.5 m diameter at breast height (DBH)). The distribution of marri ranges north to south from Geraldton (28.77°S, 114.61°E) to Cape Riche (34.61°S, 118.76°E), and from Perth (31.95°S, 115.86°E) inland beyond Narrogin (32.93°S, 117.17°E) (Churchill 1968).

Marri has environmental, conservation, economic and cultural values. From an environmental and conservation point of view, it occurs within one of the 35 global biodiversity hotspots recognised by Conservation International (FPC 2018). Furthermore, the fruits and seeds of this species are important dietary constituents for the threatened Carnaby's black cockatoo (*Calyptorhynchus latirostris* Carnaby), Baudin's black cockatoo (*Calyptorhynchus baudinii* Lear) and Forest red-tailed black cockatoo (*Calyptorhynchus banksia)* (Johnstone & Kirkby 1999; Cooper *et al.* 2003; Johnstone *et al.* 2013; Lee *et al.* 2013). Marri is also used for nesting and roosting by these cockatoos (Whitford *et al.* 2015). Economic values derived from marri include honey, timber (for various uses including furniture, flooring, and firewood), food and medicine (CCWA 2013). Marri is a local indigenous Nyoongar word for "blood" after the red gum that exudes from wounds in the bark and has an important role in Nyoongar culture (Cunningham 1998). Marri trees have been affected by canker disease caused by *Quambalaria coyrecup* (Paap *et al.* 2008). This disease has caused a severe decline of marri trees in some places, including road verges and patches of remnant native vegetation in agricultural and urban landscapes (Paap *et al.* 2016). Decline in canopy condition and loss of large mature marri trees is of concern and may lead to detrimental impact on environmental, conservation, economic and cultural values.

Neighbouring trees compete for resources, affecting their growth rate (Stoneman *et al.* 1996; Koch & Ward 2005; Forrester *et al.* 2013). Reducing stand density through thinning can reduce intra-specific competition and regain growth potential (Grigg & Grant 2009). Thinning reduces competition, leaf-area index and

---

water loss through transpiration (Ruprecht & Stoneman 1993; Stoneman *et al*. 1996; Reed *et al*. 2012; Qiu *et al*. 2013) and promotes access to light, water, and nutrients for retained trees (Stoneman *et al*. 1995; Stoneman *et al*. 1996). Thinning is also associated with increased water discharge from forest catchments (Reed *et al*. 2012), decreased fire hazard (Volkova *et al*. 2017), and increased drought resistance (Sohn *et al*. 2016; Vernon *et al*. 2018). Heavier thinning may promote regeneration through opening of the canopy (Wang *et al*. 2019).

It is well established that thinning increases the growth of individual trees; however, the effect of thinning on different specific aspects of individual tree growth is variable. For example, thinning to reduce stand density has been reported to positively influence stem diameter growth but the effect on height growth may not be consistent (Oliver 1997; Nogueira *et al*. 2015; Hébert *et al*. 2016). When thinning increases height growth, this effect is generally smaller than the effect on diameter growth (Zhang *et al*. 1997; Bhandari *et al*. 2021b; Bhandari *et al*. 2022). In cases where height growth is favoured more in un-thinned stands compared to thinned stands, this may be due to greater competition for sunlight leading to prioritization of vertical growth (Chaturvedi & Khanna 2011; Kim *et al*. 2016). Because of the different nature of diameter and height growth, and contrasting tree-growth strategies, it is always important to analyse the effect of thinning on diameter-height allometry.

Western Australia's public forests are managed under the authority of a ten-year forest management plan that applies the Montreal Process Criteria as the framework for ecologically sustainable forest management (CCWA 2013). The condition, structure and extent of these forests has been affected by clearing for agricultural production and urban development, timber harvesting, forest fire, drought, and pathogens (Kimber 1981; Bradshaw 2012; Taylor *et al*. 2012; Paap *et al*. 2016, 2017, 2018; Sapsford *et al*. 2021) and parts of the forest estate are fragmented. Silvicultural guidance documents that inform implementation of the forest management plan recognise the importance of marri trees as habitat and a food source for cockatoos and provide for retention of mature and senescent trees during timber harvesting operations. To sustainably manage these forests, it is important to understand the impact of thinning on growth and allometry. Previous research has investigated aspects of the biology and ecology of marri, but there is no published information about how thinning affects the growth and allometry of marri.

A thinning experiment was established in 1992 in an even-aged stand of karri, marri and jarrah regenerated from retained seed trees following timber harvesting in 1969 (White 1974). The aim of the experiment was to evaluate growth responses to different intensities of thinning from below (removal of smaller and slowly growing trees favour the growth of taller and fast-growing individual trees). The experiment has been measured on five occasions (1992, 1997, 2002, 2010 and 2018). The experimental design included examples of plots dominated by karri and plots dominated by marri with a secondary component of karri. This paper examines the effects of stand density on growth and allometry of marri in the marri dominant stands. We first examined the effect of stand density on individual tree and stand level variables at different time points (total DBH, total height, height-diameter ratio, crown width, stand basal area, stem number per ha), then investigated the effect of stand density on individual tree and stand-level growth. Furthermore, we fitted nine different allometric relationships between under bark DBH (DBHUB) and height. We also tested whether stand density affected allometric relationships between DBHUB and each of height, height-DBHUB ratio (HDR) and crown width (CW) at all five measurement times between plot establishment (1992) and the end of the study (2018).

MATERIALS AND METHODS

Study area

The study was conducted at Sutton forest block (34° 28' S, 116° 20' E) 38 km southeast of Manjimup, SWWA (Fig. 1). The area has a Mediterranean climate with an average annual rainfall of 986 mm (measured at the Manjimup station from 1915 to 2019, station number 9573). Average minimum and maximum temperature for February is 13.4°C and 27.2°C respectively and for July is 6.4°C and 14.4°C respectively (BOM 2020). The soils of the study site are mainly yellow and gravelly texture-contrast soils, formed on weathered mottled and pallid zone

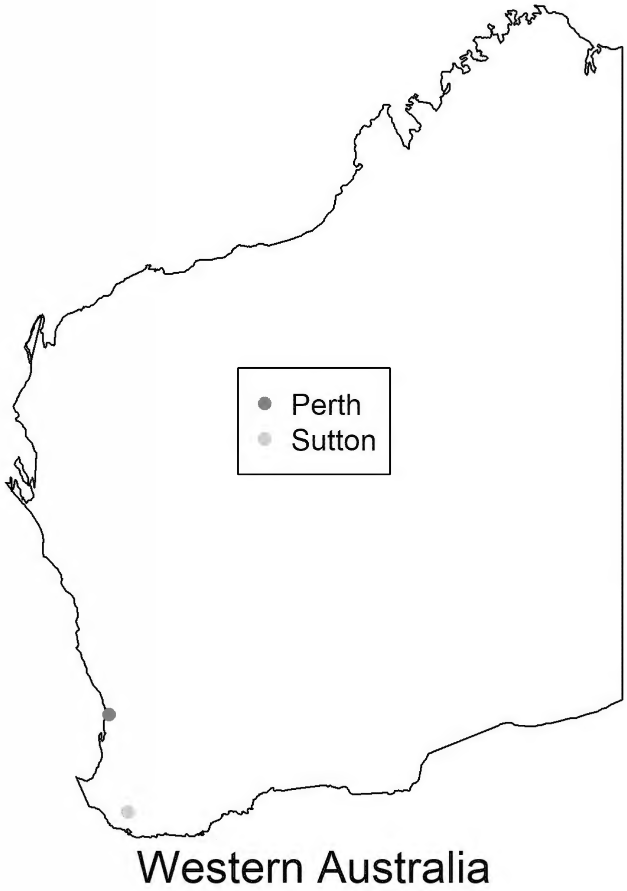

Figure 1. Location of the Sutton study site in Western Australia.

material (McArthur 2004). The regenerated forest at the experimental site remained unburnt prior to thinning and throughout the duration of the measurements reported in our study.

Treatment (thinning / stand densities)

The thinning trial at Sutton block consists of 27 plots (size 30 m × 30 m plus an outer 10 m buffer on all sides). The outer 10 m buffer was thinned to the same intensity as the inner plot, but tree measurements were carried out in the inner 30 m x 30 m. Thinning was undertaken manually with debris retained on site. Thinning plots were selected to represent marri forest where the over-bark basal area of marri was >60% of total stand basal area and top height was ≥18 m, as opposed to karri forest where the over-bark basal area of karri was >75% and top height was ≥20 m. This gave a total of eight plots for marri and 19 plots for karri. Separate experimental plots were not established for jarrah because of the small proportion of this species in the overall stand composition. In this paper, we analyse data from the eight plots dominated by marri. Results on effects of thinning and competition on growth and allometry based on karri-dominated plots are presented by Bhandari *et al.* (2021a) and Bhandari *et al.* (2022). Marri plots were managed at four different stand densities with two replicate plots placed randomly, which were established in 1992 as follows: 21.6 (T1), 11.6 (T2), 9.9 (T3) and 6.4 (T4) $m^2 ha^{-1}$ basal area under bark (BAUB, total for all species present). The BAUB of only marri trees in 1992 was 15.2 (T1), 9.4 (T2), 8.1 (T3) and 5.3 (T4) $m^2 ha^{-1}$. T1 is the un-thinned (control) and T2, T3 and T4 represent an increasing order of thinning intensity.

Data measurement

The location of each plot centre was measured using differential GPS in 1992 and the position of each tree mapped using direction and distance from the plot centre. The over bark DBH (DBHOB, cm) and bark thickness of each tree (including saplings, mm) and the total height (m) and crown radius (CR, m) of a subsample of trees of each plot was measured in 1992, 1997, 2002, 2010 and 2018. At least 10 trees located near the centre of each plot were selected for measurement of height and CR over the study period. The CR was measured as the horizontal distance from the base of the tree to the point vertically below the outward edge of the crown in the north, east, south and west orientations. Bark thickness at breast height of individual trees was measured using a syringe-type bark gauge, and the under bark DBH (DBHUB) was calculated by subtracting twice the average bark thickness from the over bark DBH. Under bark DBH (DBHUB), HDR and CW were calculated from the field measured variables. The HDR was calculated as the ratio of total height and DBH of the individual trees. The CW of each tree was calculated as twice the average of the four CR measurements. DBHUB of dominant trees (D-DOM) and height of dominant trees (H-DOM) of each plot were calculated as mean DBHUB and average height of the trees whose crowns extended above the general canopy level and thus received full light from above and some light from the sides and had the largest and fullest crowns in the stand (Smith 1962; Helms 1998). Dominance was assessed in 1992 when the trees were measured after establishment of the thinning trial.

DATA ANALYSIS

Effect of treatment on individual tree and stand level variables

The effect of thinning treatment on DBHUB, height, and CW of individual trees was evaluated using linear mixed effect models, fitted using maximum likelihood, in the R statistical software (R Core Team 2019) using the 'nlme' package (Pinheiro *et al.* 2018). Thinning treatment was included as a factor and a fixed effect (Table 1). A random effect for plot was also included to account for possible correlation among trees in the same plot. The effect of thinning treatment on stand BAUB and stem number per ha were evaluated at the plot level using standard ANOVA. The results of these plot-level ANOVA analyses should be treated with some caution, as the number of replicate plots was only two, and thus the assumption of equal variance among groups is difficult to test.

Effect of treatment on individual tree and stand-level growth

We evaluated the effect of thinning treatments on annual growth of individual DBHUB, height, CW and stand BAUB for the period of 1992 to 2018 using linear mixed effect models, fitted using maximum likelihood, in the R statistical software (R Core Team 2019) using the 'nlme' package (Pinheiro *et al.* 2018). Growth of DBHUB, height and CW of individual trees were evaluated for two different groups: all trees together and the cohort of dominant trees only. We used only marri trees to estimate the stand BAUB growth; however, the retained BAUB includes BAUB of all three species present in the plots. We included fixed effects for thinning treatment (as a factor), and random effects for plots, to account for possible spatial correlation among individual trees within the same plots, and individual trees, to account for the fact our data includes repeated measurement on the same trees at different measurement times. The effect of thinning treatment on growth of stand BAUB was evaluated at the plot level using standard ANOVA. The results of this plot-level ANOVA analyses should be treated with some caution, as the number of replicate plots was only two, and thus the assumption of equal variance among groups is difficult to test. We also tested whether the DBHUB growth varied between growth period (1992 to 1997, 1997 to 2002, 2002 to 2010 and 2010 to 2018) using growth period as fixed effect and plot as random effect.

Allometric relationship between DBH and height

Nine different linear and non-linear allometric equations (Table A1) were fitted to DBH and height data for all time points. After a preliminary analysis of all nine equations, the three best equations were selected for further analysis (Table 2). Parameters and fit statistics for each model were estimated in R using the nls and nlsLM functions in the minpack.lm package (Timur *et al.* 2016; R Core Team 2019), and models were evaluated and compared using different criteria including significance of estimated parameters (at 95% confidence level), coefficient of determination (R^2; higher values indicated better models), root mean squared error (RMSE; lower values indicate better models) (Montgomery *et al.* 2001), and Akaike

Information Criterion (AIC; lower values indicate better models) (Akaike 1972; Burnham & Anderson 2002). The distribution of residuals was also considered in selecting the best model.

Effect of treatment on allometric relationships

We also tested whether stand density (thinning treatment) affected allometric relationships between DBHUB and each of height, HDR and CW. For height, we fitted a model predicting height as a power function (Huxley & Teissier 1936) of DBHUB using a linear model including an interaction: log(height)~log(DBHUB)*T, where T was the thinning treatment as a categorical factor. We then tested whether the effect of treatment was significant in the model. The same approach was used for HDR and CW.

RESULTS

Effect of treatment on individual tree and stand level variables

Decreasing stand density resulted in a significant ($p<0.05$) increase in diameter and CW over the period 1992 to 2018 (Table 1). However, HDR, stand BAUB and number of trees per ha decreased significantly ($p<0.05$) with a decrease in stand density. Stand density had a significant effect on DBHUB, CW, height, stand BAUB, number of individual trees per ha and HDR at all five measurement times ($p<0.05$) (Table 1, Table A2, Fig. A4) except the CW in 1992 and height in 1992, 1997, 2010 and 2018. Un-thinned plots of marri had 32% fewer individual live trees in 2018 than in 1992, a net change of 1.22% yr^{-1}.

Effect of treatments on individual tree and stand level growth

Growth in DBHUB, height and CW of individual trees increased with a decrease in stand density for all trees and for dominant trees, but the rate of growth was higher for dominant trees than for all trees (Fig. 2a, b, c). The DBHUB, height and CW growth of all trees in the lowest density (T4) treatment were 108%, 41% and 82% higher than the growth in the highest density (T1) treatment respectively. Growth in stand BAUB increased with an increase in stand density (Fig. 2d). The growth of DBHUB and height increased with an increase in DBHUB (Fig. 3a, b) and the growth of DBHUB and height varied significantly with thinning treatment. Growth of CW decreased with an increase in DBHUB and varied significantly with thinning (Fig. 3c). Growth in DBHUB during the first five-year period following thinning (1992 to 1997) was significantly faster than during all subsequent periods ($p<0.05$) (Fig. 3d).

Allometric relationship between DBHUB and height

All parameters of nine height-DBHUB allometric equations were highly significant ($p<0.001$) (Table 2, Appendix Table A1) but equations M1, M2 and M3 produced higher R^2, lower RMSE and lower AIC (Table 2, Appendix Table A1) than other equations. The difference in fit statistics among these three equations was very small (Table 2), but the residuals produced by M3 are smaller and more consistent than M1 and M2 (Fig. 4b), and so M3 was considered as the best equation for the prediction of height from DBHUB.

Effect of treatment on allometric relationship

The height-DBHUB allometry varied significantly among thinning treatments in 1992 ($p=0.01$), 1997 ($p=0.003$) and 2002 ($p=0.002$) but not in 2010 ($p=0.17$) and 2018 ($p=0.24$) (Figs 4c, A3). The differences among thinning treatments were similar for 1992, 1997 and 2002. Allometry of HDR with DBHUB differed significantly with stand density in 1992 ($p=0.03$), 1997 ($p=0.003$), 2002 ($p=0.004$), but not in 2010 ($p=0.14$) and 2018 ($p=0.11$) (Figs 4d, A3). Allometry of CW and DBHUB did not differ significantly with stand density in any of the measurement years (Figs 4e, A3). Height and CW increased with an increase in DBHUB, however, HDR decreased (Fig. 4a, c, d, e).

Table 1. Arithmetic mean±standard error values of individual tree and stand characteristics according to thinning treatment for the most recent measurement (2018). For each variable, the degrees of freedom (numerator/denominator), f-value and p-value from the mixed effect model ANOVA is also shown. Note: all variables except BAUB (m^2 ha^{-1}) and Stem number per hectare (ha^{-1}) are presented for only marri trees. BAUB (m^2 ha^{-1}) and stem number per hectare given in the table includes all tree species present in the plots. Marri represents 70%, 73.1%, 74.9%, and 79.7% of the plot total basal area in T1, T2, T3 and T4 respectively.

Characteristics	**Thinning (BAUB in 1992 after thinning)**						
	T1 (21.6)	**T2 (11.6)**	**T3 (9.9)**	**T4 (6.4)**	**df**	**F-value**	**p-value**
DBHUB (cm)	15.7±0.5	21.8±0.5	27.8±0.8	30.2±1.2	3/4	44.5	0.001
DBHUB of dominant trees (cm)	26.5±1.0	27.5±0.8	33.3±1.4	34.2±2.0	3/4	15.7	0.007
Height (m)	20.4±0.6	21.1±0.6	23.7±0.7	25.8±1.1	3/4	5.1	0.075^{ns}
Height of dominant trees (m)	23.8±1.0	24.1±0.9	27.2±1.2	28.5±1.0	3/4	13.3	0.010
Height-DBHUB ratio (m cm^{-1})	1.1±0.02	1±0.02	0.9±0.02	0.8±0.03	3/4	11.6	0.019
Crown width (m)	3.3±0.2	3.3±0.2	4.5±0.3	4.7±0.4	3/4	6.8	0.047
BAUB all species (m^2 ha^{-1})	42.7±4.7	29.8±2.8	26.5±3.4	19.0±1.2	3/4	175.0	<0.001
Stem number per hectare all species (ha^{-1})	1905±383	655±67	361±28	238±39	3/4	14.7	0.012

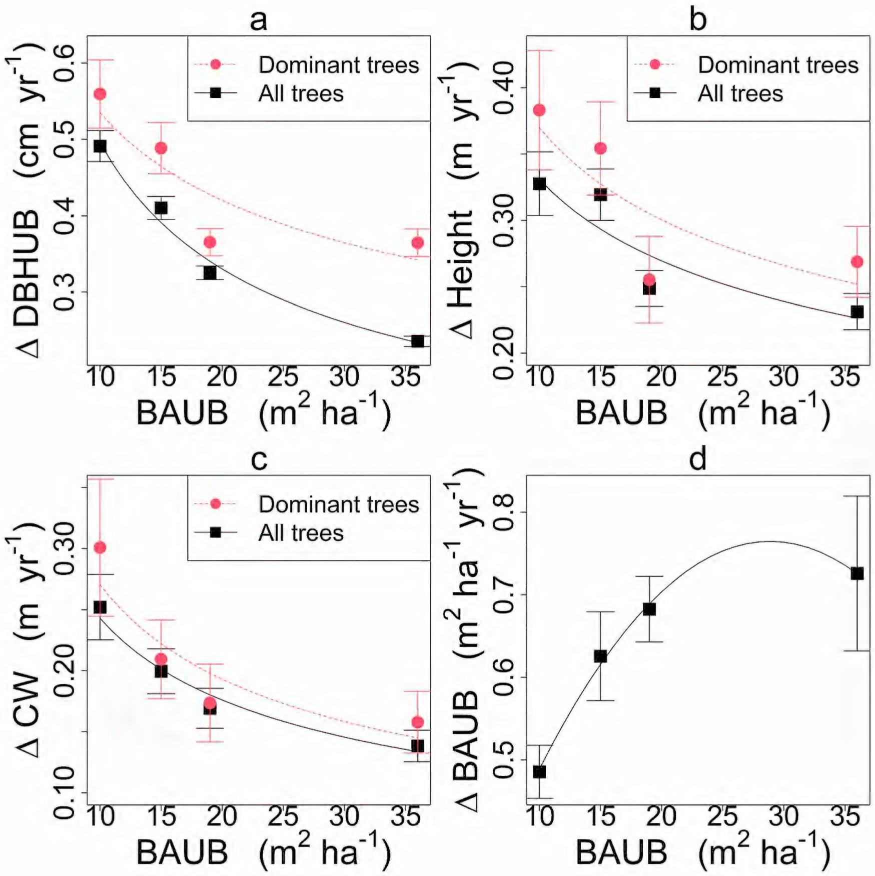

Figure 2. Effect of stand density on annual growth (1992-2018) of (a) DBHUB, (b) height, (c) CW, (d) stand BAUB. Δ denotes annual growth. Error bars denote standard error. Stand density presented in the x-axis was measured in 1992, 1997, 2002 and 2010 and the growth was from initial measurement to the next measurement year for example growth from 1992 to 1997 was plotted against stand density of 1992. The growth presented is only of marri but the BAUB presented in the x-axis is of all trees presented in the plots.

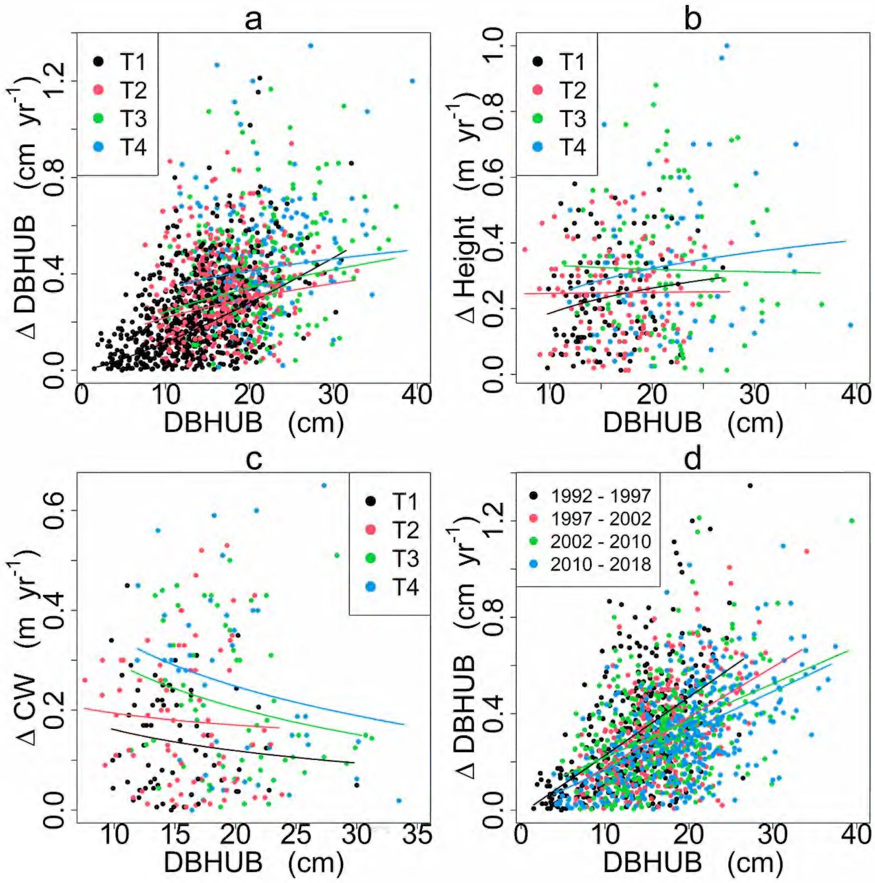

Figure 3. Effect of stand density on annual growth (1992-2018) with respect to DBHUB; (a) DBHUB, (b) height, (c) CW, (d) Effect of time period on DBHUB growth of marri only. Δ denotes annual growth. T1 (21.6 m^2ha^{-1}), T2 (11.6 m^2ha^{-1}), T3 (9.9 m^2ha^{-1}) and T4 (6.4 m^2ha^{-1}) (according to 1992 data) are thinning treatments (stand densities) in an increasing order of thinning intensity.

Table 2. Parameter values and fit statistics of different allometric equations for tree height and DBHUB (H=height in m, D=DBHUB in cm, b_1 and b_2 are parameters that were estimated). The constant value 1.3 is the height of the stem above the ground level at which DBH was measured.

Model	Equation	References	Parameter value	R^2	RMSE	AIC
M1	$H = 1.3 + b_1 + b_2 D + \varepsilon_{ij}$	Linear model	b_1=6.71 b_2=0.56	0.751	1.89	2252
M2	$H = 1.3 + b_1 \left\{ \frac{D}{(D+1)} \right\} + b_2 D + \varepsilon_{ij}$	Watts (1983)	b_1=7.47 b_2=0.54	0.751	1.89	2251
M3	$H = 1.3 + b_1 D^{b2} + \varepsilon_{ij}$	Huxley and Teissier (1936)	b_1=2.78 b_2=0.62	0.752	1.89	2251

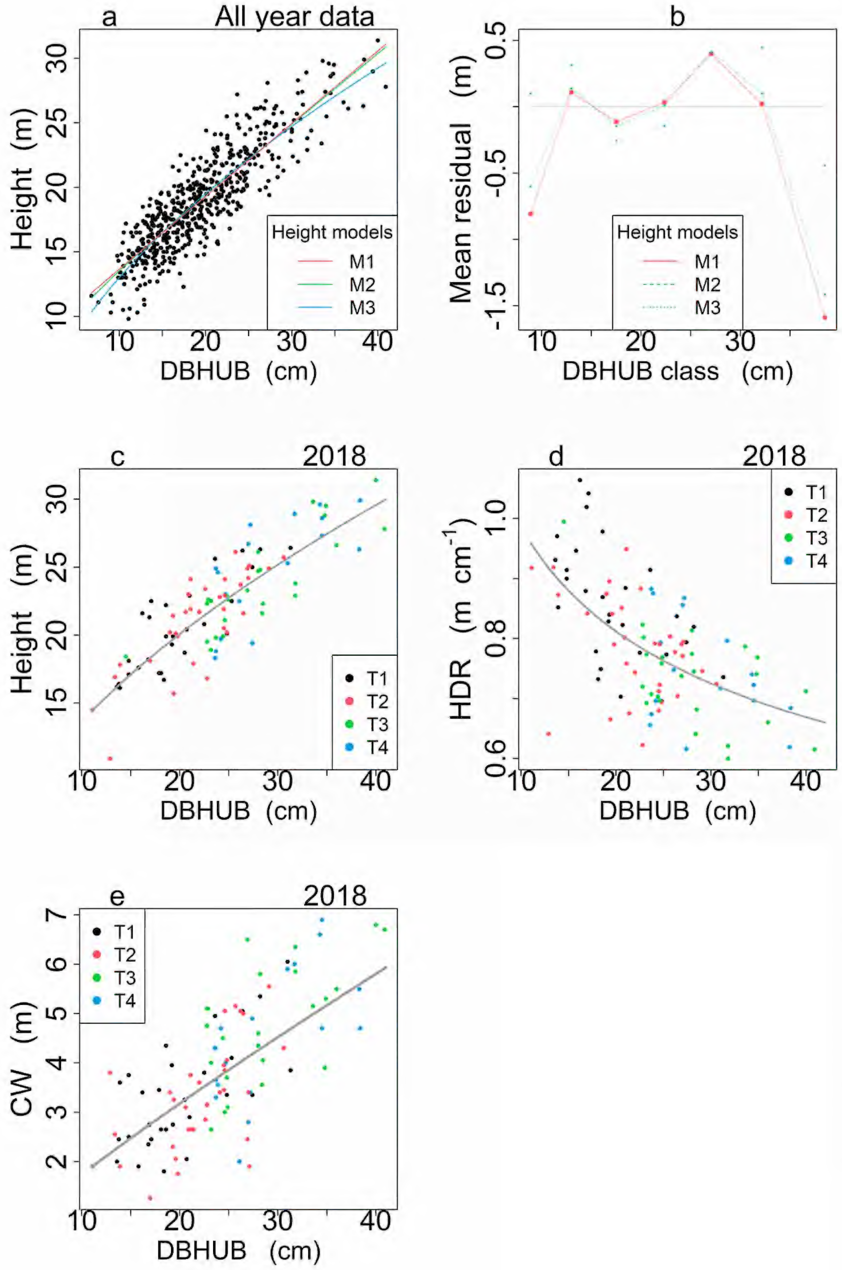

Figure 4. (a) Curves of the different DBHUB height allometry models overlaid on the observed data (data from all years), (b) Mean residual from predicted height by DBHUB class of height DBHUB allometry models, (c) Effect of stand density on allometry of DBHUB with height, (d) Effect of stand density on allometry of DBHUB with HDR, (e) Effect of stand density on allometry of DBHUB with CW. Meanings of T1 to T4 are described in Figure 3.

DISCUSSION

Effect of treatments on individual tree and stand-level variables

Low stand densities resulting from heavier thinning led to higher values of average DBHUB, height and CW at the end of the 26-year study period. In contrast, plots with low stand density resulted in lower values of HDR, stand BAUB and number of individual trees per ha. It is well established in both theory and experimental research that individual trees grow faster when competition is reduced and have greater access to light, nutrients, and water. The higher values for DBHUB and height in plots with low stand density and lower values of HDR, stand BAUB and number of individual trees per ha are consistent with the results reported for jarrah by Stoneman *et al*. (1996) and Bhandari *et al*. (2021b). Bhandari *et al*. (2022) also found similar results in the 26-year thinning experiment in karri plots at the same experimental site as this study.

Effect of treatments on individual tree and stand-level growth

Our study showed an increase in growth of DBHUB, height and CW with a decrease in stand density for the period of 1992 to 2018. Other studies have also found an increase in growth of DBH and height with a decrease in stand density (Stoneman *et al*. 1996; Grigg & Grant 2009; Forrester *et al*. 2013; Acuna *et al*. 2017; Bhandari *et al*. 2021b; Bhandari *et al*. 2022). Decreasing stand density reduces competition and increases the access to light, nutrients, and soil moisture. A similar study in *Eucalyptus* stands in Brazil found a positive effect of thinning on DBH growth but no effect on height growth of dominant trees (Medeiros *et al*. 2017). In a study carried out in jarrah forest of SWWA, Bhandari *et al*. (2021b) found that DBH growth increased continuously with an increase in thinning intensity, but the same effect was not observed consistently for height growth. Results similar to jarrah forest were also reported for the karri forest of SWWA (Bhandari *et al*. 2022). The inconsistent effect of thinning on height growth is the result of two opposing responses: 1, Thinning increases resource availability, causing remaining trees to grow faster (accumulate biomass faster); 2, Height growth is less favoured in high-light environments because more biomass is invested in diameter, branches and perhaps roots. The first is a matter of primary productivity, the second is a morphological/allometric effect. In dense plots, the individual trees tend to increase more in height in search of sunlight and thus increase their HDR. Our study also showed a lower HDR in heavily thinned plots (0.85) and higher HDR in un-thinned plots (1.05). Height growth of dominant trees was higher than that of all trees in all thinning treatments. Dominant trees even in dense stands are less influenced by light competition; however, their potential growth may be limited by below-ground competition for water and nutrients (Bhandari *et al*. 2021a, c, 2023).

Consistent with other studies (Janik *et al*. 2018; Bhandari *et al*. 2021b; Bhandari 2022), we also found that trees with greater DBHUB had greater DBHUB growth. This suggests that the DBHUB growth of individual trees of marri are still increasing and have not reached their peak. It is to be expected that DBH growth will not further increase at a certain tree DBH and will even decrease beyond that point (Gove *et al*. 2019; Chaturvedi & Khanna 2011).

Diameter growth was greatest in the first growth period after thinning (1992-1997) but decreased gradually in later growth periods. The decreasing trend in growth after the first growth period can be explained by at least two factors; the first being increased basal area in thinned plots leading to a steady increase in the inter-tree competition. A second factor leading to reduced growth over time is the decreasing trend of rainfall at the study site. Mean annual precipitation at the nearest weather station from the study site from 1992 to 1997 was 934 mm; 1997 to 2002 was 932 mm; 2002 to 2010 was 909 mm; and 2010 to 2018 was 735 mm (BOM 2020). The difference in the mean annual precipitation in the first three growth periods was small, however the significantly lower mean annual precipitation in the fourth growth period might have played a greater role in reducing the growth, along with the increased stand density.

The present study showed an increase in growth of stand BAUB with an increase in stand density. Despite the higher growth in individual tree BAUB in plots with lower stand density, we observed lower growth in stand BAUB in plots with lower stand density, primarily because of the reduction in number of individual trees. However, a trend for increasing stand BAUB growth with an increase in stand density is not likely to persist indefinitely. As inter-tree competition starts to limit growth in dense stands, growth rate starts to decrease (Bradshaw 2015a). The result of this study (increase in growth of stand BAUB with an increase in stand density) is inconsistent with observations reported by Moller (1954), Stoneman *et al*. (1996), Grigg & Grant (2009) and Bradshaw (2015a, 2015b). Studies carried out in jarrah forest (Bhandari *et al*. (2021b) and in karri forest (Bhandari *et al*. 2022) showed that stand basal area increases with an increase in stand density at stand densities below the critical threshold, but reported peak growth followed by reduced growth with further increase in stand density. Two reasons may explain our result with respect to stand density for marri in this study. The first reason for not observing reduced basal area growth in the highest density (un-thinned) stand in our study may be because this regrowth forest of relatively young age had not yet reached the critical density of trees where competition and tree allometry reduce growth rates. The second reason might be that marri is relatively tolerant of competition, perhaps due to efficient use of resources (light, moisture, and nutrients) compared to other species, but we have no direct evidence for this at present. The experimental design favoured heavier thinning treatments and did not include a treatment with a retained basal area in the range of 22-35 m^2 ha^{-1} which was the basal area range where the other studies (Bhandari *et al*. 2021b) found reduced tree growth and so the relationship between stand density and basal-area increment in denser marri stands remains uncertain.

Canker disease caused by *Quambalaria coyrecup* represents a potential threat to the health of marri forest (Paap *et al*. 2008). In a study carried out in a marri forest of SWWA, Sapsford (2017) found stand basal area was positively correlated with the proportion of trees with canker, and thus recommended thinning as an option for controlling canker disease in marri trees. Further experiments would be helpful to validate the hypothesis that reducing basal area of marri reduces the incidence of canker disease. However, thinning may increase the frequency of root diseases in some tree species such as karri (Robinson 2003). Disturbances, especially anthropogenic, need to be minimized to reduce canker disease in marri as the disturbances have a positive correlation with canker (Sapsford *et al*. 2021). Overstory species diversity was negatively correlated with the proportion of marri trees with canker (Paap *et al.* 2017; Paap *et al.* 2018). Heterogeneous forests having higher species diversity have been reported to suffer less damage from pathogens (Haas *et al.* 2011; Jactel *et al.* 2017). Thus, forest management strategies that promote species diversity may be one of the potential options for reducing the susceptibility of forest to pathogens (Holdenrieder *et al*. 2004).

Thinning resulted in a higher proportion of larger marri trees in the forest. Larger trees are likely to produce a greater quantity of fruits and seeds (Cargill *et al*. 2016), which contribute to the diet of the threatened cockatoos (Johnstone & Kirkby 1999; Cooper *et al*. 2003; Lee *et al*. 2013). In the longer term, larger trees are also likely to provide more habitat for wildlife. The formation of hollows in marri and other eucalypts is a slow process and highly dependent on age and disturbance events, natural or anthropogenic (Whitford *et al*. 2015). Older trees with larger canopies are likely to have more hollows suitable for use as nesting sites by various arboreal animals including cockatoos (Whitford 2002; Whitford & Williams 2002; Johnstone *et al*. 2013; Whitford *et al*. 2015). Marri trees are more likely to bear hollows than jarrah trees of equivalent size (Whitford & Williams 2001). At the time of writing, the maximum age of the marri trees in this study site is about 50 years and the availability of tree hollows would be expected to increase progressively over the next four to six decades. In stands comprised of a mixture of mature and regrowth trees, retention of mature trees that have a greater probability of containing large hollows is desirable from a wildlife conservation perspective even though these trees may suppress the growth of younger regeneration (Rotheram 1983)

Positive effects of a reduced number of trees due to thinning may include an increase in water yield and water discharge in a forest catchment, which may be a source of water for wildlife and may favour aquatic fauna in the forest (Stoneman & Schofield 1989; Bari & Ruprecht 2003). Thinning has also been reported to reduce fire hazard under some circumstances (Volkova *et al*. 2017; Volkova & Weston 2019). Thinning operations should be managed carefully to minimise soil disturbance and damage to retained trees and other habitat elements including mid-storey trees and large ground logs. Changes to forest management policy implemented by the Western Australian government mean that commercial timber harvesting in public native forests in SWWA will cease at the end of 2023. Thinning of younger regrowth forests to maintain and enhance ecosystem health has been identified as an option in the draft forest management plan that will apply from 2024 onwards, although the scale and nature of thinning has yet to be confirmed by government.

Effect of treatments on allometry

The allometry of DBHUB with height and HDR was significantly different among different stand densities even immediately after thinning in 1992, indicating that these differences were either introduced by bias in selection of trees for thinning, or possibly reflect random pre-existing differences among plots. This is further supported by the fact that differences in allometry between thinning treatments were not in logical order according to thinning intensity. The biggest difference was in the lowest thinning treatment (T2) and is driven by the presence of a cohort of thinner and especially shorter trees that were retained to achieve the target basal area for the thinning treatments. The significance and patterns of the differences in allometry were maintained in 1997 and 2002, but not significant in 2010 and 2018, suggesting a slow return to a more even allometry over this longer period. We did not see a clear effect of thinning treatment (stand density) on the allometric relationships between DBHUB and each of height, HDR, and CW in this study. This contrasts to the clearer effect of thinning on the allometric relationship between DBH and height reported by Deng *et al*. (2019) in *Pinus massoniana* in China; between DBH and each of height, HDR and CW reported by Bhandari *et al*. (2021b) in *Eucalyptus marginata* in SWWA and Bhandari *et al*. (2022) in *Eucalyptus diversicolor* in SWWA. The strength of the effect of thinning on allometric relationships likely depends on species, thinning intensity, inter-tree competition and time after thinning. The initial impact of thinning on inter-tree competition was reduced over the period of study as trees matured. Marri trees growing in the study area are also affected by neighbouring karri trees which contributed 20-30% of total BAUB at the start of the measurement period. Karri trees typically grow more rapidly than marri and may influence the overall growth of the marri trees, potentially attenuating the effect of thinning. The average height of karri trees was 30.8 m (Bhandari *et al*. 2022) and marri was only 22.8 m at the age of 49 years. As the number of individual trees per unit area is different in different thinning treatments, the level of competition exerted on individual trees is also different. Inter-tree competition has a crucial role in allometry of DBH and height (Lines *et al*. 2012; Forrester *et al*. 2017).

In all thinned plots, at lower stand density, height growth increased and HDR decreased with an increase in DBHUB. The HDR of un-thinned stands was higher than that of thinned stands. As described by Metzger's theory (Metzger 1893), trees growing in a low stand density prioritise girth/diameter growth even at the cost of height growth. On the other hand, trees prioritise height growth in a dense stand to improve access to light from above, as light from the side is obstructed by neighbouring competing trees. Therefore, HDR becomes smaller in thinned or open stands than in un-thinned or dense stands. Individual trees having lower HDR are stronger and therefore less prone to external forces such as wind and weight of the crown than are trees with higher HDR (Wonn & O'Hara 2001; Bobinac *et al*. 2018).

CONCLUSION

The study, using data spanning 26 years, showed that thinning reduced competition and promoted the growth of individual marri trees. Trees in heavily thinned plots had 108% higher DBHUB growth than those in un-thinned plots but un-thinned plots had higher stand basal area growth than thinned plots. Stand density affected DBHUB and height growth of individual marri trees, which in turn had a significant effect on allometry between DBHUB and each of height and HDR but not on CW. Thinning provides a technique to enable an accelerated transition from dense stands of even-aged regrowth to more open stands of larger trees that may benefit a range of forest values including water catchment management, timber production and wildlife conservation. Large-sized trees resulting from thinning are likely to provide a higher quality habitat and food resource for arboreal fauna and birds including threatened cockatoos, and more visually appealing forests.

CONFLICT OF INTEREST: The authors declare that they have no conflict of interest.

ACKNOWLEDGEMENTS

Much of the data for this study was provided by Department of Biodiversity, Conservation and Attraction (DBCA), Western Australia. We thank Ray Leemans for his cooperation in data collection. The financial support for this study was provided by Research and Training Program (RTP) and University Post Graduate Award (UPA) of University of Western Australia. We also acknowledge the constructive comments provided by two anonymous referees.

REFERENCES

Acuna M, Trandgard M, Wiedemann J & Mitchell R 2017. Impacts of early thinning of a *Eucalyptus globulus* Labill. pulplog plantation in Western Australia on economic profitability and harvester productivity. *Forests* **8**, 415. https://doi.org/10.3390/f8110415.

Akaike H 1972. A new look at statistical model identification. *IEEE Trans Autom Control* AC19 (**6**),716–723. http://dx.doi.org/10.1109/TAC.1974.1100705.

Bari MA & Ruprecht JK 2003. Water yield response to land-use change in southwest Western Australia, salinity and land-use impacts series report No. SLU31, Department of Environment, Perth.

Bhandari SK, Veneklaas EJ, McCaw L, Mazanec R & Renton M 2021a. Investigating the effect of neighbour competition on individual tree growth in thinned and unthinned eucalypt forests. *Forest Ecology and Management* **499**, 119637. https://doi.org/10.1016/j.foreco.2021.119637.

Bhandari SK, Veneklaas EJ, McCaw L, Mazanec R, Whitford K & Renton M 2021b. Effect of thinning and fertilizer on growth and allometry of *Eucalyptus marginata*. *Forest Ecology and Management* **479**. http://doi.org/10.1016/j.foreco.2020.118594.

Bhandari SK, Veneklaas EJ, McCaw L, Mazanec R, Whitford K & Renton M 2021c. Individual tree growth in jarrah (*Eucalyptus marginata*) forest is explained by size and distance of neighbouring trees in thinned and non-thinned plots. *Forest Ecology and Management* **494**, 119364. https://doi.org/10.1016/j.foreco.2021.119364.

Bhandari SK, Veneklaas EJ, McCaw L, Mazanec R & Renton M 2022. Effect of thinning on growth and allometry of *Eucalyptus diversicolor*. *Southern Forest* **84**, 298-310. https://doi.org/10.2989/20702620.2022.2155090.

Bhandari SK, Veneklaas EJ, McCaw L, Mazanec R, Whitford K & Renton M 2023. Investigating above- vs. below-ground competition by accounting for azimuth of competitors in native eucalypt forests. *Forest Ecology and Management* **542**, 121103. https://doi.org/10.1016/j.foreco.2023.121103.

Bobinac M, Andrasev S, Bauer-Zivkovic A & Susic N 2018. Effects of heavy thinning on the increment and stability of a Norway spruce stand and its trees between the age of 32 and 50. *Šumarski* **1–2**, 33–46. https://doi.org/10.31298/sl.142.1-2.3.

BOM 2020. Climate statistics for Australian location, monthly climate statistics. Manjimup (Australia): Bureau of Meteorology.

Bradshaw CJA 2012. Little left to lose: deforestation and forest degradation in Australia since European colonization. *Journal of Plant Ecology* **5**, 109–120. https://doi.org/10.1093/jpe/rtr038.

Bradshaw FJ 2015a. Reference material for karri forest silviculture, Department of Parks and Wildlife, Perth. 134p.

Bradshaw FJ 2015b. Reference material for jarrah forest silviculture. Forest Management Series FEM061, Department of Parks and Wildlife, Perth. 141p.

Burnham KP & Anderson DR 2002. *Model selection and inference: a practical information-theoretic approach*. New York: Springer-Verlag.

Cargill J, Etten EJBV, Whitford KR, McCaw LW, Stock WD 2016. A refined method for estimating capsule crops in individual jarrah (*Eucalyptus marginata*) crowns. *Australian Forestry*. **79**, 208–216. https://doi.org/10.1080/00049158.2016.1218264.

CCWA 2013. *Forest Management Plan 2014–2023*. Perth (Australia): Conservation Commission of Western Australia.

Chaturvedi AN & Khanna LS 2011. *Forest mensuration and biometry*. 5th Ed. Dheradun, India: Khanna Bandhu.

Churchill D 1968. The distribution and prehistory of *Eucalypt diversicolor* F. Muell., *E. marginata* Donn ex Sm., and *E. calophylla* R. Br. in relation to rainfall. *Australian Journal of Botany* **16**, 125–151. https://doi.org/10.1071/BT9680125.

Cooper CE, Withers PC, Mawson PR, Johnstone R, Kirkby T, Prince J, Bradshaw SD & Robertson H 2003. Characteristics of marri (*Corymbia calophylla*) fruits in relation to the foraging behaviours of the forest red-tailed black cockatoo (*Calyptorhynchus banksii naso*). *Journal of the Royal Society of Western Australia* **86**, 139–142.

Cunningham I 1998. The trees that were nature's gift I. Cunningham, Maylands, WA. [ISBN 0958556202, 9780958556200]

Deng C, Zhang S, Lu Y, Froese RE, Ming A & Li Q 2019. Thinning effects on tree height diameter allometry of masson pine (*Pinus massoniana* Lamb.). Forests **10**, 1129. https://doi.org/10.3390/f10121129.

FPC 2018. *Karri forest management plan*. Perth (Australia): Forest Products Commission.

Forrester DI, Wiedemann JC, Forrester RI & Baker TG 2013. Effects of planting density and site quality on mean tree size and total stand growth of *Eucalyptus globulus* plantations. *Canadian Journal of Forest Research* **43**, 846–851. https://doi.org/10.1139/cjfr-2013-0137.

Forrester, DI, Benneter, A, Bouriaud, O & Bauhus J 2017. Diversity and competition influence tree allometric relationships-developing functions for mixed-species forests. Journal of Ecology **105,** 761–774. https://doi.org/10.1111/1365-2745.12704.

Gove JH, Lynch TB & Ducey MJ 2019. The Chapman-Richards distribution and its relationship to the generalized beta. *Forest Ecosystems* **6**, 27. https://doi.org/10.1186/s40663-019-0184-0

Grigg AH & Grant CD 2009. Overstory growth response to thinning, burning and fertilizer in 10 to 13 years old rehabilitated jarrah (*Eucalyptus marginata*) forest after bauxite mining in southwestern Australia. *Australian Forestry* **72**, 80–86. https://doi.org/10.1080/00049158.2009.10676293.

Haas SE, Hooten MB, Rizzo DM & Meentemeyer RK 2011. Forest species diversity reduces disease risk in a generalist plant pathogen invasion. *Ecology Letters* **14**, 1108–1116.

Hébert F, Krause C, Plourde PY, Achim A, Pregent G & Menetrier J 2016. Effect of tree spacing on tree level volume growth, morphology, and wood properties in a 25-year-old *Pinus banksiana* plantation in the boreal forest of Quebec. *Forests*, **7**, 276. https://doi.org/10.3390/f7110276.

Helms JA 1998. *The Dictionary of Forestry.* Society of American Foresters, Bethesda, MD. 210p.

Hill KD & Johnson LAS 1995. Systematic studies in the eucalypts 7. A revision of the bloodwoods, genus *Corymbia* (Myrtaceae). *Telopea* **6**, 185–504.

Holdenrieder O, Pautasso M, Weisberg PJ & Lonsdale D 2004. Tree diseases and landscape processes: the challenge of landscape pathology. *Trends in Ecology & Evolution* **19**, 446–452. https://doi.org/10.1016/j.tree.2004.06.003.

Huxley JS & Teissier G 1936. Terminology of relative growth. *Nature* **137**, 780–781. https://doi.org/10.1038/137780b0.

Jactel H, Bauhus J, Boberg J, Bonal D, Castagneyrol B, Gardiner B, Gonzalez-Olabarria JR, Koricheva J, Meurisse N & Brockerhoff EG 2017. Tree diversity drives forest stand resistance to natural disturbances. *Current Forestry Reports* **3**, 223–243. https://doi.org/10.1007/s40725-017-0064-1.

Janik D, Vrska T, Hort L, Unar P & Kral K 2018. Where have all the tree diameters grown? Patterns in *Fagus sylvatica* L. diameter growth on their run to the upper canopy. *Ecosphere* **9**, e02508. https://doi.org/10.1002/ecs2.2508.

Johnstone RE & Kirkby T 1999. Food of the forest red-tailed black cockatoo *Calyptorhynchus banksii naso* in southwest Western Australia. *Western Australian Naturalist* **22**, 167–177.

Johnstone RE, Kirkby T & Sarti K 2013. The breeding biology of the Forest Red-tailed Black Cockatoo *Calyptorhynchus banksii naso* Gould in southwestern Australia. I. Characteristics of nest trees and nest hollows. *Pacific Conservation Biology* **19**, 121–142. https://doi.org/10.1071/PC130121.

Kim M, Lee WK, Kim YS, Lim CH, Song C, Park T, Son Y & Son YM 2016. Impact of thinning intensity on the diameter and height of *Larix kaempferi* stands in central Korea. *Forest Science and Technology* **12**, 77–87. http://dx.doi.org/10.1080/21580103.2015.1075435.

Kimber PC 1981. Eucalypt diebacks in the southwest of Western Australia. In: Old KM, Kile GA, Ohmart CP, editors. Eucalypt dieback in forests and woodlands. Melbourne: CSIRO; p. 37–43.

Koch JM & Ward SC 2005. Thirteen-year growth of jarrah (*Eucalyptus marginata*) on rehabilitated bauxite mines in southwestern Australia. *Australian Forestry* **68**, 176–185. https://doi.org/10.1080/00049158.2005.10674963.

Lee J, Finn H & Calver M 2013. Feeding activity of threatened black cockatoos in mine-site rehabilitation in the jarrah forest of southwestern Australia. *Australian Journal of Zoology* **61**, 119–131. https://doi.org/10.1071/ZO12101.

Lines, ER, Zavala MA, Purves DW, & Coomes DA 2012. Predictable changes in aboveground allometry of trees along gradients of temperature, aridity and competition. *Global Ecology and Biogeography* **21**, 1017–1028. https://doi.org/10.1111/j.1466-8238.2011.00746.x.

McArthur WM 2004. Reference Soils of Southwestern Australia. Department of Agriculture, Government of Western Australia, Perth.

Medeiros RA, de Paiva HN, Soares AAV, da Cruz JP & Leite HG 2017. Thinning from below: effects on height of dominant trees and diameter distribution in Eucalyptus stands. *Journal of Tropical Forest Science* **29**, 238–247.

Metzger K 1893. Der Wind als maßgebender Faktor für das Wachsthum der Bäume. *Mündener Forstliche* **3**, 35–86.

Moller C 1954. The influence of thinning on volume increment. 1. Results of investigations. In: Moller C, Abell J, Jagd T, Juncker F, editors. Thinning problems and practices in Denmark. New York: State University of New York, College of Forestry; p. 5-32.

Montgomery DC, Peck EA & Vining GG 2001. *Introduction to linear regression analysis*. New York: Wiley.

Nogueira GS, Marshall PL, Leite HG & Campos JCC 2015. Thinning Intensity and pruning impacts on eucalyptus plantations in Brazil. *International Journal of Forestry Research*, 168390. https://doi.org/10.1155/2015/168390

Oliver WW 1997. Twenty-five-year growth and mortality of planted ponderosa pine repeatedly thinned to different stand densities in northern California. *Western Journal of Applied Forestry* **12**, 122–130. https://doi.org/10.1093/wjaf/12.4.122.

Paap T, Burgess TI, McComb JA, Shearer BL & Hardy GESJ 2008. *Quambalaria* species, including *Q. coyrecup* sp. nov., implicated in canker and shoot blight diseases causing decline of *Corymbia* species in the southwest of Western Australia. *Mycological Research* **112**, 57–69. https://doi.org/10.1016/j.mycres.2007.10.005.

Paap T, Burgess TI, Calver M, McComb JA, Shearer BL & Hardy, GESJ 2016. A thirteen-year study on the impact of a severe canker disease of *Corymbia calophylla*, a keystone tree in Mediterranean-type forests. *Forest Pathology* **47**, e12292. https://doi.org/10.1111/efp.12292.

Paap T, Brouwers N, Burgess TI & Hardy GESJ 2017. Importance of climate, anthropogenic disturbance and pathogens on marri tree health in southwest Western Australia. *Annals of Forest Science* **74**, 62. https://doi.org/10.1007/s13595-017-0658-6

Paap T, Burgess TI, Rolo V, Steel E & Hardy GESJ 2018. Anthropogenic disturbance impacts stand structure and susceptibility of an iconic tree species to an endemic canker pathogen. *Forest Ecology and Management*. **425**, 145–153. https://doi.org/10.1016/j.foreco.2018.05.055.

Pinheiro J, Bates D, Debroy S, Sarkar D & R Core Team 2018. NLME: linear and non-linear mixed effects models. R package version 3.1-137, URL: https://CRAN.R-project.org/package=nlme.

Qiu S, Bell RW, Hobbs RJ & McComb AJ 2013. Overstorey and juvenile response to thinning and drought in a jarrah (*Eucalyptus marginata* Donn ex Sm.) forest of southwestern Australia. *Plant Soil* **365**, 291–305.

R Core Team 2019. R: A language and environment for statistical computing. R foundation for statistical computing, Vienna, Austria. URL https://www.R-project.org/.

Reed AJ, Barrett KL & Croton JT 2012. Future stream flow from the northern jarrah forest: learnings from the Wungong catchment trial. *Western Australian Water Corporation*.

Robinson RM 2003. Short-term impact of thinning and fertilizer application on *Armillaria* root disease in regrowth karri in Western Australia. *Forest Ecology and Management* **176**, 417–426. https://doi.org/10.1016/S0378-1127(02)00231-1.

Rotheram I 1983. Suppression of growth of surrounding regeneration by veteran trees of karri (*Eucalyptus diversicolor*). *Australian Forestry* **46**, 8–13. https://doi.org/10.1080/00049158.1983.10674368

Ruprecht JK & Stoneman GL 1993. Water yield issues in the jarrah forest of southwestern Australia. *Journal of Hydrology* **150**, 369–391. https://doi.org/10.1016/0022-1694(93)90117-R.

Sapsford SJ 2017. Factors predisposing *Corymbia calophylla* trees to canker disease caused by *Quambalaria coyrecup*. [Ph D thesis]. Perth (Australia): Murdoch University.

Sapsford SJ, Paap T, Hardy GE & Burgess TI 2021. Anthropogenic disturbance impacts mycorrhizal communities and abiotic soil properties: implications for an endemic forest disease. *Frontiers in Forest and Global Change* **3**. https://doi.org/10.3389/ffgc.2020.593243.

Smith DM 1962. *The Practice of Silviculture*. 7th ed. New York: Wiley.

Sohn JA, Saha S & Bauhus J. 2016. Potential of forest thinning to mitigate drought stress: A meta-analysis. *Forest Ecology and Management* **380**, 261–273. https://doi.org/10.1016/j.foreco.2016.07.046.

Stoneman GL, Dell B & Turner NC 1995. Growth of *Eucalyptus marginata* (jarrah) seedlings in Mediterranean-climate forest in southwest Australia in response to overstorey, site and fertiliser application. *Forest Ecology and Management* **79**, 173–184. https://doi.org/10.1016/0378-1127(95)03608-3.

Stoneman GL, Crombie DS, Whitford K, Hingstone FJ, Giles R, Portlock CC, Galbraith JH & Dimmock GM 1996. Growth and water relations of *Eucalyptus marginata* stands in response to thinning and fertilization. *Tree Physiology* **16**, 267–274. https://doi.org/10.1093/treephys/17.4.267.

Stoneman GL & Schofield NJ 1989. Silviculture for water production in jarrah forest of Western Australia: an evaluation. *Forest Ecology and Management* **27**, 273–293. https://doi.org/10.1016/0378-1127(89)90111-4.

Taylor K, Andjic V, Barber PA, Hardy GESJ & Burgess TI 2012. New species of *Teratosphaeria* associated with leaf diseases on *Corymbia calophylla* (Marri). *Mycological Progress* **11**, 159–169. https://doi.org/10.1007/s11557-011-0738-1

Timur V, Elzhov, Katharine MM, Andrej-Nikolai S & Ben B 2016. minpack.lm: R Interface to the Levenberg-Marquardt Nonlinear Least-Squares Algorithm found in MINPACK, Plus Support for Bounds. R package version 1.2-1. https://CRAN.R-project.org/package=minpack.lm.

Vernon MJ, Sherriff RL, Mantgem PV & Kane JM 2018. Thinning, tree-growth, and resistance to multi-year drought in a mixed conifer forest of northern California. *Forest Ecology and Management* **422**, 190–198. https://doi.org/10.1016/j.foreco.2018.03.043.

Volkova L, Bih, Hilton J & Weston CJ 2017. Impact of mechanical thinning on forest carbon, fuel hazard and simulated fire behaviour in *Eucalyptus delegatensis* forest of southeastern Australia. *Forest Ecology and Management* 405, 92–100. https://doi.org/10.1016/j.foreco.2017.09.032.

Volkova L & Weston CJ 2019. Effect of thinning and burning fuel reduction treatments on forest carbon and bushfire fuel hazard in *Eucalyptus sieberi* forests of Southeastern Australia. *Science of the Total Environment,* 694. https://doi.org/10.1016/j.scitotenv.2019.133708

Wang Z, Yang H, Wang D & Zhao Z 2019. Response of height growth of regenerating trees in a *Pinus tabulaeformis* Carr. plantation to different thinning intensities. *Forest Ecology and Management* **444**, 280–289. https://doi.org/10.1016/j.foreco.2019.04.042.

Watts SB 1983. *Forestry handbook for British Columbia*. 4th ed. Vancouver: Forestry Undergraduate Society.

White BJ 1974. *Regeneration methods in mixed marri-karri stands*. Forest Department of Western Australia Research Paper No 4.

Whitford KR 2002. Hollows in jarrah and marri trees. I. hollow sizes, tree attributes and ages. *Forest Ecology and Management* **160**, 201–214. https://doi.org/10.1016/S0378-1127(01)00446-7.

Whitford KR & Williams MR 2001. Survival of jarrah (*Eucalyptus marginata* Sm.) and marri (*Corymbia calophylla* Lindl.) habitat trees retained after logging. *Forest Ecology and Management* **146**, 181–197. https://doi.org/10.1016/S0378-1127(00)00459-X.

Whitford KR & Williams MR. 2002. Hollows in jarrah and marri trees, II: selecting trees to retain for hollow dependent fauna. *Forest Ecology and Management* **160**, 215–232.

Whitford KR, Wiseman D, McCaw WL & Bradshaw FJ 2015. Characteristics of nest trees and nest hollows used by the forest red-tailed black cockatoo (*Calyptorhynchus banksia naso*) in southwest Western Australia: comments on Johnstone et al. (2013). *Pacific Conservation Biology* **21**, 133–145.

Wonn HT & O'Hara KL. 2001. Height diameter ratios and stability relationships for four northern rocky mountain tree species. *Western Journal of Applied Forestry*, **16**, 87–94. https://doi.org/10.1093/wjaf/16.2.87.

Zhang S, Burkhart HE & Amateis RL 1997. The influence of thinning on tree height and diameter relationships in loblolly pine plantation. *Southern Journal of Applied Forestry* **21**, 199–205. https://doi.org/10.1093/sjaf/21.4.199.

APPENDIX

Table A1. Parameter values and fit statistics of different height DBHUB allometric equations of marri (H = height in m, D= DBHUB in cm, b_1, b_2, b_3 are parameters that were estimated). The constant value 1.3 is the height of the stem above the ground level at which DBH was measured.

Model	Equation	References	Parameter value	R2	RMSE	AIC
M1	$H = 1.3 + b_1 + b_2 D + \varepsilon_{ij}$	Linear model	b_1=6.71 b_2=0.56	0.751	1.89	2252
M2	$H = 1.3 + b_1 \left\{ \frac{D}{(D+1)} \right\} + b_2\, D + \varepsilon_{ij}$	Watts (1983)	b_1=7.47 b_2=0.54	0.751	1.89	2251
M3	$H = 1.3 + b_1 D^{b2} + \varepsilon_{ij}$	Huxley and Teissier (1936)	b_1=2.78 b_2=0.62	0.752	1.89	2251
M4	$H = 1.3 + b_1\, \{1\text{-}\exp(-b_2 D)\} + \varepsilon_{ij}$	Meyer (1940)	b_1=45.44 b_2=0.02	0.730	1.95	2312
M5	$H = 1.3 + \left\{ \frac{D}{b_1 + b_2 D} \right\}^3 + \varepsilon_{ij}$	Naslund (1936)	b_1=1.02 b_2=0.003	0.730	1.95	2312
M6	$H = 1.3 + \frac{b_1 D^2}{(D + b_2)^2} + \varepsilon_{ij}$	Hossfeld (1822)	b_1=46.73 b_2=14.96	0.720	1.99	2332
M7	$H = 1.3 + exp \left\{ b_1 + \frac{b_2}{(D+1)} \right\} + \varepsilon_{ij}$	Wykoff *et al.* (1982)	b_1=3.66 b_2=-19.53	0.708	2.03	2355
M8	$H = 1.3 + b_1\, exp \left(\frac{b_2}{D} \right) + \varepsilon_{ij}$	Buford (1986)	b_1=37.69 b_2= -17.89	0.704	2.05	2362
M9	$H = 1.3 + b_1\, \{1\text{-}exp(-b_2 D)\}^3 + \varepsilon_{ij}$	Bertalanffy (1949)	b_1=25.17 b_2=0.09	0.674	2.15	2415

Table A2. Effect of stand density on growth of marri at different time periods (Note: ^{ns} is not significant). For each variable, the degrees of freedom (numerator/denominator) and p-value from the mixed effect model ANOVA is also shown. P-value (growth) means p-value generated in Anova analysis on change of variables between two consecutive growth periods. P-value (retained) means p-value generated in Anova analysis on the retained values of the variables at the beginning of each growth period.T1 (21.6 m^2ha^{-1}), T2 (11.6 m^2ha^{-1}), T3 (9.9 m^2ha^{-1}) and T4 (6.4 m^2ha^{-1}) (according to 1992 data) are thinning treatments (stand densities) in an increasing order of thinning intensity.

Year	variables	Thinning					p-value	p-value
		T1	T2	T3	T4	df	(growth)	(retained)
1992	DBHUB (cm)	9.90	14.12	17.69	17.57	3/4		0.001
	Height (m)	15.39	15.14	16.27	17.55	3/4		0.209^{ns}
	Crown Width (m)	2.50	2.35	3.17	2.87	3/4		0.147^{ns}
	BAUB all species (m^2ha^{-1})	21.62	11.65	9.91	6.44	3/4		<0.001
	Stem number per ha all species (ha^{-1})	2794	672	366	255	3/4		0.011
1997	DBHUB (cm)	10.72	15.47	19.52	20.54	3/4	0.019	0.001
	Height (m)	16.55	16.44	17.92	19.36	3/4	0.252^{ns}	0.158^{ns}
	Crown Width (m)	3.60	3.72	4.72	4.74	3/4	0.039	0.019
	BAUB all species (m^2ha^{-1})	24.13	14.48	12.72	9.11	3/4	0.980^{ns}	<0.001
	Stem number per ha all species (ha^{-1})	2544	661	366	250	3/4	0.048	0.008
2002	DBHUB (cm)	13.93	17.03	21.49	22.84	3/4	0.001	<0.001
	Height (m)	17.52	17.44	20.26	21.54	3/4	0.011	0.041
	Crown Width (m)	3.46	3.96	4.94	4.98	3/4	0.252^{ns}	0.049
	BAUB all species (m^2ha^{-1})	25.18	17.78	15.66	11.41	3/4	0.0972^{ns}	0.003
	Stem number per ha all species (ha^{-1})	2400	655	366	250	3/4	0.057^{ns}	<0.001
2010	DBHUB (cm)	13.79	19.44	24.77	25.97	3/4	0.030	<0.001
	Height (m)	19.02	19.36	22.28	23.06	3/4	0.601^{ns}	0.062^{ns}
	Crown Width (m)	3.21	3.42	4.82	4.59	3/4	0.330^{ns}	0.017
	BAUB all species (m^2ha^{-1})	35.26	23.39	21.05	15.16	3/4	0.0124	<0.001
	Stem number per ha all species (ha^{-1})	2150	655	366	250	3/4	0.121^{ns}	0.009
2018	DBHUB (cm)	15.68	21.76	27.78	30.21	3/4	0.004	0.001
	Height (m)	20.44	21.08	23.75	25.76	3/4	0.165^{ns}	0.075^{ns}
	Crown Width (m)	3.33	3.28	4.80	4.69	3/4	0.670^{ns}	0.047
	BAUB all species (m^2ha^{-1})	42.71	29.81	26.47	19.00	3/4	0.030	<0.001
	Stem number per ha all species (ha^{-1})	1905	655	361	238	3/4	0.003	0.012

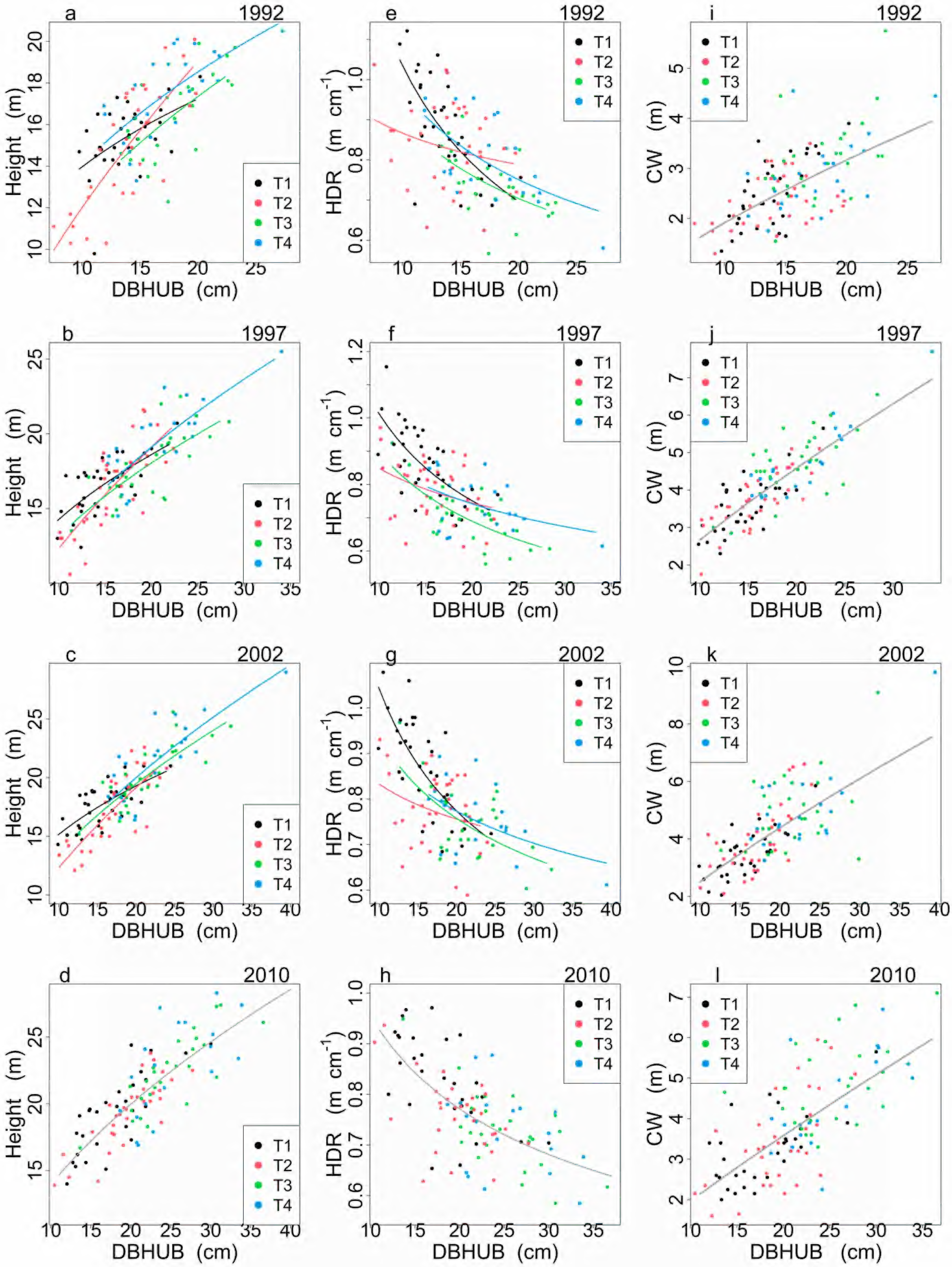

Figure A3. Effect of stand density on allometry of DBHUB with (a) height in 1992; (b) height in 1997; (c) height in 2002; (d) height in 2010; (e) HDR in 1992; (f) HDR in 1997; (g) HDR in 2002; (h) HDR in 2010; (i) CW in 1992; (j) CW in 1997; (k) CW in 2002; (l) CW in 2010. T1 (21.6 m^2ha^{-1}), T2 (11.6 m^2ha^{-1}), T3 (9.9 m^2ha^{-1}) and T4 (6.4 m^2ha^{-1}) (according to 1992 data) are thinning treatments (stand densities) in an increasing order of thinning intensity.

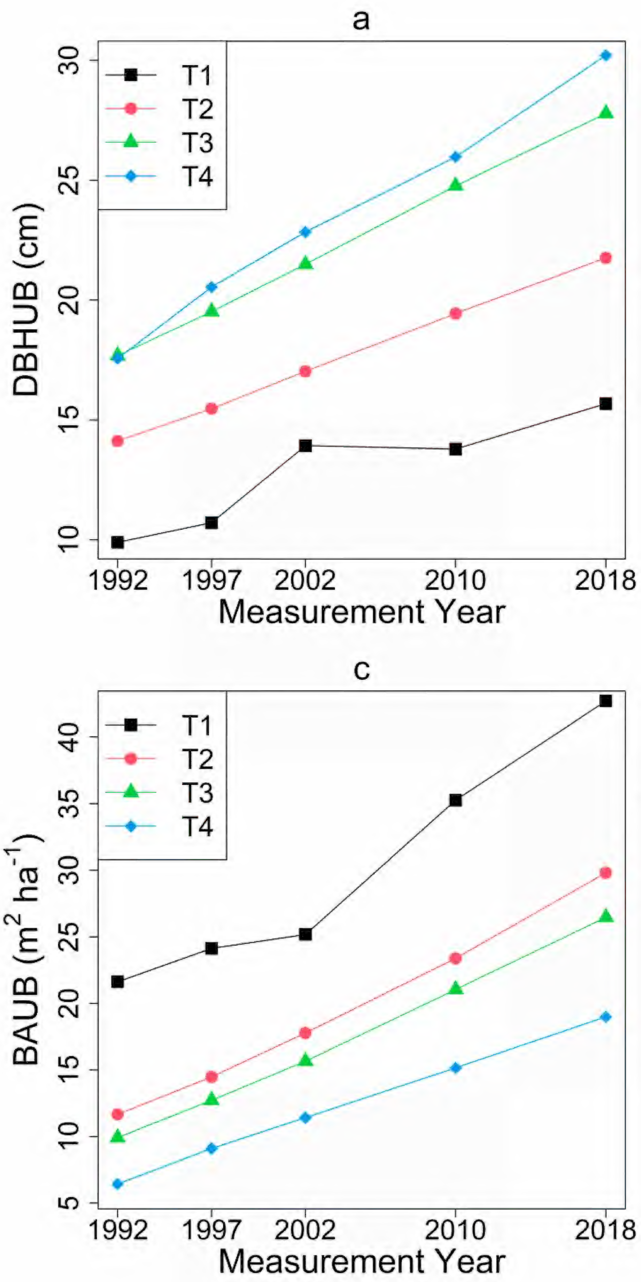

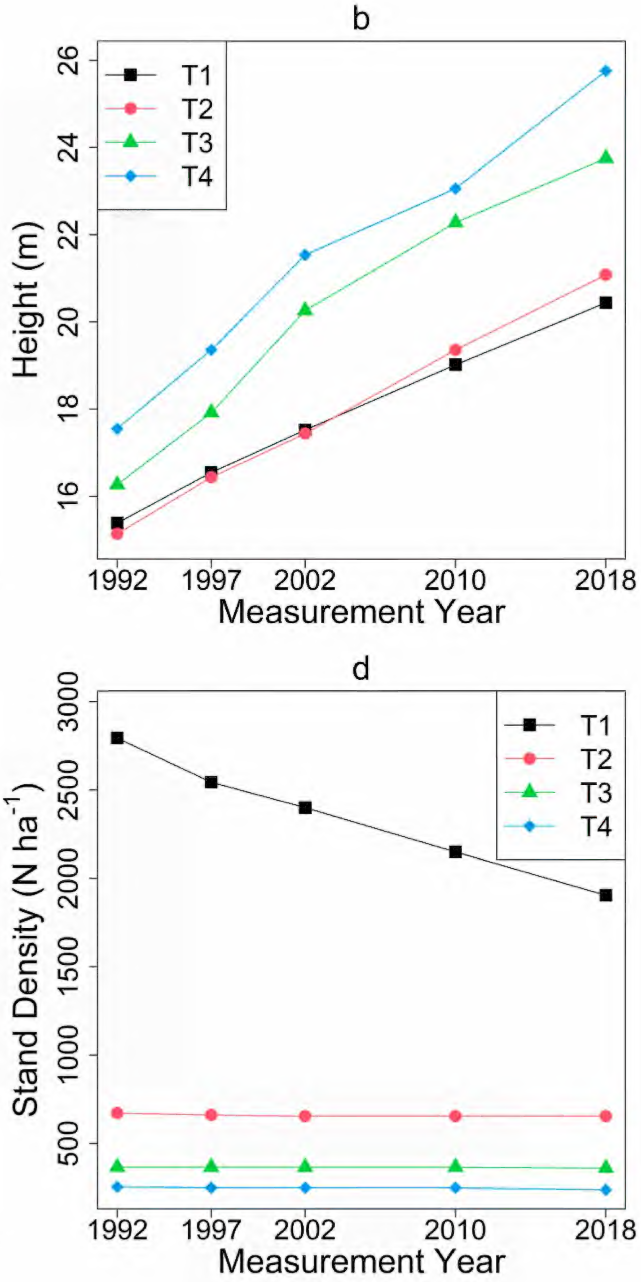

Figure A4. Variation of individual tree and stand level variables at different measurement year for different levels of stand density: (a) DBHUB; (b) height; (c) BAUB, (d) stand density. Meanings of T1 to T4 are described in Figure A2.

Journal of the Royal Society of Western Australia, 106: 61–74, 2023

A critical review of survey techniques and perceived threats for the threatened Pilbara ghost bat (*Macroderma gigas*)

HOLLY S. BRADLEY [1,*], ROBERT D. BULLEN [2], SOPHIE L. CROSS [1],
CHRIS G. KNUCKEY [3], MORGAN O'CONNELL [3], KYM OTTEWELL [4],
SCOTT REIFFER [5], SUZI WILD [6] & STEPHEN VAN LEEUWEN [1]

[1] *School of Molecular and Life Sciences, Curtin University, Kent Street, Bentley, Perth, WA 6102, Australia*

[2] *Bat Call WA, 43 Murray Drive, Hillarys, Western Australia 6025, Australia*

[3] *Biologic Environmental, 24 Wickham Street, East Perth, Western Australia 6004, Australia*

[4] *Biodiversity and Conservation Science, Department of Biodiversity, Conservation and Attractions, Kensington, Western Australia 6152, Australia*

[5] *Rio Tinto, Central Park, Level 24, 152 - 158 St Georges Terrace, Perth, Western Australia 6000, Australia*

[6] *BHP, 125 St Georges Terrace, Perth, Western Australia, 6000, Australia*

[*] *Corresponding author: ✉: h.bradley@curtin.edu.au*

ABSTRACT

Ghost bats of Western Australia's Pilbara region are widespread, although patchily distributed, and are threatened with local extirpation, largely in part due to the expanding mining footprint across the region. The extensive data collected to inform environmental impact assessments for mineral exploration projects, however, provides a key source of information to inform ghost bat policy and management. At present, the effectiveness of this resource is limited by accessibility. To help bridge this gap, we conducted a comprehensive review of the grey literature on ghost bats, summarising strategies for survey techniques, perceived threats, and threat mitigation strategies. Numerous threatening processes were identified as impacting ghost bats, with habitat loss and the cumulative impacts of mining most reported. Survey techniques were found to often include a combination of indirect and direct methods, although the suitability of different techniques is reliant on the context of the study. For this reason, it is important for future environmental assessment reports to include a detailed method rationale to support better data comparability and population estimation across the Pilbara. Overall, comprehensive and comparable research outputs will help to better assess and understand extinction risks, and to develop effective conservation management plans for this threatened species.

KEYWORDS: Abandoned mines, ecology, ghost bat, microbat, survey, threat mitigation

[**Editors' Note**: "Grey"-literature references are marked by * and cited in Appendix with link to website or library catalogue number]

INTRODUCTION

The ghost bat (*Macroderma gigas*) is Australia's only carnivorous bat and largest of the microchiroptean group (Strahan 1995; Start *et al*. 2019). Individuals weigh approximately 130 grams in the Pilbara (Guppy & Coles 1988), with a wingspan of approximately 60 centimetres (Walldorf & Mehlhorn 2014), and have pale grey to light brown fur, large ears that connect over the head, and a prominent but simple nose leaf (Tidemann *et al.* 1985). Ghost bats belong to a monotypic, endemic genus (Churchill & Helman 1990), and after a significant historic range contraction (Worthington Wilmer *et al.* 1999), are now limited to a small number of non-interbreeding populations across northern Australia, from the northwest of Western Australia to Rockhampton in Queensland (Churchill & Helman 1990; Hoyle *et al.* 2001). They are protected under both state (*Biodiversity Conservation Act 2016**; Vulnerable, Schedule 1) and federal (*Environment Protection and Biodiversity Conservation Act 1999**; Vulnerable) legislation. Pilbara populations are geographically widespread and discontinuous (Armstrong & Anstee 2000; McKenzie & Bullen 2009; Fig. 1), bordered by desert to the north and east (Bat Call 2017*). Due to geographic isolation from other extant ghost bat populations, the Pilbara population is recognised as genetically distinct at the regional level (Worthington Wilmer *et al.* 1994, 1999).

The distribution of ghost bats is limited by the presence of appropriate roosting sites, which can include both natural cave systems and disused mines, provided they have the required conditions for resting and breeding and permit access to suitable foraging habitat (Cramer *et al.* 2022). Presently, population size estimation for ghost bats in the Pilbara is between 1300 to 2000 individuals (TSSC 2016*; Ottewell *et al.* 2017*). Much of the Pilbara ghost bat population is limited to stronghold colonies roosting in disused copper and gold mines in the eastern Chichester subregion (approximately 70% of all ghost bats in the region; TSSC 2016*). Most of these roosting sites are at risk of collapse from age or from destruction by mining ventures (TSSC 2016*; Bat Call WA 2021*). Prior to conservation listing of the ghost bat under the *Environment Protection and Biodiversity Conservation Act 1999** in 2016, it was anticipated that many of the known Pilbara ghost bat roosts would be lost within 30 years in the absence of strategic intervention (Woinarski *et al.* 2014).

The Pilbara region is a hotspot for mining development and is of substantial economic importance to the rest of the state (Government of Western Australia 2014*), generating about 40% of Western Australia's gross domestic product (PEOF Overview 2019*). Almost 92% of the Pilbara IBRA (Interim Biogeographic Regionalisation for Australia) region is under mining and exploration tenure (Government of Western Australia 2014*). Consequently, mining activity and development pose a primary threat to ghost bat persistence (Cramer *et al.* 2022). There is a significant body of grey literature from decades of surveys conducted for Environmental Impact Assessment (EIA) of mining and mineral exploration projects, representing a major source of knowledge for the biodiversity in this region (Government of Western Australia 2014*). However, a limitation of this knowledge resource is a lack of communication between proponents and the absence of an easily accessible, central source of reporting and information (Government of Western Australia 2014*; Cramer *et al.* 2016). Failure to coordinate regional conservation initiatives and research can waste limited conservation funding and impede successful conservation outcomes (Pilbara Conservation Strategy 2017*).

There is no current over-arching regional management plan for the protection of Pilbara ghost bats (Armstrong 2010; Cramer *et al.* 2022). Growing interest amongst stakeholders to achieve conservation outcomes for threatened species in the Pilbara led to the launch of a workshop in March 2021 to identify research priorities for the Pilbara ghost bat (Cramer *et al.* 2022). A lack of data sharing due to confidentiality constraints and fragmented biodiversity data management systems

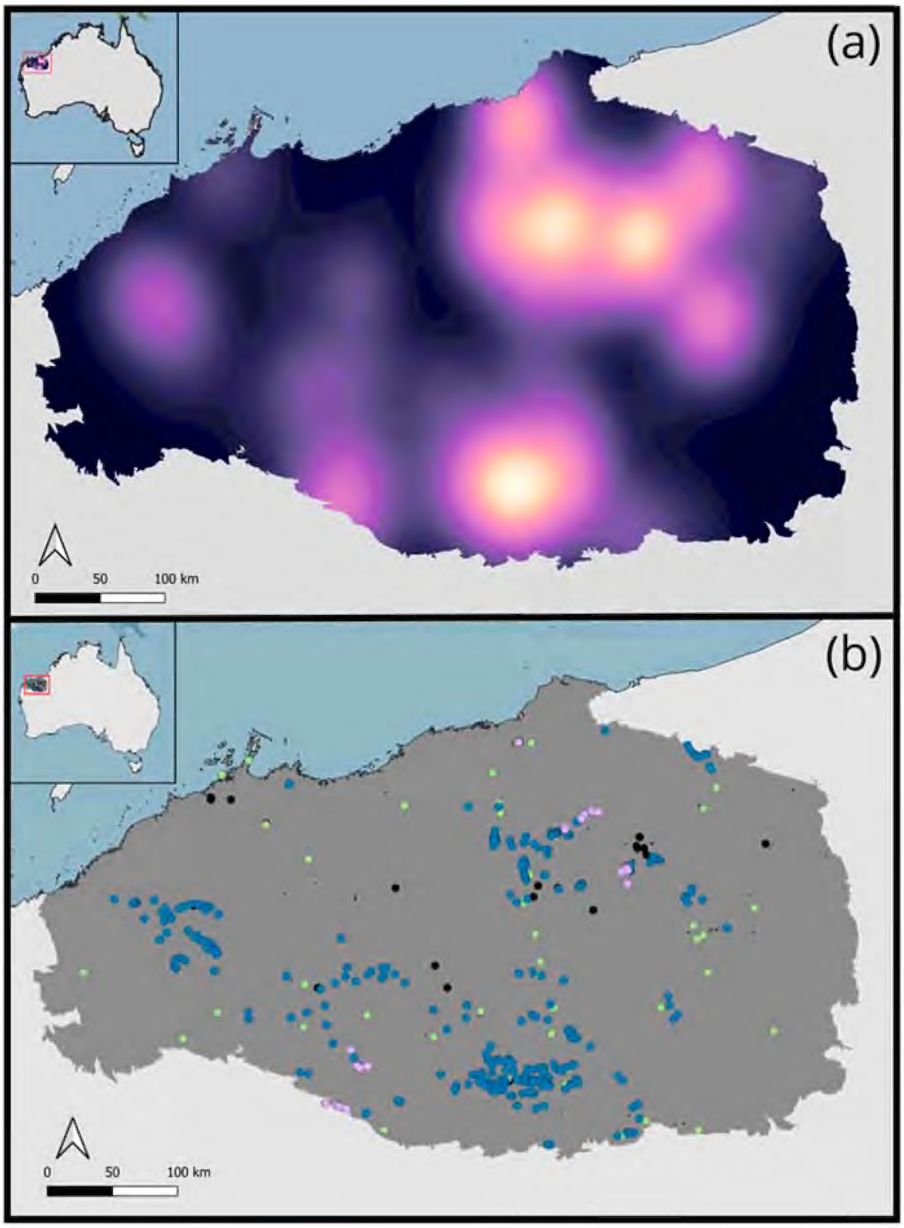

Figure 1. (a) Heatmap of ghost bat occurrence records across the Pilbara. Locations are taken from scientific and grey literature records of sightings/evidence collected between 1854 and 2022; and **(b)** occurrence records for the Pilbara ghost bat, as collected from the grey and scientific literature. Occurrence records are grouped as: black (pre-2000), green (2000–2010), blue (2010–2020), and purple (2020+), highlighting the general increase in recordings over the last decade.

and processes was identified as a major barrier to conservation planning for the species. To address this issue of largely scattered and inaccessible survey data, we collated a database of grey literature from sources ranging from multinational mining companies to sole trader consultancies. We conducted a comprehensive review of the grey literature, to: (i) identify and quantify the types of survey approaches and their frequency of use and (ii) identify the major perceived threats reported for ghost bat populations. Through recognition of these key trends and strategies, we aim to help facilitate best practice management and the ongoing conservation and recovery of the Pilbara ghost bat.

METHODS

To compile the database, we sourced available grey literature relating to ghost bat surveys and research. We limited our search to ghost bats within the Pilbara region of Western Australia as a unique management unit, due to their geographic and genetic isolation and the concentrated survey effort within this region. Literature was sourced from searches of databases, and from members of industry, government agencies, and consultancies. Searches of databases included Google Scholar, Web of Science (all databases, 1950–2021), and Scopus (all documents including secondary documents, all years; last searched March 2021), with additional publications sourced from the bibliographies of published literature. Searches of databases comprised any combination of the terms: 'ghost bat', or '*Macroderma gigas*', AND 'Western Australia', or 'Pilbara', AND 'behaviour', 'ecology', 'population', 'physiology', 'management', or 'conservation'. Grey literature included unpublished data such as government reports, environmental impact assessments, management plans, information posters, bulletins, and consulting surveys and reports; however, sourcing of grey literature was largely restricted to provision by members of industry and government due to difficulties accessing this data (Corlett 2011; Cramer *et al.* 2016). Only literature containing specific mention of ghost bats and a form of technology/method for their detection was included. Although published literature from across Australia has been referenced throughout this review to provide context, the reported statistics and trends relate only to our Pilbara-specific grey literature database, as our target questions (survey techniques and threat mitigation strategies) relate to management and policy, rather than research designed to answer a specific scientific question.

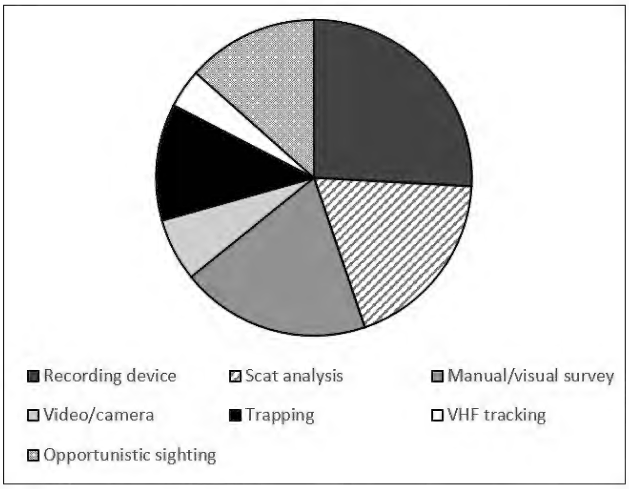

Figure 2. The relative proportions of techniques referenced for surveying ghost bats (*Macroderma gigas*), grouped according to acoustic and ultrasonic recording devices, scat analysis, manual/visual searches, video and camera devices, physical trapping of bats, VHF tracking, and opportunistic sightings. Reference to survey techniques was not mutually exclusive.

A total of 55 documents from the grey literature (from the years 2000-2022) were analysed to determine trends in the types of techniques and technologies used to survey ghost bats in the Pilbara (Fig. 2). Distribution records (between years 1899-2019) provided from the state government (Department of Biodiversity, Conservation and Attractions), were included for mapping purposes, as well as coordinates provided in the scientific and grey literature (Fig. 1). As numerous reports referred to previous survey work or surveys conducted by a different organisation, we considered survey techniques and threats those which were 'referenced' within a document.

RESULTS

Survey techniques

We found that survey techniques generally aligned to a three-step process: (i) the determination of potential roost sites and habitat; (ii) confirmation of bat presence and cave usage; and (iii) more detailed studies into population dynamics such as genetic health and colony connectivity. Overall, the use of recording devices was mentioned most often in the grey literature (26% of the total times techniques were reported; n = 52/203), followed by manual/visual searches (19%; n = 39/203) and scat analysis (19%; n = 38/203; Fig. 2).

RECORDING TECHNOLOGY

Review of the grey literature revealed most documents (84%; n = 46/55) referred to a form of acoustic or ultrasonic recording technology, with Song Meters (full spectrum detectors by Wildlife Acoustics Inc., USA) the most referenced (54%; n = 25/46), followed by AnaBat devices (early detectors by Titley Electronics, Australia; 33%; n = 15/46; Fig. 3). The type of ultrasonic recorder deployed was not specified or different in 24% (n = 11/46) of documents. Only 4% (n = 2/55) of documents referred to non-ultrasonic recording devices as a complementary recording method to the traditional ultrasonic methods.

Song Meters and AnaBat devices were the recording technologies with the highest reported use (Fig. 3); however, Song Meters have been steadily increasing in use, whereas AnaBat equipment has slowly decreased in use with time (Fig. 4). Only one report referenced a different recording technology (handheld Echo Meter; Biologic Environmental Survey 2019c*). Of the documents which used an ultrasonic recording technology (n = 37/55), only 16% (n = 6/37) justified why this technology

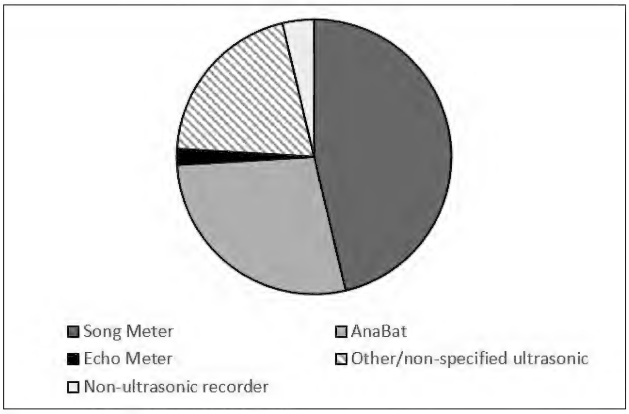

Figure 3. The relative proportions of recording equipment referenced for surveying ghost bats (*Macroderma gigas*), within documents which referenced a form of recording technology. Reference to recorder types was not mutually exclusive.

was selected. As Song Meter technology was more recently developed than AnaBat technology (Biologic Environmental Survey 2014*), justification was only relevant in later years (Song Meters appeared in the grey literature after 2009). However, justification was only present in 15% (n = 6/41) of documents dated as released after 2009 and referenced a form of acoustic or ultrasonic technology (n = 41).

OBSERVATIONAL SURVEYS

Targeted manual/visual surveys are the most common observational study method, reported in 71% (n = 39/55) of documents. Manual/visual surveys included inspections of suspected roosting sites and bat counts at cave entrances at dusk during bat emergence times (Molhar 2006*), plus aural surveys of bat calls (Bat Call WA 2013*). Both infrared cameras and motion-activated camera devices were used for bat surveys; and were evenly reported within the grey literature (infrared = 9%, n = 5/55 of documents; motion capture technology = 9%, n = 5/55 of documents).

TRAPPING & SCAT ANALYSIS

Trapping of bats using harp trapping or mist netting was referenced in 44% (n = 24/55) of documents. Collection of scats was one of the most common survey methods for ghost bats (69% of documents; n = 38/55).

Threats

For this review, perceived threats to ghost bats were reported in numerous documents (n = 42/55), with several highlighting more than one threat. The cumulative impacts from mining were reported in 98% (n = 41/42) of documents which referenced threats, and loss of habitat in 83% (n = 35/42) of those documents. Habitat modification was referenced in 74% of documents which referenced threats (n = 31/42), with feral predators (33%; n = 14/42), collisions with barbed wire fencing (29%; n = 12/42), and cane toads (17%; n = 7/42) the least often reported threats from these categories.

DISCUSSION

Survey techniques

Review of the grey literature determined a range of different techniques employed to survey and monitor Pilbara ghost bats. Acoustic and ultrasonic recorders were the survey technique used most often, followed by targeted searches and scat observation/collection. However, more novel or developing technologies such as VHF tracking for movement studies have been adopted in more recent years. The following discusses the use and context of the different survey techniques pertinent to the ongoing monitoring and management of Pilbara ghost bats.

ACOUSTIC & ULTRASONIC RECORDERS

Acoustic and ultrasonic recording is a method used to determine if caved areas are likely to be occupied by ghost bats, or to confirm presence at a particular cave site. It was the most frequently reported survey technique within the grey literature over the review period. This is likely because 95% (n = 52/55) of the documents which reported survey techniques were consultant or industry reports, primarily designed to meet a compliance requirement for the mining approval process. Determining the presence or use of an area by ghost bats is required prior to approval for mineral extraction in the Pilbara, and the deployment of ultrasonic and acoustic recorders can be a simple mechanism to survey ghost bat presence which allows the passive collection of data over consecutive days. It is also a method recommended under the Environmental Protection Authority's Technical Guidance for terrestrial vertebrate fauna surveys from environmental impact assessment in Australia (EPA 2020*).

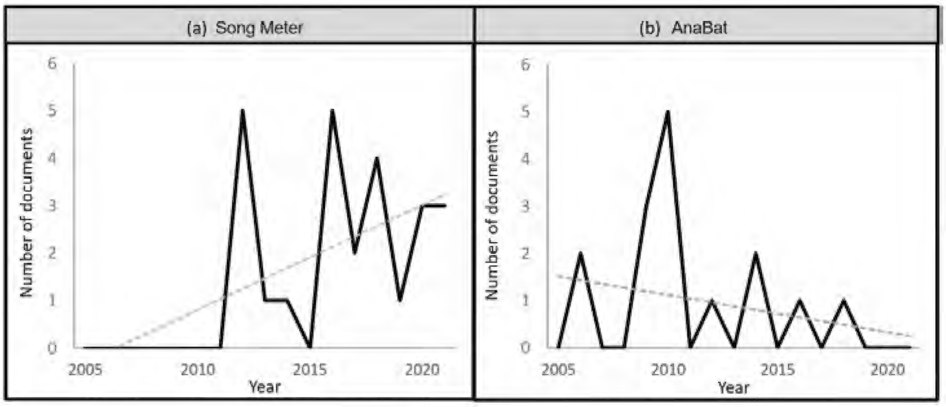

Figure 4. The number of documents (out of 55) specifying the use of (a) Song Meter devices and (b) AnaBat devices, between the years 2005 and 2021. Trendline is depicted in grey.

The collective distribution information provided by the acoustic and ultrasonic sampling data could be key to the continued regional monitoring of the Pilbara ghost bat population due to being the most feasible technology to be used at scale. However, different detectors can capture varied information (e.g., zero-crossing recordings do not capture amplitude or harmonic information; EPA 2020*) and can give different results, which impacts the comparability of results across the region and highlights the importance of reporting detector type and selected settings (Adams *et al.* 2012). The timing of the survey is also important to report, as seasonality can impact survey findings. For example, late summer when adult bats return, or the onset of winter when the population reassembles in the warmest caves, may be the most favourable times to conduct targeted colony counts, as bats will be congregated together (Toop 1985). Understanding the context of different surveys will help more accurately compare and collate population estimates across the region (Cramer *et al.* 2022).

Non-ultrasonic recorders can be used to complement ultrasonic recording surveys. The social calls of ghost bats are low pitched and range from 5-15 kHz, which is audible to humans and can be recorded on both non-ultrasonic recorders and ultrasonic recorders (Guppy *et al.* 1988; Hanrahan *et al.* 2021). As ghost bats often use visual detection to hunt (Tidemann *et al.* 1985), they are not always reliant on making ultrasonic calls (McKenzie 2016*; Outback Ecology 2012a*). New research in the Northern Territory indicates that recording social vocalisations can assist in the identification of maternity behaviours and roosting sites in a semiautomated and less invasive way than other methods which require entry into caves (Hanrahan *et al.* 2021). As many caves are not used by ghost bats, this application of the non-ultrasonic recording technology is most relevant to a secondary, detailed analysis of a site once colony occupation has been confirmed.

OBSERVATIONAL SURVEYS

Bat census surveys can confirm occupancy of a cave after selection as a potential roost site following cave assessment and acoustic surveying (Bat Call WA 2021*). Colony size can be estimated through direct observation and counts, and remote monitoring through use of video recordings can be used to conduct simultaneous assessments at multiple roost sites (e.g., Biologic Environmental Survey 2015*; 2020c*). Targeted searches and assessment of ghost bat usage of potential roost sites was the second highest reported technique among grey literature which reported survey methods. As in the acoustic surveys, this is likely an outcome of consultant and industry experimental designs targeted to assess ghost bat presence or absence for the mining approval process.

Despite the popularity of this method, a conservative approach must be taken to prevent stress to females with young or causing a colony to vacate a roost (Bat Call WA 2021*). Assessment of caves according to required roosting characteristics will help determine sites for further surveying and confirmation of ghost bat presence (Bat Call WA 2021*). A species distribution model is currently under development (K. Ottewell, pers. comm., 2022) and will also assist with targeting survey effort in the future, to gain a more comprehensive understanding of roost usage across the region. Additionally, visual inspection of bats in person and on camera can be useful to determine the presence of juveniles to confirm cave use as a maternity site (Biologic Environmental Survey 2015*). Confirmation of maternity roosting sites or critical caves is important, as these Category 1 and 2 caves (Bat Call WA 2021*) are protected for their regional significance, due to the comparative rarity of these caves with complex and stable internal structure and microclimate characteristics, in contrast to other short-term roosts (Biologic Environmental Survey 2014*).

TRAPPING

As ghost bats are easily disturbed and driven away from roosting sites, the disturbance of bats through physical entry of caves and trapping (e.g., harp trapping and mist netting) are not recommended on a repeated basis (TSSC 2016*; Ecoscape 2018*; Bat Call WA 2021*). To reduce the impact to pregnant and lactating females and their young, entry and trapping in caves should be avoided from mid-December to mid-March (Bat Call WA 2021*). Trapping should only serve a particular purpose, such as tissue collection or tracking studies (Bat Call WA 2021*). For example, tissue collection has allowed insight into the physiological resistance of ghost bats to toad toxins (Shine *et al.* 2016), an important step in prioritising and managing the threat of cane toads in the Pilbara. Capture of individuals to attach trackers for VHF tracking (e.g., Biologic Environmental Survey 2019c*; 2020d*) or GPS satellite tracking (Augusteyn 2018; Bullen *et al.* 2023) has also allowed greater insight into habitat use and likely areas of foraging, which can assist with optimising management and protection.

SCATS

The scats and middens produced by ghost bats are distinctive as they are almost twice the size of those produced by other cave-dwelling bats in the region (Biologic Environmental Survey 2020e*), and fresh scats can indicate current occupancy of a cave (Greenhall & Paradiso 1968). One limitation of this method is it relies on bats defecating directly above a ground sheet (Biologic Environmental Survey 2020e*). However, visual inspection of scat freshness away from the ground sheet can provide an indication of recent activity, although it is not possible to specify the time-period of activity (Biologic Environmental Survey 2015*). Scat presence can indicate site usage by ghost bats regardless of sampling season, as older scats can indicate historical use of a roost site and can be collected at any time. This is compared with other methods, such as acoustic recording which relies on active ghost bat presence at a site, which can be difficult given low site fidelity (Biologic Environmental Survey 2012*).

In addition to signifying cave habitation, analysis of DNA from the outer surface of ghost bat scats enables identification and tracking of individuals for mark recapture analysis and simultaneously provides information on the genetic 'health' of the population. Genotyping of DNA from scat samples creates a unique genetic fingerprint, a form of 'molecular tagging' that is used to survey individual bats in mark-recapture analyses to estimate population sizes. Molecular Tagging can be used to collect information on the temporal and spatial movements of individual ghost bats in a local area, for example to detect resident versus transient individuals and to identify 'recaptures' across years (Ottewell *et al.* 2018*; DBCA 2019*). Sex-linked markers are also available to identify sex of individuals which can assist in determination of population sex ratios, identification of maternity caves and monitoring of sex-based differences in dispersal and other behaviours. It is the only survey method currently available, besides live trapping, to provide resolution at the level of an individual. In addition to approaches using telemetry, genotyping of DNA from scat samples can provide insight into ghost bat movement patterns, including medium to long-distance dispersal events (e.g., Ottewell *et al.* 2019*) and the size of the spatial genetic neighbourhood (e.g., Ottewell *et al.* 2017*).

MOVEMENT STUDIES

Further surveying is required to understand both the presence and absence of ghost bats across the Pilbara landscape, and their basic ecology and movements (Claramunt *et al*. 2018; Cramer *et al*. 2022). Some previous studies have focussed on using VHF tracking to determine movement patterns, using VHF towers to determine relative importance of habitat areas (e.g., Biologic Environmental Survey 2019c*; 2020d*). However, as technology improves with the decrease in size of GPS tags (e.g., Weller *et al.* 2016; Conenna *et al.* 2019) and the development of satellite tags with data that can be downloaded remotely (e.g., Randhawa *et al.* 2020; Bullen *et al*. 2023), assessments of habitat usage and movement can be easier to conduct and with greater detail. The use of high-resolution GPS/satellite or VHF radio tracking can assist in identifying how movement is influenced by landscape features at various scales, such as whether long distance flights are facilitated by 'stepping-stones' of roosting sites (Cramer *et al*. 2022). A greater understanding of local movements and long-distance dispersal will enable identification of priority areas for management and conservation, and suitable buffer zones (e.g., from active mining) to assist in population conservation and management (e.g., as recommended in Biologic Environmental Survey 2016*; Bat Call WA 2017b*; Biologic Environmental Survey 2021d*).

Overall, ghost bats are a cryptic, evasive, and nocturnal species, and can be difficult to study (McKenzie 2016*). Surveying often requires a combination of techniques, including indirect and direct methods, for an effective assessment of occupancy and population size (McKenzie 2016*). We recommend the inclusion of a detailed method rationale in survey reporting to become standard practice, to support better comparability of data across the Pilbara, and generate a more accurate regional population estimation and consistent classification of roost habitat. Improved population estimation will require a substantial and coordinated effort which will be important for the assessment of regional and localised declines and inform policy and target management efforts.

Threats & mitigation management

Ghost bats are at risk of local extirpation across the Pilbara, largely due to habitat loss, the cumulative impacts of mining, collisions with barbed wire fencing, habitat modification, and competition and predation by feral predators with poisoning from cane toads an emergent risk. These are perceived threats, as it is difficult to obtain quantitative data on actual threat levels. Research priorities to quantify some of these threat levels are discussed in Cramer *et al.* (2022). The March 2021 stakeholder workshop (Cramer *et al*. 2022) identified each of these threats as a priority for mitigation to ensure the ongoing survival of ghost bats in the Pilbara, with climate change the only perceived threat not directly referenced in any of the literature. Although these perceived threats are not a novel insight and have been previously published within the scientific literature (e.g., Armstrong & Anstee 2000; Hoyle *et al.* 2001; Woinarski *et al.* 2014), our following summary can help discern if the same perceived threats are also prevalent within the grey literature.

HABITAT & ROOST LOSS

The most immediate threat to Pilbara ghost bats is the destruction of habitat from mining and other development activity (Woinarski *et al*. 2014; Cramer *et al*. 2022). Over the last decade, ghost bats were listed in the top ten threatened species in Australia to lose the most potential habitat (Ward *et al.* 2019). Without stronger protection or a change to current mining trends, many Pilbara roosting sites are predicted to be destroyed from mining activity within the next 30 years (Woinarski *et al*. 2014). The conservation of both roosting caves and foraging habitat, such as riparian corridors and productive plains with sparse, mature woodlands over *Triodia* spp. (Bat Call WA 2021*), is crucial for the long-term survival of ghost bat populations (Armstrong & Anstee 2000; Biologic Environmental Survey 2019c*; Cramer *et al*. 2022).

In addition to the protection of current habitat assets within the Pilbara, another mitigation strategy to prevent further population decline is the rehabilitation of degraded roosting sites. Ghost bats often rely on abandoned mine shafts as roosting sites, particularly in the East Pilbara (Churchill & Helman 1990; Armstrong & Anstee 2000; Woinarski *et al*. 2014). However, many abandoned underground mining structures are degraded and collapsing (Woinarski *et al*. 2014; TSSC 2016*). As there is a large backlog of rehabilitation work to fix these degraded roosting sites (Woinarski *et al*. 2014; TSSC 2016*), a strategic assessment of the regional significance of different roosting sites and an inventory of disused mines will be important to plan and prioritise rehabilitation efforts (NSW National Parks and Wildlife Service 2001*; Thomson *et al*. 2015). Under this approach, the highest value conservation assets should be protected first. A mitigation plan will also be required to limit or manage the disturbance to in situ bat populations during rehabilitation works.

The creation of new artificial roosting sites is being investigated as an additional management tool. Several factors are important to consider during the construction of artificial caves, including the physical and microhabitat requirements for the roost type. To maximise cost efficiency and minimise disturbance, the potential for conversion of an anthropogenic structure already in place (e.g., mine shafts), or addition of an adit to a pre-existing cave should be considered first, particularly as natural caves are likely to have greater longevity than an artificial structure (Biologic Environmental Survey 2014*; 2016*). If an artificial roost is created from scratch, it should be adjacent to other known roost sites or disturbed roost sites, and of a size that would support a sustainable population size for the area (as ghost bats are a top-order predator, over-abundance in certain areas could impact prey populations; Biologic Environmental Survey 2014*). Trials are underway in the Pilbara testing the creation of roosting caves through placement of a concrete cave structure (with varied chamber sizes and rough roof material for bats to grip), buried into the side of a hill to avoid drill and blasting disturbance (GCM 2016*). Monitoring is ongoing to determine usage of these artificial sites by ghost bats (BHP 2017*). Overall, whilst rehabilitation of abandoned mine infrastructure and the installation of artificial roosting habitat can be useful mitigation measures, it must be emphasised that these are not an equivalent ecological replacement to the protection of natural roosting caves, which is the priority for the ongoing survival of ghost bats (L. Ruykys pers. comm. in Bat Call WA 2021*).

CUMULATIVE IMPACTS FROM MINING

There is a substantial knowledge gap regarding the impact of active mining operations and their proximity to ghost bats, and this is a research priority for the Pilbara (Bat Call WA 2021*; Cramer *et al*. 2022). Further research is required to determine the appropriate buffer zone size to prevent roost abandonment due to altered cave conditions after dewatering or excess water disposal from mining activity (Bat Call WA 2021*). It is unknown if ghost bats return to sites that have been abandoned, and the length of time this takes if they do return (Cramer *et al.* 2022). Determination of appropriate buffer zone size is important to protect bats from the direct and indirect effects of blasting, such as exposure to potential pollutants and irritants in the dust (Bat Call WA 2021*). The investigation of disturbance thresholds that trigger a significant response from ghost bats continues to be a considerable practical challenge (Cramer *et al*. 2022) and will be key to informing policy and management.

Current limitations to understanding the cumulative impacts of mining include the lack of transparent data sharing, no central information repository for survey and monitoring data, and no central information site on clearance approvals. Advice under the *Environment Protection and Biodiversity Conservation Act 1999** states that there are currently no adequate mechanisms in place to provide the high-level planning, prioritisation, and stakeholder support required to prevent further ghost bat declines (DoE 2022*). Therefore, in addition to further research, a collaborative effort to share and centralise information will be an important step towards effective conservation management. Formal protection of Pilbara roosting sites is required, alongside policy to enforce best practice as standard for mining proponents in the region (Armstrong & Anstee 2000; TSSC 2016*). We encourage a structured review of mitigation methods, particularly a cost-benefit assessment to understand which approaches are feasible, cost-effective and have the biggest impact on improving ghost bat survival. This process will likely require a further workshop with expert elicitation.

CANE TOADS & INTRODUCED PREDATORS

Cane toad poisoning is a risk to ghost bats, as the toads are of similar size to current prey items, and native frogs are already a component of the ghost bat diet (Manger *et al*. 2001; Barritt 2012*). The western cane toad invasion front has not yet reached the Pilbara but is predicted to be potentially facilitated by artificial water point 'stepping-stones' (Florance *et al.* 2011; Tingley *et al.* 2013; Southwell *et al.* 2017). There are not any effective tools available to significantly control cane toad numbers at a landscape scale within Australia (Shanmuganathan *et al.* 2010). As such, comparison of a species distribution model for ghost bats with a fundamental niche model for cane toads will help to identify areas the two species may overlap in the Pilbara and focus localised control measures (Cramer *et al*. 2022).

Ghost bats are the only carnivorous microbat in Australia, feeding on small mammals (including other bats), reptiles, birds, and large insects (Bat Call WA 2016d*). The nutritional value and water content derived from mammalian and bird prey is greater than from smaller insects, meaning ghost bats likely preferentially target larger prey in the arid Pilbara (Claramunt *et al.* 2018). Therefore, ghost bats are likely to be potential prey items themselves as well as compete for prey with other larger introduced predators such as the feral cat, fox, and wild dog (Duncan *et al.* 1999).

HABITAT MODIFICATION & ANTHROPOGENIC DISTURBANCE

Prevention of repeated entrance to roost sites is important, as repeated disturbances may lead to roost abandonment (Bob Bullen pers. comm. 2023). Broad-scale disturbances, such as livestock grazing and altered fire regimes, can also change the spatial and temporal productivity of the landscape, potentially decreasing the foraging quality for ghost bats (Cramer *et al.* 2022). Further research is required to provide definition of what is a significant impact to the foraging habitat of ghost bats (Cramer *et al.* 2022). Active protection of roost sites and foraging areas from degradation is considered a priority in the Pilbara (TSSC 2016*); however, there is currently no regional management plan in place to coordinate this effort (Armstrong 2010). Overall, further research, formalised policy, and the regional coordination of management is required to mitigate the degradation and modification of ghost bat habitat.

BARBED WIRE

Over a quarter of the reviewed grey literature which specified threats to the ghost bat listed barbed wire as a perceived threat. However, despite the pervasiveness of this threat across the Pilbara, most ghost bat deaths from barbed wire entanglement are preventable. Barbed wire fencing is rarely essential and can be removed, replaced, or managed to reduce its impact (Little & Hall 2006*). The most effective solution to prevent entanglement deaths is to remove barbed wire completely and use alternative materials for fencing (Booth 2006*). As pastoral leases extend across more than 62 per cent of the Pilbara bioregion (PEOF Implementation Plan 2019*), the distribution of barbed wire for livestock management is likely extensive, and removal may first need to be targeted to areas with confirmed ghost bat roosting and

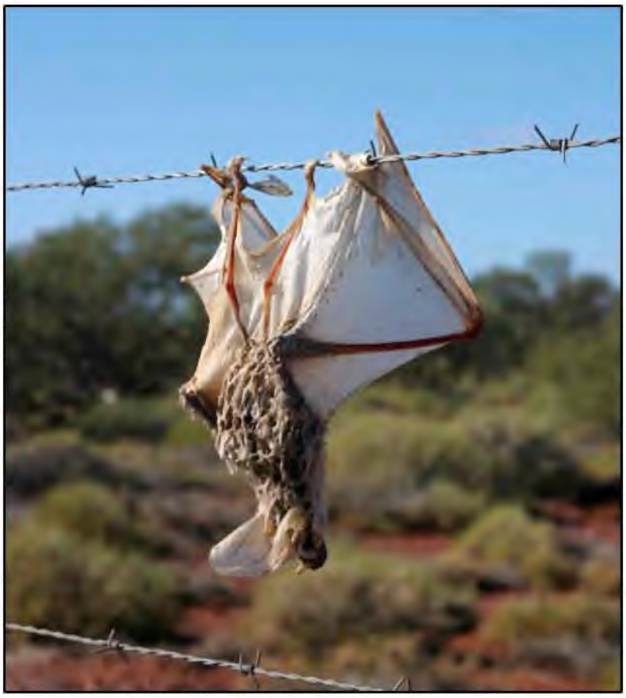

Figure 5. Example of a deceased ghost bat entangled in barbed wire fencing in the Pilbara region of Western Australia. 2005 Photograph by S. van Leeuwen.

foraging sites. An education and awareness program, such as those developed in Victoria (Maclean 2006*), may also be useful for the staged removal and replacement of barbed wire fencing by pastoralists. Some mining proponents, such as Atlas Iron Limited (2017)* and Roy Hill (2020)*, have committed to actively replacing or preventing the use of barbed wire for their projects. However, legal reforms and updated policy are required to make this mandatory for industry and land managers throughout the Pilbara (Booth 2006*).

In cases where the removal of barbed wire is not feasible, or the use of barbed wire is unavoidable, barbed sections may be covered with poly pipe, sheets of chicken mesh, or electric tape, particularly at entanglement hotspot sites (van der Ree 1999; Booth 2006*; Booth 2007*). Visible and audible additions to fences, including plastic flags, aluminium cans, metal tags, plates, and tape, may also increase the detectability of fences for bat avoidance (Booth 2006*; Booth 2007*). However, tags and flagging must be maintained or designed to be long-lasting due to deterioration in the elements and to withstand cyclonic events. Plastic options should be avoided for stock fencing as cattle (and likely other fauna) can consume plastic, which can lead to digestive problems and death (Booth 2006*; Anwar *et al.* 2013).

CONCLUSION

The extensive mining footprint across the Pilbara is a predominant threat to the ghost bat population (Cramer *et al.* 2022). However, the collective body of surveys produced as part of environmental impact assessments for mining proposals (K.N. Armstrong unpublished data cited in Armstrong 2010; Government of Western Australia 2014*) is a major source of knowledge for the biodiversity in this region (Government of Western Australia 2014*). At present, the grey literature is largely inaccessible, and the aim of this review was to collate a database of grey literature and synthesize trends in the survey techniques and perceived threats for Pilbara ghost bats. The complementary use of indirect and direct methods can be used to survey a range of factors relating to Pilbara ghost bats. The suitability of different techniques depends on the context of the study, highlighting the importance of reporting justifications for survey design. It is, therefore, recommended for future environmental assessment reports to include detailed method rationales to support better data comparability and population estimation across the Pilbara, which is important to inform policy and targeted management efforts.

Perceived threats to ghost bats are cumulative and varied, with habitat clearing and the cumulative impacts of mining often reported as perceived threats in the grey literature. Continued research and management trials will be important to develop optimal strategies for management. At present, most ghost bat surveys are conducted around mine sites, leading to a spatial bias in data collection. The grey literature consists of many once-off survey events that were the requirement for an environmental approval, leading to an *ad hoc* distribution of survey sites, and a lack of repeated assessments. There is a need for longer-term monitoring studies, plus an increased sample size of sites (particularly in under-sampled areas away from mined zones), to disentangle annual variation versus long-term trends in ghost bat ecology and population dynamics. Tenure issues may complicate the ability to select and secure long-term monitoring sites, although the Pilbara Environmental Offset Fund provides a framework and an avenue for collaboration to navigate these challenges (PEOF Implementation Plan 2019*).

While this review is an important step towards greater knowledge sharing and accessibility, the development of improved data capture systems will be important for optimised data sharing in the future. Across the world, the quantity of grey literature on some topics can far exceed that of the scientific literature (Corlett 2011), representing a vast, unexploited resource. Inclusion and analysis of grey literature studies to reviews and planning is important to help reduce the publication bias apparent in the scientific literature, where failed trials or null results are less likely to be published (Conn *et al.* 2003; Paez 2017). A more balanced understanding of the evidence (Paez 2017) is critical in a field such as threatened species management, where understanding the effectiveness of management actions is key to optimising techniques and standards. Development of a centralised data archive with free accessibility will contribute greatly to increasing visibility of the grey literature, and maximising data sharing (Corlett 2011). It is in the best interests of the scientific community to maximise the cumulative power of research, through the wider and more consistent dissemination of data (Conn *et al.* 2003), to improve conservation outcomes for threatened species, particularly those infrequently discussed in the published literature.

ACKNOWLEDGEMENTS

We respectfully acknowledge the Whadjuk people of the Noongar Nation as the Traditional Custodians of the lands on which we undertook this review. We also acknowledge the Traditional Custodians of the lands in the Pilbara for their ongoing stewardship of the Country on which this bat occurs. We would like to thank Craig Salt from Sustainable Consulting for workshop facilitation at the 2021 Ghost Bat Workshop, and for all workshop attendees for providing their expert opinion and discussion. We would also like to thank BHP for sponsorship of the workshop, and the anonymous reviewers for their expert review of the manuscript.

REFERENCES

Adams A M, Jantzen M K, Hamilton R M & Fenton M B 2012. Do you hear what I hear? Implications of detector selection for acoustic monitoring of bats. *Methods in Ecology and Evolution* **3**, 992–998.

Anwar K, Khan I, Aslam A, Mujtaba M, Din A, Amin Y & Ali Z 2013. Prevalence of indigestible rumen and reticulum foreign bodies in Achai cattle at different regions of Khyber Pakhtunkhwa. *ARPN Journal of Agricultural and Biological Science* **8**, 580–586.

Armstrong K N & Anstee S D 2000. The ghost bat in the Pilbara: 100 years on. *Australian Mammalogy* **22**, 93–101.

Armstrong K N 2010. Assessing the short-term effect of minerals exploration drilling on colonies of bats of conservation significance: a case study near Marble Bar, Western Australia. *Journal of the Royal Society of Western Australia* **93**, 165.

Augusteyn J, Hughes J, Armstrong G, Real K & Pacioni C 2018. Tracking and tracing central Queensland's *Macroderma* – determining the size of the Mount Etna ghost bat population and potential threats. *Australian Mammalogy* **40**, 243–253.

Bullen R D, Reiffer S & Trainer J 2023. Satellite tracking Ghost Bats (*Macroderma gigas* in the Pilbara, Western Australia. *Records of the Western Australian Museum* **38**, 1–10.

Churchill S K & Helman P M 1990. Distribution of the Ghost Bat, *Macroderma gigas*, (Chiroptera: Megadermatidae) in central and South Australia. *Australian Mammalogy* **13**, 149–156.

Claramunt A M A, White N E, Bunce M, O'connell M, Bullen R D & Mawson P R 2018. Determination of the diet of the ghost bat (*Macroderma gigas*) in the Pilbara region of Western Australia from dried prey remains and DNA metabarcoding. *Australian Journal of Zoology* **66**, 195–200.

Conenna I, López-baucells A, Rocha R, Ripperger S & Cabeza M 2019. Movement seasonality in a desert-dwelling bat revealed by miniature GPS loggers. *Movement Ecology* **7**, 1–10.

Conn V S, Valentine J C, Cooper H M & Rantz M J 2003. Grey literature in meta-analyses. *Nursing research* **52**, 256–261.

Corlett R T 2011. Trouble with the gray literature. *Biotropica* **43**, 3–5.

Cramer V A, Armstrong K N, Bullen R D, Ellis R, Gibson L A, Mckenzie N L, O'connell M, Spate A & Van Leeuwen S 2016. Research priorities for the Pilbara leaf-nosed bat (*Rhinonicteris aurantia* Pilbara form). *Australian Mammalogy*, **38**, 149–157.

Cramer V A, Armstrong K N, Bullen R D, Cross S L, Gibson L, Hanrahan N, Knuckey C G, Ottewell K, Reigger S, RuykyS L & Shaw R E 2022. Research priorities for the ghost bat (*Macroderma gigas*) in the Pilbara region of Western Australia. *Australian Mammalogy*, **45**(1), 1–12.

Duncan A, Baker G B & Montgomery N 1999. The action plan for Australian bats, Environment Australia, Canberra.

Florance D, Webb J K, Dempster T, Kearney M R, Worthing A & Letnic M 2011. Excluding access to invasion hubs can contain the spread of an invasive vertebrate. *Proceedings of the Royal Society B: Biological Sciences* **278**, 2900–2908.

Greenhall A M & Paradiso J L 1968. Bats and bat banding. U.S. Department of the Interior, Bureau of Sport Fisheries and Wildlife, Washington D.C.

Guppy A & Coles R B 1988. Acoustical and neural aspects of hearing in the Australian gleaning bats, *Macroderma gigas* and *Nyctophilus gouldi*. *Journal of Comparative Physiology A* **162**, 653–668.

Hanrahan N, Turnill C, Armstrong K N, Dalziell A H & Welbergen J A 2021. Ghost bats exhibit informative daily and seasonal temporal patterns in the production of social vocalisations. *Australian Journal of Zoology* **67**, 305–315.

Hoyle S D, Pople A R & Toop G J 2001. Mark–recapture may reveal more about ecology than about population trends: demography of a threatened ghost bat (*Macroderma gigas*) population. *Austral Ecology* **26**, 80–92.

Manger P R, Collins R & Rosa M G P 2001. An architectonic comparison of the ventrobasal complex of two Megachiropteran and one Microchiropteran bat: implications for the evolution of Chiroptera. *Somatosensory & Motor Research* **18**,131–140.

Mckenzie N L & Bullen R D 2009. The echolocation calls, habitat relationships, foraging niches and communities of Pilbara microbats. *Records of the Western Australian Museum* **78**, 123–155.

Paez A 2017. Gray literature: An important resource in systematic reviews. *Journal of Evidence-Based Medicine* **10**, 233–240.

Randhawa N, Bird B H, Vanwormer E, Sijali z, Kilonzo C, MSIGWA A, Ekiri A B, Samson A, Epstein J H, Wolking D J & Smith W A 2020. Fruit bats in flight: a look into the movements of the ecologically important *Eidolon helvum* in Tanzania. *One Health Outlook* **2**, 1–14.

Shanmuganathan T, Pallister J, Doody S, Mccallum H, Robinson T, Sheppard A, Hardy C, Halliday D, Venables D, Voysey R, Strive T, Hinds L & Hyatt A 2010. Biological control of the cane toad in Australia: a review. *Animal Conservation* **13**, 16–23.

Shine R, Wang S, Madani G, Armstrong K N, Zhang L & Li Y M 2016. Using genetic data to predict the vulnerability of a native predator to a toxic invader. *Endangered Species Research* **31**, 13–17.

Southwell D, Tingley R, Bode M, Nicholson E & Phillips B L 2017. Cost and feasibility of a barrier to halt the spread of invasive cane toads in arid Australia: incorporating expert knowledge into model-based decision-making. *Journal of Applied Ecology* **54**, 216–224.

Start A N, Mckenzie N L & Bullen R D 2019. Notes on bats in the diets of Ghost Bats (*Macrodermia gigas:* Megadermatidate) in the Pilbara region of Western Australia. *Records of the Western Australian Museum* **34**(1), 51–53.

Strahan R 1995. The mammals of Australia. Reed New Holland, Sydney, Australia.

Tidemann C R, Priddel D M, Nelson, J E & Pettigrew J D 1985. Foraging behaviour of the Australian Ghost Bat, *Macroderma gigas* (Microchiroptera: Megadermatidae). *Australian Journal of Zoology* **33**, 705–13.

Tingley R, Phillips B L, Letnic M, Brown G P, Shine R & Baird S J E 2013. Identifying optimal barriers to halt the invasion of cane toads *Rhinella marina* in arid Australia. *Journal of Applied Ecology* **50**, 129–137.

Toop J 1985. Habitat requirements, survival strategies and ecology of the ghost bat *Macroderma gigas* Dobson, (Microchiroptera, Megadermatidae) in central coastal Queensland. *Macroderma* **1**(2), 37–41.

Van Der Ree R 1999. Barbed wire fencing as a hazard for wildlife. *Victorian Naturalist*, **116**, 210–217.

Walldorf V & Mehlhorn H 2014. Bats: A glimpse on their astonishing morphology and lifestyle. In: *Bats (Chiroptera) as vectors of diseases and parasites* (pp. 7–24). Springer, Berlin, Heidelberg.

WARD M S, SIMMONDS J S, RESIDE A E, WATSON J E M, RHODES J R, POSSINGHAM H P, TREZISE J, FLETCHER R, FILE L & TAYLOR M 2019. Lots of loss with little scrutiny: The attrition of habitat critical for threatened species in Australia. *Conservation Science and Practice* **1**(11), e117.

WELLER T J, CASTLE K T, LIECHTI F, HEIN C D, SCHIRMACHER M R & CRYAN P M 2016. First direct evidence of long-distance seasonal movements and hibernation in a migratory bat. *Scientific Reports* **6**, 1–7.

WOINARSKI J C, BURBIDGE A A & HARRISON P L 2014. The action plan for Australian mammals, 2012. CSIRO Publishing, Collingwood, Victoria.

WORTHINGTON WILMER J, MORITZ C, HALL L & TOOP J 1994. Extreme population structuring in the threatened ghost bat, *Macroderma gigas:* evidence from mitochondrial DNA. *Proceedings of the Royal Society of London B Biological Sciences* **257**(1349), 193–198.

WORTHINGTON WILMER J, HALL L, BARRATT E & MORITZ C 1999. Genetic structure and male-mediated gene flow in the ghost bat (*Macroderma gigas*). *Evolution* **53**, 1582–1591.

APPENDIX

The grey literature in this Appendix bibliography is publicly available through the government approval websites: https://www.epa.wa.gov.au; http://epbcnotices.environment.gov.au; Government of Western Australia Department of Biodiversity, Conservation and Attractions library catalogue https://library.dbca.wa.gov.au and the Government of New South Wales, Australia.

REFERENCES (GREY LITERATURE):

Astron EnvironmentaL Services 2012. Activity assessment for bats of conservation significance. West Pilbara Iron Ore Project, prepared for API Management, Western Australia. Available from the Government of Western Australia Department of Biodiversity, Conservation and Attractions library catalogue, location 932763.

Atlas Iron Limited 2017*. Significant species management plan. Corunna Downs, Western Australia. Available from: http://epbcnotices.environment.gov.au/_entity/annotation/ffe59068-1fe1-e611-bdfe-005056ba00a8/a71d58ad-4cba-48b6-8dab-f3091fc31cd5?t=1683105833875

Atlas Iron Limited 2020. Significant species management plan. Miralga Creek DSO Project, Western Australia. Available from: https://www.epa.wa.gov.au/sites/default/files/PER_documentation2/Appendix%20K%20-%20Significant%20Species%20Management%20Plan.pdf

Bamford Consulting Ecologists 2008. Fauna assessment of the Wodgina Tailings Storage Facility 3. Prepared for EnviroWorks Consulting, Western Australia. Available from: http://epbcnotices.environment.gov.au/_entity/annotation/66b8b01c-8f69-e511-a947-005056ba00a8/a71d58ad-4cba-48b6-8dab-f3091fc31cd5?t=1683180427561

Barritt M 2012*. High end living - sandstones and floodplains of Litchfield National Park. *Wildlife Australia Magazine*, 12-17. Available from: https://search.informit.org/doi/epdf/10.3316/informit.959531729651616

Bat Call Wa 2009. Echolocation survey of bat activity in the Anson-Wogina mine site. Atlas Iron – Wodgina DSO Project Bat Survey April-May 2009, prepared for Outback Ecology, Western Australia. Available from: http://epbcnotices.environment.gov.au/_entity/annotation/2b0aaf23-e868-e511-b93f-005056ba00a7/a71d58ad-4cba-48b6-8dab-f3091fc31cd5?t=1683105589256

Bat Call Wa 2010a. Bat survey of proposed Anketell Port, Western Australia. June 2009 – March 2010. Prepared for Phoenix Environmental Science, Western Australia. Available from the Government of Western Australia Department of Biodiversity, Conservation and Attractions library catalogue, location 125761.

Bat Call Wa 2010b. Sound and vibration levels during drilling operations and impact on bat activity. Poondano Project, WA, Pilbara leaf-nosed and ghost bat monitoring November 2009, prepared for Outback Ecology, Western Australia. Available from the Government of Western Australia Department of Biodiversity, Conservation and Attractions library catalogue, location 071125.

Bat Call Wa 2012. Echolocation survey of bat activity. West Turner Project Extension Fauna Survey, prepared for Biota Environmental Sciences, Western Australia. Available from the Government of Western Australia Department of Biodiversity, Conservation and Attractions library catalogue, location 206083.

Bat Call Wa 2013*. Survey of bat activity in the Weeli Wolli Creek system of the Hamersley Range, Pilbara. Report #10 Wet Season Survey, Western Australia. Available from the Government of Western Australia Department of Biodiversity, Conservation and Attractions library catalogue, location 932813.

Bat Call Wa 2016a. Cave CO-CA-01 Pilbara leaf-nosed bat Roost Census, July 2016. Corunna Downs, Atlas Iron, prepared for MWH Global, Western Australia. Available from: https://www.epa.wa.gov.au/sites/default/files/Referral_Documentation/Appendix%20L%20MWH%202018%20Terrestrial%20Vertebrate%20Fauna%20Survey.pdf

Bat Call Wa 2016b. Echolocation survey of bat activity. Corunna Downs Project, Pilbara WA, Phase 1, February to March 2014, prepared for MWH Global, Western Australia. Available from: https://www.epa.wa.gov.au/sites/default/files/Referral_Documentation/Appendix%20L%20MWH%202018%20Terrestrial%20Vertebrate%20Fauna%20Survey.pdf

Bat Call Wa 2016c. Echolocation survey of bat activity. Corunna Downs Project, Pilbara WA, Phase 2, September to October 2016, prepared for MWH Global, Western Australia. Available from: https://www.epa.wa.gov.au/sites/default/files/Referral_Documentation/Appendix%20L%20MWH%202018%20Terrestrial%20Vertebrate%20Fauna%20Survey.pdf

Bat Call Wa 2016d*. Ghost bat roost cave assessment, July 2016. Mesa B and C, prepared for Rio Tinto, Western Australia. Available from: https://www.epa.wa.gov.au/sites/default/files/PER_documentation2/A8%20Ghost%20Bat%20Roost%20Cave%20Assessment%20%28Bat%20Call%202016%29.pdf

Bat Call Wa 2017a. Ghost bat roost cave assessment, April 2017. Robe Valley Mesa H, prepared for Rio Tinto, Western Australia. Available from the Government of Western Australia Department of Biodiversity, Conservation and Attractions library catalogue, location 206089.

Bat Call Wa 2017b*. Impact of mining on ghost bat presence and activity, April 2017, including assessment of caves on Mesas F and G. Robe Valley Mesa A to Mesa 2405A, prepared for Rio Tinto, Western Australia. Available from: https://www.epa.wa.gov.au/sites/default/files/PER_documentation2/A11%20Robe%20Valley%20Mesa%20A%20to%20Mesa%202405A%2C%20impact%20of%20mining%20on%20Ghost%20bat%20presence%20and%20activity%20%28Bat%20Call%202017a%29.pdf

Bat Call Wa 2020a. Acoustic survey of ghost bat activity, July 2018 to February 2020. Rio Tinto, Paraburdoo Western Range, Pilbara WA, prepared for Rio Tinto, Western Australia. Available from: https://www.epa.wa.gov.au/sites/default/files/PER_documentation2/A6_6%20WR%20Ghost%20Bat%20acoustic%20survey%20(Bat%20Call%202020b).pdf

Bat Call Wa 2020b. Miralga Creek review - March 2020. Western Australia. Available from: https://www.epa.wa.gov.au/sites/default/files/Referral_Documentation/Appendix%20F%20-%20Ghost%20Bat%20Review.pdf

Bat Call wa 2021*. A review of ghost bat ecology, threats and survey requirements. Prepared for the Department of Agriculture, Water and the Environment, Australian Capital Territory. Available from: https://www.dcceew.gov.au/environment/epbc/publications/review-ghost-bat

Bhp 2006. Management plan for bat species. Goldsworthy Extension Project, Revision 2 January 2006, Western Australia. Available from the Government of Western Australia Department of Biodiversity, Conservation and Attractions library catalogue, location 206304.

Bhp 2017*. Ghost bat research plan November 2017 draft. Western Australian Iron Ore, Western Australia. Available from the Government of Western Australia Department of Biodiversity, Conservation and Attractions library catalogue, location 206409.

Biodiversity Conservation Act 2016*. Version 00-d0-01. Available from: https://www.legislation.wa.gov.au/legislation/prod/filestore.nsf/FileURL/mrdoc_41658.pdf/$FILE/

Biodiversity%20Conservation%20Act%202016%20-%20%5B00-d0-01%5D.pdf?OpenElement

Biologic Environmental Survey 2012*. Targeted ghost bat survey at Karijini National Park. Prepared for BHP, Western Australia. Available from the Government of Western Australia Department of Biodiversity, Conservation and Attractions library catalogue, location 206469.

Biologic Environmental Survey 2014*. Ghost bat assessment. West Angelas - Deposit B and F, Robe River Joint Venture, Western Australia. Available from: https://www.epa.wa.gov.au/sites/default/files/API_documents/Appendix%207%20West%20Angelas%20Deposit%20B%20and%20F%20Ghost%20Bat%20Assessment%2C%20Biologic%202014_0.pdf

Biologic Environmental Survey and Bat Call Wa 2014. Pilbara regional ghost bat review. Prepared for BHP, Western Australia. Available from the Government of Western Australia Department of Biodiversity, Conservation and Attractions library catalogue, location 206467.

Biologic Environmental Survey 2015*. Central Pilbara Ghost Bat Population and Roost Assessment: 2014. Prepared for BHP, Western Australia. Available from the Government of Western Australia Department of Biodiversity, Conservation and Attractions library catalogue, location 206312.

Biologic Environmental Survey 2016*. Environmental impact assessment for ghost bat (*Macroderma gigas*). Mining Area C - Southern Flank. Prepared for BHP, Western Australia. Available from the Government of Western Australia Department of Biodiversity, Conservation and Attractions library catalogue, location 201229.

Biologic Environmental Survey 2018. 2017 West Angelas ghost bat monitoring, January 2018, prepared for Rio Tinto Iron Ore, Western Australia. Available from the Government of Western Australia Department of Biodiversity, Conservation and Attractions library catalogue, location 206478.

Biologic Environmental Survey 2019a. Conservation significant bat species impact assessment, October 2019. Warrawoona Gold Project, prepared for Calidus Resources Limited, Western Australia. Available from: http://epbcnotices.environment.gov.au/_entity/annotation/be02f2e8-b33c-ea11-b0a8-00505684324c/a71d58ad-4cba-48b6-8dab-f3091fc31cd5?t=1683104786587

Biologic Environmental Survey 2019b. Targeted vertebrate and short-range endemic invertebrate fauna assessment. Shearer's West. Prepared for BHP, Western Australia. Available from: https://www.bhp.com/-/media/bhp/regulatory-information-media/iron-ore/western-australia-iron-ore/jimblebar/jimblebar-optimisation-project---revised-draft-validation-notice---appendix-2/

Biologic Environmental Survey 2019c*. VHF bat foraging studies March 2019. Warrawoona Gold Project. Prepared for Calidus Resources Limited, Western Australia. Available from the Government of Western Australia Department of Biodiversity, Conservation and Attractions library catalogue, location 206474.

Biologic Environmental Survey 2019d. VHF bat foraging studies September 2019. Warrawoona Gold Project, prepared for Calidus Resources Limited, Western Australia. Available from: https://www.epa.wa.gov.au/sites/default/files/PER_documentation2/1-3.%20VHF%20Bat%20Foraging%20%28Biologic%29.pdf

Biologic Environmental Survey 2020a. Biologic environmental survey memo. Memo: Western Range ghost bat VHF study, prepared for Rio Tinto Iron Ore, Western Australia. Available from: https://www.epa.wa.gov.au/sites/default/files/PER_documentation2/A6_9%20Western%20Range%20Ghost%20Bat%20VHF%20Memo%20%28Biologic%202020b%29.pdf

Biologic Environmental Survey 2020b. Conservation significant vertebrate fauna impact assessment. Miralga Creek Project, prepared for Atlas Iron Limited, Western Australia. Available from: https://www.epa.wa.gov.au/sites/default/files/PER_documentation2/Appendix%20I%20-%20Vertebrate%20Fauna%20Impact%20Assessment.pdf

Biologic Environmental Survey 2020c*. Level 2 vertebrate fauna and short-range endemic invertebrate fauna assessment. Miralga Creek, prepared for Atlas Iron Limited, Western Australia. Available from: https://www.epa.wa.gov.au/sites/default/files/PER_documentation2/Appendix%20E%20-%20Level%202%20Vertebrate%20and%20SRE%20Invertebrate%20Fauna%20Assessment.pdf

Biologic Environmental Survey 2020d*. Memo: Western Range Ghost Bat VHF Study. Western Range, prepared for Rio Tinto Iron Ore, Western Australia. Available from the Government of Western Australia Department of Biodiversity, Conservation and Attractions library catalogue, location 206480.

Biologic Environmental Survey 2020e*. Western Range ghost bat scat analysis report March 2020. Prepared for Rio Tinto, Western Australia. Available from: https://www.epa.wa.gov.au/sites/default/files/PER_documentation2/A6_10%20Western%20Range%20Ghost%20Bat%20Scat%20Analysis%20Report%20(Biologic%202020c).pdf

Biologic Environmental Survey 2020f. Western Range: ghost bat VHF study April 2020. Prepared for Rio Tinto, Western Australia. Available from the Government of Western Australia Department of Biodiversity, Conservation and Attractions library catalogue, location 206479.

Biologic Environmental Survey 2021a. Consolidated terrestrial fauna report, January 2021. Sanjiv Ridge Stage2 Development Area, prepared for Atlas Iron Limited, Western Australia. Available from: https://www.epa.wa.gov.au/sites/default/files/Referral_Documentation/Appendix%20D%20-%20Verteb~-%20Stage%202%20-%20Atlas%20Iron%20Pty%20Ltd.PDF

Biologic Environmental Survey 2021b. Ghost bat and Pilbara leaf-nosed bat monitoring and regional survey. Sanjiv Ridge Stage 2, prepared for Atlas Iron Limited, Western Australia. Available from: https://www.epa.wa.gov.au/sites/default/files/Referral_Documentation/Appendix%20F%20-%20Ghost%20~-%20Stage%202%20-%20Atlas%20Iron%20Pty%20Ltd.PDF

Biologic Environmental Survey 2021c. Vertebrate fauna impact assessment. Sanjiv Ridge Stage 2, September 2021, prepared for Atlas Iron Limited, Western Australia. Available from: https://www.epa.wa.gov.au/sites/default/files/Referral_Documentation/Appendix%20E%20-%20Verteb~-%20Stage%202%20-%20Atlas%20Iron%20Pty%20Ltd.PDF

Biologic Environmental Survey 2021d*. West Angelas ghost bat monitoring 2020, February 2021. Prepared for Rio Tinto, Western Australia. Available from the Government of Western Australia Department of Biodiversity, Conservation and Attractions library catalogue, location 206484.

Biota Environmental Sciences 2009a. West Pilbara Iron Ore Project mine areas seasonal fauna survey. Prepared for API Management, Western Australia. Available from the Government of Western Australia Department of Biodiversity, Conservation and Attractions library catalogue, location 071224.

Biota Environmental Sciences 2009b. West Pilbara Iron Ore Project rail corridor fauna and fauna assemblages survey. Western Australia. Available from the Government of Western Australia Department of Biodiversity, Conservation and Attractions library catalogue, location 071230.

Booth C 2006*. Barbed wire action plan. Queensland Conservation Council, Queensland. Available from: https://wildlifefriendlyfencing.org/wp-content/uploads/2021/10/action_plan.pdf

Booth C 2007*. Caught in the devil's rope: barbed wire and wildlife. *Wildlife Australia* **44**, 16–20. Available from: https://www.proquest.com/docview/218395703?pq-origsite=gscholar&fromopenview=true

Department Biodiversity, Conservation And Attractions (DBCA) 2019*. Ghost bat (*Macroderma gigas*) genetic sampling. Robe River 2018, Government of Western Australia, Western Australia. Available from the Government of Western Australia Department of Biodiversity, Conservation and Attractions library catalogue, location 072430.

Department Of The Environment (DoE) 2022*. *Macroderma gigas* in Species Profile and Threats Database, Department of the Environment, Australian Capital Territory. Available from: https://www.environment.gov.au/sprat. Accessed 9/03/2022.

Ecologia 2000. Ghost bat management plan. West Angelas Minesite, prepared for Robe River Mining Co., Western Australia. Available from the Government of Western Australia Department of Biodiversity, Conservation and Attractions library catalogue, location 57206.

Ecoscape 2018*. Consolidated vertebrate fauna. Eliwana Project, prepared for Fortescue Metals Group, Western Australia. Available from: https://www.epa.wa.gov.au/sites/default/files/PER_documentation2/Appendix%2018%20Consolidated%20Vertebrate%20Fauna%20Survey%20Ecoscape%202017.pdf

Environmental Protection And Biodiversity Conservation Act 1999*. Available from: https://www.dcceew.gov.au/environment/epbc

Epa 2020*. Technical Guidance: Terrestrial vertebrate fauna surveys for environmental impact assessment. EPA Services, Department of Water and Environmental Regulation, Western Australia. Available from: https://www.epa.wa.gov.au/sites/default/files/Policies_and_Guidance/2020.09.17%20-%20EPA%20Technical%20Guidance%20-%20Vertebrate%20Fauna%20Surveys%20-%20Final.pdf

Fortescue Metals Group (Fmg) 2018. Conservation significant fauna management plan, February 2018. Western Australia. Available from the Government of Western Australia Department of Biodiversity, Conservation and Attractions library catalogue, location 206592.

Global Civil And Mining (Gcm) 2016*. Ghost bat roost habitat recon project - Area C. Prepared for BHP, Western Australia. Available from the Government of Western Australia Department of Biodiversity, Conservation and Attractions library catalogue, location 206408.

Government Of Western Australia 2014*. Cumulative environmental impacts of development in the Pilbara region. Advice of the Environmental Protection Authority to the Minister for Environment under Section 16(e) of the *Environmental Protection Act 1986*. Available from: https://www.epa.wa.gov.au/sites/default/files/Publications/Pilbara%20s16e%20advice%20%20270814.pdf

Kingfisher Environmental Consulting 2017. Sulphur Springs 2017 targeted fauna assessment. Prepared for Venturex Resources Limited, Western Australia. Available from: https://www.epa.wa.gov.au/sites/default/files/PER_documentation2/Appendix%2024%20-%20Sulphur%20Springs%20Targeted%20Fauna%20Assessment%20%28Kingfisher%202017%29.pdf

Little L & Hall L 2006*. John Toop, Mount Etna and ghost bats (*Macroderma gigas,* Dobson.). *The Australasian Bat Society Newsletter* (26), 28–29. Available from: https://www.ausbats.org.au/uploads/4/4/9/0/44908845/absn26.pdf

Maclean J J 2006*. Reducing the impact of barbed wire on wildlife. *The Australasian Bat Society Newsletter* (27), 33–36. Available from: https://www.ausbats.org.au/uploads/4/4/9/0/44908845/absn27.pdf

Mckenzie N L 2016*. Letter to Sarah Williamson, BHP, 16 November 2016. Available from: https://www.epa.wa.gov.au/sites/default/files/PER_documentation/Appendix%205%20-%20Ghost%20Bat%20peer%20review.pdf

Molhar 2006*. Survey for bats in disused underground mines near Nullagine. Prepared for Rapallo Consulting and Contracting Engineers and Wedgetail Exploration NL, Western Australia. Available from the Government of Western Australia Department of Biodiversity, Conservation and Attractions library catalogue, location 206401.

Nsw National Parks And Wildlife Service 2001*. Strategy for the conservation of bats in derelict mines. NSW NPWS, New South Wales. Available from: https://www.environment.nsw.gov.au/resources/nature/batsInMines.pdf

Ottewell K, Mcarthur S, Van Leeuwen S & Byrne M 2017*. Population genetics of the ghost bat (*Macroderma gigas*) in the Pilbara bioregion. Report for the Government of Western Australia, Western Australia. Available from the Government of Western Australia Department of Biodiversity, Conservation and Attractions library catalogue, location 072226.

Ottewell K, Mcarthur S, Van Leeuwen S & Byrne M 2018*. Cave use by the Ghost Bat (*Macroderma gigas*) at the West Angelas mine site, Final Report. Government of Western Australia, Western Australia. Available from the Government of Western Australia Department of Biodiversity, Conservation and Attractions library catalogue, location 072225.

Ottewell K, Mcarthur S, Van Leeuwen S & Byrne M 2019*. Ghost bat (*Macroderma gigas*) genetic monitoring: South Flank 2017–2018. Final report. Prepared for Biologic Environmental Survey. Government of Western Australia, Western Australia. Available from the Government of Western Australia Department of Biodiversity, Conservation and Attractions library catalogue, location 072635.

Outback Ecology 2010a. Terrestrial vertebrate fauna baseline survey, December 2010. Turner River Hub, prepared for Atlas Iron Limited, Western Australia. Unpublished draft report, available from the Government of Western Australia Department of Biodiversity, Conservation and Attractions library catalogue, location 206392.

Outback Ecology 2010b. Vertebrate fauna cumulative impact assessment, September 2010. Wodgina DSO Project Stage 2. Prepared for Atlas Iron Limited, Western Australia. Available from: http://epbcnotices.environment.gov.au/_entity/annotation/f519571d-8b69-e511-b93f-005056ba00a7/a71d58ad-4cba-48b6-8dab-f3091fc31cd5?t=1683103866470

Outback Ecology 2012a*. Exploration track clearance bat monitoring, August 2012. Mt Webber DSO Project, prepared for Atlas Iron Limited, Western Australia. Available from the Government of Western Australia Department of Biodiversity, Conservation and Attractions library catalogue, location 206396.

Outback Ecology 2012b. Terrestrial vertebrate fauna impact assessment. Abydos DSO Project. Prepared for Atlas iron Limited, Western Australia. Available from: http://epbcnotices.environment.gov.au/_entity/annotation/f519571d-8b69-e511-b93f-005056ba00a7/a71d58ad-4cba-48b6-8dab-f3091fc31cd5?t=1683103866470 and http://epbcnotices.environment.gov.au/_entity/annotation/c7acf50e-8f69-e511-b93f-005056ba00a7/a71d58ad-4cba-48b6-8dab-f3091fc31cd5?t=1683104393814

Phoenix Environmental Sciences 2010. Terrestrial vertebrate fauna survey for Anketell Point Rail alignment and port projects. Prepared for Australian Premium Iron Management Pty Ltd, Western Australia. Available from the Government of Western Australia Department of Biodiversity, Conservation and Attractions library catalogue, location 071240.

Pilbara Conservation Strategy 2017*. Department of Parks and Wildlife, Government of Western Australia, Western Australia. Available from: https://www.dbca.wa.gov.au/management/pilbara

Pilbara Environmental Offsets Fund (Peof) Implementation Plan 2019*. Department of Water and Environmental Regulation, Government of Western Australia, Western Australia. Available from: https://www.wa.gov.au/government/publications/pilbara-environmental-offsets-fund-implementation-plan

Pilbara Environmental Offset Fund (Peof) Overview 2019*. Department of Water and Environmental Regulation, Government of Western Australia, Western Australia. Available from: https://www.wa.gov.au/government/publications/pilbara-environmental-offsets-fund-overview

Rapallo Environmental 2012. Biological assessment of the conservation focus area. Prepared for API Management Pty Ltd, Western Australia. Available from the Government of Western Australia Department of Biodiversity, Conservation and Attractions library catalogue, location 932806.

ROY HILL 2020*. Mine vertebrate fauna management plan. Prepared for Roy Hill Iron Ore, Western Australia. Available from: https://www.epa.wa.gov.au/sites/default/files/Proponent_response_to_submissions/Appendix%2010%20-%20Roy%20Hill%20Mine%20Vertebrate%20Fauna%20Management%20Plan%20%28OP-PLN-00324%29.pdf

STANTEC 2016. Terrestrial vertebrate fauna survey. Corunna Downs Project, prepared for Atlas Iron Limited, Western Australia. Available from: http://epbcnotices.environment.gov.au/_entity/annotation/93e30a79-1fe1-e611-bdfe-005056ba00a8/a71d58ad-4cba-48b6-8dab-f3091fc31cd5?t=1485907200357

STANTEC 2018. Terrestrial vertebrate fauna survey. Corunna Downs Project, prepared for Atlas Iron Limited, Western Australia. Available from: https://www.epa.wa.gov.au/sites/default/files/Referral_Documentation/Appendix%20L%20MWH%202018%20Terrestrial%20Vertebrate%20Fauna%20Survey.pdf

THOMSON B, UNGER C & WILLIAMS W 2015. Applying best bat-practices at abandoned mines. Wildlife Australia Magazine, 42–46. Available from: https://search.informit.org/doi/epdf/10.3316/informit.330217647053551

THREATENED SPECIES SCIENTIFIC COMMITTEE (TSSC) 2016*. Conservation Advice *Macroderma gigas* Ghost Bat. Department of the Environment, Canberra, Australian Capital Territory. Available from: https://www.environment.gov.au/biodiversity/threatened/species/pubs/174-conservation-advice-05052016.pdf

Journal of the Royal Society of Western Australia, 106: 75–103, 2024

Preliminary appraisal of biota from methane-seep and associated deposits, lower Holmwood Shale, Early Permian (Sakmarian), Irwin Basin, Western Australia

DAVID W. HAIG [1*], **ANTOINE DILLINGER** [2], **GEOFFREY PLAYFORD** [3], **ROSINE RIERA** [4], **ALEKSEY SADEKOV** [5], **GRZEGORZ SKRZYPEK** [6], **ECKART HÅKANSSON** [2], **ARTHUR J. MORY** [7], **DANIEL PEYROT** [2], **CHARMAINE THOMAS** [7]

[1] *Oceans Institute, The University of Western Australia, 35 Stirling Highway, Perth, Western Australia 6009, Australia*

[2] *School of Earth Sciences, The University of Western Australia, 35 Stirling Highway, Perth, Western Australia 6009, Australia*

[3] *School of Environment, The University of Queensland, Brisbane, Queensland 4072, Australia*

[4] *Norwegian Geotechnical Institute, Level 7, 40 St Georges Terrace, Perth, Western Australia 6000, Australia*

[5] *Centre for Microscopy, Characterisation and Analysis, The University of Western Australia, 35 Stirling Highway, Perth, Western Australia 6009, Australia*

[6] *West Australian Biogeography Centre, School of Biological Sciences, 35 Stirling Highway, Perth, Western Australia 6009, Australia*

[7] *Geological Survey and Resource Strategy Division, Department of Mines, Industry Regulation and Safety, 100 Plain Street East Perth, Western Australia 6004, Australia*

* *Corresponding author:* ✉ *david.haig@uwa.edu.au*

Abstract

Fossil assemblages preserved in nodules of the methane-seep deposits, recognized by Haig *et al.* (2022) in the lower Permian (Cisuralian, Sakmarian stage) of the Irwin Basin, include representatives of three ecosystems: seep, pelagic, and coastal plain. The seep biota, new to the Australian Permian, consists of small thickets with a framework of tubeworms, less common algal-like *Tubiphytes*, and problematica (? algae or sponges). Other components include microbial mats, macrophyte alga *Litostroma* (first report from Gondwana); foraminifers; sponges with siliceous monaxon spicules; a new group of small, lightly ornamented rostroconchs; microgastropods and rare larger types; ostracods and minute scolecodonts from polychaete jaws. Elements of the pelagic ecosystem are ammonoids (abundant in enclosing shale) and marine microphytoplankton. Probable vertebrate bone (possibly amphibians) and diverse spores and pollen from land plants come from the adjoining coastal plain. The surrounding mudstone lacks benthic macrofauna but includes an unusual assemblage of siliceous agglutinated foraminifers. The seeps were oases of high organic productivity on an otherwise barren muddy seafloor. The Holmwood Shale's seep carbonates have close similarities to modern seep deposits in shallow-marine settings.

Key words: *Litostroma*, *Tubiphytes*; **foraminifers; rostroconchs; tube worms; palynomorphs**

[**Editor's Note**: Most of the content of this paper was originally archived as unpublished supplementary files to Haig, D.W., Dillinger, A., Playford, G., Riera, R., Sadekov, A., Skrzypek, G., Håkansson, E., Mory, A.J., Peyrot, D., Thomas, C., 2022. Methane seeps following Early Permian (Sakmarian) deglaciation, interior East Gondwana, Western Australia: multiphase carbonate cements, distinct carbon-isotope signatures, extraordinary biota. Palaeogeography, Palaeoclimatology, Palaeoecology 591, 110862. https://doi.org/10.1016/j.palaeo.2022.110862. It is here published with permission from the Senior Copyright's Specialist, Elsevier, in a pers. comm. to D.W. Haig dated 22 September 2023.]

INTRODUCTION

Carbonate nodules generated in methane-seeps were recognized by Haig *et al.* (2022) in blue-grey massive mudstone low in the Holmwood Shale (Fig. 1). The stratigraphic position is significant, lying at a short vertical distance (ca. 75–85 m) above the glaciogenic Nangetty Formation of the Lower Permian (Sakmarian) in the Irwin Basin (Fig. 1). The nodules are characterized by (1) cementstone with complex multiphase fabric, including yellow cement; (2) $\delta^{13}C$ values mostly within the range, -25 – -45 ‰ VPDB (Vienna Pee Dee Belemnite standard); and (3) an unusual biota with some similarities to that found living in modern seeps (Haig *et al.* 2022). These seep-deposits are the first to be recognized from the Australian Upper Paleozoic and some of very few reported from Permian strata elsewhere.

Fossil assemblages found in the seep nodules are unlike those well-known from Permian limestone units elsewhere in Australian basins (Skwarko 1993; Archbold 2000). This paper presents a preliminary appraisal of the biota in the carbonate nodules and in the surrounding shale. It outlines the reasons for identifications and discusses general implications of the biota for understanding local palaeoecology and broader biogeography of Early Permian environments in this region. Specialist taxonomic studies on most of the

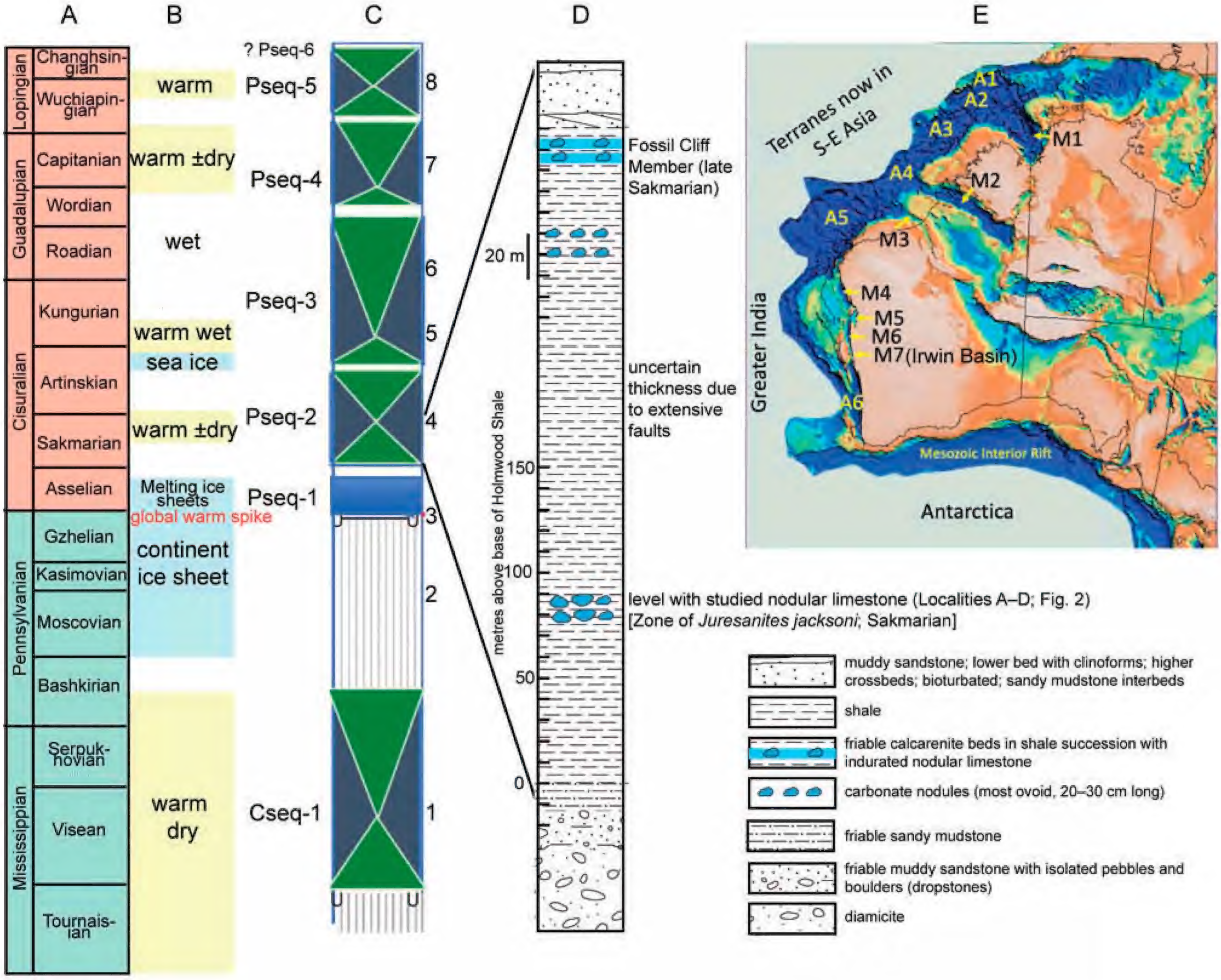

Figure 1. Stratigraphic and regional setting of studied methane-seep deposits. A, Carboniferous (green) and Permian (orange brown) chronostratigraphy following the International Chronostratigraphic Chart v2023/09 (www.stratigraphy.org accessed on 7 December 2023). B, Climate trends following Haig *et al*. (2018). C, Broad-scale sequence stratigraphy with depositional cycles Cseq-1 and Pseq-1 to Pseq-6 following Haig *et al*. (2018); rectangles with green triangles on blue background indicate retrogradational phases (deepening - green triangle with apex upward) and progradational phases (shallowing - green triangle with apex downward and with junction of triangles the maximum marine flooding level) of the major cycles. Numbers on the side of column C are among the most recent references on each cycle: **1**, Vachard *et al*. 2014; **2**, Backhouse & Mory 2020 (regional hiatus); **3**, Davydov *et al*. 2013, 2014; **4**, Haig *et al*. 2014, 2022, Taboada *et al*. 2015, Tremblin & Haig 2023; **5**, Haig *et al*. 2017, Haig 2018; **6**, Haig & Mory 2016; **7**, Nogami 1963, Haig *et al*. 2018; **8**, McCartain *et al*. 2006; Haig *et al*. 2018. D, Schematic stratigraphic log of the Holmwood Shale in the study area (from Haig *et al*. 2022). E, Basement terrane map of the Western Australian part of the East Gondwana Lowlands (compiled by FROGTECH, www.frogtech.com,au accessed 7 December 2023) with dark blue areas along the present-day western margin of the continent outlining late Paleozoic depocentres with axial basins of the East Gondwana Interior Rift labelled A1 to A6, and marginal rift basins labelled M1 to M7 (see Haig *et al*. 2018, 2022 for details). The site of the present study is the Irwin Basin (M7).

groups still must be made and this preliminary account aims to encourage future more detailed systematic studies of this remarkable biota.

LOCALITY DESCRIPTIONS

Locality A

The locality is at Macaroni Hill on the western side of Nangetty Station (Fig. 2A) at 28.9714°S, 115.0471°E. It is located on a shale breakaway at the edge of a large mesa about 1.5 km northwest of Nangetty Homestead (Fig. 2A). Nodular limestone (cementstone) forms three units on the hill in an exposed stratigraphic thickness of about 4 m (Figs. 2D). The limestone units seem to have limited lateral extent. Locality/sample co-ordinates are given in Appendix 1, and a description of rock types is provided by Haig *et al*. (2022). The section with limestone forming the hill seems to be a mound that was, before modern erosion, encased in grey shale. The shale includes sparsely scattered small carbonate mudstone nodules some of which contain the large ammonoid *Juresanites jacksoni*.

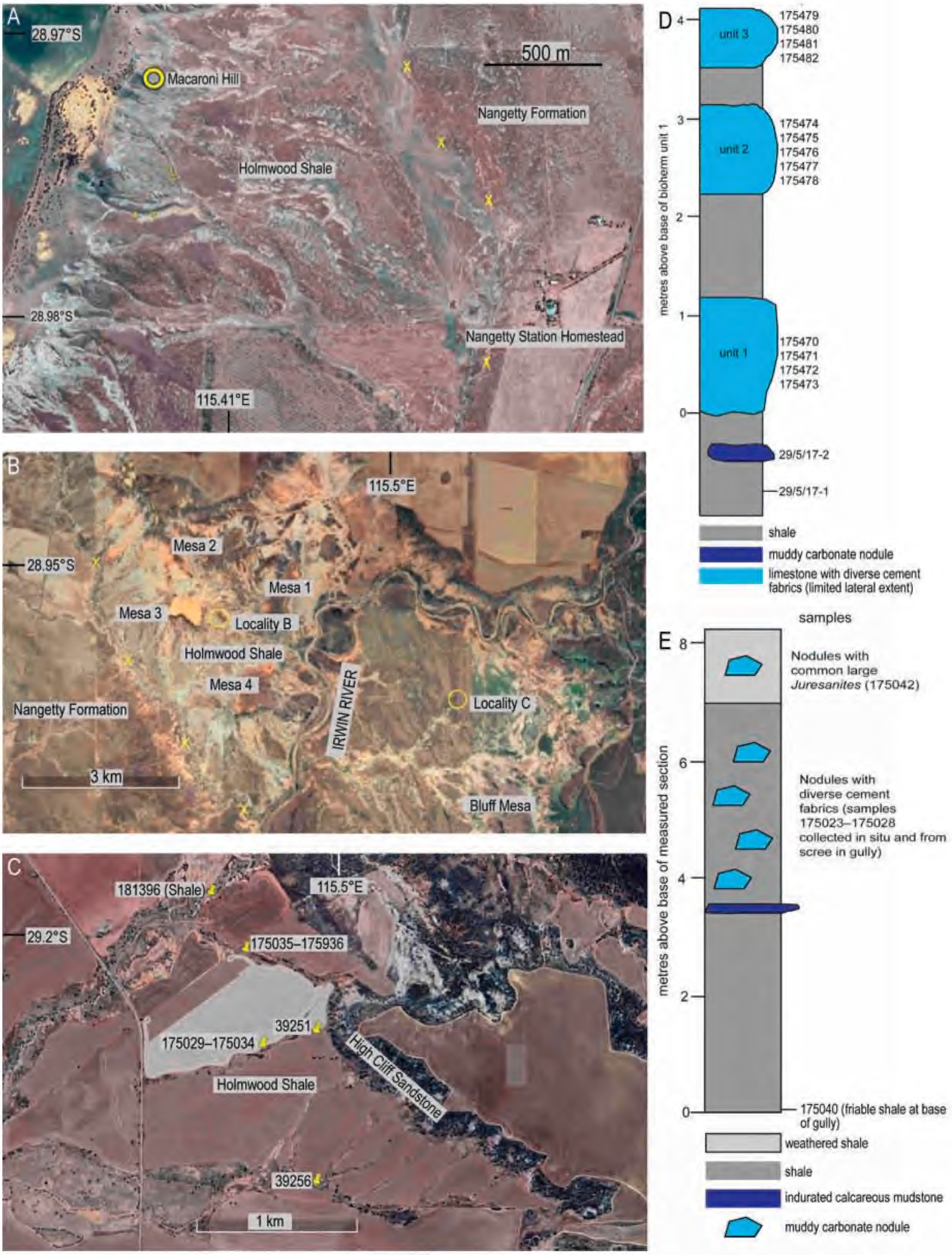

Figure 2. A–C, Google-Earth images. A, Country west of Nangetty Station Homestead. Note position of Macaroni Hill (Locality A) on "breakaway" (escarpment) with Holmwood Shale outcrop. The probable contact between the underlying glaciogenic Nangetty Formation and the Holmwood Shale is marked by yellow crosses. B, Positions of Localities B and C. The names of Mesas follow Clarke *et al*. (1951). A yellow X marks the contact between the glaciogenic Nangetty Formation (west) and the Holmwood Shale (east). Note: Locality B lies on a *Juresanites* ammonoid horizon marked on the Clarke *et al*. (1951) map. Locality C lies on a fossiliferous horizon marked by Clarke *et al*. (1951). To the immediate west of Locality C, the strata are structurally disturbed. Clarke *et al*. (1951) showed major faults in this area. Localities B and C are stratigraphically close and the strata around Locality C have been repeated by faulting. C, Position of sampling sites in Woolaga Creek area (Locality D, see Appendix 1 for details). D and E, schematic stratigraphic logs of sections containing methane-seep nodules at Locality A (D) and Locality B (E).

Locality B

Locality B lies at 28.9597°S, 115.4664°E on a mudstone scarp between prominent mesas in the northeastern sector of Nangetty Station (Fig. 2B). The stratigraphic log (Fig. 2E) was taken from the succession exposed in the major gully on the southern side of the scarp. Samples are listed in Appendix 1, and rock types are described in Haig *et al*. (2022). The nodular limestone level at Locality B is at the same altitude as Locality A. Given the negligible dip, it likely represents the same stratigraphic position.

Locality C

Locality C covers a flat area among cultivated paddocks strewn with dislocated nodules, around 28.9771°S and 115.5120°E (Fig. 2B). The nodules follow a trend along the structural strike of the Holmwood Shale here, near the boundary fence between Nangetty and Holmwood stations. This is in a faulted part of the succession. Similarities in the biota and cement fabrics (see Haig *et al*. 2022) suggest that the nodular carbonates here lie at the same level as those at localities A and B. Samples localities are listed in Appendix 1.

Locality D

Locality D covers a cultivated area (Fig. 2C) around 29.30°S, 115.655°E where scattered carbonate nodules have been moved to gutters besides the ploughed paddocks and along the southern gully leading northward into Woolaga Creek. Samples studied from this site are listed in Appendix 1 and include two from Playford's (1959) study. Rock types are described by Haig *et al*. (2022). As a result of his detailed mapping of the area, Playford (1959) estimated that the nodular limestone outcrops (which he called the Woolaga Limestone Member of the Holmwood Shale) were at least 76 m above the base of the Holmwood Shale.

METHODS

Multiple samples of nodular limestone were collected from each locality. These were slabbed with a diamond saw and acetate peels taken from the slabbed surfaces (several per sample). The surfaces were etched in 2% HCl acid for 4 minutes and then gently washed in a still water bath and air dried without touching the etched surface. Once dry, the surface was flooded with acetone and a sheet of acetate film (clear, 0.003 inch thick; commercially obtained) was carefully placed on the surface before the acetone evaporated. After several minutes, the film was removed producing a peel of the surface. Each peel was placed between glass plates and examined and photographed under a compound biological microscope. The advantages of acetate peels over thin sections for a preliminary investigation such as this is the much greater area available for study in a peel compared to a standard thin section. The peel also offers enhanced clarity of the cement fabrics and carbonate skeletal microstructures as evidenced in the photographic images illustrated in Haig *et al*. (2022) and in this paper.

Friable mudstone (shale) was disaggregated in water and the clean sand residue retained after successive decants of muddy water from the disaggregated slurry. Microfossils were picked from the dried sand fractions using a very fine 000 sable-hair brush and placed on gridded carboard micropaleontological slides.

Procedures used for processing samples for palynomorphs follow Playford (2021). All rock samples, acetate peels, washed sand residues and picked foraminiferal slides are housed in the collections of the Earth Science Museum at the University of Western Australia. The illustrated palynomorphs are curated in collections of the Geological Survey of Western Australia.

Results of the analysis of the biota are listed in Appendices 2 and 3. Curatorial details for the palynomorphs are listed in Appendix 4.

BIOTA

Bacterial indicators

Bacteria have been shown elsewhere to play an important role in carbonate cementation of nodules within organic-rich shale facies (Case *et al*. 2015; Zhu & Dittrich 2016). However, direct observations in ancient nodules of microbial activities are limited. Among the chaotic

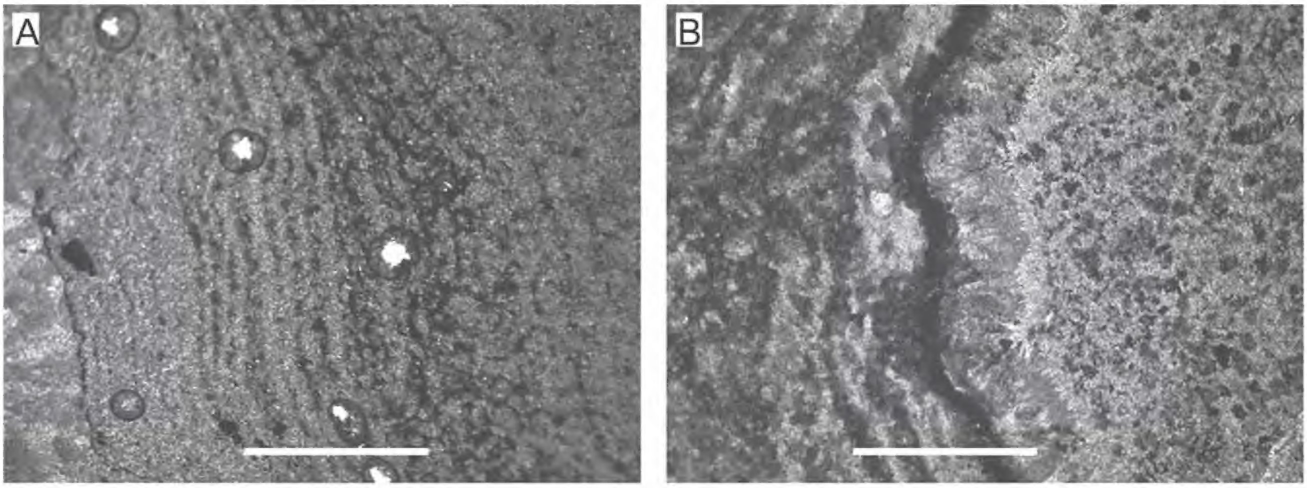

Figure 3. Laminations probably produced by successive microbial (bacterial) mats; from sample 175034. Bar scale = 0.5 mm.

cement fabrics of the studied nodules (Haig *et al*. 2022), laminations are present in some patches. These consist of alternating light and dark layers, < 0.1 mm thick, of microgranular carbonate (Fig. 3) with banded to streaky laminar architecture (as defined by Grey & Awramik 2020). This is consistent with the presence of microbial mats (Wilmeth *et al*. 2018). No evidence of cyanobacterial borings (or other endoliths, as defined by Günther 1990) in carbonate skeletons has been observed in the nodules.

Since publication of Haig *et al*. (2022), samples from each locality have been analysed for AOM (anaerobic oxidation of methane) biomarkers by Joern Peckmann and his research team at the University of Hamburg (J. Peckmann pers. comm. to D.W. Haig, 9 October 2023). They found good preservation of the biomarkers and different compound inventories of AOM biomarkers at different localities. These exciting results are being prepared for publication.

ALGAE

Unicellular algae

Algal microfossils form a minor component of the palynomorph preparations from Locality-D nodules, with eight species recorded (Playford 2021). Playford illustrated these aquatic species and noted with reference to Brenner & Foster (1994), Grenfell (1995), and Mays *et al*. (2021): (i) the probable non-marine (freshwater or brackish) habitat of *Maculatasporites* spp., *Quadrisporites horridus*, *Spongocystia eraduica*, and *Tetraporina* sp.; and (ii) the variable marine or non-marine habitat of *Leiosphaeridia* sp. and *Cymatiosphaera gondwanensis* (see Playford 2021, for taxonomic identifications).

Litostroma

Litostroma oklahomense Mamay 1959 is present in nodules from each locality (Fig. 4A–F). It is most abundant at Locality C where concentrations of thalli are preserved in some nodules (Fig. 4A). At other sites, *L. oklahomense* occurs as isolated skeletal plates. Some of the thalli are >10 cm long. The identification is based on the monostromatic skeleton that is flexible, unattached, and apparently composed of dark organic material. The thalli are small and plate-like but their original shapes and the cell arrangements in horizontal view cannot be ascertained in the acetate peels. In oblique view (e.g., Fig. 4D), cells appear polygonal in cross-section. In vertical view (Fig. 4B, C), cells are of similar dimensions and shapes to those in the type specimens figured by Mamay (1959). The cells are normally just over 100 µm

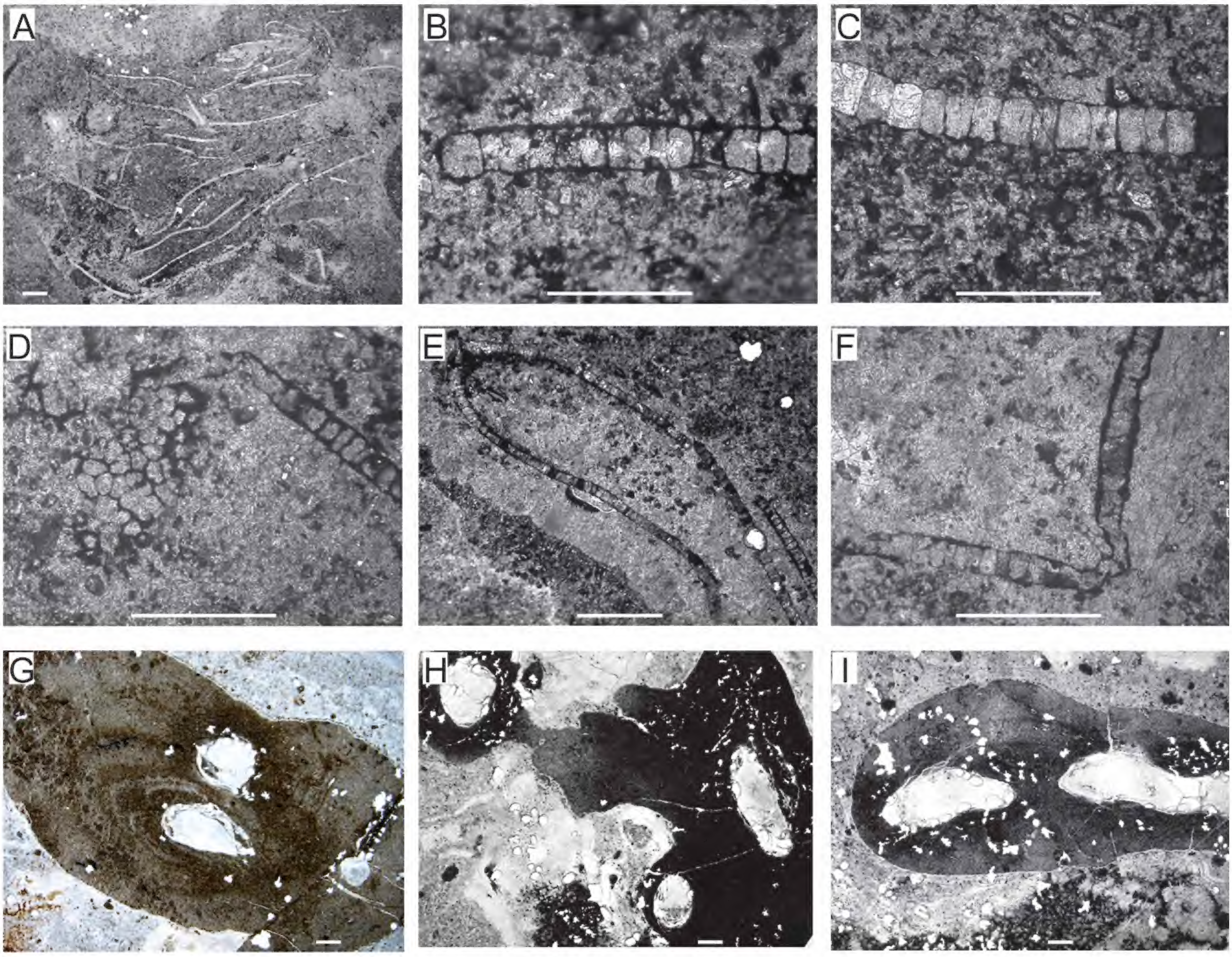

Figure 4. "Algae" in nodular limestone. Bar scales = 1 mm (A, G–I) and 0.5 mm (B–F). A–F, *Litostroma oklahomense* Mamay; all specimens from Locality C, sample 175019. G–I, *Tubiphytes* sp., all specimens from Locality A, sample 175005.

wide and slightly exceed 160 µm in height. The outer walls of the "cells" tend to be slightly convex giving a slightly lobate outline with cell contacts incised at the surface. The terminal faces of the final cells in a thallus are convex. The thalli do not appear to subdivide. Regular passageways between cells cannot be observed. The cells are infilled by cement. The flexible nature of the thalli is illustrated in Fig. 4E where a thallus has been tightly folded, and in Fig. 4F where the thallus has been sharply kinked. Some of the thalli (e.g., Fig. 4E) provided a substrate for encrusting porcelaneous and agglutinated foraminifers (see below).

Litostroma Mamay 1959, typified by *L. oklahomense* differs from *Eolithoporella* Johnson 1966 (their pl. 176, figs. 9, 10), which has cells with rectangular shapes in vertical section and flat rather than convex surfaces. It differs from *Nostocites* in which cells have circular cross-sections (see Groves 1983; and *Litostroma* sp. of Jansa *et al*. 1978, with "subrounded" cell cross-sections).

The type material of *L. oklahomense* is from the Boggy Shale of Early Pennsylvanian age in Oklahoma (dated by Thompson 1935, on the basis of fusulinids). It was originally described from a carbonate nodule (8 cm in maximum dimension) present in a shallow-marine shale succession that overlies a coal seam. Coal balls with a diverse marine assemblage occur in the shale (Mamay & Yochelson 1962), but the relative positions of these and the nodule containing the type material of *L. oklahomense* are not known. Accompanying the type specimens in the nodule are rare bivalves, gastropods, inarticulate brachiopod debris, foraminifers, and fish debris. Mamay (1959) illustrated porcelaneous foraminifers encrusting some of the thalli of *Litostroma*; these were described by Henbest (1958; see below). Beyond the type locality, *Litostroma oklahomense* has been described from the lower part of the Lower Permian of the Carnic Alps, Austria (Homann 1972) in facies interpreted as shallow-marine.

Because of the rectangular shape of cells with flat surfaces in vertical cross-section, *L. europaea* Kochansky-Devidé (1970, p. 15, figs 3–5), from the Pennsylvanian of Croatia, should be transferred to *Eolithoporella*. *Litostroma* has not been recorded previously from Australian or other Gondwanan successions. In the Irwin Basin, rare examples are present in carbonate nodules higher in the Holmwood Shale at a level about 50–60 m below the top of the formation (Tremblin & Haig 2023) and at the stratigraphic level of the Fossil Cliff Member in the uppermost part of the Holmwood Shale.

Bomfleur *et al*. (2009) characterized *Litostroma oklahomense* as a "putative red alga". Homann (1972) included it among the "Rhodophycophyta incertae sedis".

Tubiphytes

The algal affinities of *Tubiphytes* are uncertain (Vachard *et al*. 2001; Senowbari-Daryan 2013). Specimens observed in the nodular limestone from Locality A (Fig. 4G–I), have the typical tongue-shaped "segments", large central cavities, thick dark skeleton with "focculent microfabric", and crude layering that characterize *Tubiphytes* (see Vachard *et al*. 2001; Senowbari-Daryan 2013). However, studied specimens are very large in comparison to those normally illustrated for *Tubiphytes*, some reaching almost 1.5 cm in maximum cross-sectional diameter.

Elsewhere in the Permian of the East Gondwana Interior Rift, *Tubiphytes* has been recorded from the upper Gzhelian, upper Sakmarian–lower Artinskian, and upper Artinskian–lower Kungurian in Timor (Davydov *et al*. 2013; Haig *et al*. 2014, 2017); and in the upper Sakmarian (viz. lower Callytharra Formation in the Merlinleigh Basin and equivalents of the Nura Nura Member in the Canning Basin; Haig *et al*. 2014) and upper Artinskian–lower Kungurian in the Noonkanbah Formation of the Canning Basin (Haig *et al*. 2017).

Problematica

Three groups which may have affinity to algae or sponges, or may be inorganic, are included here, informally labelled A, B, and C. Problematicum A has been found at Localities B–D and, very rarely, in nodules within the Fossil Cliff Member equivalents in the upper part of the Holmwood Shale. Problematica B and C have only been identified in nodular limestone at Locality A.

Problematicum A is usually represented by curved fragments (Fig. 5B) of objects that probably had a circular or ovoid cross-section (Fig. 5A, C). These consist of very thin, dark-coloured elements, ca. 0.3 mm long, with many branching approximately half-way lengthwise. The branches face outward toward the convex side, and some terminate with a small bifurcation on the outer (convex) periphery. The elements are preserved in a very fine, clear, granular matrix. Two interpretations of Problematicum A seem possible. (i) The matrix represents recrystallized skeleton (e.g., originally aragonite) and the elements are fine tubules infilled with micrite and perhaps with finely disseminated pyrite. If this is the case, these objects may be dasycladacean algae (see, e.g., poorly preserved skeletons illustrated by Homann 1972, pl. 7, figs. 56–58, as *Salopekiella*). (ii) The dark elements may be solid skeletal structures and the granular matrix may be a cavity with cement-infill.

Problematicum B includes cement-filled cavities up to 3–4 mm in maximum dimension (Fig. 5D, G). Bordering the inner edge of these major cavities is a zone containing "elements" set in a clear granular matrix. These resemble those in Problematicum A but are brown in colour in acetate peels. Surrounding the major cavities is a dark brown network that includes cavities (0.15–0.25 mm maximum diameter) with a roughly stellate outline (Fig. 5F).

Problematicum C forms part of the framework of the small bioherms represented in the nodular limestone at Locality A. It encrusts on skeletal plates (e.g. Fig. 5I) and forms irregularly erect columns (several centimetres in diameter) with circular cross-sections that branch (Fig 5H).

We have not recognized Problematicum B or C elsewhere in the Western Australian Permian. Very rare Problematicum A is also present at a level much higher than the studied horizon in nodular limestone of the Fossil Cliff Member near the top of the Holmwood Shale.

Foraminifera

Two different foraminiferal associations with little in

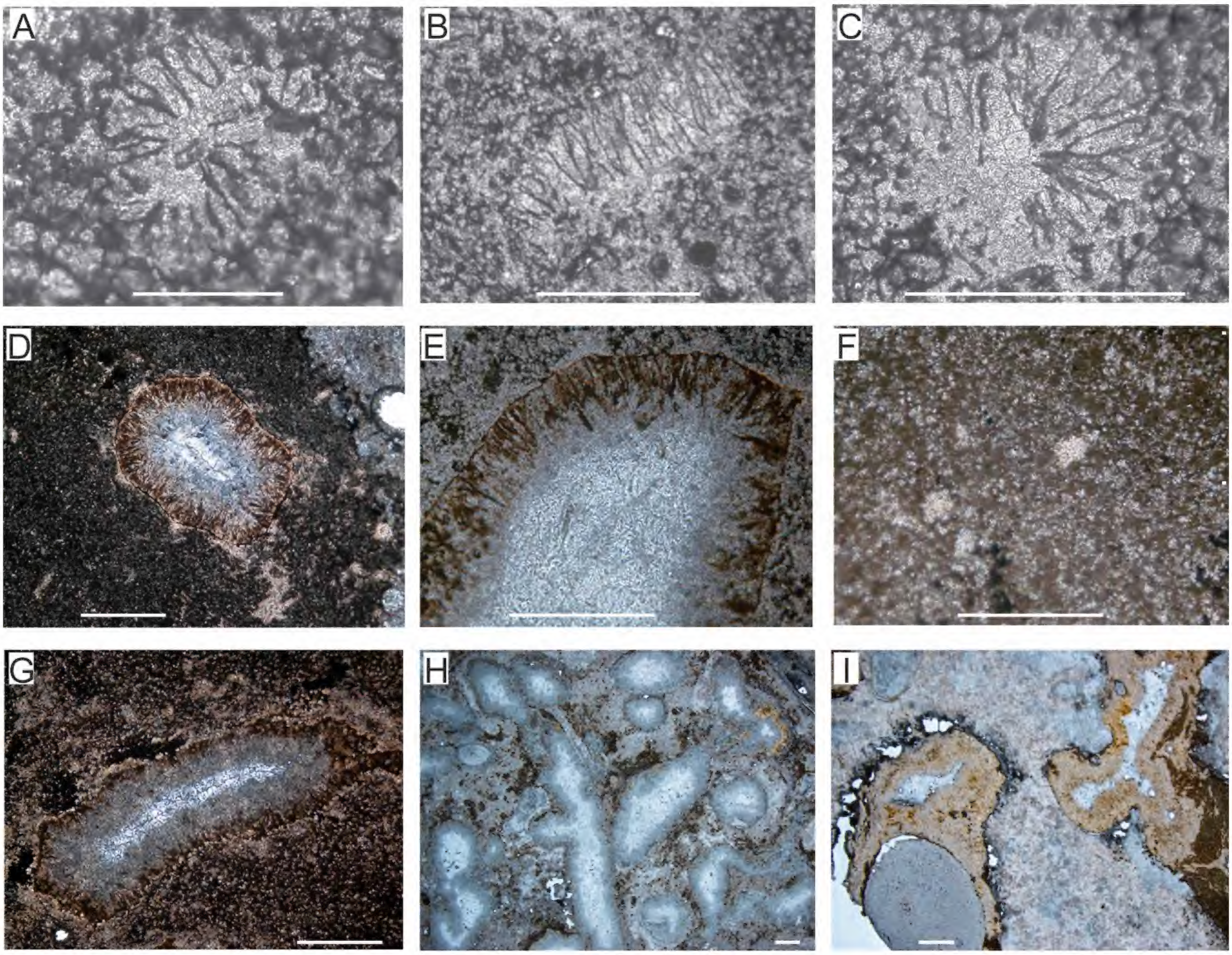

Figure 5. Problematica from nodular limestone. Bar scales = 0.5 mm (A–G) and 1 mm (H, I). A–C, Problematicum A from Locality D, sample 175029. D–G, Problematicum B from Locality A, unit 3, sample 175482. H, I, Problematicum C from Locality A, unit 1, H from sample 175470, I from sample 181377.

common are present in the studied interval within the Holmwood Shale: (i) an organic-cemented siliceous agglutinated fauna with mainly single-chambered morphotypes extracted from friable-shale samples (Fig. 6); and (ii) sparse assemblages of multichambered coiled agglutinated species as well as calcareous, porcelaneous, free and attached forms in the carbonate nodules (Fig. 7). These are outlined separately below.

Shale-facies foraminifers

Foraminifers were recovered from friable shale samples collected from Localities A, B, and D, and from similar rocks in a transect across the lower Holmwood Shale in Beckett's Gully (Appendix 3). In the latter, the ammonoid *Juresanites jacksoni* (see below) is preserved in a nodule within shale at about 61 m above the exposed top of the Nangetty Formation. This ammonoid was also found in the shale at Localities A and B and has been reported from Locality D (Skwarko 1993; and recorded as *Metalegoceras campbelli* by Playford 1959, see Glenister *et al*. 1993 for synonymy).

The foraminiferal assemblage is composed entirely of organic-cemented siliceous agglutinated tests belonging to 14 species. The tests now have secondary silica cement agglutinating the quartz grains of the wall (probably as silica overgrowths on these grains, precipitated during silica diagenesis during burial). They show the typical preservation of organic-cemented types that have undergone burial deformation in shale.

All but one of the species are single-chambered morphotypes (Fig. 6) belonging to *Thuramminoides sphaeroidalis*, *Thurammina texana*, *Sansabaina elegantissima*, *Sansabaina*? *acicula*, *Kechenotsike hadzeli*, *Hyperammina coleyi*, *Sacculinella australae*, *Placentammina ampulla*, *Placentammina*? sp., *Pseudohyperammina*? sp., *Lagenammina* sp., *Glomospirella nyei*, and *Ammodiscus nitidus*. A minute trochamminid with irregular coiling is only found in two samples in the Beckett Gully section just above the *Juresanites* level. Skwarko (1993, p. 89, 90) listed a similar assemblage of agglutinated species from the Holmwood Shale, as distinct from the more diverse microfauna, including calcareous species, recorded from the Fossil Cliff Member in the upper part of the formation. No foraminifers were recorded by Skwarko (1993) in the Woolaga Limestone Member of the Holmwood Shale. Precise localities were not documented

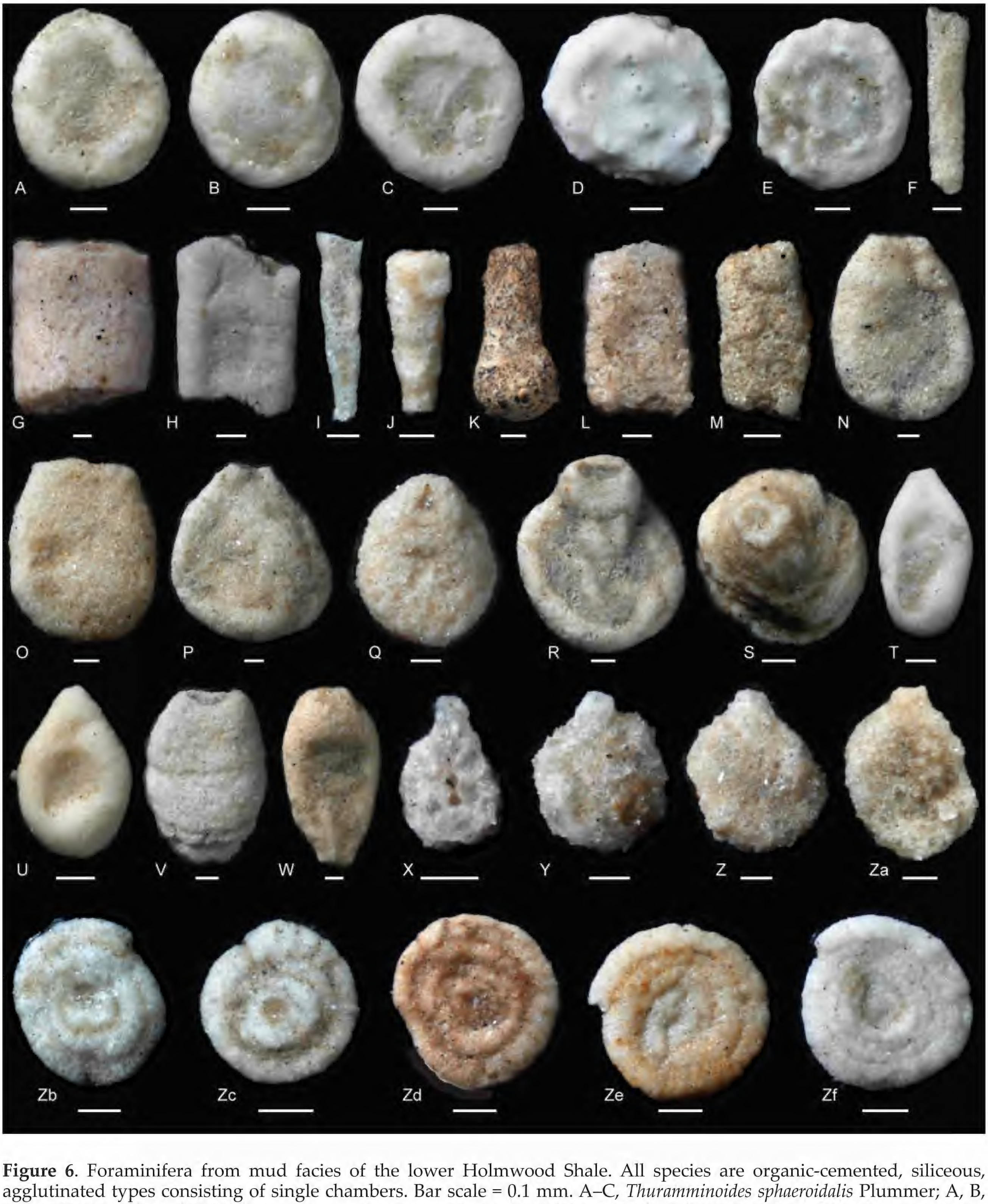

Figure 6. Foraminifera from mud facies of the lower Holmwood Shale. All species are organic-cemented, siliceous, agglutinated types consisting of single chambers. Bar scale = 0.1 mm. A–C, *Thuramminoides sphaeroidalis* Plummer; A, B, from 181397; C from 181384. D, E, *Thurammina texana* Cushman & Waters; D from 181385; E from 181384. F, *Sansabaina elegantissima* (Plummer); from 181397. G, H, *Sansabaina*? *acicula* (Parr); G from 181386; H from 181384. I, J, *Kechenotiske hadzeli* (Crespin); I from 181397; J from 181385. K–M, *Hyperammina coleyi* Parr; K, L from 181386; M from 181381. N–P, *Sacculinella australae* Crespin; N, P from 181384; O from 181397. Q–S, *Placentammina ampulla* Crespin; Q from 181390; R, S, from 181384. T, U, *Placentammina*? sp.; T from 181385; U from 181397. V, W, *Pseudohyperammina*? sp.; V from 181390; W from 181397. X–Za, *Lagenammina* sp.; from 181394. Zb–Ze, *Glomospirella nyei* Crespin; from 181394. Zf, *Ammodiscus nitidus* Parr; from 181394.

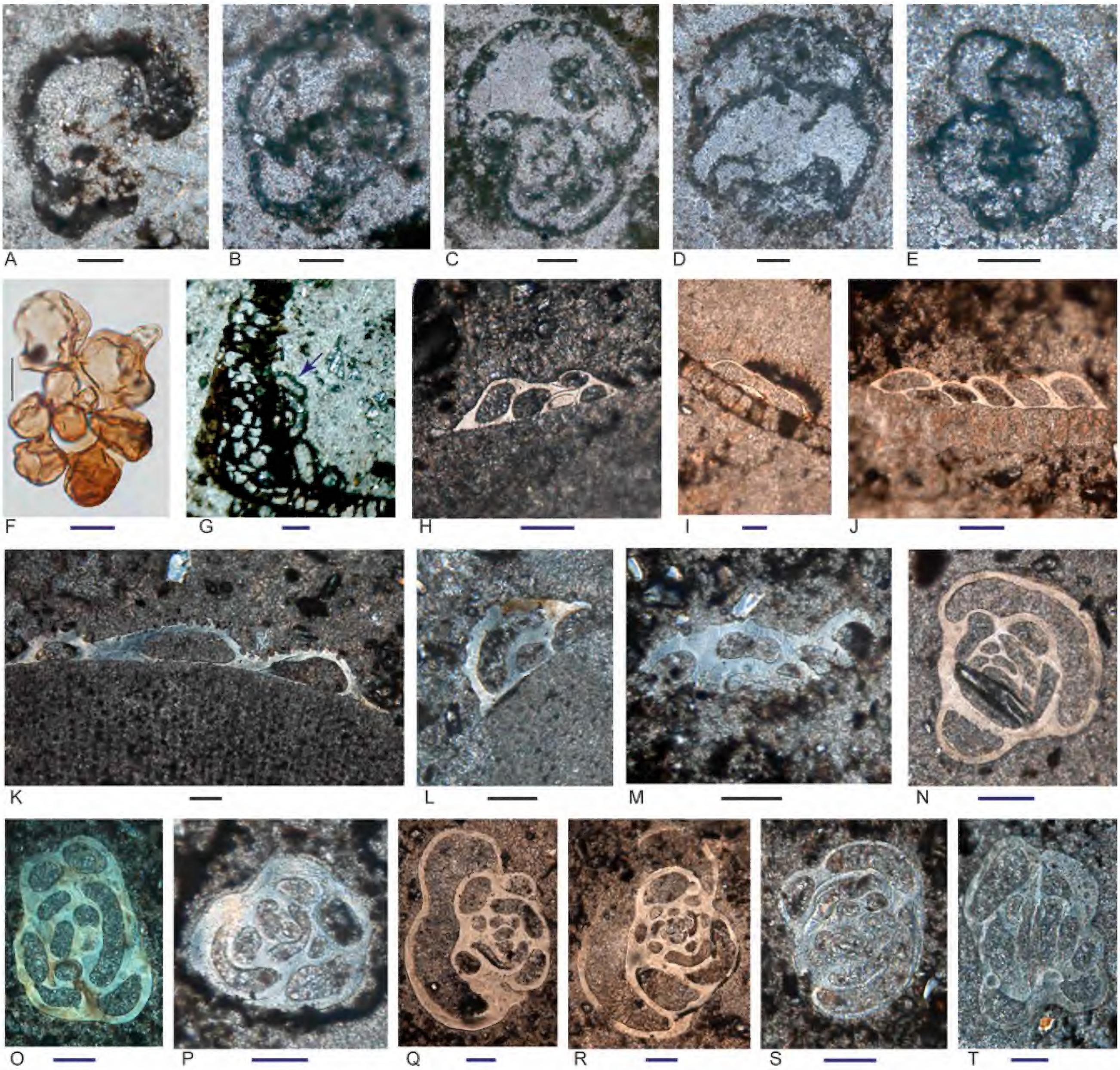

Figure 7. Foraminifera from nodular limestone at studied localities A–D. Images A–E and G–T are from acetate peels. Note that walls (e.g. whether dark or light) have different appearances than in thin sections because in the peels light does not pass through a mineralized wall. Well-preserved porcelaneous walls are usually pale. Bar scales = 0.1 mm. A–D, Multichambered forms with thick agglutinated tests probably *Verispira holmesorum* Tremblin & Haig (2023, fig. 7), A from 175472, B–D from 175481. E, Equatorial section of either a planispiral test or a very low trochospiral agglutinated morphotype, from 175474. F, An organic lining from a foraminiferal wall, observed in palynomorph preparation from 175035. G, *Tolypammina* encrusted onto *Litostroma* alga from 175019. H–J, *Calcitornella* sp.; I and J are attached to *Litostroma*; the attachment surface for H is recrystallized; H from 175034; I and J from 175019. K–M, *Hedraites* sp.; K and L are attached to crinoid columnals; the attachment surface for M is not preserved; K and L from 175034; M from 175035. N?, possible transitional morphotype between *Calcitornella* Cushman & Waters and *Glomomidiella* Vachard, Rettori, Angiolini & Checconi; the early whorls are attached to a small fragment of Problematicum A, the final stage of growth may have been unattached; from 175034. O–S, ?T, *Glomomidiella* sp.; apparently free-living morphotypes; O from 175027; P, S and T from 175035; Q and R from 175029.

by Skwarko (1993) nor by Palmieri (1993) in the same bulletin. Assemblages from the Fossil Cliff Member in the uppermost Holmwood Shale were described and illustrated by Crespin (1958), Foster *et al*. (1985), and Ferdinando (2001).

Elsewhere in Australian Permian basins, similar agglutinated assemblages with a range of single-chambered siliceous-agglutinated morphotypes seem to be best represented in basal marine transgressive muds of the Early Permian in Queensland's Bowen Basin (Crespin 1958; Palmieri 1994, 1998), the Sydney–Hunter basins of New South Wales (Crespin 1958; Scheibnerová 1982) and in Tasmania (Conkin & Conkin 1993). In North American interior basins of the Pennsylvanian, similar microfaunas from shallow-marine shale successions have been recorded and reviewed by Plummer (1945). However, most of these assemblages also contain multichambered agglutinated types.

Carbonate-nodule foraminifers

Carbonate nodules at all studied localities contain a sparse foraminiferal assemblage (Fig. 7; Appendix 2) of very different aspect to that in the surrounding shale. Two distinct groups are represented. Coiled chambered agglutinated morphotypes have walls with scattered grains (? quartz) in a dense microgranular matrix. Coiling in the agglutinated group seems to be of two types: (i) Irregular to streptospiral coiling observed in random sections (Fig. 7A–D) with rapid increase in chamber size; and (ii) planispiral or very low trochospiral coiling (Fig. 7E, F) with gradual increase in chamber size. Morphotype (i) may belong to the organic-cemented agglutinated *Verispira holmesorum* Tremblin & Haig (2023, p. 277, fig. 7, nos. 1a–6c) which has *Ataxophragmium*-like coiling. This species was described from carbonate mudstone nodules higher in the Holmwood Shale at about 50–60 m below the top of the formation. No similar morphotypes have been found elsewhere in the Western Australian Permian, but *Verispira* was first described as a globivalvulinid from Artinskian shale in the Permian of the Bowen Basin in Queensland by Palmieri (1988). The planispiral or very low trochospiral tests (Fig. 7E, F) may be either a *Haplophragmoides* or a low spired *Trochammina*. Very rare tubular, coiled, agglutinated *Tolypammina* sp. lived as epiphytes on the alga Litostroma (Fig. 7G). All the agglutinated types are organic-cemented types.

The calcareous porcelaneous species are tubular calcivertellines (Miliolata). These were either free living in the benthic environment (e.g., *Glomomidiella* sp.; Fig. 7O–S, ?N, ?T) or attached. The latter include *Calcitornella* sp. with smooth outer wall, attached to the alga *Litostroma* (Fig. 7H–J); and *Hedraites* sp. with spinose granules on outer wall, attached for example to the sides of crinoid columnals (Fig. 7K–M). Some porcelaneous foraminifers recorded here are present in the Fossil Cliff Member in the uppermost Holmwood Shale (Crespin 1958; Foster *et al*. 1985; Ferdinando 2001). However, *Hemigordius*, which is common in the Fossil Cliff Member, is absent from the assemblages in the carbonate nodules studied here.

Elsewhere in the Permian of the East Gondwana Interior Rift, elements of a coeval porcelaneous assemblage are known from the Merlinleigh (Southern Carnarvon) and Canning basins (Crespin 1958; Dixon & Haig 2004, Haig *et al*. 2014); and in Timor (Haig *et al*. 2014). In eastern Australian basins, similar porcelaneous morphotypes to those present in the studied nodules have not been illustrated from coeval strata (e.g., by Crespin 1958, and Palmieri 1994). The porcelaneous assemblage recorded here resembles microfaunas, associated with siliceous agglutinated foraminifers, recorded from the Pennsylvanian interior basins of southern North America (Cushman & Waters 1928a, b). From the lower Pennsylvanian of Oklahoma, Henbest (1958) and Mamay (1959) described and illustrated an association, like that recorded here, of *Calcitornella* sp. epiphytic on the alga *Litostroma*.

Sponges

Monaxon siliceous sponge spicules are rare in some nodules at all studied localities (Appendix 2). The Problematica A–C described above may be of sponge affinity.

Brachiopods

Very rare thin-shelled brachiopod debris occurs in some nodules at Localities B–D, and possibly in one nodule from Unit 2 at Locality A (Appendix 2). The brachiopods have pseudopunctate shell microstructure. Their rarity here contrasts with their usual notable abundance in other Permian carbonate units in Western Australia.

Rostroconchs

The main bivalved group in the nodules are probably rostroconchs, an enigmatic molluscan group extinct at the end of the Paleozoic (Pojeta & Runnegar 1976). Small bivalved morphotypes (Fig. 8A–G) that have non-functional hinges and are identified as rostroconchs have been observed in all units at Locality A and in one nodule from Locality D. At all localities, many nodules contain rare disarticulated and fragmented shells with similar microstructure to those identified as rostroconchs. Clarke *et al*. (1951) noted that a "species of *Conocardium*", a genus now referred to the Class Rostroconchia (Pojeta & Runnegar 1976), is present in the Macaroni Hill "serpulid reef". We could not find clear macrofossil examples of the genus in the nodular limestone at Locality A, nor in samples from the study of Clarke *et al*. (1951) in the collections of the Earth Science Museum at the University of Western Australia. Skwarko (1993, p. 90) recorded as Bivalvia, a single incomplete specimen identified as *Conocardium* sp. A from the Fossil Cliff Member in the upper Holmwood Shale. This specimen had been figured by Dickins (1963, pl. 16, fig. 1) and shows strong ribbing characteristic of the genus but not present on the material present in the methane-seep deposits. '*Conocardium* sp.' was also listed by Skwarko (1993, p. 91; perhaps the internal cast identified as *Conocardium* sp. B in Skwarko, 1993, their appendix) from an unknown level in Holmwood Shale. The genus has not been recognized elsewhere in the Western Australian Permian.

The species recorded from the carbonate nodules (Fig. 8A–G) lacks the coarse ribbing characteristic of *Conocardium* (see Pojeta & Runnegar 1976, p. 69, pl. 37–40; and Ambler 2016), and is considerably smaller than most species attributed to this genus. The shells had dorsal-ventral heights ranging from 7.4 to 6.5 mm, but this is

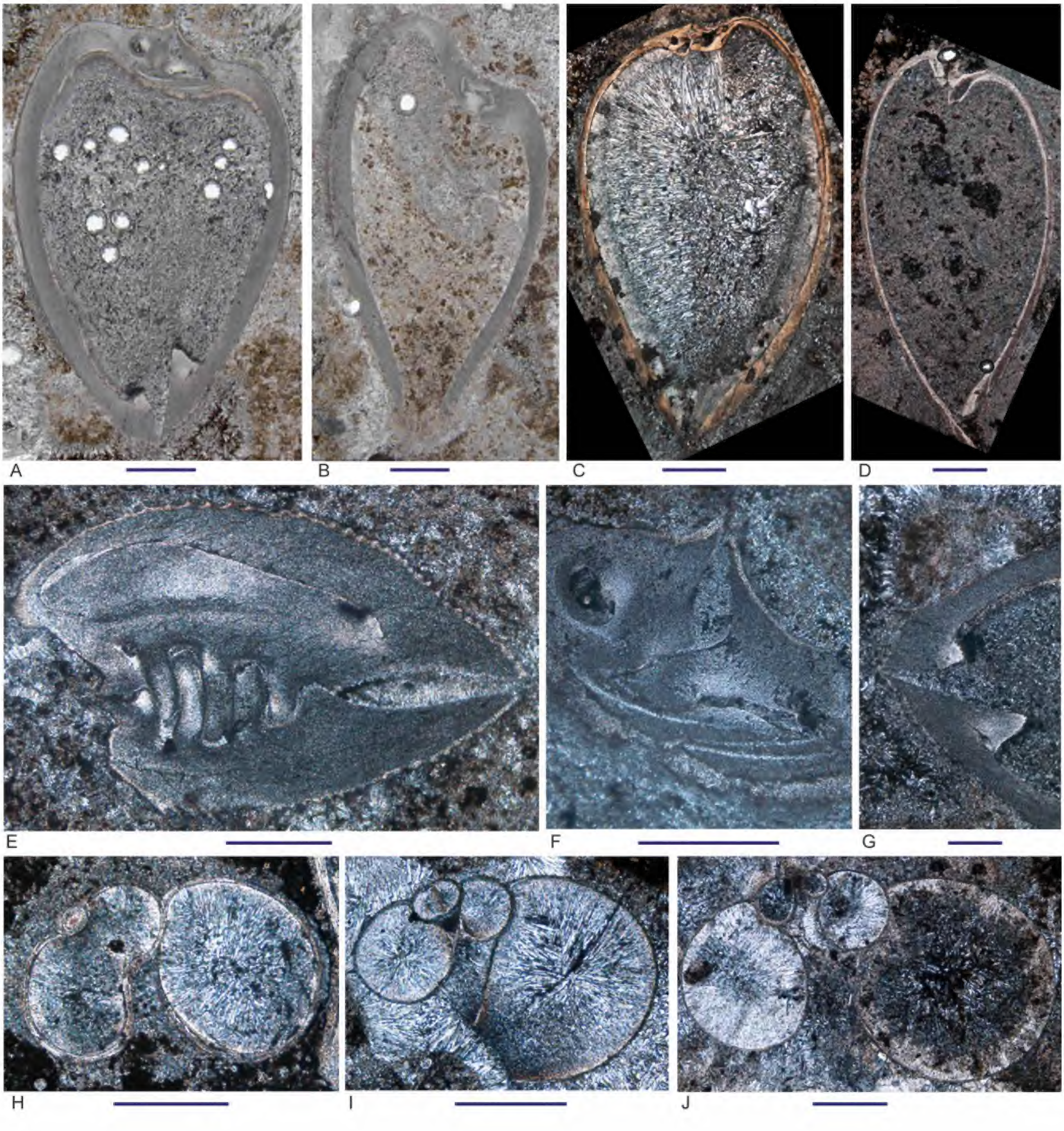

Figure 8. Molluscs occurring commonly in the nodular limestone. Bar scales = 1 mm (A–D), and 0.5 mm (E–J). A–G, Probable rostroconchs: A–D are dorsal–ventral cross-sections through the valves with the hinge dorsally placed. These probably belong to one species; differences being attributed to sections at different anterior to posterior positions. Note: (1) hinge structures that appear non-functional, with F an enlarged view of the hinge in A; (2) "shelves", perhaps in the anterio-ventral part of the valves, in A and C and in G an enlarged view of the shelves in A; A and B from 175477; C from 175470; D from 175481. E, dorsal section cut approximately tangential along the hinge; from 175477. In E, the gap between valves, the large depression on one valve and the "fractures" in the hinge area match with similar structures observed in the dorsal–ventral cross-section shown in A and suggest that the right-hand side of E may be the anterior side (as A contains anterior-ventral shelves). H–J, Gastropod A.; note very thin wall, globose chambers, and large umbilical cavity; H and I from 175482; J from 175474.

probably dependent on where the sections fall along the anterior-posterior axis. The valves are asymmetric. One valve seems slightly larger than the other and the hinge structures are asymmetric. The outer surface of the wall is made up of a very thin clear external layer that forms fine corrugations due to thickening of the layer (e.g. Fig. 8A, B and E). The hinge as viewed in dorsal-ventral section is clearly non-functional with, in Fig. 8A at least, shell material extending along the inner side across the junction between valves. In tangential view along the dorsal side, closely interlocking "teeth" are present. On the ventral side of two sections (Fig. 8A and C), distinct shelves (e.g. Fig. 8G) are composed of skeletal material of different (microgranular) microstructure than featured by the laminated valves (shown best in Fig. 8C). These may correspond to the anterior longitudinal shelves described by Pojeta & Runnegar (1976). Their anterior position is supported by the deduction made in the caption to Fig. 8 about the relationship of Figs. 8A and E. In addition to the arguments advanced there, the abrupt termination of the left-hand side of the section in Fig. 8E probably indicates that this is the posterior side where a rostrum is developed (see Rogalla *et al*. 2003, fig. 1). Sections shown in Fig. 8B and D may be on the posterior side of the shell.

The species observed in the studied carbonate nodules probably belongs to a new conocardioid genus. Taxonomic study, beyond the scope of the present study, would best be done by using serial acetate peels and then reconstructing a three-dimensional model of the shell.

Bivalves

Some of the unidentified bivalved shell fragments observed in the acetate peels (Appendix 2) may belong to the Bivalvia. Shell fragments with prismatic calcitic microstructure are attributed to the Bivalvia; others with different microstructure may also belong here. Un-named nuculid bivalves were reported by Clarke *et al*. (1951) from the Macaroni Hill "serpulid"-rich limestone. We could not recognize them in the field. These are probably among the indeterminant shell material observed in the acetate peels. Skwarko (1993) recorded '*Sanguinolites*' sp. from the Woolaga Limestone Member of the Holmwood Shale (Locality D of this paper) but did not include it in the systematic descriptions in his accompanying compilation of the Permian bivalves of Western Australia.

Gastropods

Clarke *et al*. (1951, p. 52) noted that the gastropod fauna in the Macaroni Hill "serpulid" limestone (Locality A of this study) was "peculiar" but did not identify the types present. We observed rare moderately high-trochospiral morphotypes with thick shells at this site, some having transverse and longitudinal ribs. However, because these were visible only as sections in hard rock, they proved unidentifiable. The most common gastropods, observed only in the acetate peels, are minute shells (Fig. 8H–J; Appendix 2, designated as Gastropod A) with some resemblance to skeneimorphs described from Cretaceous seep deposits in Japan (Kaim *et al*. 2009, fig. 14). They are characterized by an inflated low trochospiral shell with a very thin smooth wall and a deep "cylindrical" umbilical cavity beneath the spire. No gastropods of this type have been previously recorded from the Western Australian Permian (see Dickins 1963; Skwarko 1993)

Ammonoids

Two ammonoids are well known from the studied localities. The large metalegoceratid *Juresanites jacksoni* (Etheridge) was reviewed and illustrated by Glenister & Furnish (1961, p. 705, 706, pl. 81, figs 1, 2), Glenister *et al*. (1973, p. 1033–1035, pl. 2, figs. 2, 3), and Glenister *et al*. (1993, pl.52, figs 1–5). It is scattered within the calcareous mudstone nodules in shale deposits surrounding the Macaroni Hill nodular limestone (Locality A). We have collected in situ specimens in nodules in a gully immediately west and at the same stratigraphic level as Unit 1 of the Macaroni Hill limestone succession. *Juresanites jacksoni* is abundant in shale deposits associated with calcareous mudstone nodules at Locality B. It was recorded by Glenister *et al*. (1973) together with its synonym *J. campbelli* (see Glenister *et al*., 1993) from Woolaga Creek Locality D. Glenister & Furnish (1961, p. 706) noted that "several parallel exposures" of beds containing *J. jacksoni*, e.g., as mapped by Clarke *et al*. (1951), are probably fault repeats of the same bed. Where we have found *J. jacksoni* in the shale succession (in nodules), it is the only macrofossil present. Glenister & Furnish (1961, p. 705) noted that in a thin bed designated the "Beckett Member", the species forms an almost monospecific "ammonoid coquina" associated with very rare indeterminant nautiloids, gastropods and bivalves.

The other ammonoid, *Uraloceras irwinense* Teichert & Glenister (1952; following the nomenclature of Leonova 2011), is a small evolute species. We have found very rare specimens in Unit 1 at Locality A, and at Locality C. Glenister & Furnish (1961) noted that it is abundant together with *Juresanites* at one site in Locality D.

Echinoderms

Rare crinoid columnal plates are preserved in the nodular limestone at localities B and D (Appendix 2). The plates are present in small stem segments or as isolated columnals with circular cross sections. Very rare indeterminate skeletal material of possible echinoderm origin is present in units 2 and 3 at Locality A. Most of the nodular limestone shows no evidence of crinoidal or other echinodermal debris. Elsewhere in the Lower Permian limestones of Western Australia, crinoid debris forms one of the main biogenic components.

Ostracods

Ostracods are found in the nodular limestone at all studied localities (Appendix 2). Specimens having thin, smooth, articulated valves are most common (Fig. 9). Without three-dimensional images, the ostracods are impossible to identify. By comparison to diverse assemblages described from the Fossil Cliff Member of the uppermost Holmwood Shale (Foster *et al*. 1985; Ferdinando 2001), it is clear that the ostracod assemblages at the studied localities lack the thick-walled ornamented species so conspicuous in the Fossil Cliff fauna.

Polychaetes

Tube worms

Tube-worm calcareous skeletons (Fig. 10) form a major part of the framework, together with Problematica B and C and minor *Tubiphytes*, of the small thickets in all units at Locality A and are also scattered in the nodular limestone

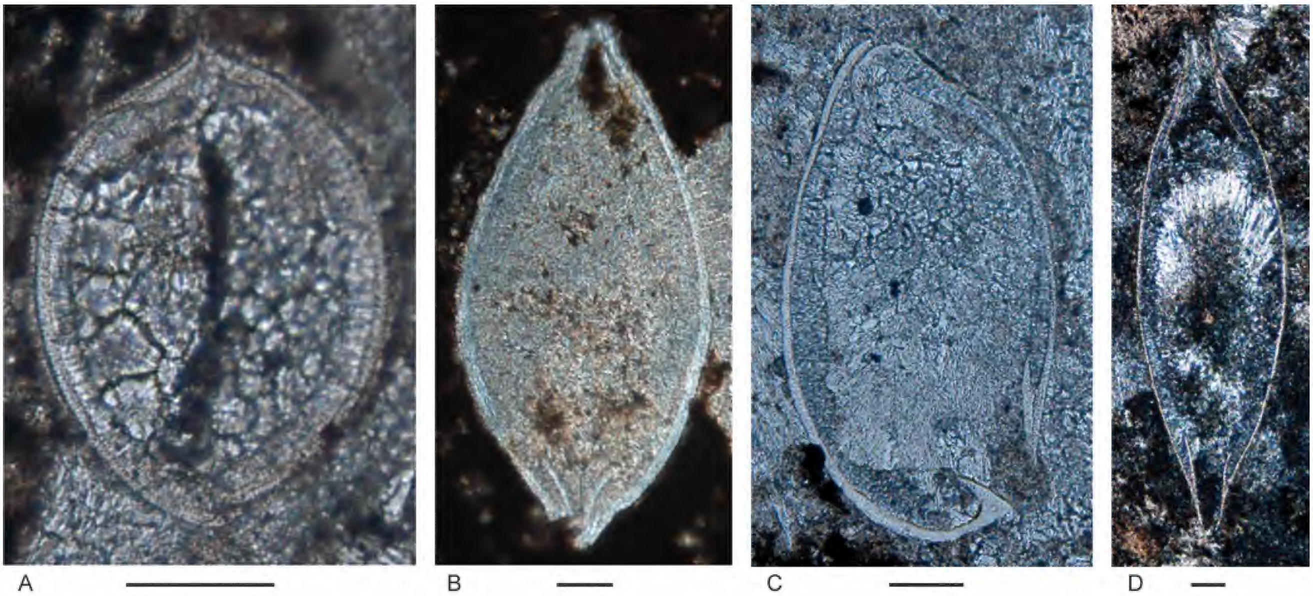

Figure 9. Representative ostracods from the nodular limestone. Bar scales = 0.1 mm. Note the smooth very thin walls without lamination, the inner lamella and selvage in each valve, and slight differences in valve size in each specimen. A and C from 175470, B from 175471, D from 175472.

at Locality D. They are rare in the carbonate nodules at localities B and C (Appendix 2).

There is no evidence to suggest that the calcareous skeletons in many of the tubes from the Locality A thickets are either extensively recrystallized or a product of replacement. The skeleton is finely laminated, probably with an original fine fibrous microstructure (Fig. 10A, B). In some specimens, the outer laminae have partially defoliated from the inner wall layers with cement infilling the gaps created. The tubes are cylindrical; the wall is very thin compared to the tube diameter (Fig. 10C). In many of the tubes, as observed in both acetate peels and thin sections, the wall has a brown colour, perhaps reflecting an organic (chitinous) component (e.g. Fig. 10B–D, H). Most tubes are approximately circular in cross-section with diameters < 2 mm, but a few have more irregular outlines (e.g. Fig. 10E, F). Irregularly positioned low longitudinal keels, involving a thickening of the wall, are present in many tubes (e.g. Fig. 10D–H). The inner and outer wall surfaces are sharply defined in the acetate peels. The tubes are not cemented to neighbouring tubes, but close contact can modify the cross-sectional shape (Fig. 10F). On their wall surfaces, they do not carry epibionts with mineralized skeletons, nor are they bored.

Georgieva *et al*. (2019, p. 288) noted that, among modern tube worms, "calcareous tubes are almost exclusively confined to the Family Serpulidae". Other tubeworms may have organic or agglutinated skeletons. Modern organic-walled sigoglinids (notably vestimentiferans) are widely distributed and abundant around methane seeps as well as hydrothermal vents (Bright & Lallier 2010; Hass *et al*. 2009; Hilário *et al*. 2011; Georgieva *et al*. 2019). Vestimentiferans lack a digestive system and most rely on sulphide oxidizing, intercellular bacterial symbionts (Bright & Lallier 2010; Reveillaud *et al*. 2018). Around seeps, even in shallow water, vestimentiferans form small thickets/bioherms (e.g. Hashimoto *et al*. 1993; Miura *et al*. 1997; Karaseva *et al*. 2020) and their "root-balls" (= posterior part of tubes that grow downward into the sediment) are closely associated with carbonate nodules forming within the sediment at the seeps (Hass *et al*. 2009). Among modern vestimentiferans are examples (e.g. at deep-water seeps in the Congo fan) where the posterior tubes of a living species are variably replaced by diagenetic aragonite when still in growth position (Peckmann *et al*. 2005; Hass *et al*. 2009; Hilário *et al*. 2011). In the Congo-fan examples most of the outer wall layers remain in place whereas the inner layers are delaminated, and needle-like clumps of aragonite seem optically continuous through the layers. Accordingly, some late Paleozoic tube worms have been referred to the vestimentiferans (e.g. Peckmann *et al*. 2005; Himmler *et al*. 2008; Georgieva *et al*. 2019) although the molecular phylogeny of the modern species suggests a Cretaceous evolutionary divergence established the group (Little & Vrijenhoek 2003; Campbell 2006).

The tube-worm skeletons studied here show some similarities to those described by Himmler *et al*. (2008) from methane-seep carbonates in the Gzhelian (uppermost Pennsylvanian) of the glaciomarine Dwyka Group in southern Namibia. The African types are slender tubes with partly delaminated walls that characterize the Western Australian examples. The wall laminae have a similar brown colour (see thin section illustrated in Hilário *et al*. 2011, fig. 5F). However, keels and variability in cross-sectional shapes were not described and the tubes seem poorly preserved. Himmler *et al*. (2008) noted that the Dwyka Group tube worms were "vestimentiferan-like". The tube worms described by Peckmann *et al*. (2005) from the Middle Devonian of Morocco and suggested as possible vestimentiferans also show a delaminated wall but seem much more poorly preserved than the Dwyka Group and Western Australian examples.

The tube worms at the studied Irwin Basin localities either form small thickets (i.e., colonies of apparently

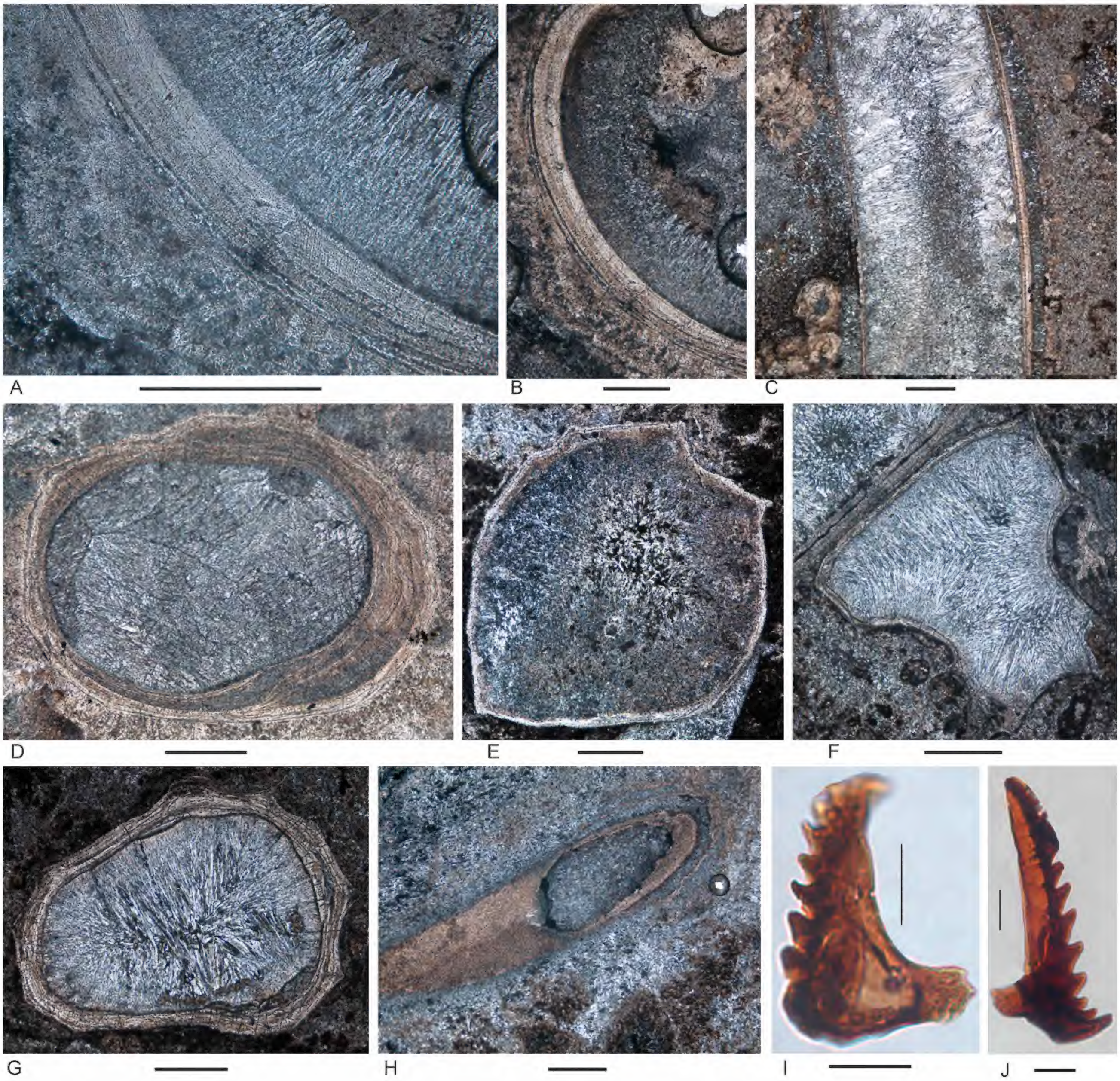

Figure 10. Polychaetes from the nodular limestone. Bar scales = 0.5 mm (A–H) and 0.1 mm (I, J). A–H, Tube worms; note laminated crystalline carbonate wall (not diagenetically replaced); longitudinal keels positioned irregularly on some tubes (observed mainly in cross-section). A, Enlarged view of wall shown in B revealing very fine laminae in inner part of wall, from 181377; C, longitudinal section, from 175470; D, slightly oblique cross section, from 175479; E, cross section, from 175481; F, G, cross sections, from 175482; H, oblique section, from 175476. I, J, Scolecodonts; I from palynomorph preparation 175035; J from palynomorph preparation 175029.

unconnected individuals, e.g., in units 1–3 at Locality A) or are isolated individuals, as observed in nodules from Locality D. In the thickets it is not possible at this stage to confirm that these are "root balls" formed from the posterior parts of tubes. Although more detailed petrography is required, the carbonate in most of the skeletons from Locality A seems to be primary rather than a replacement. Notably, laminations appear much finer in the inner wall (Fig. 10A) than in the modern vestimentiferans. The tubes of the Irwin Basin examples have well defined inner and outer surfaces and delamination has taken place between outer lamellae rather than from the inner layers as reported in modern mineralized vestimentiferan tubes. The presence of keels and variability in cross-sectional shape of tubes has not been described previously for the Paleozoic tube worms considered of vestmentiferan affinities. These features are like those recorded in modern serpulids (Ten-Hove & Kupriyanova 2009).

The tube worms found at the studied localities probably belong to a group separate from the vestimentiferans (and perhaps the parent sigoglinids) as well as the serpulids. They may have possessed characters that include (i) a primary calcareous skeleton with incorporated layers perhaps rich in chitinous crystallites (Neville *et al*., 1976); (ii) outer layers tending to delaminate during diagenesis; and (iii) variable development among colonial individuals of cross-sectional shape of the tube and the presence of low keels formed by wall thickening (not through delamination).

Scolecodonts

The presence of other polychaete groups at the studied sites is indicated by very rare scolecodonts, from the jaw apparatuses, in palynomorph preparations from nodule samples at Locality D (Fig. 10I, J; and Playford 2021, their fig. 9J, K). From a very small sample, several morphotypes are present.

Possible vertebrate bone fragments

Fragmental skeletal elements that reach > 1 cm long (Fig. 11) from an unknown animal are present at localities B and D. The fragments are irregularly shaped with a smooth outline. Although the fragments are dense, laminated and fibrous fabrics are locally observed. Large cavities of variable shape are present together with small elongate cavities arranged in layers around the larger cavities. These may constitute large medullary and smaller vascular cavities in bone.

The fragments could be from fish, amphibians (see bone cross-sections from Triassic examples illustrated

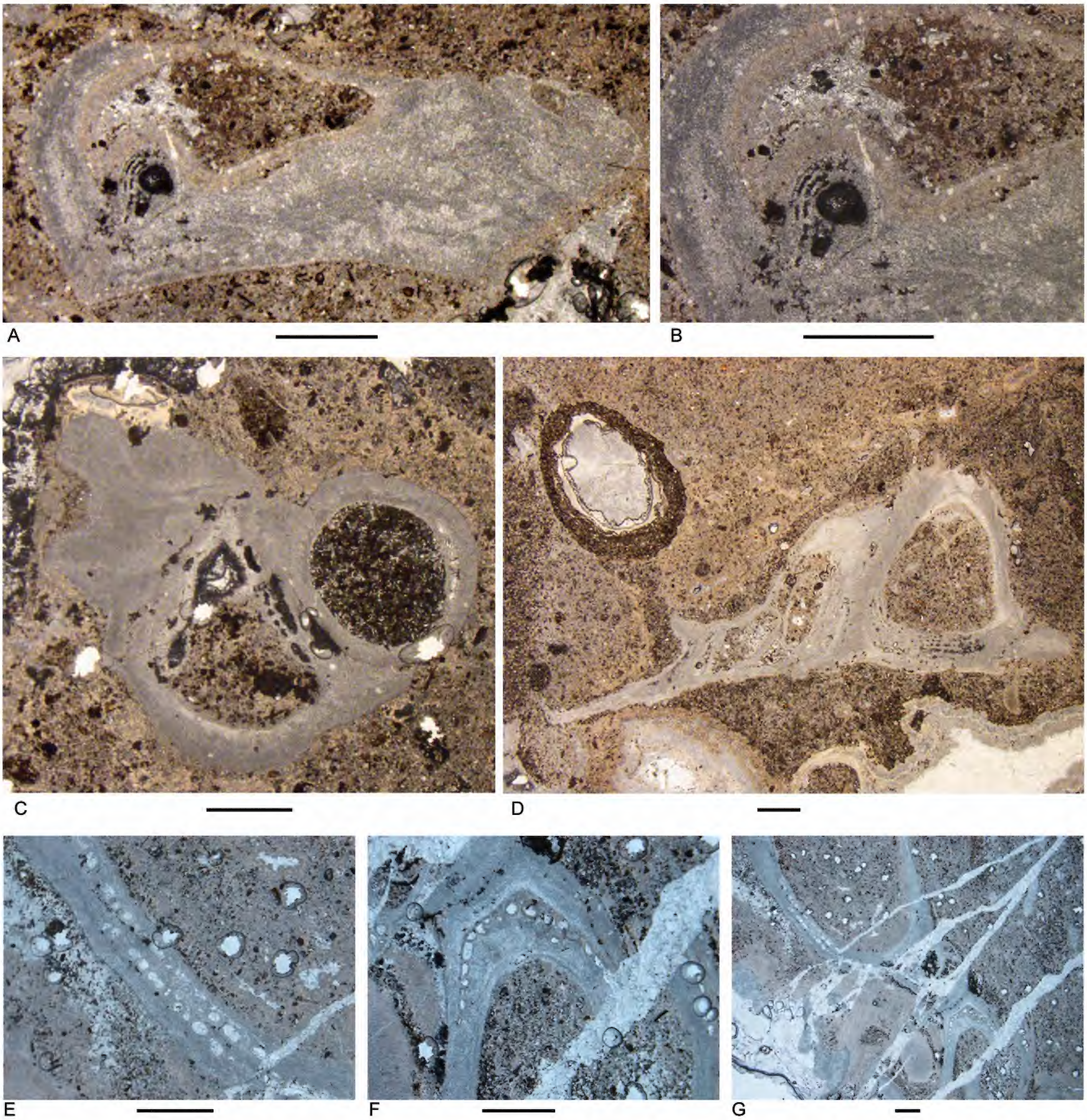

Figure 11. Skeletal fragments of possible vertebrates (? amphibians). Bar scales = 1 mm. Note irregular large cavities within dense skeleton that are infilled by sediment, and rows of smaller elongate cavities infilled by cement around the larger cavities. Also note ball and socket joint in C, suggestive of a tetrapod. A and B from 39251; C from 175034, D from 175035, E–G from 175028.

by Konietzko-Meier & Sander 2013 and Canoville & Chinsamy 2015) or primitive reptiles. The articulation between two separate parts of a skeleton illustrated in Fig. 11C may represent the articulation of limb bones (e.g. ulna and humerus). This suggests that these fragments are from tetrapods, most likely amphibians.

Much more work needs to be done on these interesting structures, including acid digestion of the nodules and micro-CT scanning of the rock, before their taxonomic affinities can be ascertained.

Palynomorphs from land plants

As reported by Playford (2021), nodules from Locality D preserve an abundance and diversity of palynomorphs: predominantly spores and pollen grains (Figs. 12, 13), together with some algal microfossils, rare scolecodonts, and foraminiferal cell linings. The quality of both palynopreservation and -yield is of high standard, unusually so, given that the samples are from weathered outcrop and from a commonly sparsely palyniferous lithology.

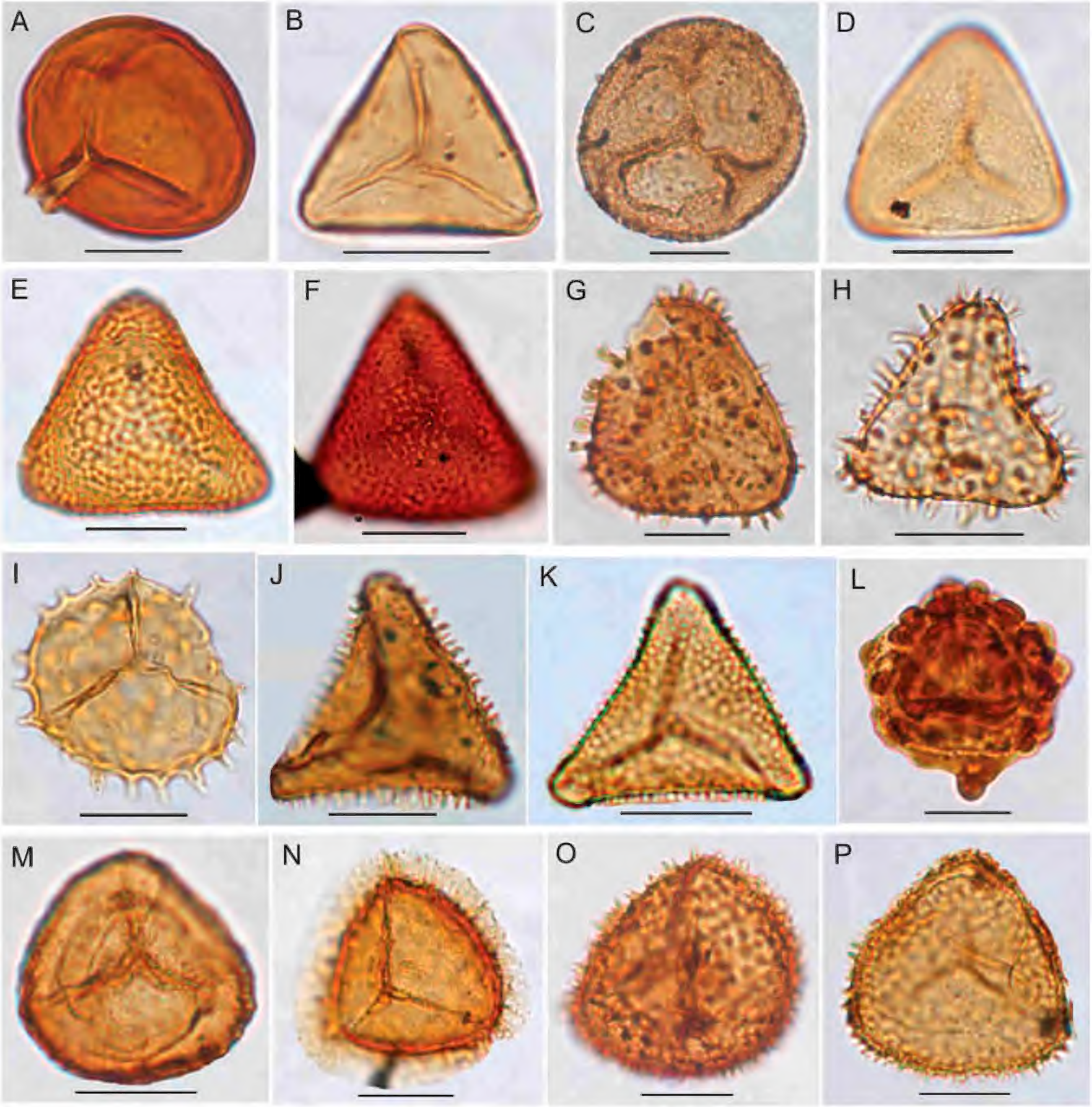

Figure 12. Representative spores from nodules at Locality D (B, F–J, L, M from 175029; A, C–E, K, N–P from 175035), *Punctatisporites gretensis* Balme & Hennelly. B, *Leiotriletes directus* Balme & Hennelly. C, *Apiculiretusispora* sp. D, *Microbaculispora tentula* Tiwari. E, F, *Converrucosisporites confluens* (Archangelsky & Gamerro). G, H, *Horriditriletes ramosus* (Balme & Hennelly). I, *Brevitriletes cornutus* (Balme & Hennelly). J, *Diatomozonotriletes townrowii* Segroves. K, *Diatomozonotriletes* sp. L, *Secarisporites lacunatus* (Tiwari). M, *Densoisporites solidus* Segroves. N, *Indotriradites niger* (Segroves). O, P, *Gondisporites ewingtonensis* Backhouse. Scale bars = 20 µm. For full taxonomic attribution and other spore species present in the samples, see Playford (2021). For curatorial details see Appendix 4.

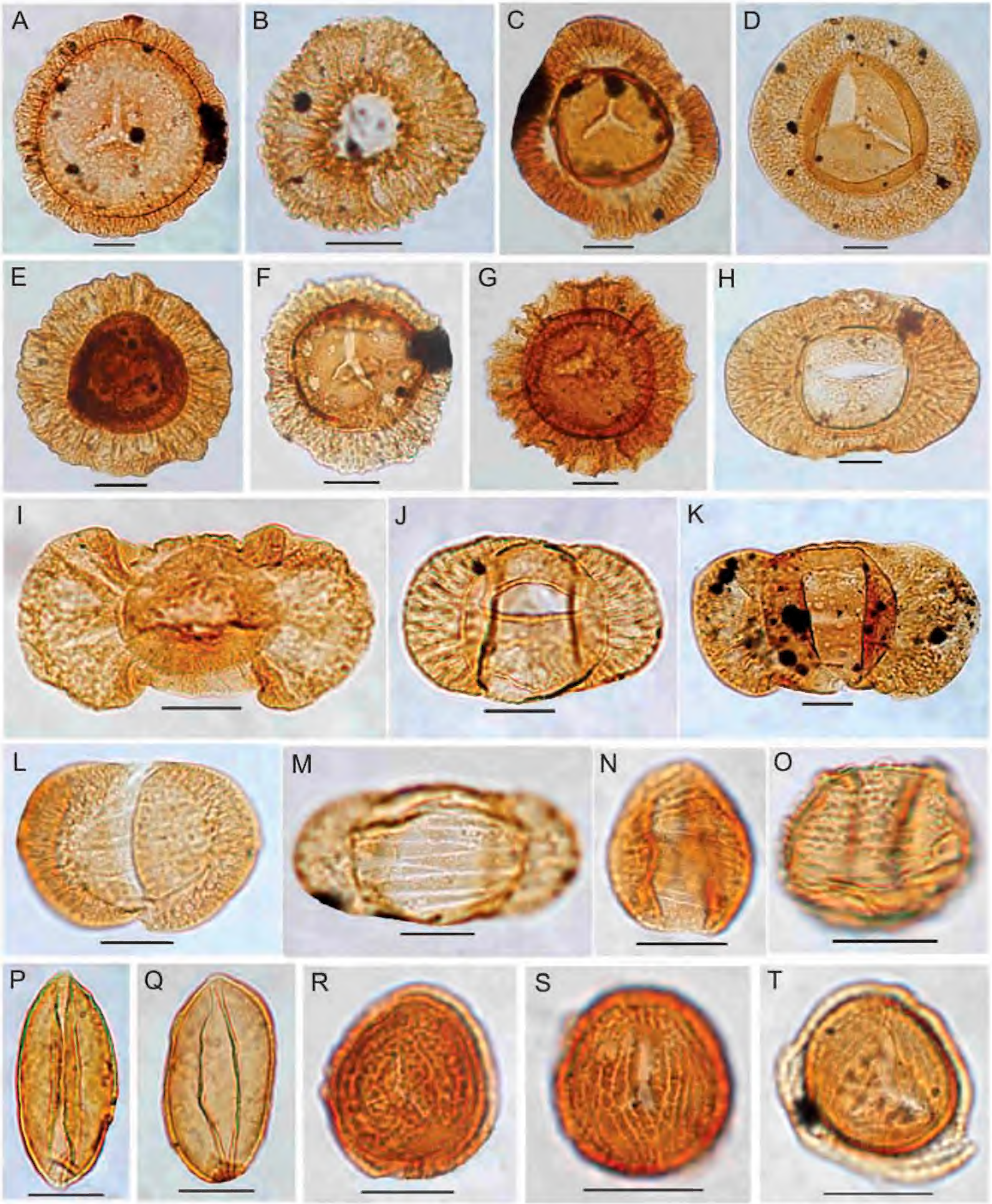

Figure 13. Representative pollen grains from nodules at Locality D (A–E, G–I, K, P–S from 175029; F, J, L–O, T from 175035). A, *Cannanoropollis janakii* Potonié & Sah. B, cf. *Cannanoropollis* sp. C, *Barakarites* sp. D, *Plicatipollenites gondwanensis* (Balme & Hennelly). E, *Plicatipollenites densus* Srivastava. F, *Plicatipollenites malabarensis* (Potonié & Sah). G, *Plicatipollenites* sp. cf. *P. malabarensis*. H, *Potonieisporites novicus* Bhardwaj. I, *Caheniasaccites* sp. J, *Limitisporites rectus* Leschik. K, *Protohaploxypinus amplus* (Balme & Hennelly). L, *Protohaploxypinus limpidus* (Balme & Hennelly). M, *Striatoabieites multistriatus* (Balme & Hennelly). N, *Vittatina fasciolata* (Balme & Hennelly). O, *Vittatina scutata* (Balme & Hennelly). P, Q, *Cycadopites cymbatus* (Balme & Hennelly). R, S, *Marsupipollenites striatus* (Balme & Hennelly). T, *Marsupipollenites* sp. cf. *M. striatus*. Scale bars = 20 µm. For full taxonomic attribution and other spore species present in the samples, see Playford (2021). For curatorial details see Appendix 4.

Reiterating Playford (2021), it would seem very likely that rapid lithification of the hosting calcareous sediment effectively protected the palynomorphs from oxidation at the methane-seep site and also from weathering desiccation. Early cementation of the nodules prevented burial-induced flattening.

DISCUSSION

Ecosystems represented in biota

Haig *et al*. (2022) distinguished representatives of three ecosystems in fossil assemblages from the carbonate nodules: (i) local marine seep ecosytem; (ii) broader marine pelagic ecosystem; and (iii) terrestrial ecosystem (probably coastal plain). They discussed possible palaeoecological relationships among these ecosystems, and the surrounding very poorly fossiliferous marine shale ecosystem. The biotic composition known from each ecosystem is summarized below.

The seep ecosystem includes (i) AOM archaea and bacteria (producing carbonate cement), (ii) microbial communities forming sediment laminations, (iii) small thickets of tube worms (that may have relied on chemosymbionts) and less common *Tubiphytes* and problematica B and C; (iv) other sessile inhabitants such as the organic macrophyte *Lithostoma* and its epiphytic porcelaneous and agglutinated foraminifers), rostroconch molluscs, very rare brachiopods and crinoids, and sponges that produced minute siliceous spicules. Benthic vagile foraminifers, gastropods, including microgastropods, ostracods, and polychaetes were also present. As Haig *et al*. (2022) noted, normal marine salinity is indicated by the seep fossil assemblage.

The marine pelagic ecosystem includes ammonoids, marine phytoplankton, and rare fish debris. Indeterminant nautiloids were also listed by Skwarko (1993). In muddy limestone nodules in the shale surrounding the seep deposits, the large ammonoid *Juresanites* (to at least 30 cm in diameter and in places forming a coquina) are common. Ammonoids are very rare elsewhere in the Western Australian Permian and the *Juresanites* occurrence suggests that (i) it was an opportunistic species attracted by the high organic productivity in the region of the methane seeps, and (ii) a more open-marine normal habitat for the ammonoid existed to the west of the Irwin Basin (the genus is not known further north in the contiguous marginal rift basins shown on Fig. 1E).

The marine shale ecosystem has benthic organisms with mineralized skeletons that are entirely different from those in the seep nodules. They consist only of organic-cemented siliceous agglutinated foraminifers. Haig *et al*. (2022) discounted the possibility that the shale hosted a benthic macrofauna whose calcareous skeletons suffered post-burial dissolution. They interpreted the shale deposits as suggesting very low-oxygen levels in the mud substrate and possible toxic pore water.

The coastal plain ecosystem includes spores and pollen grains preserved in the seep nodules. These were produced by diverse land plants probably living on the adjacent coastal plain. Some microphytoplankton preserved in the nodules signify freshwater inflow, via sediment-laden surface-water plumes from rivers and streams, coming from the coastal plain into the shallow interior sea.

The possible vertebrate remains (e.g., questionably very small amphibians) may have come from transitional shoreline environments. The animals may have been opportunistic feeders in surface waters above the seeps, being trapped and killed in methane eruptions sending their remains to the seafloor.

Criteria for water depth

Water depth is interpreted based on two main lines of evidence: (i) Stratigraphic criteria independent of fossil evidence; and (ii) fossil evidence.

Stratigraphic criteria independent of fossil evidence

Non-palaeontological palaeobathymetric evidence is derived from: (i) the low dip of strata and uniform thickness across the basin (see Clarke *et al*. 1951), and (ii) evidence for the water depth of the change between shallower sand facies and deeper mud facies in the interior sea (positioned hundreds of kilometres from the open Mesotethyan Ocean; Haig *et al*. 2022). Apart from Mesozoic faulting related to the breakup of Gondwana and later re-activation of faults due to late Miocene orogenesis on the far north-western margin of the Australian continent (Haig *et al*. 2018; Nano *et al*. 2023), the Permian strata in the Irwin Basin are little deformed and were not covered by any substantial thickness of post-Permian strata. The seafloor topography was locally flat grading into an extensive low coastal plain to the south, upland areas to the east (across the Darling Fault, see Clarke *et al*. 1951) and west (the Gascoyne Platform, recognized as a topographic high by Iasky *et al*. 2003, p. 30) and contiguous shallow seas to the north.

The water depth of the facies change is derived from the contact between the High Cliff Sandstone and the uppermost Holmwood Shale at High Cliff in the North Branch of the Irwin River (at 28.947°S, 115.548°E; Fig. 14). A muddy sandstone bed (2 m thick) at the base of the High Cliff Sandstone overlies carbonaceous mudstone of the uppermost Holmwood Shale (Fig. 14). The sandstone unit contains clinoforms, marked by more muddy horizons that extend from an erosion surface at the top of the bed to the basal planar contact with the Holmwood Shale (Fig. 14A). The clinoforms dip 5–10° SW, in the same dip direction as a higher 2 m thick tabular cross-bedded coarse sandstone (see Fig. 14 and Dillinger *et al*. 2021, fig. 7). There is no evidence for substantial sea-floor gradients in this area. Major bedding surfaces in the High Cliff Sandstone parallel the contact with the Holmwood Shale and with beds in the Fossil Cliff Member. The uppermost part of the Holmwood Shale is devoid of a shelly fauna except for a very low diversity assemblage of siliceous organic-cemented agglutinated foraminifers with simple tubular morphology. As indicated in Fig. 14B, beneath the uppermost shale is a unit equivalent to the highly fossiliferous Fossil Cliff Member with a shelly fauna indicating normal-marine salinities (Haig *et al*. 2014). The basal bed of the High Cliff Sandstone at this location is interpreted as a small deltaic deposit that prograded over a flat muddy seafloor (of the Holmwood Shale). The unfossiliferous uppermost part of the

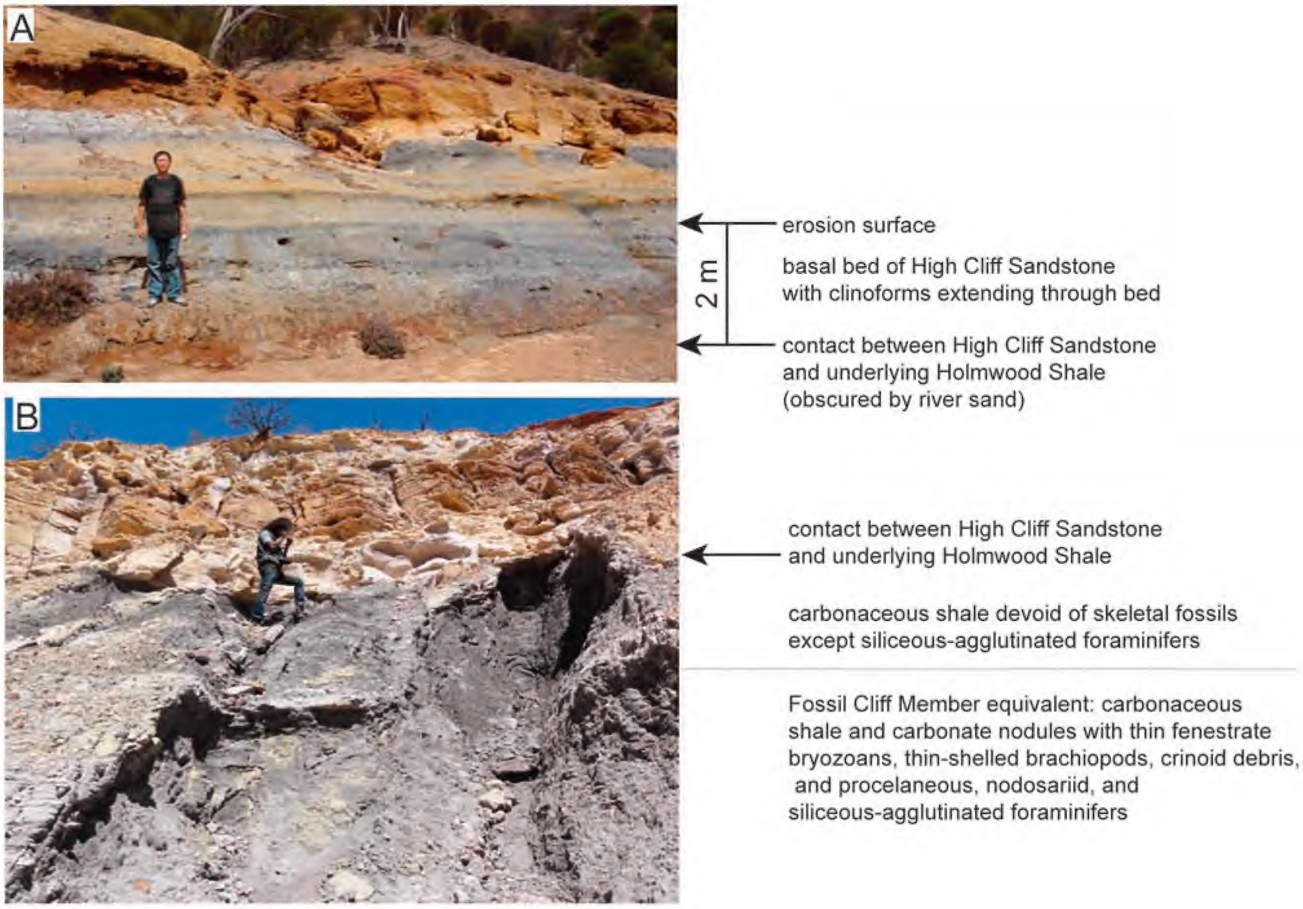
A
erosion surface
basal bed of High Cliff Sandstone with clinoforms extending through bed
2 m
contact between High Cliff Sandstone and underlying Holmwood Shale (obscured by river sand)
B
contact between High Cliff Sandstone and underlying Holmwood Shale
carbonaceous shale devoid of skeletal fossils except siliceous-agglutinated foraminifers
Fossil Cliff Member equivalent: carbonaceous shale and carbonate nodules with thin fenestrate bryozoans, thin-shelled brachiopods, crinoid debris, and procelaneous, nodosariid, and siliceous-agglutinated foraminifers

Figure 14. The Holmwood Shale–High Cliff Sandstone contact, North Branch of Irwin River. This is a critical section for interpretation of the depositional water depth for the upper part of the Holmwood Shale.

Holmwood Shale probably reflects an advancing brackish water front associated with the prograding delta. The erosional top of the basal sandstone bed may be close to sea level in the interior sea which would have had a low energy, probably microtidal, shoreline. The sand/mud facies change was probably at a few metres water depth assuming that the erosional surface was at approximate sea level.

Fossil assemblage evidence

The presence of probable photosynthetic *Litostroma* (possible red macrophytic algae) in the seep nodules and at other levels higher in the Holmwood suggests very shallow water, not much less than 30 m as deduced by Haig *et al*. (2022). This is supported by the presence of large porcelaneous (Miliolata) foraminifers which are most abundant in the inner neritic zones of normal-marine seas and absent in brackish environments (Murray 1991). The other components (including possible calcareous algae) of the seep assemblage are compatible with the shallow-water environments. The presence of calcareous fauna at several levels in the Holmwood Shale (including the methane-seep level) perhaps indicates intervals of maximum marine flooding.

Age

The age of the methane-seep deposits is based on ammonoids *Juresanites jacksoni* and *Uraloceras irwinense* that indicate a Sakmarian (Early Permian, Cisuralian) age based on stratigraphic ranges of the genera and evolutionary trends of species in classical sections of the Permian in Russia (see discussion in Haig *et al*. 2022). Playford (2021) and Haig *et al*. (2022) indicated that the well-preserved diverse spore-pollen assemblage belongs to either the *Converrucosisporites confluens* Zone or to the succeeding *Pseudoreticulatispora pseudoreticulata* Zone (as defined by Mory & Backhouse 1997). The boundary between these zones is poorly marked in the Irwin Basin.

CONCLUSIONS

From Haig *et al*. (2022) and the descriptions above, the methane seeps are interpreted as sanctuaries of high organic productivity on an otherwise barren, shallow, muddy seafloor. They supported a biota that included forms resembling modern seep inhabitants that rely on chemosynthesis (AOM microbial suites) and photosynthesis (red monostromatic alga like *Litostroma*), as well as metazoans that possibly hosted chemosymbionts (e.g., vestimentiferan-like tube worms).

The shale surrounding the seep deposits lacks a benthic macrofauna. However, it includes a peculiar assemblage of organic-cemented foraminifers, mainly single chambered, that suggest low dissolved oxygen conditions on the seafloor. Carbonate nodules in the shale contain the skeletons of ammonoids including common large *Juresanites* (to 30 cm diameter) considered to be opportunistic feeders on organic material generated at the seeps.

Episodic influxes of freshwater (perhaps glacial meltwater) are evidenced by some of the microphytoplankton and the spores-pollen. Water-column stratification resulted with mud-laden freshwater surface plumes coming into the shallow interior from rivers on the nearby vegetated coastal plain.

The seep-nodule fossil assemblage is unlike any previously described from the Australian Permian. It warrants detailed taxonomic study and search for additional occurrences in the Irwin Basin and in other Australian basins.

ACKNOWLEDGEMENTS

We thank the owners of Nangetty, Holmwood, and Woolaga Creek stations for permission to access the study sites. Jenny Bevan, Sarah Martin, Rodney Burrell, Isaias Barros, and Clement Tremblin are thanked for assistance with field work in the Irwin Basin and for sharing views about the stratigraphy. Peter Jell, Daniel Vachard, Daniel Mantle, Michael Amler, Shi Yukun, Kailah Thorn, and Marco Taviani provided valuable comments concerning the biota. Joern Peckmann, Tom Algeo, two anonymous Palaeo3 reviewers, and Guang Shi and Ken McNamara provided many helpful suggestions that have improved the manuscript. David Haig is very grateful to The University of Western Australia and its Oceans Graduate School and Oceans Institute for providing a stimulating and enjoyable venue for his research while in retirement. Haig's work was mainly self-funded, with some logistical support in the field from the Geological Survey of Western Australia. Arthur Mory and Charmaine Thomas publish with the permission of the Director, Geological Survey of Western Australia.

REFERENCES

Archbold, N W 2000. Palaeobiogeography of the Australasian Permian. *Memoir of the Association of Australasian Palaeontologists* **23**, 287–310.

Backhouse J & Mory A J 2020. Mid-Carboniferous – lower Permian palynology and stratigraphy, Canning Basin, Western Australia. *Report of the Geological Survey of Western Australia* **207**, 1–133.

Bomfleur B, Krings M, Kaštovský J, & Kerp H 2009. An enigmatic non-marine thalloid organism from the Triassic of East Antarctica. *Review of Palaeobotany and Palynology* **157**, 317–325.

Brenner W & Foster C B 1994. Chlorophycean algae from the Triassic of Australia. *Review of Palaeobotany and Palynology* **80**, 209–234.

Bright M & Lallier F H 2010. The biology of vestimentiferan tubeworms. *Oceanography and Marine Biology: An Annual Review* **48**, 213–266

Campbell K A 2006. Hydrocarbon seep and hydrothermal vent paleoenvironments and paleontology: Past developments and future research developments. *Palaeogeography, Palaeoclimatology, Palaeoecology* **232**, 362–407.

Canoville A & Chinsamy A 2015. Bone microstructure of the stereospondyl *Lydekkerina huxleyi* reveals adaptive strategies to the harsh post Permian-extinction environment. *The Anatomical Record* **298**, 1237–1254.

Case D H, Pasulka A L, Marlow J J, Grupe B M, Levin L A, & Orphan V J 2015. Methane seep carbonates host distinct, diverse, and dynamic microbial assemblages. *mBio* **6**(6), e01348-15. doi:10.1128/mBio.01348-15.

Clarke E de C, Prendergast K L, Teichert C, & Fairbridge R W 1951. Permian succession and structure in the northern part of the Irwin Basin, Western Australia. *Journal of the Royal Society Western Australia* **35**, 31–84.

Conkin J E & Conkin B M 1993. Permian Foraminifera of Tasmania. *University of Louisville Studies in Paleontology and Stratigraphy* **21**, 1–36.

Crespin I 1958. Permian Foraminifera of Australia. *Bulletin of the Bureau of Mineral Resources, Geology and Geophysics* **48**, 1–207.

Cushman J A & Waters J A 1928a. Some Foraminifera from the Pennsylvanian and Permian of Texas. *Contributions from the Cushman Laboratory for Foraminiferal Research* **4**, 31–55.

Cushman J A & Waters J A 1928b. Upper Paleozoic Foraminifera from Sutton County, Texas. *Journal of Paleontology* **2**, 358–371.

Davydov V I, Haig D W, M & McCartain E 2013. A latest Carboniferous warming spike recorded by a fusulinid-rich bioherm in Timor Leste: Implications for East Gondwana deglaciation. *Palaeogeography, Palaeoclimatology, Palaeoecology* **376**, 22–38.

Davydov V I, Haig D W, & McCartain E 2014. Latest Carboniferous (Late Gzhelian) fusulinids from Timor Leste and their paleobiogeographic affinities. *Journal of Paleontology* **88**, 588–605. DOI: 10.1666/13-007. Supplementary Material is available at: http://dx.doi.org/10.5061/dryad.qc580.

Dickins J M 1963. Permian pelecypods and gastropods from Western Australia. *Bulletin of the Bureau of Mineral Resources, Geology and Geophysics* **63**, 1–203.

Dillinger A George A D & Vaucher R 2021. Evolution of a complex early Permian coarse-grained shoreline along a rift basin margin. *Journal of Sedimentary Research* **91**, 317–347.

Dixon M, & Haig D W 2004. Foraminifera and their habitats within a cool-water carbonate succession following glaciation, Early Permian (Sakmarian), Western Australia. *Journal of Foraminiferal Research* **34**, 308–324.

Ferdinando D 2001. Ostracode and foraminiferal taxonomy and palaeoecology of the Fossil Cliff Member of the Holmwood Shale, northern Perth Basin, Western Australia. PhD Thesis, The University of Western Australia, Perth.

Foster C B, Palmieri V, & Fleming P J G 1985. Plant microfossils, Foraminiferida, and Ostracoda, from the Fossil Cliff Formation (Early Permian, Sakmarian), Perth Basin, Western Australia. Spec. Publ. S. Aust. Dep. Mines Energy **5**, 61–105.

Georgieva M N, Little C T S, Watson J S, Sephton M A, Ball A D & Glover A G 2019. Identification of fossil worm tubes from Phanerozoic hydrothermal vents and cold seeps. *Journal of Systematic Palaeontology* **17**, 287–329.

Glenister B F & Furnish W M 1961. The Permian ammonoids of Australia. *Journal of Paleontology* **35**, 673–736.

Glenister B F, Windle D L & Furnish W M 1973. Australasian Metalegoceratidae (Lower Permian ammonoids). *Journal of Paleontology* **47**, 1031–1043.

Glenister B F, Rogers F S & Skwarko, S K 1993. Ammonoids. *Geological Survey ofWestern Australian Bulletin* **136**, 54–63 (plus Appendix).

Grenfell H R 1995. Probable fossil zygnematacean algal spore genera. *Review of Palaeobotany and Palynology* **84**, 201–220.

Grey K & Awramik S M 2020. Handbook for the study and description of microbialites. *Geological Survey of Western Australia Bulletin* **147**, 1–275.

Groves J R 1983. Calcareous foraminifers and algae from the type Morrowan (Lower Pennsylvanian) region of northeastern Oklahoma and northwestern Arkansas. *Oklahoma Geological Survey Bulletin* **133**, 1–66.

Günther A 1990. Distribution and bathymetric zonation of shell-boring endoliths in recent reef and shelf environments: Cozumel, Yucatan (Mexico). *Facies* **22**, 233–262.

Haig D W 2018. Permian (Kungurian) Foraminifera from Western Australia described by Walter Parr in 1942: reassessment and additions. *Alcheringa: An Australasian Journal of Palaeontology* **42**, 37–66. https://doi.org/10.1080/03115518.2017.1374459

Haig D W & Mory A J 2016. Middle Permian (Roadian) Foraminifera from mudstone facies of the type Baker Formation, Southern Carnarvon Basin, Western Australia. *Journal of the Royal Society of Western Australia* **99**, 61-75.

Haig D W, McCartain E, Mory A J, Borges G, Davydov V I, Dixon M, Ernst A, Groflin S, Håkansson E, Keep M, Dos Santos Z, Shi G R & Soares J 2014. Postglacial Early Permian (late Sakmarian–early Artinskian) shallow-marine carbonate deposition along a 2000 km transect from Timor to west Australia. *Palaeogeography, Palaeoclimatology, Palaeoecology* **409**, 180–204.

Haig D W, Mory A J, McCartain E, Backhouse J, Håkansson E, Ernst A, Nicoll R S, Shi G R, Bevan J C, Davydov V I, Hunter A, Keep M, Martin S, Peyrot D, Kossavaya O & Dos Santos Z, 2017. Late Artinskian–Early Kungurian (Early Permian) warming and maximum marine flooding in the East Gondwana interior rift, Timor and Western Australia, and comparisons across East Gondwana. *Palaeoegography, Palaeoclimatology, Palaeoecology* 468, 88–121.

Haig D W, Foster C B, Howe R W, Mantle D, Backhouse J, Peyrot D & Vitacca J 2018. Fossil protists (algae and testate protozoans) in the marine Phanerozoic of Western Australia: a review through latitudinal change, climate extremes and breakup of a supercontinent. *Journal of the Royal Society of Western Australia* **101**, 44–67.

Haig D W, Dillinger A, Playford G, Riera R, Sadekov A, Skrzypek G, Håkansson E, Mory A J, Peyrot D & Thomas C 2022. Methane seeps following Early Permian (Sakmarian) deglaciation, interior East Gondwana, Western Australia: Multiphase carbonate cements, distinct carbon-isotope signatures, extraordinary biota. *Palaeogeography, Palaeoclimatology, Palaeoecology* **591**, 110862.

https://doi.org/10.1016/j.palaeo.2022.110862. Supplementary Material is available at https://doi. org/10.1016/j.palaeo.2022.110862.

Hashimoto J, Miura T, Fujikura K & Ossaka J 1993. Discovery of vestimentiferan rube-worms in the Euphotic Zone. *Zoological Science* **10**, 1063–1067.

Hass A, Little C T S, Sahling H, Bohrmann G, Himmler T & Peckmann J 2009. Mineralization of vestimentiferan tubes at methane seeps on the Congo deep-sea fan. *Deep-Sea Research 1* **56**, 283–293.

Henbest L G 1958. Ecology and life association of fossil algae and foraminifera in a Pennsylvanian limestone, McAlester, Oklahoma. *Contributions from the Cushman Foundation for Foraminiferal Research* **9**, 104–111.

Hilário A, Capa M, Dahlgren T G, Halanych K M, Little C T S, Thornhill D J, Verna C & Glover A G 2011. New perspectives on the ecology and evolution of sigoglinid tubeworms. *PLoS ONE* **6(2)**: e16309. doi:10.1371/journal.pone.0016309

Himmler T, Freiwald A, Stollhofen H, & Peckmann J 2008. Late Carboniferous hydrocarbon-seep carbonates from the glaciomarine Dwyka Group, southern Namibia. *Palaeogeography, Palaeoclimatology, Palaeoecology* 257, 185–197.

Homann W 1972. Unter-und tief-mittelpermische Kalkalgen aus den Rattendorfer Schichten, dem Trogkofel-Kalk und dem Tressdorfer Kalk der Karnischen Alpen (Österreich). *Senckenbergiana lethaea* **53**, 135–313.

Iasky R P, D'Ercole C, Ghori K A R, Mory A J & Lockwood A M 2003. Structure and petroleum prospectivity of the Gascoyne Platform, Western Australia. *Report of the Geological Survey of Western Australia* **87**, 1–56.

Jansa L F, Mamet B & Roux A 1978. Viséan limestone from the Newfoundland Shelf. *Canadian Journal of Earth Sciences* **15**, 1422–1436.

Johnson J H 1966. New Mississippian algae from Alberta. *Journal of Paleontology* **40**, 1385–1387.

Kaim A, Jenkins R G & Hikida Y 2009. Gastropods from Late Cretaceous Omagari and Yasukawa hydrocarbon seep deposits in the Nakagawa area, Hokkaido, Japan. *Acta Palaeontologica Polonica* **54**, 463–490.

Karaseva N, Gantsevich M, Obzhirov A, Shakirov R, Starovoitov A, Smirnov R, & Malakhov V 2020. Correlation of the sigoglinid (Annelida: Siboglinidae) distribution to higher concentrations of hydrocarbons in the Sea of Okhotsk. *Marine Pollution Bulletin* **158**, https://doi.org/10.1016/j.marpolbul.2020.111448

Kochansky-Devidé V 1970. Die Kalkalgen des Karbons von Velebit-Gebirge (Moskovien und Oklahoma. *Journal of Paleontology* **9**, 291–306.

Konietzko-Meier D & Sander M 2013. Long bone histology of *Metoposaurus diagnosticus* (Temnospondyli) from the Late Triassic of Krasiejów (Poland) and its paleobiological implications. *Journal of Vertebrate Paleontology* **33**, 1003–1018.

Leonova T B 2011. Permian ammonoids: biostratigraphic, biogeographical, and ecological analysis. *Paleontological Journal* **45**, 1206–1312.

Little C T S & Vrijenhoek R C 2003. Are hydrothermal vent animals living fossils. *Trends in Ecology and Evolution* **18**, 582–588.

Mamay S H 1959. *Litostroma*, a new genus of problematical algae from the Pennsylvanian of Oklahoma. *American Journal of Botany* **46**, 283–292.

Mamay S H & Yochelson E L 1962. Occurrence and significance of marine animal remains in American coal balls. *Geological Survey of United States Professional Paper* **354-1**, 193–224.

Mays C, Vajda V & McLoughlin S 2021. Permian–Triassic non-marine algae of Gondwana—distributions, natural affinities and ecological implications. *Earth-Science Reviews* **212**, 1–29.

McCartain E, Backhouse J, Haig D, Balme B & Keep M 2006. Gondwana-related Late Permian palynoflora, foraminifers and lithofacies from the Wailuli Valley, Timor Leste. *Neues Jahrbuch für Geologie und Paläontologie Abhandlungen* **240**, 53–80.

Miura T, Tsukahara J & Hashimoto, J. 1997. *Lamellibrachia satsuma*, a new species of vestimentiferan worms (Annelida: Pogonophora) from a shallow hydrothermal vent in Kagoshima Bay, Japan. *Proceedings of the Biological Society of Washington* **110**, 447–456.

Mory A J & Backhouse J 1997. Permian stratigraphy and palynology of the Carnarvon Basin, Western Australia. Report of the *Geological Survey of Western Australia* **51**, 1–46.

Murray J 1991. *Ecology and Palaeoecology of Benthic Foraminifera*. Longman Scientific & Technical, Harlow, 397 pp.

Nano J, Haig D.W, Fraga E, Soares M, Barros I S, McCartain E & Baillie P 2023. Debris-slides, olistoliths and turbidites: keys to understanding the tectonostratigraphic affinities of a terrane block in a young orogenic belt, Timor-Leste. *Journal of the Geological Society, London*, https://doi.org/10.1144/jgs2023-079. Supplementary Material is available at https://doi.org/10.6084/m9.figshare.c.6852387.

Neville A C, Parry D A D & Woodhead-Galloway J 1976. The chitin crystallite in arthropod cuticle. *Journal of Cell Science* **21**, 73–82.

Nogami Y 1963. Fusulinids from Portuguese Timor (Palaeontological Study of Portuguese Timor, 1). *Memoirs of the College of Science, University of Kyoto, Series B*, **30 (2)**, 59–67.

Palmieri V 1988. Globovalvulinid foraminifera from the Permian of Queensland: *Alcheringa* **12**, 27–47.

Palmieri V 1993. Foraminifers. *Bulletin of the Geological Survey of Western Australia* **136**, 30–32.

Palmieri V 1994. Permian Foraminifera in the Bowen Basin, Queensland. *Queensland Geology* **6**, 1–125.

Palmieri V 1998. Foraminifera zonation in the Permian stratigraphy of the Denison Trough (Bowen Basin), Central

Queensland. *Proceedings of the Royal Society of Victoria* **110**, 173–195.

Peckmann J, Little C T S, Gill F & Reitner J 2005. Worm tube fossils from the Hollard Mound hydrocarbon-seep deposit, Middle Devonian, Morocco: Palaeozoic seep-related vestimentiferans? *Palaeogeography, Palaeoclimatology, Palaeoecology* **227**, 242–257.

Playford G 1959. Permian stratigraphy of the Woolaga Creek area, Mingenew District, Western Australia. *Journal Royal Society of Western Australia* **42**, 7–29.

Playford G 2021. Lower Permian (Sakmarian) palynoflora from the Woolaga Limestone Member of the Holmwood Shale, northern Perth Basin, Western Australia. *Journal of the Royal Society of Western Australia* **104**, 45–63.

Plummer H J 1945. Smaller Foraminifera in the Marble Falls, Smithwick, and Lower Strawn strata around the Llano Uplift in Texas. *The University of Texas, Publication* **4401**, 209–271.

Pojeta J & Runnegar B 1976. The paleontology of rostroconch mollusks and the early history of the Phylum Mollusca. *U.S. Geological Survey Professional Paper* **968**, 1–88.

Reveillaud J, Anderson R, Reves-Sohn S, Cavanaugh C & Huber J A 2018. Metagenomic investigation of vestimentiferan tubeworm endosymbionts from Mid-Cayman Rise reveals new insights into metabolism and diversity. *Microbiome* **6:19,** DOI 10.1186/s40168-018-0411-x

Rogalla N S, Carter J G & Pojeta J 2003. Shell microstructure of the Late Carboniferous rostroconch mollusc *Apotocardium lanterna* (Branson, 1965). *Journal of Paleontology* **77**, 655–673.

Scheibnerová V 1982. Permian Foraminifera of the Sydney Basin. *Memoirs of the Geological Survey of New South Wales, Palaeontology* **19**, 1–125.

Senowbari-Daryan B 2013. *Tubiphytes* Maslov, 1956 and description of similar organisms from Triassic reefs of the Tethys. *Facies* **59**, 75–112.

Skwarko S K 1993. A list of Permian fossils from the Collie, Perth, Carnarvon, and Canning Basins. *Bulletin of the Geological Survey of Western Australia* **136**, 89–109.

Taboada A C, Mory A J, Shi G-R, Haig D W & Pinilla M K 2015. An Early Permian brachiopod-gastropod fauna from the Calytrix Formation, Barbwire Terrace, Canning Basin, Western Australia. *Alcheringa* **39**, 207–223. http://dx.doi.org/10.1080/03115518.2015.965921

Teichert C & Glenister B F 1952. Lower Permian ammonoids from the Irwin Basin, Western Australia. *Journal of Paleontology* **26**, 12–23.

Ten Hove H A & Kupriyanova E K 2009. Taxonomy of Serpulidae (Annelida, Polychaeta): The state of affairs. Zootaxa **2036**, 1–126.

Thompson M L 1935. Fusulinids from the Lower Pennsylvanian Atoka and Boggy Formations of Oklahoma. Journal of Paleontology **9**, 291–306.

Tremblin C M & Haig D W 2023. Evolution of trochamminoids (trochospiral organic-cemented agglutinated Foraminifera): Examples from the Lower Permian of Western Australia. *Journal of Foraminiferal Research* **53**, 269–285.

Vachard D, Hauser M, Martini R, Zaninetti L, Matter A & Peters T 2001. New algae and problematica of algal affinity from the Permian of the Aseelah Unit of the Batain Plain (East Oman). *Geobios* **34**, 375–404.

Vachard D, Haig D W & Mory A J 2014. Lower Carboniferous (middle Visean) foraminifers and algae from an interior sea, Southern Carnarvon Basin, Australia. *Geobios* **47**, 57–74. http://dx.doi.org/10.1016/j.geobios.2013.10.005. Supplementary Material is available at: https://ars.els-cdn.com/content/image/1-s2.0-S0016699514000047-mmc1.pdf

Wilmeth D T, Johnson H A, Stamps B W, Berelson W M, Stevenson B S, Nunn H S, Grim S L, Dillon M L, Paradis O, Corsetti F A & Spear J R 2018. Environmental and biological influences on carbonate precipitation within hot spring microbial mats in Little Hot Creek, CA. *Frontiers in Microbiology* doi: 10.3389/fbioe.2016.00004

Zhu T & Dittrich M 2016. Carbonate precipitation through microbial activities in natural environment, and their potential in biotechnology: a review. *Frontiers in Bioengineering and Biotechnology* doi: 10.3389/fbioe.2016.00004

Appendix 1. Localities and lists of studied samples

UWA Number	Field No.	°S	°E	Area	Basin	Formation/Age	Description
Limestone Nodules							
Locality A: Unit 1							
175470	1_5_19-1	28.97144	115.4071	WA	Irwin Basin	Holmwood Shale, Permian	Macaroni Hill, "Serpulid" bioherm, unit 1 at base of succession; muddy limestone
175471	1_5_19-2	28.97144	115.4071	WA	Irwin Basin	Holmwood Shale, Permian	Macaroni Hill, "Serpulid" bioherm, unit 1 at base of succession; muddy limestone
175472	1_5_19-3	28.97144	115.4071	WA	Irwin Basin	Holmwood Shale, Permian	Macaroni Hill, "Serpulid" bioherm, unit 1 at base of succession; muddy limestone
175473	1_5_19-4	28.97144	115.4071	WA	Irwin Basin	Holmwood Shale, Permian	Macaroni Hill, "Serpulid" bioherm, unit 1 at base of succession; muddy limestone
181377	1_5_19-5	28.97144	115.4071	WA	Irwin Basin	Holmwood Shale, Permian	Macaroni Hill, "Serpulid" bioherm, unit 1 at base of succession; muddy limestone
Locality A: Unit 2							
175474	2_5_19_1	28.97144	115.4071	WA	Irwin Basin	Holmwood Shale, Permian	Macaroni Hill, "Serpulid" bioherm, unit 2; muddy limestone
175475	2_5_19_2	28.97144	115.4071	WA	Irwin Basin	Holmwood Shale, Permian	Macaroni Hill, "Serpulid" bioherm, unit 2; muddy limestone
175476	2_5_19_3	28.97144	115.4071	WA	Irwin Basin	Holmwood Shale, Permian	Macaroni Hill, "Serpulid" bioherm, unit 2; muddy limestone
175477	2_5_19_4	28.97144	115.4071	WA	Irwin Basin	Holmwood Shale, Permian	Macaroni Hill, "Serpulid" bioherm, unit 2; muddy limestone
175478	2_5_19_5	28.97144	115.4071	WA	Irwin Basin	Holmwood Shale, Permian	Macaroni Hill, "Serpulid" bioherm, unit 2; muddy limestone
181378	27_5_21_2	28.97144	115.4071	WA	Irwin Basin	Holmwood Shale, Permian	Macaroni Hill, "Serpulid" bioherm, unit 2; muddy limestone
Locality A: Unit 3							
175479	2_5_19_6	28.97144	115.4071	WA	Irwin Basin	Holmwood Shale, Permian	Macaroni Hill, "Serpulid" bioherm, unit 3 at top of succession; muddy limestone
175480	2_5_19_7	28.97144	115.4071	WA	Irwin Basin	Holmwood Shale, Permian	Macaroni Hill, "Serpulid" bioherm, unit 3 at top of succession; muddy limestone
175481	2_5_19_8	28.97144	115.4071	WA	Irwin Basin	Holmwood Shale, Permian	Macaroni Hill, "Serpulid" bioherm, unit 3 at top of succession; muddy limestone
175482	2_5_19_9	28.97144	115.4071	WA	Irwin Basin	Holmwood Shale, Permian	Macaroni Hill, "Serpulid" bioherm, unit 3 at top of succession; muddy limestone
Locality A: scree samples							
175000	28/11/2016	28.9714	115.40705	WA	Irwin Basin	Holmwood Shale, Permian	Macaroni Hill, "Serpulid" Reef, Nangetty Station ; 2 large slabs
175001	28/11/16_2	28.9714	115.40705	WA	Irwin Basin	Holmwood Shale, Permian	Macaroni Hill, "Serpulid" Reef, Nangetty Station ; 4 slabs
175002	28/11/16-3	28.9714	115.40705	WA	Irwin Basin	Holmwood Shale, Permian	Macaroni Hill, "Serpulid" Reef, Nangetty Station ; 2 slabs
175003	28/11/16-4	28.9714	115.40705	WA	Irwin Basin	Holmwood Shale, Permian	Macaroni Hill, "Serpulid" Reef, Nangetty Station ; 2 slabs
175004	28/11/16-5	28.9714	115.40705	WA	Irwin Basin	Holmwood Shale, Permian	Macaroni Hill, "Serpulid" Reef, Nangetty Station ; 4 slabs
175005	28/11/16_1	28.9714	115.40705	WA	Irwin Basin	Holmwood Shale, Permian	Macaroni Hill, "Serpulid" Reef, Nangetty Station ; 3 slabs (large tubes with concentric infill)
Locality B							
175023	9/9/16-7	28°57'34.9"	115°27'59.0"	WA	Irwin Basin	Holmwood Shale, Permian	Breakaway between mesas; 2 slabs of nodule
175024	9/9/16-7	28°57'34.9"	115°27'59.0"	WA	Irwin Basin	Holmwood Shale, Permian	Breakaway between mesas; 2 slabs of nodule
175025	9/9/16-7	28°57'34.9"	115°27'59.0"	WA	Irwin Basin	Holmwood Shale, Permian	Breakaway between mesas; 1 slab of nodule
175026	9/9/16-7	28°57'34.9"	115°27'59.0"	WA	Irwin Basin	Holmwood Shale, Permian	Breakaway between mesas; 1 slab of nodule
175027	9/9/16-7	28°57'34.9"	115°27'59.0"	WA	Irwin Basin	Holmwood Shale, Permian	Breakaway between mesas; 2 slabs of nodule
175028	9/9/16-7	28°57'34.9"	115°27'59.0"	WA	Irwin Basin	Holmwood Shale, Permian	Breakaway between mesas; 1 slab of nodule

UWA Number	Field No.	°S	°E	Area	Basin	Formation/Age	Description
Locality C							
175007	10/9/16/1	28°58'37.6"	115°30'45.5"	WA	Irwin Basin	Holmwood Shale, Permian	2 slabs of nodule; collected approximately along strike line in flat paddock
175012	10/9/16-2	28°58'37.4"	115°30'44.4"	WA	Irwin Basin	Holmwood Shale, Permian	2 slabs of nodule; collected approximately along strike line in flat paddock
175016	10/9/16-3	28°58'37.5"	115°30'43.1"	WA	Irwin Basin	Holmwood Shale, Permian	2 slabs of nodule collected by Arthur Mory in paddock about 100-200 m north of 175016
175019	10/9/16-5	28°58'37.5"	115°30'43.1"	WA	Irwin Basin	Holmwood Shale, Permian	2 slabs of nodule collected by Arthur Mory in paddock about 100-200 m north of 175016
175020	10/9/16-4	28°58'37.5"	115°30'43.1"	WA	Irwin Basin	Holmwood Shale, Permian	2 slabs of nodule collected by Arthur Mory in paddock about 100-200 m north of 175016
175021	10/9/16-8	28°58'37.5"	115°30'43.1"	WA	Irwin Basin	Holmwood Shale, Permian	4 slabs of nodule collected by Arthur Mory in paddock about 100-200 m north of 175016
175022	10/9/16-9	28°58'37.5"	115°30'43.1"	WA	Irwin Basin	Holmwood Shale, Permian	2 slabs of nodule collected by Arthur Mory in paddock about 100-200 m north of 175016
Locality D							
175029	5/9/16-1	29°12'12.7"	115°39'17.7"	WA	Irwin Basin	Holmwood Shale, Permian	1 slab of blocks of indurated fossiliferous carlcareous mudstone; moved and concentrated at edge of paddock; Woolaga Creek area
175033	5/9/16-1	29°12'12.7"	115°39'17.7"	WA	Irwin Basin	Holmwood Shale, Permian	2 slabs of blocks of indurated fossiliferous carlcareous mudstone; moved and concentrated at edge of paddock
175034	5/9/16-1	29°12'12.7"	115°39'17.7"	WA	Irwin Basin	Holmwood Shale, Permian	2 slabs of blocks of indurated fossiliferous carlcareous mudstone; moved and concentrated at edge of paddock
175035	5/9/16-2	29°11'53.5"	115°39'13.7"	WA	Irwin Basin	Holmwood Shale, Permian	2 slabs of blocks of indurated fossiliferous carlcareous mudstone; moved and concentrated at edge of paddock
175036	5/9/16-2	29°11'53.5"	115°39'13.7"	WA	Irwin Basin	Holmwood Shale,	2 slabs of blocks of indurated fossiliferous carlcareous mudstone; moved and concentrated at edge of paddock
39251		29°12'10"	115°39'30"	WA	Irwin Basin	Holmwood Shale, Permian	nodular limestone
39256		29°12'40"	115°39'30"	WA	Irwin Basin	Holmwood Shale, Permian	nodular limestone
Shale samples							
Beckett's Gully (Samples collected along Beckett's Gully and tributaries)							
181379	6_9_16-3	29°01'25.8"	115°31'05.1"	WA	Irwin Basin	Holmwood Shale, Permian	Shale outcrop in Beckett Gully, estimated 46 m above top Nangetty outcrop
181380	6_9_16-8	29°01'21.0"	115°31'16.6"	WA	Irwin Basin	Holmwood Shale, Permian	
181381	8_9_16-6	29°01'23.3"	115°31'21.2"	WA	Irwin Basin	Holmwood Shale, Permian	same level as ammonoid (*Jurensanites*; 8_9_16_5); about 60 m above top Nangetty
181382	8_9_16-7(2)	29°01'23.2"	115°31'21.9"	WA	Irwin Basin	Holmwood Shale, Permian	
181383	8_9_16-7(4)	29°01'23.2"	115°31'21.9"	WA	Irwin Basin	Holmwood Shale, Permian	
181384	8_9_16-10	29°01'25.5"	115°31'45.7"	WA	Irwin Basin	Holmwood Shale, Permian	
181385	8_9_16-12	29°01'16.7"	115°31'54.6"	WA	Irwin Basin	Holmwood Shale, Permian	
181386	8_9_16-15	28°57'43.0"	115°31'51.2"	WA	Irwin Basin	Holmwood Shale, Permian	
181397	8_9_16-2	29°01'24.0"	115°31'17.8"	WA	Irwin Basin	Holmwood Shale, Permian	Stratigraphically below *Juresanites* level (181381)

UWA Number	Field No.	°S	°E	Area	Basin	Formation/Age	Description
Locality A (shale in interval with *Juresanites* in calcareous mudstone nodules)							
181387	10_9_16-10	28°58'34.5"	115°24'24.7"	WA	Irwin Basin	Holmwood Shale, Permian	
181388	10_9_16-11	28°58'34.6"	115°24'22.2"	WA	Irwin Basin	Holmwood Shale, Permian	
181389	10_9_16-13	28°58'28.7"	115°24'27.1"	WA	Irwin Basin	Holmwood Shale, Permian	
181390	10_9_16-14	28°58'29.6"	115°24'27.8"	WA	Irwin Basin	Holmwood Shale, Permian	
181391	29_5_17-1	28.9714°	115.40705°	WA	Irwin Basin	Holmwood Shale, Permian	about 1 m below base of Unit 1 of "Serpulid" nodular limestone
Locality B							
175040	9_9_16-7	28°57'34.9"	115°27'59.0"	WA	Irwin Basin	Holmwood Shale, Permian	at base of measured section
181392	9_9_16-8	28°57'34.9"	115°27'59.0"	WA	Irwin Basin	Holmwood Shale, Permian	about 0.85 m above base
181393	9_9_16-9	28°57'34.9"	115°27'59.0"	WA	Irwin Basin	Holmwood Shale, Permian	about 1.7 m above base
181394	9_9_16-10	28°57'34.9"	115°27'59.0"	WA	Irwin Basin	Holmwood Shale, Permian	about 2 m above base
181395	9_9_16-11	28°57'34.9"	115°27'59.0"	WA	Irwin Basin	Holmwood Shale, Permian	about 3.5 m above base; just below level with *Juresanites* in nodules
Locality D							
181396	28/5/21-1	29.19494°	115.65154°	WA	Irwin Basin	Holmwood Shale, Permian	shale exposed on small scarp, Woolaga Creek

Appendix 2. List of biota in studied nodules.

							Foraminifera							**Mollusca**										
	Microbial (bacterial) lamination	*Litostroma oklahomensis*	*Tubiphytes* sp.	Problematica A	Problematica B	Problematica C	Microgranular /agglutinated morphotypes	*Tolypammina* sp.	*Calcitornella* sp.	*Glomomidiella* sp.	*Hedraites* sp.	monaxon siliceous sponge spicules	Brachiopod debris - pseudopunctate shells	Rostroconchs	Bivalve debris with prismatic microstructure	Bivalved shells of uncertain affinity	Gastropod A	Gastropods - other morphotypes	? *Uraloceras* sp.	Crinoid debris	? Echinoderm	Ostracods	Tube worms	probable vertebrate bone fragments (?amphibians)
Loc. A																								
Unit 1																								
175470					?	X	X							X		X	X	X	X			X	X	
175471		X					X			?				X		X	X					X	X	
175472							X				X			X		X	X					X	X	
175473				?		X	X				?	X				X						X	X	
181377		X				X	X		X			X				X	X	X				X	X	
Unit 2																								
175474							X							X			X	X				X	X	
175475							X		X							X	X	X			X	X	X	
175476							X		X					X		X	X					X	X	
175477					?		X							X		X	X	X				X	X	
175478							X						?			X	X					X	X	
181378			X		?		X							X		X						X	X	
Unit 3																								
175479						?											X					X	X	
175480														X			X	X				X	X	
175481		X	?		X	?	X			?				X		X	X	X			X	X	X	
175482					X		X		X					X	X	X	X				X	X	X	
scree																								
175001						X									X								X	
175002						X									X							X	X	
175003			?																				X	
175004						X	X		?					X		X	X						X	
175005			X		X		X									X	X					X	X	
Loc. B																								
175023		X																						
175024		X					X		?				X									X		
175025		X		X																				
175026		X		X								X										X		
175027		X								X														
175028				X								X			X			X		X		X	X	X

							Foraminifera							**Mollusca**										
	Microrobial (bacterial) lamination	*Litostroma oklahomensis*	*Tubiphytes* sp.	Problematica A	Problematica B	Problematica C	Microgranular /agglutinated morphotypes	*Tolypammina* sp.	*Calcitornella* sp.	*Glomomidiella* sp.	*Hedraites* sp.	monaxon siliceous sponge spicules	Brachiopod debris - pseudopunctate shells	Rostroconchs	Bivalve debris with prismatic microstructure	Bivalved shells of uncertain affinity	Gastropod A	Gastropods - other morphotypes	? *Uraloceras* sp.	Crinoid debris	? Echinoderm	Ostracods	Tube worms	probable vertebrate bone fragments (?amphibians)
Loc. C																								
175007		X										?												
175012		X		X																				
175016		X		X								X											X	
175019	X	X		X				X	X			X	?		X	X			X			X		
175020		X										X												
175021		X		X									X		X			X						
175022		X		X								X	X		X	X								
Loc. D																								
175029		X		X			X			X		X				X	X			X		X	X	
175033									X			X						X		X			X	X
175034	X	X		X					X	X	X	X				X	X			X		X	X	X
175035		X		X			X		X	X	X	X				X				X		X	X	X
39251					X				X			X		X		X				X		X	X	X
39256												X	X			X		X		X			X	

Appendix 3. List of biota from studied shale samples.

Foraminifera. (R = > 5 specimens; C = 5-20; A = >20)	*Thuramminoides sphaeroidalis*	*Thurammina texana*	*Sansabaina elegantissima*	*Sansabaina? acicular*	*Kechenotiske hadzeli*	*Hyperammina coleyi*	*Sacculinella australae*	*Placentammina ampulla*	*Placentammina?* sp.	Pseudohyperammina? sp.	*Lagenammina* sp.	*Glomospirella nyei*	*Ammodiscus nitidus*	?minute trochamminid	Fish teeth	*Jureasnites*
Beckett's Gully																
181379	R	R	C				C	A	R	R						
181380			R				R			R		R	R			
181381	R	R	R			A				?		A			X	X
181382	R		R				?				R	A		C		
181383	R			?				R			C	A	R	R	X	
181384	R	R	R				A	A	R							
181385	R	R	R		R		C	C	R		R					
181386			A	R	R	R	?					C				
181397	C		A		R		C		R	R						
Locality A (in interval with *Juresanites* in nodules)																
181387	R		R				C					R				
181388			R		R		R									
181389	C	R	R				R	R								
181390	C		R				R	R		R						
181391	R						R					A				
Locality B (immediately below level with *Juresanites*																
175040	C					A	R					A				
181392	C		R			R	R	R			R	A			X	
181393					R						R	A				
181394	R				R				R		R	A	R			
181395			R		R						R	A			X	
Locality D																
181396			C	R				?				R				

Appendix 4. Curatorial details for figured palynomorphs (Figs. 12, 13)

Palynomorphs	Fig. no.	Sample no.	Slide no.	EF coords	Photo no.	GSWA no.
Punctatisporites gretensis	12A	175035	3	V27/1	WL706	F55166
Leiotriletes directus	12B	175029	5	D16	WL74	F55167
Apiculiretusispora sp.	12C	175035	12	F18	WL1162	F55168
Microbaculispora tentula	12D	175035	3	T25	WL699	F55169
Converrucosisporites confluens	12E	175035	2	Q40	WL504	F55170
Converrucosisporites confluens	12F	175029	16	Q25	WL1301	F55171
Horriditriletes ramosus	12G	175029	16	T8	WL1292	F55172
Horriditriletes ramosus	12H	175029	16	P31/1	WL1305	F55173
Brevitriletes cornutus	12I	175029	9	Q21	WL169	F55174
Diatomozonotriletes townrowii	12J	175029	14	N30/1	WL1247	F55175
Diatomozonotriletes sp.	12K	175035	2	P28/2	WL437	F55176
Secarisporites lacunatus	12L	175029	14	W39/4	WL1254	F55177
Densoisporites solidus	12M	175029	5	L45	WL100	F55178
Indotriradites niger	12N	175035	2	U17	WL337	F55179
Gondisporites ewingtonensis	12O	175035	1	O25/3	WL41	F55180
Gondisporites ewingtonensis	12P	175035	2	H47	WL553	F55181
Cannanoropollis janakii	13A	175029	8	E45	WL164	F55182
cf. *Cannanoropollis* sp.	13B	175029	13	V9	WL1192	F55183
Barakarites sp.	13C	175029	17	N34/4	WL1332	F55184
Plicatipollenites gondwanensis	13D	175029	14	G42	WL1258	F55185
Plicatipollenites densus	13E	175029	17	T36/4	WL1333	F55186
Plicatipollenites malabarensis	13F	175035	10	J27/3	WL1066	F55187
Plicatipollenites cf. *malabarensis*	13G	175029	13	E14/3	WL1198	F55188
Potonieisporites novicus	13H	175029	16	K10/2	WL1294	F55189
Caheniasaccites sp.	13I	175029	8	S18/3	WL112	F55190
Limitisporites rectus	13J	175035	2	T48/1	WL561	F55191
Protohaploxpinus amplus	13K	175029	5	S44	WL98	F55192
Protohaploxpinus limpidus	13L	175035	2	V39/4	WL503	F55193
Striatoabieites multistriatus	13M	175035	2	R10/2	WL209	F55194
Vittatina fasciolatus	13N	175035	2	E13	WL266	F55195
Vittatina scutata	13O	175035	12	R14/1	WL1153	F55196
Cycadopites cymbatus	13P	175029	14	R27	WL1243	F55197
Cycadopites cymbatus	13Q	175029	13	V19/4	WL1205	F55198
Marsupipollenites striatus	13R	175029	17	U21/1	WL1329	F55199
Marsupipollenites striatus	13S	175029	15	J40	WL1289	F55200
Marsupipollenites cf. *striatus*	13T	175035	10	E32/2	WL1076	F55201
Foraminiferal test lining	7F	175035	11	W30/3	WL1129	F55202
Scolecodont	10I	175035	11	S34/3	WL1133	F55203
Scolecodont	10J	175029	13	F45/2	WL1227	F55204